

ELUCIDATING THE MOLECULAR DRIVERS OF NAIROVIRUS OTU
INTERACTIONS WITH UB AND ISG15

by

JOHN VINCENT DZIMIANSKI

(Under the Direction of Scott Pegan)

ABSTRACT

The family *Nairoviridae* consists of a group of tick-borne viruses in the order *Bunyavirales*. Several nairoviruses have been demonstrated to cause human disease, the most notable being Crimean-Congo hemorrhagic fever virus that can have fatality rates greater than 30%. Encoded in the nairovirus genome is an ovarian tumor domain protease (OTU) that reverses posttranslational modifications of proteins by ubiquitin (Ub) and the Ub-like protein interferon (IFN)-stimulated gene product 15 (ISG15). This activity of the OTU and proteases from other viruses as deubiquitinases/deISGylases has been connected with suppression of the type I IFN response, a key part of early cellular responses to viral infections. As a result, they have been proposed to be virulence factors and are considered potential therapeutic targets. Interestingly, it has been observed that OTUs from different nairoviruses do not possess the same activity or relative preference for Ub and ISG15. This raises the prospect that these viruses may not engage the immune response in the same way. Additionally, ISG15 shows significant interspecies diversity that has been shown to impact interactions with viral proteins and potentially host tropism. Regrettably, prior investigations of OTUs were only able to characterize the activity of a few nairoviruses,

leaving it unclear on how substrate specificity may differ across the family. This work addresses this gap in knowledge through structural and biochemical approaches to understand the impact of virus and host diversity on nairovirus-host interactions. OTUs from diverse nairoviruses representing the whole virus family were broadly assessed for their activity against Ub and 12 species' ISG15. This revealed that DUB and deISGylase activity is predominantly restricted to a few, closely related virus lineages, and that ISG15 preference generally correlates with known host associations. Six novel OTU structures were solved by X-ray crystallography, revealing the impact of sequence diversity on structural features. Combined with mutational analysis, this revealed the molecular drivers for interaction with Ub and ISG15, including the ability to shift preferences of one substrate versus another. Overall, this work provides a foundation to develop tools to further probe the role of the OTU during infection and its potential as a therapeutic target.

INDEX WORDS: Nairovirus, OTU, Ubiquitin, ISG15, Interferon, Innate immune response, Host tropism, Structure, DUB, deISGylase

ELUCIDATING THE MOLECULAR DRIVERS OF NAIROVIRUS OTU
INTERACTIONS WITH UB AND ISG15

by

JOHN VINCENT DZIMIANSKI

B.S.A, The University of Georgia, 2014

A Dissertation Submitted to the Graduate Faculty of The University of Georgia in Partial
Fulfillment of the Requirements for the Degree

DOCTOR OF PHILOSOPHY

ATHENS, GEORGIA

2019

© 2019

John Vincent Dzimianski

All Rights Reserved

ELUCIDATING THE MOLECULAR DRIVERS OF NAIROVIRUS OTU
INTERACTIONS WITH UB AND ISG15

by

JOHN VINCENT DZIMIANSKI

Major Professor:	Scott Pegan
Committee:	Cory Momany
	Arthur Roberts
	William Lanzilotta
	Ralph Tripp

Electronic Version Approved:

Suzanne Barbour
Dean of the Graduate School
The University of Georgia
May 2019

DEDICATION

A dissertation is often presented as an individualistic endeavor—the crowning achievement of a single person making it through a rigorous graduate program and becoming an expert in their subject area. In a sense, this is true. At its best, a dissertation requires and demonstrates that an individual be able to independently formulate, articulate, and defend their own ideas. Getting to that point, however, involved countless points of interaction with others that shaped the ideas and development of the person. In a very real way, no successful PhD is a solo effort. In my Departmental Grantsmanship course, the instructor would remind us of the importance of previous work—that in developing a good grant, we are always “standing on the shoulders of giants” (quote by Sir Isaac Newton: “If I have seen further it is by standing on the shoulders of giants”). In a similar way, various people have had a profound impact on me and the culmination of my PhD. It is to some of these “giants” that I dedicate my dissertation.

First, to my parents, Mike and Debbie, who provided an environment that fostered inquisitiveness and modeled patient endurance in life and professional pursuits.

To David McKinney, previously the graduate TA for my undergraduate biology lab with whom I later developed a strong and lasting friendship. Our conversations over the years deeply shaped the way I think about life and science, and his advice proved invaluable as I considered and eventually pursued graduate study.

To my advisor, Scott Pegan, for his mentorship and providing the environment for my development as a scientist. Also, to my committee members and collaborators who have challenged and expanded my thinking on various scientific questions and projects.

To my lab members over the years from whom I have learned much in working with, and who helped shape and refine the ideas I was learning and developing. Two in particular should be specifically mentioned. Octavia Goodwin's time as a postdoc in the lab started soon after I joined. Her advice and council benefitted me tremendously in learning the principles of protein purification, how to think about lab operation and dynamics, and keeping a balanced perspective of research and life. Courtney Daczkowski was a graduate student one year my senior and took on the task of training me when I first joined. There may not be an individual to whom I owe more individually during my graduate career than Courtney, who brought me from a (sometimes) frustrating junior student to the level of a respected colleague. Working with her not only helped me professionally, but also personally—I learned a lot about myself during that time and gained a greater degree of clarity regarding my personal goals for life and career. It would be hard to measure the impact that she has had, and I am indebted for the investment she made in me. I couldn't have asked for a better labmate, mentor, and friend during the three years that our time overlapped in the lab.

To family and friends who have been a solid structure during both the good and difficult times of graduate school. Worthy of special mention are my brothers Daniel and Timothy, two of my best friends in the world. It's hard for life to be boring when you know them. They have been a refreshing and stabilizing presence during my time in

graduate school, and have been both the core and catalyst of the most meaningful relationships I have developed outside the lab.

Finally, to the previous generations of scientists that have laid the foundation for the small work I've been able to accomplish. In particular, the “giants” who were key to the historical development of science, many with whom I feel a common motivation: that in studying nature we learn more about the nature and glory of God. In the words of Johannes Kepler, that in studying nature we are “thinking God’s after him”.

Soli Deo gloria.

TABLE OF CONTENTS

	Page
LIST OF TABLES	x
LIST OF FIGURES	xi
CHAPTER	
1 INTRODUCTION AND LITERATURE REVIEW	1
Forward	1
The <i>Nairoviridae</i> family.....	2
Nairovirus replication cycle and molecular biology.....	4
Nairovirus mechanisms to evade host immune responses	5
Viral DUBs: an emerging paradigm in immune suppression.....	8
The simplicity and complexity of Ub	10
2 ISG15: IT'S COMPLICATED.....	16
Introduction	19
Discovery of ISG15	19
The intracellular role of ISG15.....	20
ISG15 as an extracellular cytokine.....	23
ISG15 and viral proteins	24
ISG15 possesses interspecies diversity that translates to variation in protein structure	26

	ISG15 sequence and structural diversity impacts virus protein-protein interactions	32
	Current outlook and challenges to evaluating the specific effects of ISG15	35
	Potential applications to leverage ISG15 interspecies diversity.....	38
	Conclusion.....	41
3	PROBING THE IMPACT OF NAIROVIRUS GENOMIC DIVERSITY ON VIRAL OVARIAN TUMOR DOMAIN PROTEASE (vOTU) STRUCTURE AND DEUBIQUITINASE ACTIVITY	51
	Introduction	54
	Results	61
	Discussion.....	87
	Methods	95
4	DETERMING THE MOLECULAR DRIVERS OF SPECIES-SPECIFIC INTERFERON-STIMULATED GENE PRODCUT 15 INTERACTIONS WITH NAIROVIRUS OVARIAN TUMOR DOMAIN PROTEASES.....	109
	Introduction	112
	Results	117
	Discussion.....	142
	Materials and Methods	148
5	DISCUSSION.....	163
	The implications of OTU-substrate activity and preference	163

Utilizing structure-function: opportunities to develop novel applications	
.....	168
Conclusion.....	172
REFERENCES	173
APPENDICES	
A SUPPLEMENTAL INFORMATION FOR CHAPTER 3.....	184
B SUPPLEMENTAL INFORMATION FOR CHAPTER 4.....	189

LIST OF TABLES

	Page
Table 3.1: Data collection and refinement statistics for vOTU crystal structures.....	68
Table 3.2: Isothermal Titration Calorimetry of TAGV-Ub binding.....	76
Table 4.1: Data collection and refinement statistics	122
3.S1 Table: Viruses and sequence accession numbers.....	185

LIST OF FIGURES

	Page
Fig 2.1: ISG15 is conjugated to a wide range of viral and cellular proteins, influencing immune responses.	21
Fig 2.2: Structure of human ISG15 (PDB entry 1Z2M)	27
Fig 2.3: ISG15 structural diversity.....	30
Fig 3.1: Sequence and structural diversity of nairovirus vOTUs	56
Fig 3.2: Diversity of vOTU specific activity.....	62
Fig 3.3: vOTU preferences for different di-Ub linkages.....	64
Fig 3.4: Structural comparison of new vOTU structures	69
Fig 3.5: Selectivity pocket of nairovirus vOTUs.....	74
Fig 3.6: Structure of the FARV vOTU.....	80
Fig 3.7: Model of molecular contributors to FARV mono- and poly-Ub activity	83
Fig 3.8: Second site of FARV vOTU interaction with di-Ub.....	86
Fig 4.1: Sequence alignment of OTUs and ISG15	115
Fig 4.2: Activity of nairovirus OTUs for proISG15 from different species.....	119
Fig 4.3: Structure of KUPEV OTU in complex with CshISG15.....	123
Fig 4.4: Structure of GANV OTU in complex with shISG15	127
Fig 4.5: Molecular contributors to species-variable ISG15 interactions with nairovirus OTUs.....	129
Fig 4.6: Additional residues influencing species-specific OTU-ISG15 interactions.....	132

Fig 4.7: Targeting the OTU “selectivity helix” to alter ISG15 preference	136
Fig 4.8: Selectively altering CCHFV OTU interactions with hISG15 and mISG15.....	140
3.S1 Fig: Comparison of commercially available di-UB FRET TAMRA/QXL substrates.....	186
3.S2 Fig: Global structural comparison of vOTUs.....	187
3.S3 Fig: ITC Isotherms of TAGV vOTU-Ub binding and biochemical environment of FARV vOTU Leu13	188
4.S1 Fig: Expanded nairovirus OTU sequence alignment	190
4.S2 Fig: Related to Fig 4.2.....	191

CHAPTER 1

INTRODUCTION AND LITERATURE REVIEW

Forward

The discovery of bacteria and viruses as causative agents of disease in the mid to late 19th century ushered in a new era of combatting illness and life-threatening conditions. This led to unprecedented success as the golden age of antibiotics and vaccines led to the control and, in some cases, eradication of devastating diseases. In the shadow of these tremendous successes are conditions, however, for which there is no cure-all. In other words, some disease-causing agents still exist for which no effective therapeutics have been successfully developed. As the easy problems have been solved and given way to harder ones, finding remedies and cures for diseases continually relies on patient, persistent research in characterizing pathogens—of gaining a fundamental understanding of the molecular biology of bacteria and viruses and their complex interactions with their hosts.

This study focuses on one such aspect in the case of nairovirus interactions with their hosts. Nairoviruses encode an ovarian tumor domain protease (OTU) that is known to interact with the host proteins ubiquitin (Ub) and interferon-stimulated gene product 15 (ISG15). Specifically, the activity of the OTU is centered on reversing the post-translational modification of proteins by Ub (deubiquitinating) and ISG15 (deISGylating). These interactions carry with them the potential to influence host immune responses, creating important implications for outcomes of viral infection. Prior to this work little was known regarding the role of the OTU in relation to host adaption and whether it had a

conserved role in nairoviruses, leaving an incomplete picture of the overall impact of this virus-host interface. What follows is my work approaching this problem from a structural and biochemical perspective to identify the molecular features underlying these virus-host interactions. In particular, it delves into the dual-impact of virus and host genetic diversity on the functional outcomes at this interface. For the remainder of this chapter, I provide a larger context for the activity of the OTU, including a brief review of nairoviruses, the utilization of deubiquitinases (DUBs) as a viral strategy for immune evasion, and the general structural features and roles of Ub, including its involvement in cellular responses to infection. Following this are three first-author manuscripts I have published or submitted for publication as a part of this project. CHAPTER 2 is a literature review of ISG15, going more in depth on the complexities and nuances created by its interspecies diversity. CHAPTER 3 presents a study investigating the impact of nairovirus diversity on substrate interactions with a particular focus on Ub, while CHAPTER 4 carries this into the influences of ISG15 diversity and how it relates to nairovirus host ranges. CHAPTER 5 ties these things together, providing my concluding thoughts and discussion of this work's implications for the field.

The *Nairoviridae* family

The seminal work in the literature leading to the characterization of nairoviruses was the report by Montgomery in 1917 of gastroenteric disease causing high mortality in sheep and goats in East Africa [1, 2]. The causative agent, known as Nairobi Sheep Disease virus (NSDV), was identified and observed to transmit through ticks. In the century since this discovery more than 40 viruses have been classified as a nairovirus or “nairovirus-like”. The classification originally depended on antigenic characteristics that led to

clustering within seven serogroups. Recently this shifted to a dynamic re-classification system based on increasing genomic data and phylogenetic analysis, leading to a current estimate of ~16-17 species split across 3 genera (*Orthonairovirus*, *Shaspivirus*, and *Striwavivirus*), with the classical “nairoviruses” falling within the *Orthonairovirus* genus [3-7].

Nairoviruses have been found in regions of every major continent, giving this family of viruses a global geographic distribution [7]. Consistent with their nature as tick-borne viruses, most have been isolated from ticks, though a few were discovered in vertebrates such as bats and shrews [6, 8-11]. Several have been associated with human disease, including an Asian variant of NSDV found in India known as Ganjam virus (GANV), Dugbe virus (DUGV) and Kasokero virus (KASV) in Africa, Issyk-kul virus (ISKV) in eastern Europe, Erve virus (ERVEV) in western Europe, and Crimean-Congo hemorrhagic fever virus (CCHFV) throughout regions of eastern and southern Europe, Asia, the Middle East, and Africa [10, 12-16]. In most cases these viruses cause mild inflammatory illness. Infections with CCHFV, however, in some cases progresses to severe hemorrhagic disease with fatality rates ranging from 5-40% depending on the size of the outbreak, virus strain, and geographical region [12]. Notably, CCHFV is asymptomatic in most non-human animals. This not only presents challenges from the perspective of disease surveillance but has also presented obstacles to therapeutic development due to the lack of animal models. Recent advancements include the use of immunocompromised mice (*Stat1*^{-/-} and *IFNAR1*^{-/-}) that lack an interferon (IFN) response and recapitulate human signs of disease, as well as the development of a non-human primate model with a particular CCHFV strain [17-19].

Nairovirus replication cycle and molecular biology

Most of our knowledge of nairovirus biology has been derived from studying the highly pathogenic CCHFV, as well as the milder NSDV, DUGV, and Hazara (HAZV) viruses. Nairoviruses are part of the order *Bunyavirales*, which consist of enveloped, negative-sense, single stranded RNA viruses containing a tripartite genome consisting of small (S), medium (M), and large (L) segments. The S segment encodes the nucleoprotein (NP) that associates with and packages the viral genome. The M segment is expressed as a polyprotein encoding the two glycoprotein components, Gn and Gc, and is processed by host proteases and undergoes extensive post-translational modifications [20-24]. The L segment, which is much larger in nairoviruses compared to other bunyaviruses, encodes a single, multifunctional protein (L protein) possessing multiple domains with distinct enzymatic and non-enzymatic functions. This includes the OTU domain and an endonuclease domain near the N-terminus, the RNA-dependent RNA polymerase (RdRp) within the C-terminal half, and regions that are known to interact with NP [25, 26].

The replication cycle occurs by mechanisms similar to other members of *Bunyavirales* yet has some features distinct to nairoviruses (Reviewed in [27, 28]). Cell entry is triggered by receptor-mediated endocytosis that is thought to occur by a clathrin-dependent mechanism [29]. The current understanding is that Gc is the critical player in cell attachment by association with an unidentified cell-surface receptor [27, 30]. Following endosomal escape, pre-packaged L protein begins transcription of the viral genome via the RdRp. Concurrently, the endonuclease domain performs a snatch-capping function, removing the 7-methylguanosine cap from cellular mRNAs and subsequently utilizing it as a primer for transcription [31]. Following transcription, the viral mRNAs

undergo translation occurs by host ribosomes, with the destination for the NP and L proteins being the cytoplasm and the immature M the endoplasmic reticulum (ER), where it undergoes further processing [20, 27, 32, 33]. Within the cytoplasm, NP and the L protein undergo increasing colocalization as it progresses from early to late stages of replication, likely reflecting cooperative activity in genome replication and formation of the ribonucleoprotein (RNP) [33]. Maturation of the M-derived glycoproteins proceeds through the ER and typically culminates in the Golgi complex, where assembly of the viral proteins occurs, leading to budding and exocytotic release of the nascent virion [34].

Nairovirus mechanisms to evade host immune responses

To counter viral threats, cells encode various mechanisms to detect and control viral replication. In early stages particularly, cells detect pathogen-associated molecular patterns (PAMPs) through the action of pattern recognition receptors (PRRs) that trigger innate immune pathways to induce an antiviral state. One pathway of specific importance for nairovirus infection is the retinoic acid inducible gene I (RIG-I) pathway that triggers the type I interferon (IFN) response. Upon detection of viral RNA, RIG-I present in the cytosol undergoes activation that results in its association with the mitochondrial-associated antiviral signaling (MAVS) protein [35-37]. This results in the synthesis of IFN α/β through NF- κ B-driven expression, which is secreted and exhibits autocrine/paracrine effects by binding the type I IFN receptor (IFNAR), triggering the Jak-Stat signaling pathway and leading to the production of numerous IFN-stimulated genes (ISGs) that induce the antiviral state.

Given the impact of these pathways, it is not surprising that viruses encode countermeasures to suppress or directly antagonize the immune response. This can

sometimes include many components of viral genome. With nairoviruses there are currently three factors known or suspected to mediate suppressive or disruptive effects on host antiviral mechanisms.

L protein endonuclease

One of the distinctive features leading to RIG-I activation is the presence of a 5'-triphosphate on mature viral RNAs [38]. In addition to the activity of the nairovirus endonuclease “snatching” and incorporating a cellular 7-methylguanosine cap into viral mRNAs, it has also been suggested to employ a mechanism referred as “prime and re-align” that results in the removal of 5' nucleotides, resulting in a monophosphorylated 5' RNA [27, 39, 40]. This presents a preventive mechanism that partially shields the virus from detection by RIG-I, resulting in a less robust initial activation of the system.

S segment nonstructural protein (NSs)

While the main role of the S segment in bunyaviruses is the production of NP, in some cases it also encodes a nonstructural protein termed the NSs protein. The NSs of nairoviruses is encoded in the reverse frame as the nucleoprotein, rendering it the only part of the nairovirus genome that is currently known to be ambisense. While in some bunyaviruses the NSs has been associated with shutdown of host translation, in nairoviruses it has been directly connected with modulating apoptosis [41]. In CCHFV, in particular, it is known that apoptosis is inhibited in early stages of replication and promoted in later stages [42, 43]. The CCHFV NSs has recently been demonstrated to trigger apoptosis by disrupting the mitochondrial membrane potential [41]. The details on how this may benefit the virus and whether this pro-apoptotic activity is significant in the

context of viral infection have yet to be elucidated, and requires further investigation [27, 41].

The L protein OTU

Of the features in nairoviruses that have been viewed as possible immune antagonists, the OTU domain has received the most attention for its potential effects. In contrast to the endonuclease, which only passively influences the immune response, and the potential effects of the NSs, which would impact late stages of viral replication, the OTU has the potential to be a direct suppressor of early responses to viral infection. Interestingly, the OTU is not a universal feature among bunyaviruses, only being present in nairoviruses and relatively distantly related tenuiviruses. Even within the *Nairoviridae* family, the presence of the OTU has not yet been identified in the recently classified *Shaspivirus* and *Striwavirus* genera. This presents the strong possibility that viruses in the *Orthonairovirus* genus independently acquired this domain and has utilized it for adaptive functions.

When first identified, it was considered that the OTU might play a role in proteolytic processing of the L protein. However, *in vitro* study revealed that the replication function of the CCHFV L protein can proceed in the absence of the OTU, indicating that OTU proteolytic activity is not necessary for polymerase maturation [44]. Additionally, cellular studies examining the localization of the L and NP proteins in NSDV confirmed by Western Blot that the L protein functions as a single, intact protein that did not undergo specific cleavage [33]. The discovery that the CCHFV OTU possesses deubiquitinating and deISGylating activity raised the prospect that the primary role of the OTU was suppression of the innate immune response [45]. Subsequent studies

overexpressing the OTU in cellular systems were able to demonstrate the potential impact of OTU activity in CCHFV, NSDV, and DUGV, and was predominantly associated with suppression of the RIG-I pathway [45-47]. A recent reverse genetics system for CCHFV was able to further demonstrate this in the context of an authentic viral infection, providing more clarity and details on the effect of the OTU [48]. This demonstrated ability of the OTU to impact cellular responses to viral infection thrust it into a larger developing narrative of viruses utilizing deubiquitinases (DUBs) to suppress host immune responses.

Viral DUBs: an emerging paradigm in immune suppression

The concept of viral DUBs acting to suppress immune responses is a relatively recent idea, with this viral activity only being known for about 15 years. The 2002-2003 outbreak of severe acute respiratory syndrome in China led to the rapid identification and attempts to characterize the novel causative agent, severe acute respiratory syndrome-related coronavirus (SARS-CoV). Within a few years significant functional knowledge had been gained on the virus genome and its protein products. This included a papain-like protease domain (PLP) present within the nsp3 protein, which was known to have a critical function in polyprotein processing to generate the mature replicase complex of this positive-sense RNA virus. Interestingly, a sequence analysis revealed a similarity of the PLP domain to known Ub-specific proteases (USPs), particularly the HAUSP protein [49]. This homology combined with the fact that the conserved polyprotein cleavage site, LXGG, resembled the C-terminus of Ub and ISG15, led to the hypothesis that the PLP may possess deubiquitinating and deISGylating activity [49-53]. The confirmation of this hypothesis laid the foundation for identifying similar functions in a wider range of viruses. This includes other viruses in the *Coronaviridae* family, such as mouse hepatitis virus

(MHV) and the more recently emergent Middle East respiratory syndrome-related coronavirus (MERS-CoV), that have shown similar activities [54-56]. Other virus groups include the arteriviruses—such as porcine reproductive and respiratory syndrome virus (PRRSV) and equine arteritis virus (EAV)—that possess an OTU domain within the nsp2 protein, and the aforementioned nairovirus OTUs [45, 57-60]. Similar to coronaviruses, arteriviruses are also positive-sense single-stranded RNA viruses in which the OTU performs a dual function of processing a polyprotein and possessing DUB/deISGylase activity. For each of these virus families the DUB has been demonstrated to exhibit immune suppressive effects related to its ability to interact with Ub and/or ISG15, with the RIG-I pathway often implicated as being impacted [48, 60]. As with nairovirus OTUs, initial assessments of coronavirus and arterivirus DUBs relied on overexpression of the DUB domain, with recently developed reverse genetics systems confirming and clarifying the function in the context of viral infection [59, 61, 62]. In addition to these cellular studies, structural and biochemical analyses have provided complementary insights into these interactions. Structures have been solved of DUBs from each of these virus groups bound to Ub or ISG15, providing the molecular level details of these interactions and serving as a base to further probe its impact. As a result of these studies describing the immune-suppressive effects of viral DUBs, they are a current focus as potential therapeutic targets through both the development of specific inhibitors and approaches to selectively reduce or eliminate the DUB activity for the purpose of vaccine development [63-65].

Interestingly, the levels of DUB activity vary between viruses, even between those within the same family. In nairoviruses, for example, the CCHFV OTU possesses potent activity for both Ub and ISG15, while the DUGV and ERVEV OTUs appear to lack

substantial activity towards ISG15 and Ub, respectively [66]. Similarly, SARS- and MERS-CoV possess different levels of *in vitro* DUB/deISGylating activity as well [54]. This presents the question of how differing DUB/deISGylase activities relate to viral pathogenesis. A recent paper on SARS- and SARS-like-CoV's demonstrated a difference in DUB activity between strains that correlated with the relative pathogenicity of the virus, leading to the authors concluding it to be a distinctive virulence trait [61]. Whether such clear relationships for other viruses remains to be determined, but it presents important potential implications for the impact of viral OTUs and PLPs and viral pathogenesis.

The simplicity and complexity of Ub

Investigations into viral DUB-Ub interactions have produced extensive insight into this virus-host interface. One limitation, however, is related to the nature of Ub itself. Specifically, Ub does not occur in cells exclusively as a single moiety, but can take on multiple modified forms that are involved in different functions. Many of these functions have only begun to be uncovered over the course of the last decade, limiting the tools available to assess how viral DUBs may interact with them. For those that are known, the impact of the DUB on the specific form has been inferred based on *in vitro* biochemical characterization. In addition, most DUB mutants to date have exclusively dealt with overall DUB/deISGylase activity and lacked sensitivity to discriminate between different forms of modified Ub. As further knowledge and tools continue to develop, undoubtedly additional insights will be gained into the bigger picture of these interactions.

Ub itself is a small protein consisting of just 76 amino acids with a simple, compact structure. As the name suggests, it is one of the most abundant proteins present within the cell. In addition to this it also one of the most conserved proteins at an amino acid level in

eukaryotes, almost perfectly identical among mammals and differing by only a few amino acid residues between yeast, plants, and animals [67]. Consistent with this high degree of conservation, virtually every aspect of cellular biology is regulated in some capacity by Ub.

The effects of Ub are mediated by its addition as a post-translational modification to proteins. This is performed by a series of enzymes known as activating (E1), conjugating (E2), and ligating (E3) enzymes that attach the C-terminal glycine of Ub to a primary amine, most commonly to the ϵ -amine group of lysine residues in substrate proteins. Ub itself contains seven lysine residues (K6, K11, K27, K29, K33, K48, and K63), that with the primary amine at the N-terminus allow it to be linked to itself in 8 distinct ways to form polymeric chains. To control all these aspects of Ub linkage, numerous different E1, E2, and E3 enzymes are encoded for substrate, localization, and temporal regulation. In addition, cells also express numerous DUBs to negatively regulate Ub signaling and recycle Ub.

Initially poly-Ub was found to be associated with tagging proteins for degradation by the proteasome. It was later found that this was primarily mediated by K48-linked poly-Ub, and that other forms of poly-Ub regulated other cellular processes. In addition, recent work has continued to uncover the nuances of poly-Ub function, showing that it can involve multiple linkage types (“heterotypic” compared to “homotypic”) as well as form branched chains. The reader is referred to excellent reviews on these emerging insights into Ub signaling [68-70]. Below is a summary of the major functions identified so far for each linkage type.

Linear

Linear poly-Ub is synthesized by a single E3 enzyme, LUBAC. It is a major regulator of NF- κ B signaling and is specifically involved with the TNF signaling pathway to upregulate inflammatory factors [71]. It primarily mediates its effects through facilitating the recruitment of other signaling factors, such as NEMO, to initiate the signaling cascade.

K6

K6-linked poly-Ub lay in obscurity for years. Some studies initially linked K6 to cellular responses to DNA damage [72]. More recently, however, K6 has emerged as an important player in mitophagy [73, 74]. Mitochondria are dynamic organelles undergoing constant regulation. In addition to having a central role in metabolism, they are also at the crossroads of numerous other signaling processes, including immune functions and apoptosis, making the maintenance of healthy mitochondria an important priority. Damaged and dysfunctional mitochondria are coated by a poly-Ub “carpet” that predominantly consists of K6-linked Ub chains formed by the E3 ligase parkin [73]. This marks the mitochondria for an autophagic pathway leading to fusion with lysosomes for degradation.

K11

The main role of K11 chains is its well-studied function in controlling the cell cycle. Poly-ubiquitination targets the check point protein APC/C for degradation, permitting the continuation of the cell cycle. K11 linked poly-Ub is an important part of this process and is mediated by the E2 enzyme UBE2S [75]. In addition to this well-characterized function,

K11 has recently been more connected with regulating TNF signaling, presenting a potential role in mediating immune responses [76].

K27

K27-linkages are the least understood poly-Ub linkages. Currently its known roles are connected with DNA damage responses, with other functions identified as regulating secretion or autophagy of specific proteins [77-79].

K29

K29-linked chains are also among the less studied linkages. Current studies have associated it with a role in signaling for proteasome mediated protein degradation [80, 81], as well as in the regulation of Wnt signaling [82, 83].

K33

K33 poly-Ub has been associated with signaling in T-cells, serving as a feedback mechanism to dampen T-cell receptor signaling by inhibiting association of the kinase ZAP70 with the receptor [84]. Additional roles have been identified more recently with protein trafficking through the Golgi [85].

K48

Easily the most studied linkage type, K48 poly-Ub is predominantly involved in marking proteins for proteasomal degradation. Although one role is to maintain a general homeostasis of proteins, it serves in a regulatory function through targeted protein degradation. A specific case includes the RIG-I pathway, where the factor IKK is held in an inhibited state by association with I κ B. Upon activation of the pathway, K48-linked polyubiquitination of I κ B targets it for degradation, removing the inhibition [70]. In

addition, viral proteins can be marked for degradation by K48 poly-Ub, leading to inhibition of viral replication [86, 87].

K63

Apart from K48 linkages, K63 is the most well-studied of the polymeric Ub forms. Like linear poly-Ub, it has a strong association with NF- κ B signaling and pro-inflammatory responses. It plays a key role in innate immune signaling, particularly within the RIG-I pathway. Upon detection of viral RNA, RIG-I undergoes K63 polyubiquitination that facilitates its association with MAVS. This interaction triggers MAVS aggregation that propagates the signal through downstream factors [36, 37]. In addition to RIG-I, other downstream components in the pathway such as IRF3 also require K63 polyubiquitination to carry out their function [88].

Ub: a common viral target across multiple hosts?

The fact that Ub is so highly conserved across eukaryotes naturally raises the prospect of whether this provides a common point of action that viruses could use against a variety of potential hosts. When it comes to vertebrate hosts, this seems especially straightforward as many antiviral mechanisms, such as RIG-I, serve analogous functions in different species. This would support, for example, a transition from bats to humans as is thought to have occurred with the SARS- and MERS-CoVs. With arthropod-borne viruses, especially those that are highly dependent on the arthropod host for long-term maintenance in nature (such as nairoviruses with their tick hosts), it's less clear whether there could be a possible cross-over effect. The Ub system of arthropods has been characterized much less extensively, with no reports currently addressing whether it has a role in regulating antiviral signaling.

All of the modifications and variable forms of Ub give it a level of nuanced complexity that allows it to perform many different functions in numerous cellular contexts. When it comes to the interactions with viral DUBs, however, this largely simplifies to interactions with the different chain types. With the high conservation of Ub between species, the actual interface of DUBs with Ub and the underlying interactions remain largely the same even across different hosts. This contrasts greatly with the other main target of viral DUBs, ISG15, which brings additional layers of complexity to virus-host interactions.

CHAPTER 2

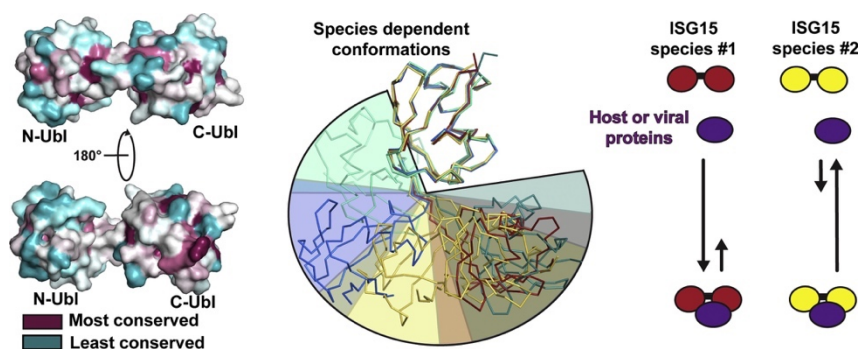
ISG15: IT'S COMPLICATED ¹

¹ Dzimianski, J.V., F.E.M. Scholte, É. Bergeron, and S.D. Pegan. 2019. Accepted by *Journal of Molecular Biology*. Doi: 10.1016/j.jmb.2019.03.013 Reprinted here with permission of the publisher.

Abstract

Interferon stimulated gene product 15 (ISG15) is a key component of host responses to microbial infection. Despite having been known for four decades, grasping the functions and features of ISG15 has been a slow and elusive process. Substantial work over the past two decades has greatly enhanced this understanding, revealing the complex and variable nature of this protein. This has unveiled multiple mechanisms of action that are only now beginning to be understood. In addition, it has uncovered diversity not only between how ISG15 affects different pathogens, but also between the function and structure of ISG15 itself between different host species. Here we review the complexity of ISG15 within the context of viral infection, focusing primarily on its antiviral function and the mechanisms viruses employ to thwart its effects. We highlight what is known regarding the impact of ISG15 sequence and structural diversity on these interactions and discuss the aspects presenting the next frontier towards elucidating a more complete picture of ISG15 function.

Graphical Abstract



Highlights

- ISG15 is one of the most highly upregulated IFN-stimulated proteins
- ISG15 is involved in numerous pathways with multiple mechanisms of action
- Viruses encode specific countermeasures to combat ISG15 function
- ISG15 possesses interspecies sequence diversity impacting structure, function, and viral interactions
- Key advances have been made, much work remains to grasp the complexity of ISG15

Introduction

Interferon (IFN)-stimulated gene product 15 (ISG15) is one of the most highly induced genes in response to viral infection. ISG15 is part of a class of proteins sharing structural homology to ubiquitin (Ub), known as Ub-like (proteins), that also includes SUMO, Nedd8, and FAT10 [1–9]. Both Ub and Ubl proteins are key mediators and regulators of numerous cellular processes, and ISG15 is no exception. Despite being the first Ubl protein discovered, efforts to attain a cohesive characterization of ISG15 lagged behind relative to most of its sister Ubl proteins. While its immunological function, particularly as an antiviral protein, was inferred based on its upregulated levels upon IFN treatment, a detailed understanding of its roles was lacking. Recent studies have begun to unveil the more specific mechanisms of ISG15 action, revealing varied and apparently contrasting functions for ISG15. These have introduced a complexity to our understanding of ISG15, showing it to not only to be intrinsically multifunctional but also to display functional and structural diversity between different species. Understanding these differences will be key to ascertaining the impact on the microbe-host interface, as well as the potential connections this could have to host immune responses, microbe species tropism, and pathogenesis. In this review, we focus on ISG15 within the context of its antiviral function and especially how various viruses have evolved strategies to counter the effects of ISG15. We highlight the emerging picture of how ISG15 species diversity influences its immune function and the ability of viral proteins to thwart its effects.

Discovery of ISG15

ISG15 was first identified in 1979 in IFN-treated cells [10], although its Ub-like nature was not reported until 1987, when it was found to cross-react with Ub antibodies

[11]. ISG15 was renamed in 1987 from general references to a “15-kDa protein” to its current name after the discovery that its transcription was driven by IFN- β , and the term “interferon-stimulated gene” was coined [12,13]. This IFN-dependent expression prompted studies investigating the contribution of ISG15 to antiviral responses. The innate immune response is the first line of defense against invading pathogens, which are sensed by host pattern-recognition receptors. For example, viral RNA is detected by cytoplasmic sensors such as RIG-I and MDA5 (Fig. 2.1a). This triggers various downstream signaling pathways resulting in the expression of type I IFNs and proinflammatory cytokines. Type I IFNs are released from infected cells and subsequently bind to IFN α/β receptors of the infected cell as well as neighboring cells, thus exerting both autocrine and paracrine effects. Binding of secreted IFN to its receptor activates downstream signaling that ultimately results in the expression of hundreds of IFN-stimulated genes (ISGs), whose promoters contain IFN response stimulated elements (ISRE) (Fig. 2.1a). ISG-encoded proteins, including ISG15, are critical orchestrators of the host cell defense arsenal to viral infection. The role of ISG15 in antiviral immunity has been investigated extensively in mouse models, and several viruses were found to be more pathogenic in ISG15 KO mice [14].

The intracellular role of ISG15

In keeping with its similarity to Ub, our current knowledge about ISG15 suggests its role to be predominantly intracellular through its conjugation to lysine (K) residues in a process called ISGylation, although unconjugated (free) ISG15 also has various functions. ISGylation requires a three-step enzymatic cascade involving an E1 activating enzyme (Ube1L), an E2 conjugating enzyme (UbcH8), and an E3 ligase (Herc5 or TRIM25/EFP). ISGylation is reversed by Ub-specific protease USP18 [15]. Like ISG15, the

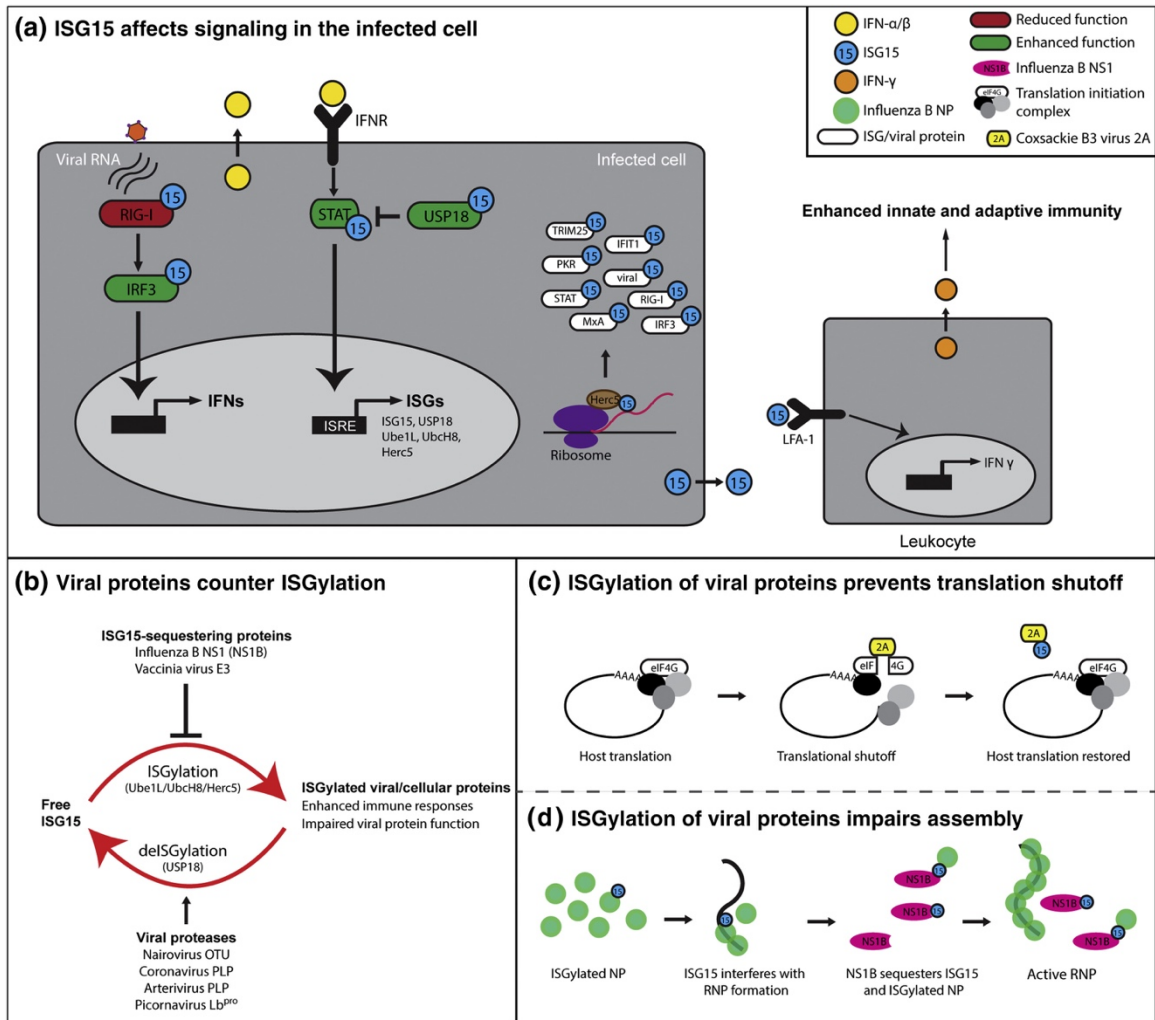


Fig. 2.1. ISG15 is conjugated to a wide range of viral and cellular proteins, influencing immune responses. (a) The infected host cell senses viral RNA via RIG-I, which induces signaling leading to the expression and secretion of type I IFN. Type I interferon binding to IFN receptor (IFNR) result in the expression of IFN-stimulated genes (ISGs), including ISG15 and its conjugating enzymes (Ube1L, UbcH8, and Herc5). Herc5 association to ribosomes result in the ISGylation of newly synthesized host and viral proteins including several ISGs (white). ISG15 conjugation can inhibit (red) or enhance (green) the activation state of innate immune signaling proteins. USP18 is a negative regulator of IFNR signaling by limiting STAT activation. USP18 protected from degradation by ISG15 binding, thereby enhancing the inhibition of IFNR signaling. Extracellular ISG15 binds to LFA-1 receptors of leukocytes and induces the expression and secretion of IFN- γ . (b) Viral proteins can counter ISGylation by sequestering ISG15/ISGylated proteins, or by deconjugating ISG15. (c) The 2A protease of Coxsackie B3 virus induces host translational shutoff by cleaving eIF4G. ISGylation of 2A restores host translation by preventing eIF4G cleavage. (d) ISGylation of viral proteins interferes with virus replication. ISGylation of Influenza B virus NP reduces the oligomerization and formation of viral ribonucleoprotein complexes (RNPs). NS1B counters ISGylation by sequestering ISG15 and ISGylated NP.

expression of its conjugating enzymes and USP18 is upregulated by IFN (Fig. 2.1a). In contrast to the hundreds of E1–E2–E3 enzymes available for formation of complex poly-Ub chains, ISG15 is conjugated to target proteins as a monomer by a very limited set of E1–E2–E3 enzymes. ISGylation appears to take place predominantly at the ribosomes, due to the localization of the dominant ISG15 E3 ligase (Herc5), which largely limits ISGylation to newly synthesized proteins [16]. Therefore, during viral infection, actively translated proteins such as ISGs and viral proteins are preferentially ISGylated (Fig. 2.1a) [16–22].

The effects of free ISG15 and ISGylation on cell biology are diverse and can be stimulatory as well as inhibitory. ISGylation can enhance antiviral signaling pathways by prolonging the activation state of signaling proteins (e.g., IRF3, STAT1), resulting in a higher production of type I IFN and ISGs [23,24]. Although ISG15 plays an important role activating antiviral immunity, it also provides negative feedback suppression of antiviral signaling pathways. Type I IFN activation is tightly regulated to prevent excessive immune responses. ISG15 negatively regulates type I IFN signaling at multiple levels. For example, ISGylation of RIG-I results in reduced levels of IFN promoter activity, and ISG15 binding targets RIG-I for autophagic degradation [25,26]. USP18 regulates antiviral responses by removing ISG15 conjugates and can directly inhibit type I IFN receptor signaling by binding the subunit 2 of the receptor via STAT-2 [27,28]. This interaction prevents the dimerization of the IFNAR subunits and recruitment of JAK1 necessary for the phosphorylation and activation of STAT1, which induces the transcription activation of ISGs. Therefore, USP18 dampens the immune responses by reversing protein ISGylation and directly inhibiting IFN signaling (Fig. 2.1a,b). In human cells, binding of ISG15 to

USP18 increases USP18 levels by preventing its degradation [29], further reinforcing the inhibition of IFN receptor signaling. Therefore, USP18 and/or ISG15 depletion results in prolonged type I IFN signaling and enhanced levels of ISGs [30]. Similar to human cells, murine USP18 dampens IFN signaling by binding to the IFN receptor, but mouse USP18 is not stabilized by mouse or human ISG15 [30]. This greatly limits the extrapolation of conclusions obtained in murine systems to humans and emphasizes evolutionary divergence of ISG15 between species and potential different roles in regulating the antiviral responses. ISG15 KO mice are more susceptible to various viruses, and in most cases, the antiviral activity of ISG15 appeared to require conjugation, as preventing conjugation by knocking out Ube1L recapitulated the increased viral replication observed in ISG15 KO mice [14]. Unlike mice, ISG15-deficient patients are not more susceptible for viral infection; in fact, they appear to be more resistant due to higher basal levels of ISG expression [29].

ISG15 as an extracellular cytokine

Given its structural similarity to Ub, a somewhat surprising feature of ISG15 is its ability to function as an extracellular signaling molecule. ISG15 is secreted or released by various cell types, including fibroblasts, neutrophils, monocytes, and lymphocytes [31–34]. The receptor for extracellular ISG15 was identified recently as the leukocyte function-associated antigen-1 (LFA-1), an adhesion molecule of the integrin family composed of an α L and β 2 subunit [35]. LFA-1 binding to the intercellular adhesion molecule 1 is critical in the homing of leukocytes to sites of inflammation. ISG15 does not compete with intercellular adhesion molecule 1 binding to LFA-1. Instead, secreted ISG15 acts on natural killer cell and T lymphocytes to enhance the secretion of IFN- γ (type II IFN) secretion,

which is important for the activation of innate and adaptive immune responses [34,36]. ISG15-deficient patients are highly susceptible to mycobacterial disease because of their IFN- γ deficiency [31]. In addition, ISG15 induces natural killer cell proliferation and enhanced lytic capabilities of lymphokine-activated killer-like cells [36].

ISG15 and viral proteins

Beyond ISG15 conjugation to host proteins, various viral proteins have also been identified as ISG15 targets. ISGylation of viral proteins can affect their function by interfering with their localization, protease activity, or ability to interact with host proteins or other viral proteins. For example, ISGylation of Coxsackie B3 virus (CVB3) 2A protease prevents the induction of cellular host shut-off by preventing cleavage of eIF4G (Fig. 2.1c) [37]. ISGylation of viral proteins that oligomerize, required for the formation of viral replication complexes and/or particle assembly, is especially efficient, as only a small fraction of viral proteins has to be modified in order to cause a dominant inhibitory effect. This has been described for NP of Influenza B virus (Fig. 2.1d) and the human papillomavirus L1 capsid protein [16,38]. A particularly well-studied ISGylated viral protein is NS1 of Influenza A virus, a major virulence factor. ISGylation of Influenza A virus NS1 prevents its ability to form homodimers and interaction with PKR, which is required for suppression of host antiviral responses. Mutating the lysine residues predominantly targeted for ISGylation in NS1 produces viruses that demonstrate increased viral growth in infected cells, and enhanced virulence in mice [22].

Considering the potential negative impact of ISG15 on viral processes, it is not surprising that viruses have evolved various mechanisms to inhibit or reverse ISGylation. The main viral strategies to counter ISGylation fall into two general categories: the use of

viral proteins to sequester ISG15/ISGylated proteins (e.g., Vaccinia virus E3 and NS1 of Influenza B (Fig. 2.1c)), or the use of virally-encoded proteases to remove ISG15 conjugates from their target proteins (Fig. 2.1b). Viruses that encode viral proteases able to reverse ISG15 conjugation include nairoviruses [e.g., Crimean-Congo hemorrhagic fever virus (CCHFV), Nairobi sheep disease virus, and Erve virus] [39], arteriviruses [e.g. equine arteritis virus (EAV) and porcine reproductive and respiratory syndrome virus] [39], picornaviruses (e.g. foot and mouth disease virus) [40], and coronaviruses [e.g. severe acute respiratory syndrome-related coronavirus (SARS-CoV), Middle East respiratory syndrome-related coronavirus (MERS-CoV), and mouse hepatitis virus] [41]. These cysteine proteases typically also possess substantial activity in reversing Ub conjugation and thus are often referred to as viral deubiquitinating proteins (DUBs). These DUBs are generally classified as ovarian tumor domain proteases (OTUs), papain-like proteases (PLPs), or leader proteases (Lb^{pro}) with some overlap in the descriptions. Although viral proteins are a primary target of ISGylation and thus a natural target for deISGylating activity, it is equally likely that viral DUBs counter ISGylation of host proteins to disrupt immune regulation. Nairovirus OTUs are one of the better characterized viral DUB families with a total of 12 x-ray crystal structures solved, including three OTU–ISG15 complex structures. OTU activity has been associated with immune suppression and reduction in ISG15 conjugates [42–44]. In addition, a recent study has tentatively associated the deISGylase activity of nairovirus OTUs with higher levels of the L protein in CCHFV [43]. Coronavirus PLPs have also been studied relatively extensively at the molecular and cellular level. This includes five PLP-ISG15 complex structures. The SARS-CoV PLP was among the first viral DUBs to be recognized as possessing deISGylase

activity and has been associated with the reduction of ISG15 conjugates and enhanced immune suppression [41,44,45]. Similar effects were observed in the more recently emergent MERS-CoV, suggesting an association between coronavirus pathogenicity and the presence of strong deISGylating activity [46]. Currently, the precise role for viral deISGylase activity is unknown, as no specific cellular targets have been firmly established. However, the fact that human pathogens like CCHFV, SARS-CoV, and MERS-CoV all possess robust deISGylase activity, which in the case of SARS-CoV exceeds its deubiquitinating activity, suggests that it may have an important function [45–47]. In addition to the more extensively studied nairovirus OTUs and coronavirus PLPs, deISGylating activity has also been observed in arterivirus OTU-like PLPs, EAV PLP2, and the porcine reproductive and respiratory syndrome virus PLP2 [42,48–52]. Picornavirus Lb^{pro}s also possess deISGylating activity, and for foot and mouse disease virus this is the most prominent deconjugating activity [40]. Overall, the widespread occurrence of viral proteins targeting ISG15 conjugation suggests that the ISG15-virus interface is a major factor impacting the balance between host responses and viral countermeasures.

ISG15 possesses interspecies diversity that translates to variation in protein structure

In comparison to Ub and other Ubl proteins, the sequence diversity of ISG15 has long stood out as an intriguing feature. ISG15 consists of two Ubl domains bearing the characteristic β -grasp fold containing four β -sheets and single α -helix per domain. These two domains are connected by a polypeptide sequence described as a “hinge” [53] (Fig. 2.2). ISG15 ultimately terminates with the familiar LRLRGG sequence, also found in Ub,

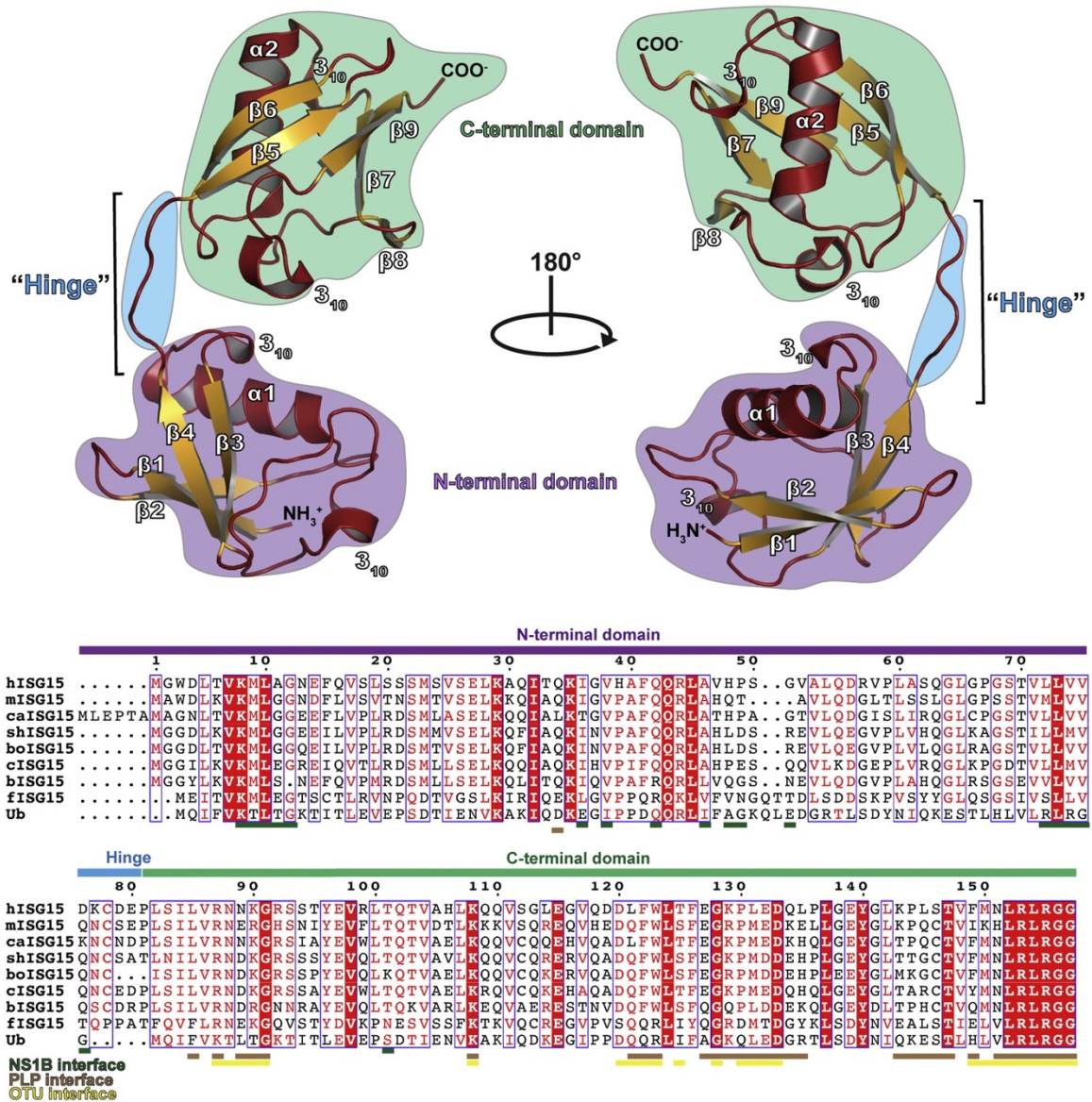


Fig. 2.2. Structure of human ISG15 (PDB entry 1Z2M). The secondary structure is denoted with helices and loops shown in red and sheets shown in gold. The C-terminal domain is denoted by a green background, hinge region by a blue background, and the N-terminal domain by a purple background. A sequence alignment of human ISG15 (hISG15), mouse ISG15 (mISG15), canine ISG15 (caISG15), sheep ISG15 (shISG15), bovine ISG15 (boISG15), camel ISG15 (cISG15), vesper bat ISG15 (bISG15), fish ISG15 (fISG15), and Ub is shown with the domain architecture indicated with colored bars. The residues of ISG15 known to interact with the influenza B NS1 protein, coronavirus PLPs, and nairovirus OTUs are indicated. The sequence alignment graphic was generated using the ESPrnt server [54].

that is critical for conjugation to proteins as a posttranslational modification. Beyond the C-terminus and other select regions of the protein, however, ISG15 shows substantial sequence variation (Fig. 2.2). In the most extreme cases, such as between some mammalian and fish species, ISG15s can share sequence identities of just 30%-35%. Even between two different mammals, the sequence identities can be less than 60%. Although substantial, this marked variance is not entirely unexpected, as it would be in keeping with ISG15's function as an immune molecule [55]. Related to this, it has been suggested that only certain features of ISG15, such as those driving the Ubl folds and interactions with proteins in the conjugation system, need to be conserved in order to serve its functions [56]. The cross-species compatibility of ISG15 enzymes is generally consistent with this idea [57,58] and may account for the higher degree of sequence variability in ISG15 compared to its interactive partners in the conjugation system. Other observations, however, suggest a more nuanced picture and that sequence diversity could have functional implications. Pattyn and coworkers [57] reported that ISG15 from Old World monkeys demonstrated a higher degree of ISGylation in human and mouse cells compared to the native ISG15s. Mapping of the differences within the predicted interface with the E1 enzyme Ube1L revealed the causal residues mediating this effect. Interestingly, some of the positions with the most influence possessed highly similar residues, such as an asparagine *versus* aspartate at position 89, demonstrating that even subtle differences may contribute to species-species differences. Whether the differences in ISGylation efficiency are meaningful in the context of a viral infection remains to be determined. It conceptually lends possible credence, however, to the suggested mechanism for the differences in the effects of ISG15 on USP18 in humans versus mice [30]. Human ISG15 was observed to bind more strongly

to USP18 compared to mouse ISG15, accounting for the protection of USP18 from degradation in human cells. The sequence divergence of ISG15 and USP18 between humans and mice led the authors to suggest that this may lie at the root of this difference in function. While a crystal structure of mouse USP18–ISG15 has been utilized to account for the specificity of ISG15 over Ub, analyses have yet to be performed that clearly determine the cause for the differences in USP18–ISG15 interactions between humans and mice [59,60].

Beyond the effect of species variance within potential protein–protein interfaces, evidence has been accumulating suggesting that ISG15 sequence diversity impacts the tertiary structure, particularly the orientation of the two Ubl domains relative to each other (Fig. 2.3a). Prior to 2017, the only full-length structure of ISG15 available was human. This included crystal structures of the ISG15 by itself and in complex with viral proteins, including the NS1 protein from Influenza B and the OTU from CCHFV [53,61–63]. Although present in different biochemical and crystallographic environments, the ISG15 molecules in these structures showed a remarkable degree of consistency in the orientation of the Ubl domains. From this alone, it would be natural to assume that all ISG15s possess similar structural characteristics. Structures of mouse ISG15 crystallized alone and in complex with USP18, however, revealed this to not be the case [59,64]. These structures revealed a wide variability in the interdomain arrangement of both individual mouse ISG15 molecules and in comparison to the human ISG15 structures. Examination of the interface between the two domains uncovered specific points of divergence in mouse *versus* human ISG15 that may account for the differences observed in the structures. In particular, at residue position 39 human ISG15 possesses a histidine, in contrast to proline for most other

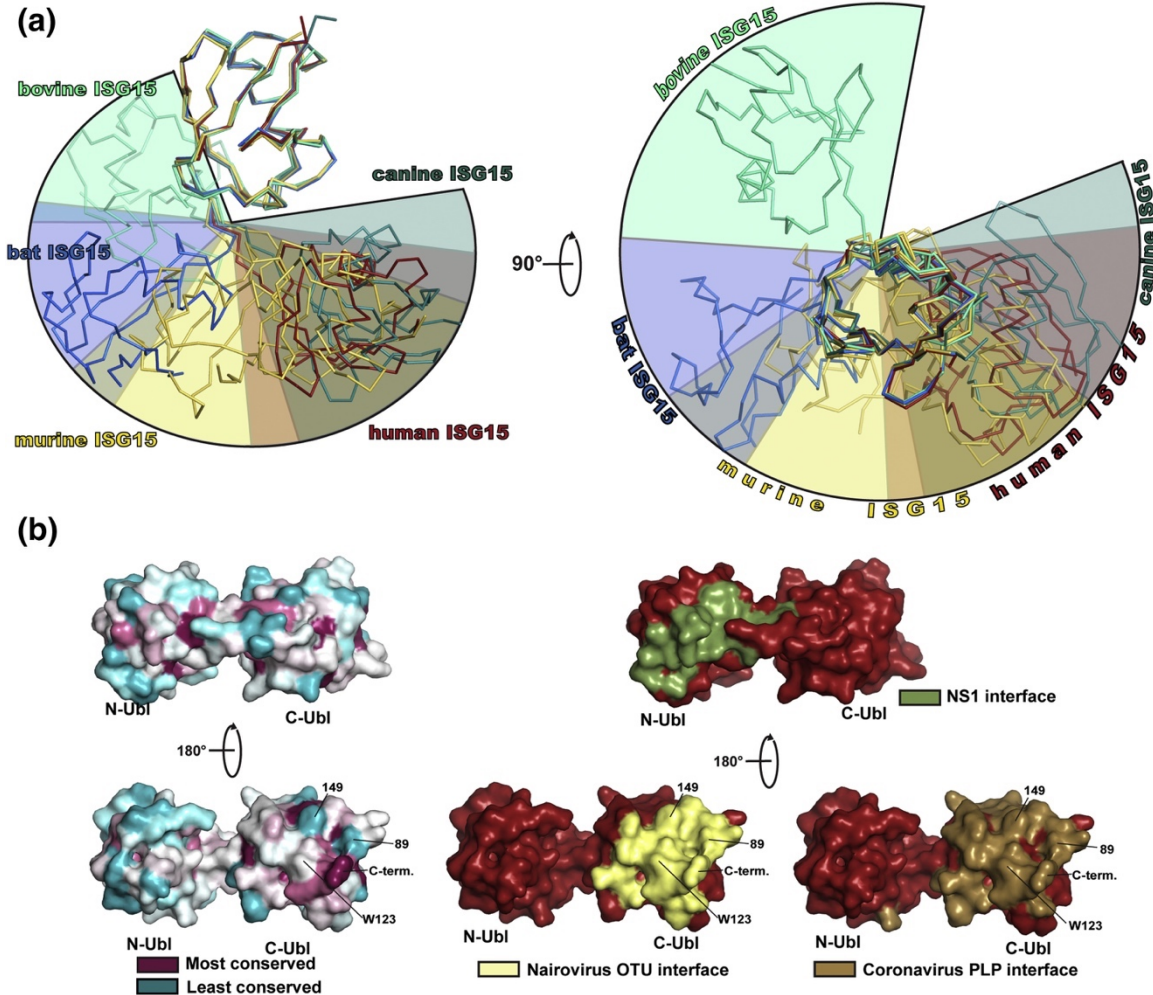


Fig. 2.3. ISG15 structural diversity. (a) The C-terminal domains of ISG15 chains from human ISG15 (red, [53,61–63] and PDB entries 3R66 and 6BI8), murine ISG15 (gold, [59,64,65] and PDB entries 5CHF and 5CHW), bat ISG15 (blue, [66]), bovine ISG15 (cyan green, [65]), and canine ISG15 (dark teal, [65]) were overlaid to identify the trends in domain–domain orientations between species. Representative chains were selected for each species. For murine ISG15, two structures were included to show the wider range of conformations that have been observed. Colored wedges show the approximate spatial range occupied by the N-terminal domain of ISG15 from each species. (b) Surface rendering of ISG15 showing the relative conservation among >100 species (left). Calculations and renderings were performed using the ConSurf server and PyMOL [67–71]. Surface of ISG15 known to interact with viral proteins based on x-ray crystal complex structures (right), with the interface with the influenza B NS1 protein shown in green, nairovirus OTU interface in yellow, and coronavirus PLP in brown. The template ISG15 structure for surface renderings was human ISG15 (PDB entry 1Z2M).

ISG15s, that may contribute steric and electrostatic factors limiting the conformations it is able to adopt [64]. Mouse ISG15, on the other hand, possesses a wider hydrophobic interface that is less constricting of the interdomain arrangement. This theme was further bolstered with the recently reported structure of vesper bat ISG15 that showed an even wider range of structural modes than previously observed [66]. It also revealed the central role of a highly conserved phenylalanine (Phe40/41) in the N-terminal domain in forming the interdomain contact regardless of the overall structure. Mutation of this residue diminished binding with the SARS-CoV PLP, which is known to interact with both Ubl domains of ISG15, showing this structure-stabilizing effect of the interdomain interface to be of biochemical importance. Beyond this direct domain–domain interaction, the vesper bat ISG15 structure also unveiled an underappreciated role of the hinge region in influencing tertiary structure. Specifically, the sequence composition of the hinge region in bat ISG15 allows it to form a type I reverse turn that is absent from human and mouse ISG15, possibly stabilizing the structural conformation. While this particular role of the hinge region is a novel observation, it is not the only example of species diversity in the hinge region having structural impact. Sorensen and colleagues [72] demonstrated that the lack of three residues within the hinge region of bovine ISG15 compared to sheep ISG15 contributed to the lower stability of bovine ISG15 in solution, potentially as a result of different spatial arrangement of the two Ubl domains. The recently reported crystal structure of bovine ISG15 bound to the Influenza B NS1 protein tentatively supports this conclusion, as the two Ubl domains are twisted in a completely different orientation compared to what has been observed in other ISG15s [65]. Solving the structure of the

highly similar sheep ISG15 would be valuable in validating the contribution of these hinge region residues to the tertiary structure.

Overall, the current structural evidence suggests that ISG15 species diversity influences tertiary structure characteristics. The primary drivers center around conserved residues forming a hydrophobic interface between the domains that permits an array of possible conformations, with other interdomain interactions and characteristics of the hinge region limiting the range of motion. Regrettably, limited information exists to determine the full structural dynamics of different ISG15s as the only full-length structures available were determined by x-ray crystallography. Although NMR assignments have been made for human ISG15, a complete structure has not been determined [73]. Further structural characterization would bring greater clarity. In addition, it remains to be seen what effects this could have within the ISGylation system of different species, and what magnitude of biochemical effects are needed to observe cellular ones. While the N-terminal Ubl domain of ISG15 has been shown to influence ISG15 conjugation, it is not clear how it contributes to this and whether variability in preferred ISG15 interdomain arrangements would influence it [57,74]. Furthermore, it is unclear what degree of difference in the efficiency of ISGylation would be necessary to have a biological impact. Additional work will be needed in order to address these questions.

ISG15 sequence and structural diversity impacts virus protein–protein interactions

Although it appears that ISG15 diversity may affect cellular proteins involved in the ISGylation/deISGylation system, the impact of ISG15 interspecies differences on endogenous proteins and processes still remains ambiguous. In contrast, ISG15 sequence diversity has been shown to unequivocally affect the countermeasures some viruses have

mounted against it. The most well-studied case remains the first characterized example of viral protein ISG15 species specificity with the Influenza B NS1 protein. Influenza B has a narrow host tropism, with humans serving as one of the primary hosts. The observation that the NS1B protein was able to more efficiently bind human and non-human primate ISG15 compared to other species' ISG15, such as mouse, canine and bovine, suggested that it could be a major factor in determining host susceptibility [58,75,76]. Studies utilizing mutagenesis and structural approaches were able to map the determinant interactions for strong binding to the N-terminal Ubl domain and hinge region of ISG15 (Fig. 2.2, Fig. 2.3b) [58,62,63,65,76]. Mutations to key residues within the hinge region alone are sufficient to drastically impact the binding [65,76]. Exchanging two residues in human ISG15 with the corresponding ones in murine, canine, and bovine ISG15 reduced binding to levels comparable with each of those species. Conversely, the opposite exchange increased the binding of murine, canine, and bovine ISG15 to similar levels as human ISG15. This provides a molecular mechanism that can account for the different cellular phenotypes observed in response to influenza B infection in different species and indicates that the hinge may be the primary driver of species specificity for NS1B.

Although Influenza B via the NS1 protein is the best-characterized example of a virus affected by ISG15 interspecies diversity, recent studies indicate that the impact may extend to other viruses. Nairovirus OTUs have been observed to interact with ISG15s from different species to different degrees *in vitro* [77,78]. Comparison between crystal structures of the Erve virus OTU bound to the C-terminal Ubl domain of mouse ISG15 and the OTU of CCHFV bound to human ISG15 provided insights into the possible contributing factors to these differences. This highlighted four residues (residue positions

89 and 149–151 in human ISG15) that show a high variability among ISG15s [78]. Interestingly, position 150 is not within the direct binding interface. Instead, the difference in this position between human and mouse ISG15, methionine and lysine, respectively, influences the orientation of the residue present in position 89, illustrating that factors beneath the protein surface can impact the binding interface with viral OTUs. In a similar vein, coronavirus PLPs were demonstrated to possess substantial variation in their ability to interact with different ISG15s [64]. Importantly, it also reflected differences in the known breadth of host ranges between different coronaviruses. The PLP2 from mouse hepatitis virus, which primarily infects mice, showed essentially no activity for some ISG15s (including human) while possessing robust activity for mouse ISG15. In contrast, the PLPs from SARS-CoV and MERS-CoV, which are known to have a wider host range, were somewhat promiscuous deISGylases. In addition to these substrate specificity trends, crystal structures of the SARS-CoV PLP bound to the C-terminal Ubl domains of human and mouse ISG15 revealed novel insights into how interspecies sequence diversity influences the nature of enzyme substrate binding. Surprisingly, mouse ISG15 bound in an orientation shifted 27° compared to human ISG15, with corresponding shifts in the protease structure to accommodate it. Coupling the structural analysis with isothermal titration calorimetry data revealed that the C-terminal Ubl domain of mouse ISG15 contained less optimal elements for protease binding, and that the N-terminal Ubl domain contributed substantially more to binding when compared to human ISG15. While the regions of SARS-CoV PLP that interact with both domains of ISG15 are known, it remains to be determined what portion(s) of the N-terminal Ubl domain of ISG15s is involved in this interaction and how potential differences in the domain–domain orientation impact the

interface [45,64,79]. Interestingly, similar analyses with the MERS-CoV PLP revealed it to interact solely with the C-terminal Ubl domain, indicating that the driving factors for interaction may not be universal even within a family of viruses [80].

Altogether, a picture is emerging of ISG15 sequence and structural diversity impacting the ability of viruses to counteract its effects. In the case of Influenza B, these differences could be highly influential in determining host tropism. For other viruses affected by ISG15 species diversity, including nairoviruses and coronaviruses, it remains to be determined what the threshold of difference may be in order to observe host-specific effects. The fact that various viruses interact with different portions of the ISG15 molecule opens the possibility that most, or all, of the ISG15 surface could be targeted by viral proteins. Thus, in addition to there being host-specific effects due to ISG15 diversity, the potential also exists for diverse and virus-specific mechanisms to disrupting ISG15 function. Further complicating these is the potential that, as in the case of humans compared to mice, ISG15 from different species may not necessarily play analogous roles. Differences in the relative importance of ISG15 between species could raise the importance of other IFN antagonists and produce unique relationships at each virus–host interface.

Current outlook and challenges to evaluating the specific effects of ISG15

While the effects and function of ISG15 are slowly emerging, many details remain to be determined regarding the mechanism of its action. Although ISG15 and ISGylation knockouts have been key to establishing the basic modes of action against several viruses, more nuanced methods may be necessary to fully grasp ISG15 function and viral countermeasures. One approach consists in specifically attenuating the action of ISG15-interacting viral proteins and assessing the activity using mutant viruses. Beyond the

technical hurdles associated with developing reverse genetics systems required to modify the viral genomes, another challenging aspect to achieving this lies in the fact that viruses often encode multiple protein antagonists targeting the innate immune responses at multiple levels. This complicates the study to identify individual contribution of each protein, especially when they have redundant or overlapping functions. Therefore, the function of an individual viral protein, or domain thereof, is often studied in biochemical assays using purified forms, allowing insight into mechanistic details that can complement studies using mutant recombinant viruses and their pathogenic role *in vivo*. In addition to the challenges of distinguishing between the individual contributions of different immune antagonists, the multifunctional nature of many viral proteases can make it difficult even within a single protein to selectively influence one interaction it displays over others. For example, viral deISGylating enzymes such as OTUs and PLPs often possess substantial deubiquitinating activity and in some cases play a critical role in virus polyprotein processing required for polymerase maturation. Due to such critical roles in the viral life cycle, elucidating the function cannot rely on simply deleting the protease from the genome or removing its baseline catalytic activity, and must instead rely on specific reduction in the ability to interact with Ub and/or ISG15. While this presents a challenging task, several encouraging advancements have been made recently that indicate this to be a feasible approach. A reverse genetics system for EAV was successfully developed with structure-guided OTU mutants that reduced deubiquitinating activity while leaving the proteolytic function unperturbed [42]. This study was able to show the impact of the loss on the ability of EAV to block the expression of IFN- β in cellular systems. Further work was able to successfully apply these mutants to *in vivo* assessment in shetland mares as a possible

vaccine candidate [81]. This provided protection against EAV infection and demonstrated the feasibility of creating viable DUB-deficient mutant recombinant viruses as vaccine candidates, though under the conditions studied it could not be established that this provided greater benefit compared to wild-type virus. Another recent achievement demonstrated a similar decoupling of activity with PLP mutants in a SARS-CoV reverse genetics system, also providing key insights into virus immune suppression and pathogenesis [44]. Regrettably, these studies focused solely on the effect of these mutants on ubiquitination. It would be interesting to revisit these mutants to assess whether they have any impairment in deISGylase activity, or possibly pursue additional ones that might provide insight into the impact of ISGylation for these viruses. Currently, the only reverse genetics system that has been utilized to investigate the impact on ISGylation is for CCHFV [43,82]. This was able to substantiate different effects that were mediated by ubiquitination *versus* ISGylation in the context of a nairovirus infection by comparing a mutant lacking both Ub and ISG15 activity with one deficient in only Ub activity. Unfortunately, current insights are limited by the lack of a deISGylase-specific OTU mutant, as the most promising candidates to date have also yielded an impairment in deubiquitinase activity [43,61,83]. Similar difficulty has been encountered with the SARS-CoV PLP, with mutants typically exhibiting a moderate effect or substantially impacting both Ub and ISG15 activities [64,79]. Recently, however, Daczkowski and co-workers [80] were able to perform structure-guided mutagenesis to selectively reduce *in vitro* deISGylase activity of the MERS-CoV PLP without appreciably impacting the other enzymatic functions. Application of these mutants to cellular and *in vivo* assays would

provide novel insights into the relative importance of ISGylation in combatting coronavirus infection.

The nonconserved nature of ISG15 remains another challenge. Apart from specific examples of how this impacts innate immunity and virus–host interactions, we still have a poor understanding of the full influence of this diversity. Much work remains to ascertain the functional drivers of ISG15 variability and how this impacts its role between species. Until there is a good grasp of these aspects, each ISG15 species will have to be tested separately to evaluate the nuances in function. This may ultimately reveal whether there are lineage-specific characteristics or motifs in ISG15 that serve as the primary drivers in dictating its function.

Potential applications to leverage ISG15 interspecies diversity

Although ISG15's genetic diversity has created challenges to elucidating its function, this same feature may also present the opportunity to leverage it for biomedical purposes. Classical biosurveillance methods rely on a laborious process of sample acquisition and testing that can be time-consuming and expensive. Knowledge of how ISG15 interspecies diversity impacts viral protein interactions could expedite this process. In the case of emerging or re-emerging viruses that possess ISG15-interacting proteins, *in vitro* assays could be performed in a medium- to high-throughput manner to determine the relative preference for different species' ISG15s. This would guide a more targeted approach in the field for those species most likely to be susceptible to the virus. In an age of increasingly available genomic data, the utility of such a methodology will only grow over time. As more becomes known on the features of ISG15 that are most influential for

particular families of viruses, this also lends itself to computational approaches to predict interactions *in silico*.

In addition to the identification of competent hosts in the present, ISG15 genetic diversity could provide insight into long-term trends in virus evolution. Although cell entry is the first step to virus infection and a predominant factor governing virus tropism, intracellular factors also play a role, and over time a virus will naturally become adapted to these components of the host immune system. If a virus has moved to a different host, it is possible it may retain some of the features for optimization with the prior host. Thus, although ISG15 may not be a primary determining factor for all viruses, it could serve as a tracer for the natural history of the virus. Adding to the value of ISG15 in such a probe is the fact that viruses in the same family possess the same repertoire of potential ISG15-interacting proteins, likely creating a common interface for comparison. While viruses in the same family sometimes utilize different cell-surface receptors, ISG15 may present a consistent point of interaction that makes it ideal for tracing a virus's evolutionary past. Alternatively, interspecies ISG15 diversity may have predictive value regarding the potential hosts to which the virus could most easily adapt. For example, MERS-CoV is unable to infect mouse cells due to an inability to interact with the mouse DPP4 receptor. Exogenous or transgenic expression of the human DPP4 receptor results in successful infection that after serially passaging can produce mouse-adapted pathogenic strains [84–86]. Interestingly, non-adapted MERS-CoV PLP is already able to interact with mouse ISG15, and while some of the mutations generated in the mouse-adapted strains are present in the nsp3 protein, none of them map to the PLP domain [64,85–87]. Looking at the residues of ISG15 that PLPs are known to engage reveals that there is a mix of conserved

and variable features with which the PLP interacts (Fig. 2.3b). This includes, for example, Trp123 that is highly conserved among mammals, and the almost perfectly conserved C-terminal tail. However, there are also notable areas of variation, particularly at positions 89 and 149, that the PLP must be able to accommodate. While the conserved regions may provide a platform for interaction with mammalian ISG15s in general, these other less conserved regions can markedly influence how well the PLP engages specific species' ISG15 [64]. This is reflected in the relatively broad, but not universal activity of the PLP for different ISG15 species. For example, although bat, camel, and human ISG15 only share 62%-66% sequence identity to each other, they all show susceptibility to the MERS-CoV PLP as would be consistent with the virus's known and predicted host range. For other species, including sheep, shrews, and fish that are not predicted to be hosts for the virus, the activity is noticeably lower suggesting the need to accommodate specific sequence variations. Considering this, the combination of the PLP's ability to interact with mouse ISG15 and the lack of mutations in the PLP of mouse-adapted strains suggests that the MERS-CoV, in a sense, may have been partially “pre-adapted” to mice as potential hosts, and that overcoming the threshold of cell entry was all that was required to replicate and eventually fully adapt. It would be interesting to apply this reasoning to other systems to ascertain its predictive value. Such knowledge could aid in understanding the risk posed by a particular virus during the course of genetic drift, as well as inform the design of appropriate model systems of disease.

Beyond surveillance and research applications, the features of ISG15 diversity also raise questions regarding its potential for direct therapeutic use. Could a modified ISG15, or one from a different species, be used to combat viral infection? Given the central place

of ISGylation in antiviral mechanisms, such a strategy would rely on providing the conjugation machinery or assuming cross-species compatibility of the conjugation system enzymes. Though far from comprehensive, the current data suggests the latter to possibly be the case [57,58]. From this standpoint, it could be envisioned how some agriculturally important animals could be genetically engineered for ISG15 to enhance resistance to particular virus threats. Alternatively, perhaps ISG15, or an ISG15 gene, could be administered to transiently introduce a modified or different species version of ISG15 to combat acute viral infection. Further work will be needed to assess the potential of these intriguing possibilities.

Conclusion

ISG15 is an influential component in mediating and regulating host responses to viral infection. Study of its form and function has yielded several surprises, and many aspects remain to be fully comprehended. Grasping its roles has proven elusive due to diverse mechanisms of action that can vary in importance between different pathogens, and possibly even between different host species. The sequence and structural diversity of ISG15 adds an additional layer to this complexity, particularly in how it impacts virus–host interfaces. Although much remains to be known, the tools and knowledge base needed to probe these questions have begun to come together, presenting exciting and unprecedented opportunities to understand and leverage ISG15 function.

Acknowledgments

This work was supported by the National Institutes of Health application number 1R01AI109008 (to S.D.P. and E.B.). The findings and conclusions in this report are those of the authors and do not necessarily represent the official position of the Centers for

Disease Control and Prevention. The authors thank Xinquan Wang and Yinan Jiang for sharing the structure coordinates for the NS1B-bound murine ISG15, canine ISG15, and bovine ISG15 structures in advance of PDB deposition.

References

- [1] M. Liu, R. Reimschuessel, B.A. Hassel, Molecular cloning of the fish interferon stimulated gene, 15 kDa (ISG15) orthologue: a ubiquitin-like gene induced by nephrotoxic damage, *Gene*. 298 (2002) 129–139. <http://www.ncbi.nlm.nih.gov/pubmed/12426101>.
- [2] R. Mahajan, C. Delphin, T. Guan, L. Gerace, F. Melchior, A small ubiquitin-related polypeptide involved in targeting RanGAP1 to nuclear pore complex Protein RanBP2, *Cell*. 88 (1997) 97–107. doi:10.1016/S0092-8674(00)81862-0.
- [3] M.J. Matunis, E. Coutavas, G. Blobel, A novel ubiquitin-like modification modulates the partitioning of the Ran-GTPase-activating protein RanGAP1 between the cytosol and the nuclear pore complex., *J. Cell Biol.* 135 (1996) 1457–1470. <http://www.ncbi.nlm.nih.gov/pubmed/8978815>.
- [4] T. Kamitani, K. Kito, H.P. Nguyen, E.T. Yeh, Characterization of NEDD8, a developmentally down-regulated ubiquitin-like protein., *J. Biol. Chem.* 272 (1997) 28557–28562. <http://www.ncbi.nlm.nih.gov/pubmed/9353319>.
- [5] S. Kumar, Y. Tomooka, M. Noda, Identification of a set of genes with developmentally down-regulated expression in the mouse brain, *Biochem. Biophys. Res. Commun.* 185 (1992) 1155–1161. doi:10.1016/0006-291X(92)91747-E.
- [6] E.E.M. Bates, O. Ravel, M.-C. Dieu, S. Ho, C. Guret, J.-M. Bridon, S. Ait-Yahia, F. Brière, C. Caux, J. Banchereau, S. Lebecque, Identification and analysis of a novel member of the ubiquitin family expressed in dendritic cells and mature B cells, *Eur. J. Immunol.* 27 (1997) 2471–2477. doi:10.1002/eji.1830271002.
- [7] J.R. Gruen, S.R. Nalabolu, T.W. Chu, C. Bowlus, W.F. Fan, V.L. Goei, H. Wei, R. Sivakamasundari, Y. Liu, H.X. Xu, S. Parimoo, G. Nallur, R. Ajioka, H. Shukla, P. Bray-Ward, J. Pan, S.M. Weissman, A transcription map of the major histocompatibility complex (MHC) class I region., *Genomics*. 36 (1996) 70–85. <http://www.ncbi.nlm.nih.gov/pubmed/8812418>.
- [8] W. Fan, W. Cai, S. Parimoo, D.C. Schwarz, G.G. Lennon, S.M. Weissman, Identification of seven new human MHC class I region genes around the HLA-F locus., *Immunogenetics*. 44 (1996) 97–103. <http://www.ncbi.nlm.nih.gov/pubmed/8662070>.
- [9] Y.C. Liu, J. Pan, C. Zhang, W. Fan, M. Collinge, J.R. Bender, S.M. Weissman, A MHC-encoded ubiquitin-like protein (FAT10) binds noncovalently to the

spindle assembly checkpoint protein MAD2., *Proc. Natl. Acad. Sci. U. S. A.* 96 (1999) 4313–4318. <http://www.ncbi.nlm.nih.gov/pubmed/10200259>.

[10] P.J. Farrell, R.J. Broeze, P. Lengyel, P. Farrell, Paul J., Broeze, Robert J., Lengyel, Accumulation of an mRNA and protein in interferon-treated Ehrlich ascites tumour cells, *Nature*. 279 (1979) 523–525.

[11] A.L. Haas, P. Ahrens, P.M. Bright, H. Ankel, Interferon induces a 15-kilodalton protein exhibiting marked homology to ubiquitin, *J. Biol. Chem.* 262 (1987) 11315–11323. <https://www.ncbi.nlm.nih.gov/pubmed/2440890>.

[12] D.S. Kessler, D.E. Levy, J.E. Darnell, Two interferon-induced nuclear factors bind a single promoter element in interferon-stimulated genes, *Proc. Natl. Acad. Sci. U. S. A.* 85 (1988) 8521–8525.

[13] N. Reich, B. Evans, D. Levy, D. Fahey, E. Knight Jr., J.E. Darnell Jr., Interferon-induced transcription of a gene encoding a 15-kDa protein depends on an upstream enhancer element, *Proc. Natl. Acad. Sci. U. S. A.* 84 (1987) 6394–6398. <https://www.ncbi.nlm.nih.gov/pubmed/3476954>.

[14] D.J. Morales, D.J. Lenschow, The antiviral activities of ISG15, *J. Mol. Biol.* (2013) 1–14.

[15] M.P. Malakhov, O.A. Malakhova, K.I. Kim, K.J. Ritchie, D.E. Zhang, UBP43 (USP18) specifically removes ISG15 from conjugated proteins, *J. Biol. Chem.* 277 (2002) 9976–9981. doi:10.1074/jbc.M109078200.

[16] L.A. Durfee, N. Lyon, K. Seo, J.M. Huibregtse, and J.M.H. Durfee, Larissa A., Nancy Lyon, Kyungwoon Seo, The ISG15 conjugation system broadly targets newly synthesized proteins: implications for the antiviral function of ISG15, *Mol. Cell.* 38 (2010) 722–732. doi:10.1016/j.molcel.2010.05.002.

[17] M.P. Malakhov, K.I. Kim, O.A. Malakhova, B.S. Jacobs, E.C. Borden, D.E. Zhang, High-throughput immunoblotting. Ubiquitin-like protein ISG15 modifies key regulators of signal transduction, *J. Biol. Chem.* 278 (2003) 16608–16613. doi:10.1074/jbc.M208435200.

[18] T. Takeuchi, S. Inoue, H. Yokosawa, Identification and Herc5-mediated ISGylation of novel target proteins, *Biochem. Biophys. Res. Commun.* 348 (2006) 473–477. doi:10.1016/j.bbrc.2006.07.076.

[19] C. Zhao, C. Denison, J.M. Huibregtse, S. Gygi, R.M. Krug, Human ISG15 conjugation targets both IFN-induced and constitutively expressed proteins functioning in diverse cellular pathways., *Proc. Natl. Acad. Sci. U. S. A.* 102 (2005) 10200–10205.

[20] N.V. Giannakopoulos, J.-K. Luo, V. Papov, W. Zou, D.J. Lenschow, B.S. Jacobs, E.C. Borden, J. Li, H.W. Virgin, D.-E. Zhang, Proteomic identification of proteins

conjugated to ISG15 in mouse and human cells., *Biochem. Biophys. Res. Commun.* 336 (2005) 496–506. doi:10.1016/j.bbrc.2005.08.132.

[21] J.J. Wong, Y.F. Pung, N.S. Sze, K.C. Chin, HERC5 is an IFN-induced HECT-type E3 protein ligase that mediates type I IFN-induced ISGylation of protein targets, *Proc. Natl. Acad. Sci. U. S. A.* 103 (2006) 10735–10740. doi:10.1073/pnas.0600397103.

[22] Y. Tang, G. Zhong, L. Zhu, X. Liu, Y. Shan, H. Feng, Z. Bu, H. Chen, C. Wang, Herc5 attenuates influenza A virus by catalyzing ISGylation of viral NS1 protein., *J. Immunol.* 184 (2010) 5777–5790.

[23] M. Ganesan, L.Y. Poluektova, D.J. Tuma, K.K. Kharbanda, N.A. Osna, Acetaldehyde disrupts interferon alpha signaling in hepatitis C virus-infected liver cells by up-regulating USP18., *Alcohol. Clin. Exp. Res.* 40 (2016) 2329–2338. doi:10.1111/acer.13226.

[24] H.X. Shi, K. Yang, X. Liu, X.Y. Liu, B. Wei, Y.F. Shan, L.H. Zhu, C. Wang, Positive regulation of interferon regulatory factor 3 activation by Herc5 via ISG15 modification, *Mol. Cell. Biol.* 30 (2010) 2424–2436. doi:10.1128/MCB.01466-09.

[25] M.-J. Kim, S.-Y. Hwang, T. Imaizumi, J.-Y. Yoo, Negative feedback regulation of RIG-I-mediated antiviral signaling by interferon-induced ISG15 conjugation., *J. Virol.* 82 (2008) 1474–1483.

[26] Y. Du, T. Duan, Y. Feng, Q. Liu, M. Lin, J. Cui, R. Wang, LRRC25 inhibits type I IFN signaling by targeting ISG15-associated RIG-I for autophagic degradation, *EMBO J.* (2017) e96781. doi:10.15252/embj.201796781.

[27] O.A. Malakhova, M. Yan, M.P. Malakhov, Y. Yuan, K.J. Ritchie, K. Il Kim, L.F. Peterson, K. Shuai, D.E. Zhang, Protein ISGylation modulates the JAK-STAT signaling pathway, *Genes Dev.* 17 (2003) 455–460. doi:10.1101/gad.1056303.

[28] K.I. Arimoto, S. Löchte, S.A. Stoner, C. Burkart, Y. Zhang, S. Miyauchi, S. Wilmes, J.-B.B. Fan, J.J. Heinisch, Z. Li, M. Yan, S. Pellegrini, F. Colland, J. Piehler, D.-E.E. Zhang, STAT2 is an essential adaptor in USP18-mediated suppression of type I interferon signaling, *Nat. Struct. Mol. Biol.* 24 (2017) 279–289. doi:10.1038/nsmb.3378.

[29] X. Zhang, D. Bogunovic, B. Payelle-Brogard, V. Francois-Newton, S.D. Speer, C. Yuan, S. Volpi, Z. Li, O. Sanal, D. Mansouri, I. Tezcan, G.I. Rice, C. Chen, N. Mansouri, S.A. Mahdavian, Y. Itan, B. Boisson, S. Okada, L. Zeng, X. Wang, H. Jiang, W. Liu, T. Han, D. Liu, T. Ma, B. Wang, M. Liu, J.-Y. Liu, Q.K. Wang, D. Yalnizoglu, L. Radoshevich, G. Uzé, P. Gros, F. Rozenberg, S.-Y. Zhang, E. Jouanguy, J. Bustamante, A. García-Sastre, L. Abel, P. Lebon, L.D. Notarangelo, Y.J. Crow, S. Boisson-Dupuis, J.-L. Casanova, S. Pellegrini, Human intracellular ISG15 prevents interferon- α/β over-amplification and auto-inflammation., *Nature.* 517 (2015) 89–93.

- [30] S.D. Speer, Z. Li, S. Buta, B. Payelle-Brogard, L. Qian, F. Vigant, E. Rubino, T.J. Gardner, T. Wedeking, M. Hermann, J. Duehr, O. Sanal, I. Tezcan, N. Mansouri, P. Tabarsi, D. Mansouri, V. Francois-Newton, C.F. Daussy, M.R. Rodriguez, D.J. Lenschow, A.N. Freiberg, D. Tortorella, J. Piehler, B. Lee, A. Garcia-Sastre, S. Pellegrini, D. Bogunovic, ISG15 deficiency and increased viral resistance in humans but not mice, *Nat. Commun.* 7 (2016) 11496. doi:10.1038/ncomms11496.
- [31] D. Bogunovic, M. Byun, L.A. Durfee, A. Abhyankar, O. Sanal, D. Mansouri, S. Salem, I. Radovanovic, A.V. Grant, P. Adimi, N. Mansouri, S. Okada, V.L. Bryant, X. Kong, A. Kreins, M.M. Velez, B. Boisson, S. Khalilzadeh, U. Ozcelik, I.A. Darazam, J.W. Schoggins, C.M. Rice, S. Al-muhsen, M. Behr, G. Vogt, A. Puel, J. Bustamante, P. Gros, J.M. Huibregtse, Mycobacterial disease and impaired IFN- γ immunity in humans with inherited ISG15 deficiency, *Science* (80-.). 2 (2012) 1684–1689.
- [32] J. D'Cunha, S. Ramanujam, R.J. Wagner, P.L. Witt, E. Knight Jr., E.C. Borden, In vitro and in vivo secretion of human ISG15, an IFN-induced immunomodulatory cytokine, *J. Immunol.* 157 (1996) 4100–4108. <https://www.ncbi.nlm.nih.gov/pubmed/8892645>.
- [33] E. Knight Jr., B. Cordova, IFN-induced 15-kDa protein is released from human lymphocytes and monocytes, *J. Immunol.* 146 (1991) 2280–2284. <https://www.ncbi.nlm.nih.gov/pubmed/2005397>.
- [34] M. Recht, E.C. Borden, E. Knight Jr., A human 15-kDa IFN-induced protein induces the secretion of IFN-gamma, *J. Immunol.* 147 (1991) 2617–2623. <https://www.ncbi.nlm.nih.gov/pubmed/1717569>.
- [35] C.D. Swaim, A.F. Scott, L.A. Canadeo, J.M. Huibregtse, Extracellular ISG15 signals cytokine secretion through the LFA-1 integrin receptor, *Mol. Cell* 68 (2017) 581–590.e5. doi:10.1016/j.molcel.2017.10.003.
- [36] J. D'Cunha, E. Knight Jr., A.L. Haas, R.L. Truitt, E.C. Borden, Immunoregulatory properties of ISG15, an interferon-induced cytokine, *Proc. Natl. Acad. Sci. U. S. A.* 93 (1996) 211–215. <https://www.ncbi.nlm.nih.gov/pubmed/8552607>.
- [37] A. Rahnefeld, K. Klingel, A. Schuermann, N.L. Diny, N. Althof, A. Lindner, P. Bleienheuft, K. Savvatis, D. Respondek, E. Opitz, L. Ketscher, M. Sauter, U. Seifert, C. Tschöpe, W. Poller, K.-P. Knobeloch, A. Voigt, Ubiquitin-like protein ISG15 (interferon-stimulated gene of 15 kDa) in host defense against heart failure in a mouse model of virus-induced cardiomyopathy., *Circulation.* 130 (2014) 1589–600. doi:10.1161/CIRCULATIONAHA.114.009847.
- [38] C. Zhao, H. Sridharan, R. Chen, D.P. Baker, S. Wang, R.M. Krug, K.R. Loeb, A.L. Haas, H. Sridharan, C. Zhao, R.M. Krug, B. Skaug, Z.J. Chen, M.P. Malakhov, O.A. Malakhova, K.I. Kim, K.J. Ritchie, D.E. Zhang, C. Zhao, M.N. Collins, T.Y. Hsiang, R.M. Krug, W. Yuan, R.M. Krug, S. Guerra, A. Caceres, K.P. Knobeloch, I. Horak, M. Esteban, N. Frias-Staheli, D.J. Lenschow, C. Lai, D.J. Morales, T.Y. Hsiang, C. Zhao, R.M. Krug, C. Zhao, T.Y. Hsiang, R.L. Kuo, R.M. Krug, Y. Tang, L.A. Durfee, N. Lyon, K.

Seo, J.M. Huibregtse, S.W. Werneke, D. Bogunovic, X. Zhang, O.A. Malakhova, S.D. Speer, G.A. Versteeg, R. Guan, A.K. Ng, L. Sherry, M. Smith, S. Davidson, D. Jackson, L. Ketscher, A.J. Einfeld, G. Neumann, Y. Kawaoka, S. Reich, W. Zheng, Y.J. Tao, Q. Ye, R.M. Krug, Y.J. Tao, A. Mondal, G.K. Potts, A.R. Dawson, J.J. Coon, A. Mehle, L. Turrell, J.W. Lyall, L.S. Tiley, E. Fodor, F.T. Vreede, Y.F. Shen, J. Schneider, B. Dauber, K. Melen, I. Julkunen, T. Wolff, Q. Ye, E. Hoffmann, J. D’Cunha, E. Knight, A.L. Haas, R.L. Truitt, E.C. Borden, V.C. Huber, L.H. Kleimeyer, J.A. McCullers, E. Fodor, Influenza B virus non-structural protein 1 counteracts ISG15 antiviral activity by sequestering ISGylated viral proteins, *Nat. Commun.* 7 (2016) 12754. doi:10.1038/ncomms12754.

[39] N. Frias-Staheli, N.V. Giannakopoulos, M. Kikkert, S.L. Taylor, A. Bridgen, J. Paragas, J.A. Richt, R.R. Rowland, C.S. Schmaljohn, D.J. Lenschow, E.J. Snijder, A. García-Sastre, H.W. Virgin, Ovarian tumor domain-containing viral proteases evade ubiquitin- and ISG15-dependent innate immune responses., *Cell Host Microbe* 2 (2007) 404–416.

[40] K.N. Swatek, M. Aumayr, J.N. Pruneda, L.J. Visser, S. Berryman, A.F. Kueck, P.P. Geurink, H. Ovaa, F.J.M. van Kuppeveld, T.J. Tuthill, T. Skern, D. Komander, Irreversible inactivation of ISG15 by a viral leader protease enables alternative infection detection strategies, *Proc. Natl. Acad. Sci. U. S. A.* 115 (2018) 2371–2376. doi:10.1073/pnas.1710617115.

[41] H.A. Lindner, N. Fotouhi-Ardakani, V. Lytvyn, P. Lachance, T. Sulea, R. Ménard, The papain-like protease from the severe acute respiratory syndrome coronavirus is a deubiquitinating enzyme., *J. Virol.* 79 (2005) 15199–15208.

[42] P.B. van Kasteren, B.A. Bailey-Elkin, T.W. James, D.K. Ninaber, C. Beugeling, M. Khajehpour, E.J. Snijder, B.L. Mark, M. Kikkert, Deubiquitinase function of arterivirus papain-like protease 2 suppresses the innate immune response in infected host cells., *Proc. Natl. Acad. Sci. U. S. A.* 110 (2013) E838-E847. doi:10.1073/pnas.1218464110.

[43] F.E.M. Scholte, M. Zivcec, J.V. Dzimianski, M.K. Deaton, J.R. Spengler, S.R. Welch, S.T. Nichol, S.D. Pegan, C.F. Spiropoulou, É. Bergeron, Crimean-Congo hemorrhagic fever virus suppresses innate immune responses via a ubiquitin and ISG15 specific protease., *Cell Rep.* 20 (2017) 2396–2407. doi:10.1016/j.celrep.2017.08.040.

[44] D. Niemeyer, K. Mösbauer, E.M. Klein, A. Sieberg, R.C. Mettelman, A.M. Mielech, R. Dijkman, S.C. Baker, C. Drosten, M.A. Müller, The papain-like protease determines a virulence trait that varies among members of the SARS-coronavirus species., *PLoS Pathog.* 14 (2018) e1007296. doi:10.1371/journal.ppat.1007296.

[45] H.A. Lindner, V. Lytvyn, H. Qi, P. Lachance, E. Ziomek, R. Ménard, Selectivity in ISG15 and ubiquitin recognition by the SARS coronavirus papain-like protease., *Arch. Biochem. Biophys.* 466 (2007) 8–14. doi:10.1016/j.abb.2007.07.006.

- [46] A.M. Mielech, A. Kilianski, Y.M. Baez-Santos, A.D. Mesecar, S.C. Baker, MERS-CoV papain-like protease has deISGylating and deubiquitinating activities., *Virology*. 450–451 (2014) 64–70.
- [47] G.C. Capodagli, M.A. McKercher, E.A. Baker, E.M. Masters, J.S. Brunzelle, S.D. Pegan, Structural analysis of a viral ovarian tumor domain protease from the Crimean-Congo hemorrhagic fever virus in complex with covalently bonded ubiquitin, *J. Virol.* 85 (2011) 3621–3630. doi:10.1128/JVI.02496-10.
- [48] P.B. van Kasteren, C. Beugeling, D.K. Ninaber, N. Frias-Staheli, S. van Boheemen, A. Garcia-Sastre, E.J. Snijder, M. Kikkert, Arterivirus and nairovirus ovarian tumor domain-containing deubiquitinases target activated RIG-I to control innate immune signaling, *J. Virol.* 86 (2011) 773–785.
- [49] D. Patel, Y. Nan, M. Shen, K. Ritthipichai, X. Zhu, Y.-J. Zhang, Porcine reproductive and respiratory syndrome virus inhibits type I interferon signaling by blocking STAT1/STAT2 nuclear translocation., *J. Virol.* 84 (2010) 11045–11055.
- [50] Z. Sun, Y. Li, R. Ransburgh, E.J. Snijder, Y. Fang, Nonstructural protein 2 of porcine reproductive and respiratory syndrome virus inhibits the antiviral function of interferon-stimulated gene 15, *J. Virol.* 86 (2012) 3839–3850. doi:10.1128/JVI.06466-11.
- [51] M.K. Deaton, A. Spear, K.S. Faaberg, S.D. Pegan, The vOTU domain of highly-pathogenic porcine reproductive and respiratory syndrome virus displays a differential substrate preference, *Virology*. 454–455 (2014) 247–253. doi:10.1016/j.virol.2014.02.026.
- [52] S.M. Bester, C.M. Daczkowski, K.S. Faaberg, S.D. Pegan, Insights into the porcine reproductive and respiratory syndrome virus viral ovarian tumor domain protease specificity for ubiquitin and interferon stimulated gene product 15, *ACS Infect Dis.* 4 (2018) 1316–1326. doi:10.1021/acsinfecdis.8b00068.
- [53] J. Narasimhan, M. Wang, Z. Fu, J.M. Klein, A.L. Haas, J.J. Kim, Crystal structure of the interferon-induced ubiquitin-like protein ISG15, *J. Biol. Chem.* 280 (2005) 27356–27365. doi:10.1074/jbc.M502814200.
- [54] X. Robert, P. Gouet, Deciphering key features in protein structures with the new ENDscript server, *Nucleic Acids Res.* 42 (2014) W320–W324. doi:10.1093/nar/gku316.
- [55] A. Catic, E. Fiebigler, G.A. Korbel, D. Blom, P.J. Galardy, H.L. Ploegh, Screen for ISG15-crossreactive deubiquitinases, *PLoS One* 2 (2007) e679. doi:10.1371/journal.pone.0000679.
- [56] L.A. Durfee, M.L. Kelley, J.M. Huibregtse, The basis for selective E1-E2 interactions in the ISG15 conjugation system, *J. Biol. Chem.* 283 (2008) 23895–23902. doi:10.1074/jbc.M804069200.

- [57] E. Pattyn, A. Verhee, I. Uyttendaele, J. Piessevaux, E. Timmerman, K. Gevaert, J. Vandekerckhove, F. Peelman, J. Tavernier, HyperISGylation of Old World monkey ISG15 in human cells, *PLoS One* 3 (2008) e2427. doi:10.1371/journal.pone.0002427.
- [58] G.A. Versteeg, B.G. Hale, S. van Boheemen, T. Wolff, D.J. Lenschow, A. Garcia-Sastre, Species-specific antagonism of host ISGylation by the influenza B virus NS1 protein, *J. Virol.* 84 (2010) 5423–5430. doi:10.1128/JVI.02395-09.
- [59] A. Basters, P.P. Geurink, A. Rocker, K.F. Witting, R. Tadayon, S. Hess, M.S. Semrau, P. Storici, H. Ovaa, K.P. Knobloch, G. Fritz, Structural basis of the specificity of USP18 toward ISG15, *Nat. Struct. Mol. Biol.* 24 (2017) 270–278. doi:10.1038/nsmb.3371.
- [60] A. Basters, K.-P. Knobloch, G. Fritz, How USP18 deals with ISG15-modified proteins: structural basis for the specificity of the protease., *FEBS J.* 285 (2018) 1024–1029. doi:10.1111/febs.14260.
- [61] T.W. James, N. Frias-Staheli, J.-P. Bacik, J.M. Levingston Macleod, M. Khajehpour, A. García-Sastre, B.L. Mark, Structural basis for the removal of ubiquitin and interferon-stimulated gene 15 by a viral ovarian tumor domain-containing protease., *Proc. Natl. Acad. Sci. U. S. A.* 108 (2011) 2222–2227.
- [62] R. Guan, L.C. Ma, P.G. Leonard, B.R. Amer, H. Sridharan, C. Zhao, R.M. Krug, G.T. Montelione, Structural basis for the sequence-specific recognition of human ISG15 by the NS1 protein of influenza B virus, *Proc. Natl. Acad. Sci. U. S. A.* 108 (2011) 13468–13473. doi:10.1073/pnas.1107032108.
- [63] L. Li, D. Wang, Y. Jiang, J. Sun, S. Zhang, Y. Chen, X. Wang, Crystal structure of human ISG15 protein in complex with influenza B virus NS1B, *J. Biol. Chem.* 286 (2011) 30258–30262. doi:10.1074/jbc.C111.257899.
- [64] C.M. Daczkowski, J.V. Dzimianski, J.R. Clasman, O. Goodwin, A.D. Mesecar, S.D. Pegan, Structural insights into the interaction of coronavirus papain-like proteases and interferon-stimulated gene product 15 from different species, *J. Mol. Biol.* 429 (2017) 1661–1683. doi:10.1016/j.jmb.2017.04.011.
- [65] Y. Jiang, X. Wang, Structural insights into the species preference of the influenza B virus NS1 protein in ISG15 binding., *Protein Cell.* (2018). doi:10.1007/s13238-018-0598-4.
- [66] C. Langley, O. Goodwin, J.V. Dzimianski, C.M. Daczkowski, S.D. Pegan, Structure of interferon-stimulated gene product 15 (ISG15) from the bat species *Myotis davidii* and the impact of interdomain ISG15 interactions on viral protein engagement, *Acta Crystallogr. Sect. D Struct. Biol.* 75 (2019). doi:10.1107/S2059798318015322.
- [67] F. Glaser, T. Pupko, I. Paz, R.E. Bell, D. Bechor-Shental, E. Martz, N. Ben-Tal, ConSurf: identification of functional regions in proteins by surface-mapping of

phylogenetic information., *Bioinformatics*. 19 (2003) 163–164. <http://www.ncbi.nlm.nih.gov/pubmed/12499312>.

[68] M. Landau, I. Mayrose, Y. Rosenberg, F. Glaser, E. Martz, T. Pupko, N. Ben-Tal, ConSurf 2005: the projection of evolutionary conservation scores of residues on protein structures., *Nucleic Acids Res.* 33 (2005) W299-W302. doi:10.1093/nar/gki370.

[69] H. Ashkenazy, E. Erez, E. Martz, T. Pupko, N. Ben-Tal, ConSurf 2010: calculating evolutionary conservation in sequence and structure of proteins and nucleic acids., *Nucleic Acids Res.* 38 (2010) W529-33. doi:10.1093/nar/gkq399.

[70] G. Celniker, G. Nimrod, H. Ashkenazy, F. Glaser, E. Martz, I. Mayrose, T. Pupko, N. Ben-Tal, ConSurf: Using evolutionary data to raise testable hypotheses about protein function, *Isr. J. Chem.* 53 (2013) 199–206. doi:10.1002/ijch.201200096.

[71] H. Ashkenazy, S. Abadi, E. Martz, O. Chay, I. Mayrose, T. Pupko, N. Ben-Tal, ConSurf 2016: an improved methodology to estimate and visualize evolutionary conservation in macromolecules., *Nucleic Acids Res.* 44 (2016) W344-W350. doi:10.1093/nar/gkw408.

[72] C.M. Sorensen, L.A. Rempel, S.R. Nelson, B.R. Francis, D.J. Perry, R.V. Lewis, A.L. Haas, T.R. Hansen, The hinge region between two ubiquitin-like domains destabilizes recombinant ISG15 in solution, *Biochemistry*. 46 (2007) 772–780. doi:10.1021/bi061408x.

[73] C. Yin, J.M. Aramini, L.C. Ma, J.R. Cort, G.V. Swapna, R.M. Krug, G.T. Montelione, Backbone and Ile-delta1, Leu, Val methyl 1H, 13C and 15N NMR chemical shift assignments for human interferon-stimulated gene 15 protein, *Biomol NMR Assign.* 5 (2011) 215–219. doi:10.1007/s12104-011-9303-8.

[74] Y.G. Chang, X.Z. Yan, Y.Y. Xie, X.C. Gao, A.X. Song, D.E. Zhang, H.Y. Hu, Different roles for two ubiquitin-like domains of ISG15 in protein modification, *J. Biol. Chem.* 283 (2008) 13370–13377. doi:10.1074/jbc.M800162200.

[75] C. Lai, J.J. Struckhoff, J. Schneider, L. Martinez-Sobrido, T. Wolff, A. Garcia-Sastre, D.E. Zhang, D.J. Lenschow, Mice lacking the ISG15 E1 enzyme UBE1L demonstrate increased susceptibility to both mouse-adapted and non-mouse-adapted influenza B virus infection, *J. Virol.* 83 (2009) 1147–1151. doi:10.1128/JVI.00105-08.

[76] H. Sridharan, C. Zhao, R.M. Krug, Species specificity of the NS1 protein of influenza B virus: NS1 binds only human and non-human primate ubiquitin-like ISG15 proteins, *J. Biol. Chem.* 285 (2010) 7852–7856. doi:10.1074/jbc.C109.095703.

[77] G.C. Capodagli, M.K. Deaton, E.A. Baker, R.J. Lumpkin, S.D. Pegan, Diversity of ubiquitin and ISG15 specificity among nairoviruses' viral ovarian tumor domain proteases, *J. Virol.* 87 (2013) 3815–3827. Diversity of Ubiquitin and ISG15 Spec.

- [78] M.K. Deaton, J.V. Dzimianski, C.M. Daczkowski, G.K. Whitney, N.J. Mank, M.M. Parham, E. Bergeron, S.D. Pegan, Biochemical and structural insights into nairoviral deISGylases preference for interferon-stimulated-gene-product 15 originating from certain species, *J. Virol.* (2016). doi:10.1128/JVI.00975-16.
- [79] K. Ratia, A. Kilianski, Y.M. Baez-Santos, S.C. Baker, A. Mesecar, Structural basis for the ubiquitin-linkage specificity and deISGylating activity of SARS-CoV papain-like protease, *PLoS Pathog.* 10 (2014) e1004113. doi:10.1371/journal.ppat.1004113.
- [80] C.M. Daczkowski, O.Y. Goodwin, J.V. Dzimianski, J.J. Farhat, S.D. Pegan, Structurally guided removal of DeISGylase biochemical activity from papain-like protease originating from Middle East respiratory syndrome coronavirus, *J. Virol.* 91 (2017). doi:10.1128/JVI.01067-17.
- [81] P.B. van Kasteren, R.C.M. Knaap, P. van den Elzen, E.J. Snijder, U.B.R. Balasuriya, E. van den Born, M. Kikkert, In vivo assessment of equine arteritis virus vaccine improvement by disabling the deubiquitinase activity of papain-like protease 2., *Vet. Microbiol.* 178 (2015) 132–137. doi:10.1016/j.vetmic.2015.04.018.
- [82] É. Bergeron, M. Zivcec, A.K. Chakrabarti, S.T. Nichol, C.G. Albariño, C.F. Spiropoulou, Recovery of recombinant Crimean Congo Hemorrhagic fever virus reveals a function for non-structural glycoproteins cleavage by furin, *PLoS Pathog.* 11 (2015) e1004879. doi:10.1371/journal.ppat.1004879.
- [83] M. Akutsu, Y. Ye, S. Virdee, J.W. Chin, D. Komander, Molecular basis for ubiquitin and ISG15 cross-reactivity in viral ovarian tumor domains, *Proc. Natl. Acad. Sci. U. S. A.* 108 (2011) 2228–2233. doi:10.1073/pnas.1015287108.
- [84] C.M. Coleman, J.M. Sisk, G. Halasz, J. Zhong, S.E. Beck, K.L. Matthews, T. Venkataraman, S. Rajagopalan, C.A. Kyratsous, M.B. Frieman, CD8+ T cells and macrophages regulate pathogenesis in a mouse model of Middle East respiratory syndrome., *J. Virol.* 91 (2017). doi:10.1128/JVI.01825-16.
- [85] A.S. Cockrell, B.L. Yount, T. Scobey, K. Jensen, M. Douglas, A. Beall, X.-C. Tang, W.A. Marasco, M.T. Heise, R.S. Baric, A mouse model for MERS coronavirus-induced acute respiratory distress syndrome., *Nat. Microbiol.* 2 (2016) 16226. doi:10.1038/nmicrobiol.2016.226.
- [86] K. Li, C.L. Wohlford-Lenane, R. Channappanavar, J.-E. Park, J.T. Earnest, T.B. Bair, A.M. Bates, K.A. Brogden, H.A. Flaherty, T. Gallagher, D.K. Meyerholz, S. Perlman, P.B. McCray, Mouse-adapted MERS coronavirus causes lethal lung disease in human DPP4 knockin mice., *Proc. Natl. Acad. Sci. U. S. A.* 114 (2017) E3119–E3128. doi:10.1073/pnas.1619109114.
- [87] M.G. Douglas, J.F. Kocher, T. Scobey, R.S. Baric, A.S. Cockrell, Adaptive evolution influences the infectious dose of MERS-CoV necessary to achieve severe respiratory disease., *Virology.* 517 (2018) 98–107. doi:10.1016/j.virol.2017.12.006.

CHAPTER 3

PROBING THE IMPACT OF NAIROVIRUS GENOMIC DIVERSITY ON VIRAL
OVARIAN TUMOR DOMAIN PROTEASE (vOTU) STRUCTURE AND
DEUBIQUITINASE ACTIVITY ¹

¹ Dzimianski, J.V, B.S. Beldon, C.M. Daczkowski, O.Y. Goodwin, F.E.M. Scholte, É. Bergeron, and S.D. Pegan. 2019. *PLOS Pathogens*. 15(1):e1007515. doi: 10.1371/journal.ppat.1007515. Reprinted here with permission of the publisher.

Abstract

Post-translational modification of host and viral proteins by ubiquitin (Ub) and Ub-like proteins, such as interferon stimulated gene product 15 (ISG15), plays a key role in response to infection. Viruses have been increasingly identified that contain proteases possessing deubiquitinase (DUB) and/or deISGylase functions. This includes viruses in the *Nairoviridae* family that encode a viral homologue of the ovarian tumor protease (vOTU). vOTU activity was recently demonstrated to be critical for replication of the often-fatal Crimean-Congo hemorrhagic fever virus, with DUB activity suppressing the type I interferon responses and deISGylase activity broadly removing ISG15 conjugated proteins. There are currently about 40 known nairoviruses classified into fourteen species. Recent genomic characterization has revealed a high degree of diversity, with vOTUs showing less than 25% amino acids identities within the family. Previous investigations have been limited to only a few closely related nairoviruses, leaving it unclear what impact this diversity has on vOTU function. To probe the effects of vOTU diversity on enzyme activity and specificity, we assessed representative vOTUs spanning the *Nairoviridae* family towards Ub and ISG15 fluorogenic substrates. This revealed great variation in enzymatic activity and specific substrate preferences. A subset of the vOTUs were further assayed against eight biologically relevant di-Ub substrates, uncovering both common trends and distinct preferences of poly-Ub linkages by vOTUs. Four novel X-ray crystal structures were obtained that provide a biochemical rationale for vOTU substrate preferences and elucidate structural features that distinguish the vOTUs, including a motif in the Hughes orthonairovirus species that has not been previously observed in OTU domains. Additionally, structure-informed mutagenesis provided the first direct evidence of a second

site involved in di-Ub binding for vOTUs. These results provide new insight into nairovirus evolution and pathogenesis, and further enhances the development of tools for therapeutic purposes.

Author Summary

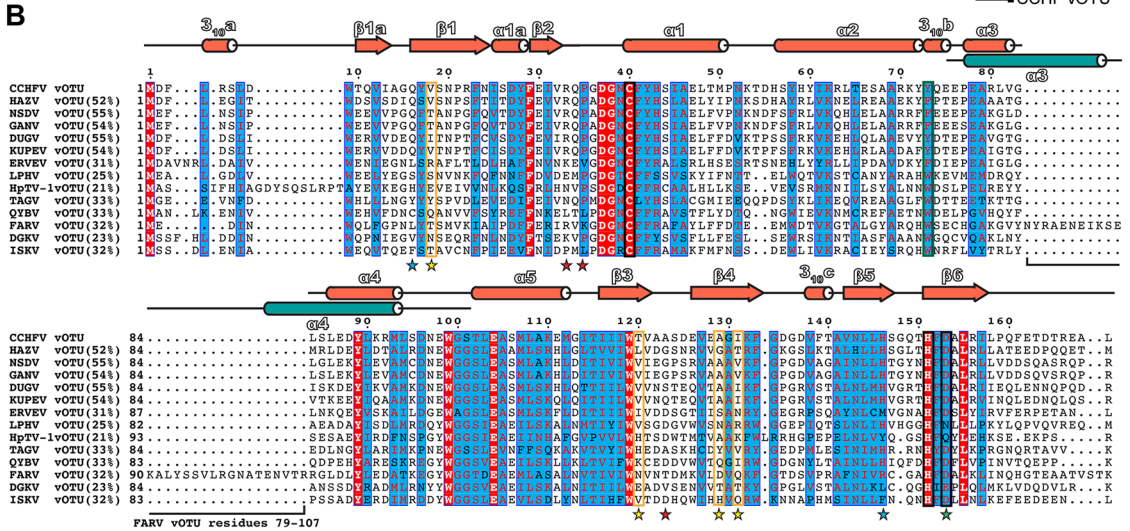
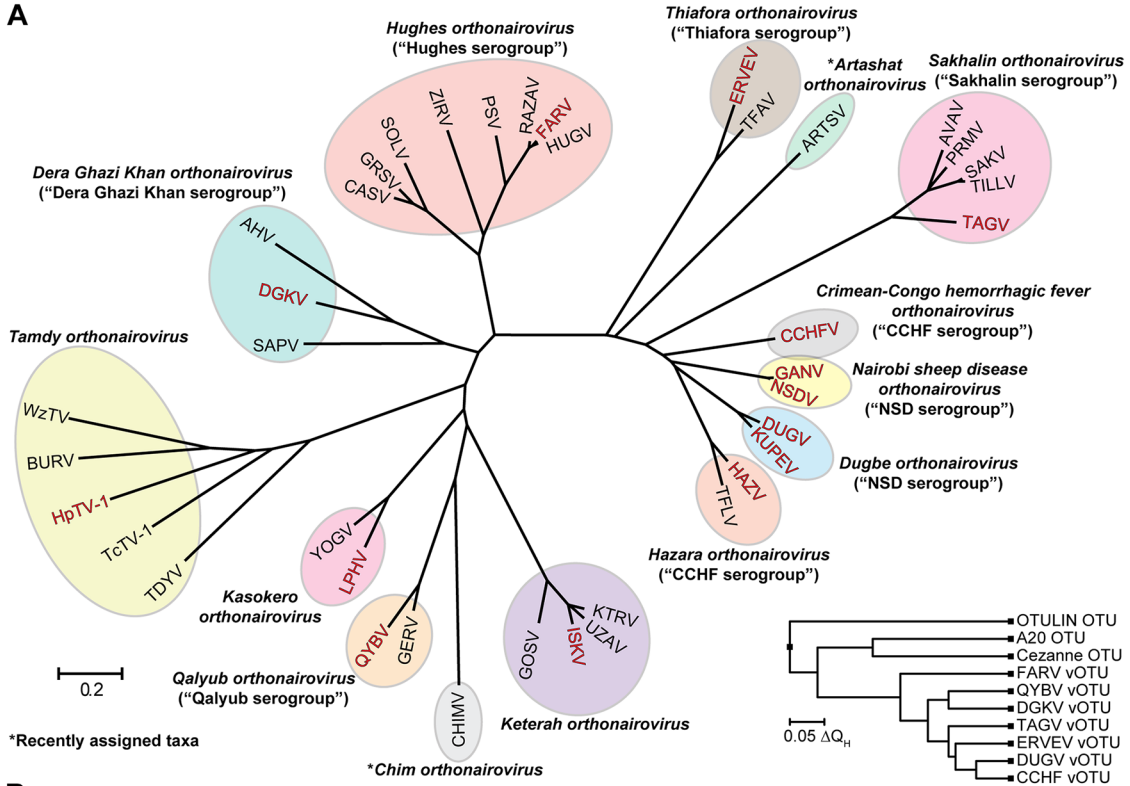
Viruses utilize a variety of mechanisms to manipulate and suppress host responses to infection. One specific mechanism used by nairoviruses is the production of a deubiquitinating enzyme, termed the vOTU, that disrupts the innate immune response. This enzyme has been shown to play a key role in efficient replication of Crimean-Congo hemorrhagic fever virus (CCHFV), a severe human pathogen causing outbreaks with high case fatality rates. Recent genomic studies have revealed a high degree of sequence variation for the vOTU among nairoviruses, but knowledge relating to the functional impact of this diversity is lacking. Here we investigated the effects of this diversity on the structure and function of vOTUs from a wide range of nairoviruses. This revealed that vOTUs from different nairoviruses possess distinct preferences for certain host proteins. In addition, we found that different vOTUs possess distinguishing structural features, including a unique motif present in one that was previously undescribed. Utilizing this information, we were able to provide a rational basis for the observed differences in the vOTUs. This work provides a foundation to understand nairovirus evolution by providing insight into a mechanism that influences virus host adaptation and pathogenesis.

Introduction

Nairoviruses are negative sense single stranded RNA [(-) ssRNA] viruses within the order *Bunyavirales*. Initial classification of nairovirus species relied on antigenic cross-reactivity, leading to the clustering of viruses into seven serogroups; however, with the recent increase in the number of available viral sequences the classifications have shifted to a comparative genomics approach. This not only confirmed the diversity observed based on the serogroup classification, but also further accentuated how these viruses vary across the *Nairoviridae* family. The family *Nairoviridae* now consists of approximately 40 viruses that are currently classified into 14 species (Fig 3.1; [1-5]).

Most nairoviruses are tick-borne viruses infecting multiple vertebrate host species they parasitize in nature. Several have been implicated in human disease, the most notable being Crimean-Congo hemorrhagic fever virus (CCHFV), which has reported case fatality rates in humans that can exceed 30% [6]. Other nairoviruses associated with human disease include Dugbe virus (DUGV), Nairobi sheep disease virus (NSDV) and the Asian variant Ganjam virus (GANV), Erve virus (ERVEV), Issyk-kul virus (ISKV) and Kasokero virus (KASV). These viruses have been reported to cause a myriad of symptoms, some of which include fever, headache, and diarrhea [7-12]. Nairoviruses have also been observed to cause fatal animal disease. For example, NSDV has been reported to have a >90% mortality rate in sheep and goats making it a significant economic as well as human health concern [13]. A recently characterized nairovirus, Leopards Hill virus (LPHV), was isolated from bats and causes severe gastroenteric hemorrhaging and hepatic disease in mice [14]. Hazara virus (HAZV) was isolated from ticks collected from the Royle's mountain vole and has been proposed as a model system to study CCHFV based on its

Fig 3.1. Sequence and structural diversity of nairovirus vOTUs. (A) Phylogenetic tree of CLUSTALW aligned nairovirus vOTUs. The tree was constructed utilizing the Jones-Thornton-Taylor model in the MEGA7 program [70]. Current species groupings are indicated by colored ovals, and the assigned species denoted. Previous serogroup classification, if applicable, is shown in parentheses. Virus vOTUs included in this study are denoted by red lettering. Inset is a structure-based phylogenetic tree of vOTUs, with the mammalian Cezanne, A20, and OTULIN OTUs included for comparison. The tree was constructed using PDB IDs 3PRP, 4HXD, 5JZE, 6DX1, 6DX2, 6DX3, 6DX5, 5LRV, 5LRX, and 3ZNZ in the MultiSeq module of VMD [71]. Sequence accession numbers are included in 3.S1 Table. CCHFV, Crimean-Congo hemorrhagic fever virus; GANV, Ganjam virus; NSDV, Nairobi sheep disease virus; DUGV, Dugbe virus; KUPEV, Kupe virus; HAZV, Hazara virus; TFLV, Tofla virus; TAGV, Taggert virus; TILLV, Tillamook virus; SAKV, Sakhalin virus; PRMV, Paramushir virus; AVAV, Avalon virus; ARTSV, Artashat virus; TFAV, Thiafora virus; ERVEV, Erve virus; HUGV, Hughes virus; FARV, Farallon virus; RAZAV, Raza virus; PSV, Punta Salinas virus; ZIRV, Zirqa virus; SOLV, Soldado virus; GRSV, Great Saltee virus; CASV, Caspiy virus; AHV, Abu Hammad virus; DGKV, Dera Ghazi Khan virus; SAPV, Sapphire II virus; WzTV, Wēnzhōu tick virus; BURV, Burana virus; HpTV-1, Huángpí tick virus 1; TcTV-1, Tǎchéng tick virus 1; TDYV, Tamdy virus; YOGV, Yogue virus; LPHV, Leopards Hill virus; QYBV, Qalyub virus; GERV, Geran virus; CHIMV, Chim virus; GOSV, Gossas virus; ISKV, Issyk-kul virus; UZAV, Uzun-Agach virus; KTRV, Keterah virus. (B) Nairovirus vOTUs tested in this study aligned using the T-Coffee sequence alignment program [72]. Percentages show the sequence identity relative to CCHFV vOTU. Generic vOTU secondary structure based on Define Secondary Structure of Proteins (DSSP) algorithm calculations for the vOTUs is shown in reddish orange, with the $\alpha 3$ and $\alpha 4$ helices of FARV vOTU shown in teal. The catalytic triad is boxed in black and the selectivity pocket in orange. Mutation sites related to the selectivity pocket are shown by yellow stars, sites related to differences in how FARV vOTU engages mono-Ub by blue stars, and the DGKV vOTU catalytic triad mutant by a green star. Mutation sites for the second Ub binding site in FARV vOTU are denoted by red stars. The region deleted in the FARV vOTU ^{$\Delta 79-107$} construct is indicated by a bracket.



ability to cause similar fatal disease in interferon (IFN)-receptor knockout mice [15, 16]. Beyond these viruses causing disease in mammalian hosts, other nairovirus have been associated with a broad taxonomic diversity of vertebrate hosts such as birds, fish, and reptiles. For example, viruses in the *Hughes orthonairovirus* species, such as Farallon virus (FARV), have been implicated in infecting birds [17].

Nairoviruses possess a tripartite genome consisting of small (S), medium (M), and large (L) segments that encode the viral nucleoprotein, glycoproteins, and RNA-dependent RNA polymerase, respectively. Interestingly, the nairoviral L segment also encodes a viral homologue of the ovarian tumor protease (OTU) at the N-terminus. This feature uniquely distinguishes the *Nairoviridae* family and genus *Tenuivirus* from other members of the order *Bunyvirales*. The viral OTU (vOTU) does not appear to play a direct role in genome replication and is dispensable in minigenome replication systems [18]. Instead, the vOTU's primary function appears to be the reversal of post-translational modifications by ubiquitin (Ub) and the Ub-like protein interferon stimulated gene product 15 (ISG15). This vOTU-encoded deubiquitinase (DUB) and deISGylase activity has been implicated in evading the innate immune response [19-21]. Ub is an 8.5 kDa protein that is involved in a wide range of cellular processes, including key regulatory functions in innate immunity. Ub is conjugated to target proteins by means of a three step process involving activating (E1), conjugating (E2), and ligating (E3) enzymes, and can either occur as a single Ub moiety (mono-Ub) or in polymeric and branched forms (poly-Ub). These chains can be formed by linkage through either the N-terminus (linear) or one of seven lysine residues in Ub (K6, K11, K27, K29, K33, K48, and K63), with different forms often mediating different downstream effects. The most thoroughly studied forms, K48 and K63, play

important roles in regulation of the innate immune responses. Specifically, K48-mediated proteasomal degradation has been associated with feedback control, while K63 polyubiquitination is required for pathway activation, including retinoic acid-inducible protein I (RIG-I), mitochondrial antiviral signaling protein (MAVS), Tumor necrosis factor (TNF) receptor associated factor 3 (TRAF3), TANK binding kinase 1 (TBK1), and IFN regulatory factor 3 (IRF3). This signaling cascade leads to the production of IFN- α/β , which ultimately results in the upregulation of numerous IFN-stimulated genes, including ISG15 [22, 23]. The role of ISG15 is complex and not well understood but is generally associated with mediating and regulating antiviral responses both as a co-translational modification and as free ISG15 in the cytosol and secreted form inducing the secretion of IFN- γ and IL-10 by binding cell surface receptor LFA-1 [24-29].

Initial studies on nairoviruses, including CCHFV, DUGV, and NSDV, established the potential immune modulatory effects of vOTU activity based on overexpression of the respective isolated OTU domain in cell culture [19-21]. The ability to probe the specific role of the vOTU during the viral replication cycle remained elusive, however, until the recent development of a reverse genetics system for CCHFV. These studies revealed distinct roles for DUB versus deISGylating activity during the course of a CCHFV infection [30]. Specifically, that CCHFV vOTU DUB activity is not as promiscuous towards ubiquitinated host proteins as it first seemed based on the overexpression studies, but appears to be restricted to a targeted subset of cellular substrates associated with suppression of RIG-I-mediated early cellular responses to infection. In particular, wildtype CCHFV was able to reduce the induction of several immune components, including RIG-I, while CCHFV with a vOTU specifically lacking DUB activity resulted in enhanced

cellular responses to infection and establishment of a cellular antiviral state that reduced viral titers. In contrast, deISGylating activity appears to play a role in later stages of CCHFV infection. A recent study demonstrated a similar impact of DUB activity in viral immune suppression during the replication cycle of severe acute respiratory syndrome coronavirus (SARS-CoV) [31]. Specifically, when the DUB activity of the SARS-CoV papain-like protease (PLpro) was selectively disrupted, the virus showed increased sensitivity to IFN and slower growth kinetics. Furthermore, domain exchanges of PLpro's between different SARS-CoV variants supported this observation, establishing DUB activity to be a distinguishing virulence trait. These emerging insights into the impact of DUB activity in the CCHFV vOTU and SARS-CoV PLpro during viral replication emphasizes the importance of robust DUB activity among pathogenic viruses. The demonstrated vOTU-associated DUB/deISGylase activity of other nairoviruses such as DUGV, ERVEV, and NSDV/GANV, further highlights a potentially substantial role of the vOTU in viral replication and immune suppression for viruses in the *Nairoviridae* family [19-21, 32].

Remarkably, the nairoviral vOTU domain shows a great degree of sequence diversity, with sequence identities that can drop below 25% between species (Fig 3.1). A particularly striking case of this diversity is found in members of the *Hughes orthonairovirus* species, such as FARV, which possess 26-30 additional residues in the middle of the OTU domain (Fig 3.1B). These sequence differences between vOTUs suggest a plasticity in the OTU domain that could play a role in evolutionary adaptation. Currently, exploration into the phenotypical effects of this diversity has been restricted to only a few taxa that include CCHFV, DUGV, NSDV/GANV, and ERVEV [32, 33]. These

studies revealed that vOTUs possess different enzymatic and structural characteristics. In particular, vOTUs display a wide degree of variation in the efficiency with which they engage Ub and ISG15 that is driven by specific sequence and structural features. These substantial differences in viruses within closely related taxa raises questions on the impact of vOTU diversity across the *Nairoviridae* family. Specifically, how vOTUs from viruses in each species vary in structure and activity, and the implications of this for the potential to suppress the innate immune response and affect viral pathogenesis and host tropism.

To better understand the impact of vOTU diversity, we sought to obtain a more complete perspective of the functional and structural features of vOTUs within the *Nairoviridae* family. *In vitro* assays revealed that vOTUs across diverse taxa possess Ub activity, but that activity towards ISG15 appears more restricted. Further characterization of vOTU activity uncovered distinct trends and preferences for specific poly-Ub linkages. To better understand the molecular mechanisms driving Ub activity and specificity, novel X-ray crystal structures were solved revealing features that distinguish the vOTUs from each other, including a pocket that correlates with Ub specificity. Additionally, a structure of the FARV vOTU provides details into the structural nature of the additional residues in *Hughes orthonairovirus* vOTUs. Structure-informed mutagenesis of FARV vOTU identified residues involved specifically in di-Ub binding, representing the first report of the role of a second site involved in di-Ub binding in nairovirus vOTUs. This novel enzymatic and structural data not only provides insight into the nature of vOTU diversity, but also lays a foundation for understanding the impact of the vOTU interaction with the innate immune response and its connection to viral pathogenesis.

Results

vOTU Enzymatic Diversity

To gauge vOTU diversity across the *Nairoviridae* family, viruses representing the divergent species were selected and the OTU domain recombinantly expressed. Initially selected based on the traditional serogroups as well as emerging genetic characterization, these viruses include members of the most distantly related taxa and represent 12 of the currently recognized 14 species in the dynamic classification landscape of nairoviruses (Fig 3.1). Included were the vOTUs from CCHFV, NSDV and GANV, DUGV and Kupe virus (KUPEV), HAZV, Taggart virus (TAGV), ERVEV, FARV, Dera Ghazi Khan virus (DGKV), Huángpí Tick virus 1 (HpTV-1), LPHV, Qalyub virus (QYBV), and ISKV (Fig 3.1). To better understand the global diversity of nairoviral engagement with Ub and ISG15 substrates, these vOTUs were assessed for activity towards Ub and human ISG15 fluorogenic substrates. These specific activities were measured by the accumulation of the fluorescent molecule 7-amino-4-methylcoumarin (AMC) as a result of cleavage from the C-terminus of Ub or ISG15 (Fig 3.2).

Intriguingly, the vOTUs showed a diverse range of activity towards Ub. In general, vOTUs can be divided into groups possessing high (CCHFV, HAZV, NSDV/GANV, TAGV), moderate (DUGV, KUPEV, FARV, QYBV, ISKV), or low activity (ERVEV, DGKV, LPHV, HpTV-1) (Fig 3.2A). For some of these vOTUs, their deubiquitination activity mirrors that observed in DUB-deficient CCHFV mutants that impact cellular ubiquitination levels leading to an impaired ability to suppress the IFN response [30, 34]. To a large degree, viruses more closely related phylogenetically with CCHFV possess the most robust activity (Fig 3.1A and Fig 3.2A). Beyond this, there is not an obvious

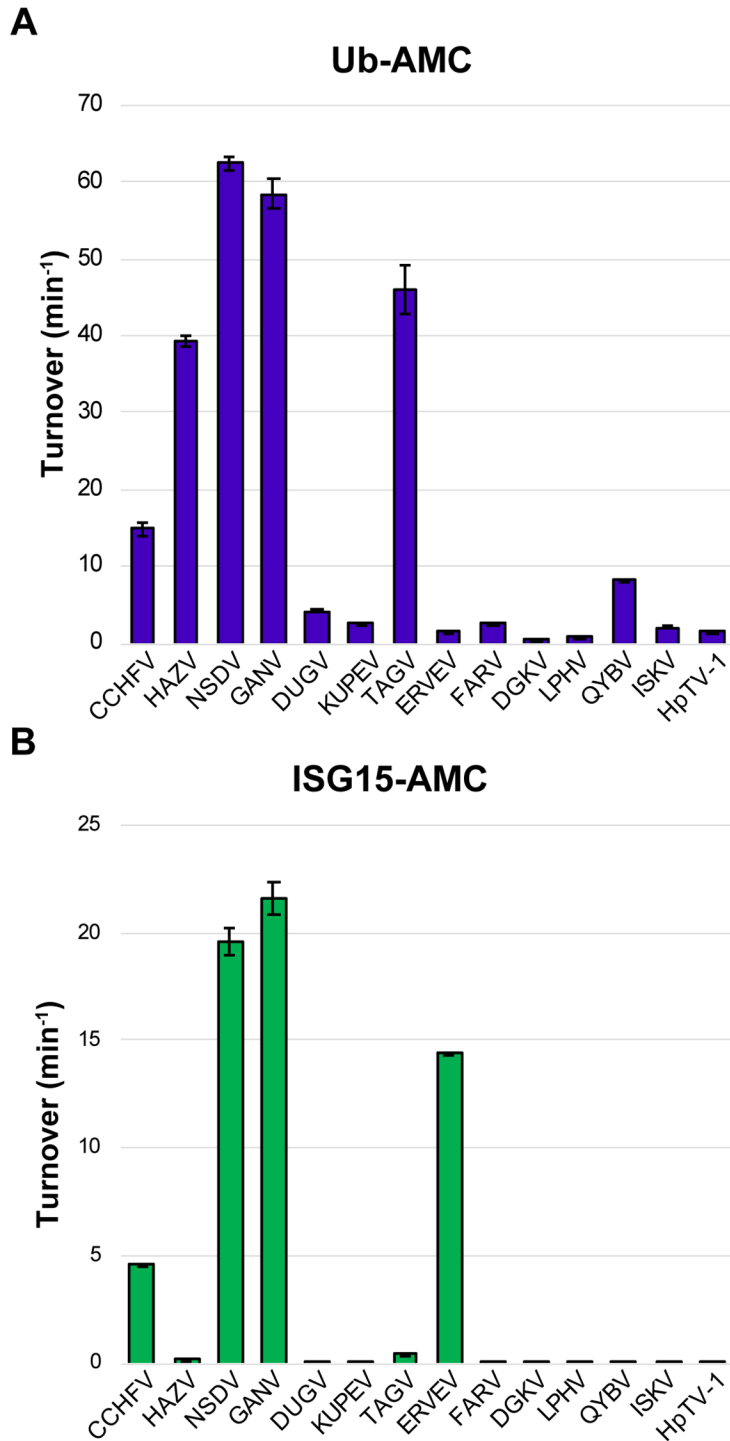


Fig 3.2. Diversity of vOTU specific activity. Activity of vOTUs towards Ub-AMC (A) and human ISG15-AMC (B). Values shown are the mean \pm standard deviation of two independent experiments.

phylogenetic trend to how well the vOTUs cleave Ub-AMC, with disparate taxa showing similar low to mid-range activity. Overall, engagement with Ub is observed to be a feature that can be present in diverse species in the *Nairoviridae* family, with some taxa demonstrating enhanced activity.

The patterns of activity for Ub are in stark contrast to those of ISG15-AMC, which shows a more dichotomous pattern as a substrate for the vOTUs (Fig 3.2B). Specifically, there appears to be an abrupt break phylogenetically between groups that contain vOTUs with deISGylating activity, compared to others for which activity is almost negligible. This break appears to exist at the node separating the *Thiafora*, *Artashat*, *Sakhalin*, *Crimean-Congo hemorrhagic fever*, *Nairobi Sheep Disease*, *Dugbe*, and *Hazara orthonairovirus* species from the remaining seven (Fig 3.1A). Interestingly, the presence of ISG15 activity does not encompass every vOTU in these species, suggesting individual factors may have driven the development or retention of ISG15 activity for viruses within this clade. Naturally, this also implies that DUB activity could be a more broadly utilized mechanism to evade cellular responses. This led us to further explore the dynamics of different nairovirus vOTU's interactions with Ub.

Di-Ub linkage preferences of vOTUs

While the Ub-AMC assay provides general information on the ability of vOTUs to engage monomeric Ub, cellular substrates are typically modified by poly-Ub chains through various linkage types [35]. Additionally, DUBs in general and vOTUs in particular have been observed to prefer some linkage types over others [32, 36-40]. To assess the patterns of Ub linkage preferences of diverse vOTUs, a subset of the vOTUs were analyzed against di-Ub FRET-TAMRA substrates (Fig 3.3A). HAZV vOTU and GANV vOTU

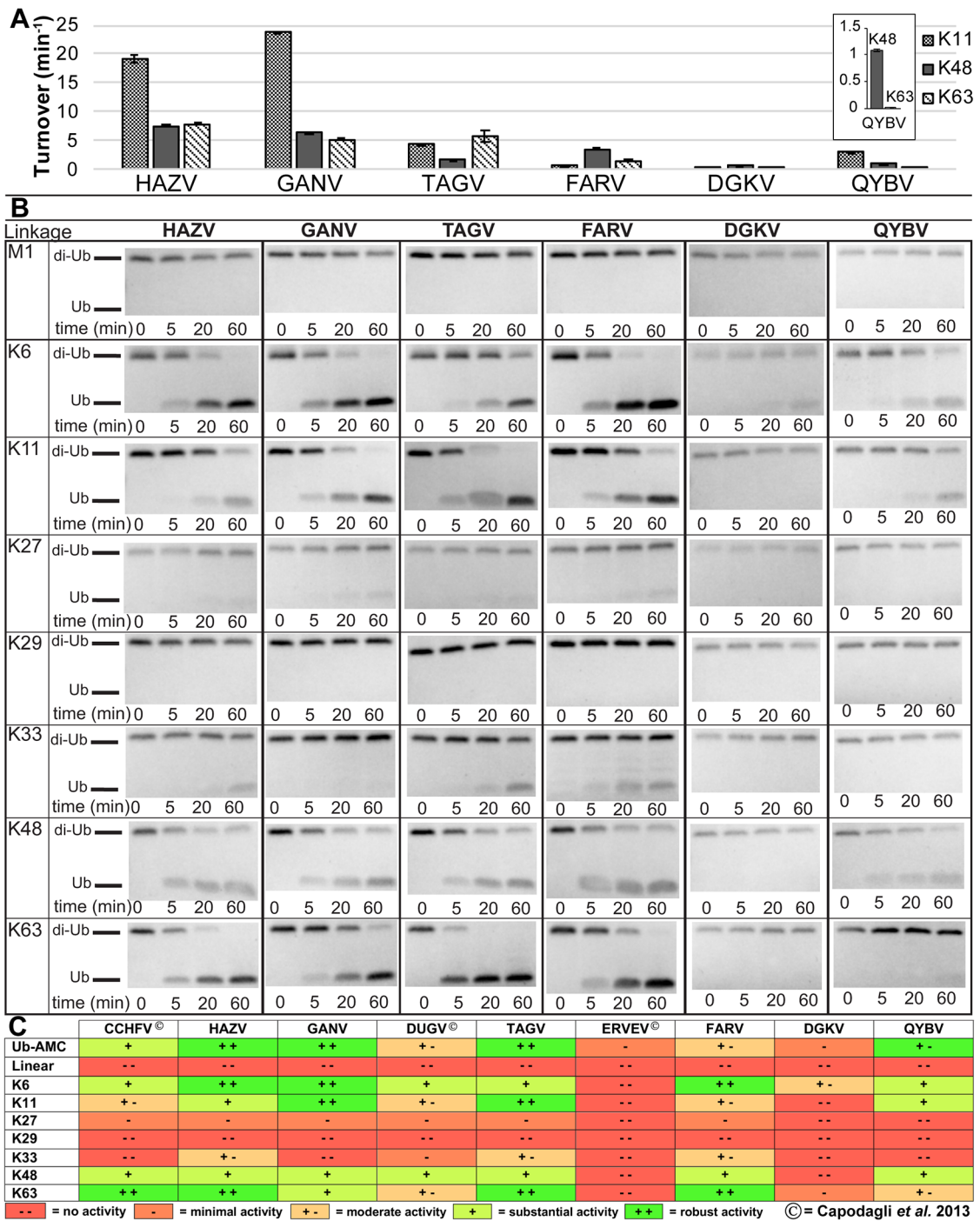


Fig 3.3. vOTU preferences for different di-Ub linkages. (A) Activity towards K48, K63, and K11 linked di-Ub FRET-TAMRA substrates. Values shown are the mean \pm standard deviation of two independent experiments. (B) Gel cleavage assay of unlabeled di-Ub, visualized by Commassie Blue staining. (C) Summary of currently investigated vOTU di-Ub activity (present study and [32]).

were selected because they have been considered to be a potential model system for CCHFV and have significant health and economic impact, respectively. TAGV vOTU represents a more distantly related vOTU that also has substantial DUB activity, while the vOTUs encoded by QYBV, FARV, and DGKV display diminished activity towards mono-Ub. To reduce the influence of interactions with the FRET pairs that may disrupt interaction, multiple FRET pair configurations were assessed when available and the one displaying the highest activity selected (two positions each for K48 and K63; 3.S1 Fig).

Comparison of vOTU activities towards different di-Ub FRET substrates reveals that each species' vOTU has distinct preferences for specific di-Ub linkages. While HAZV vOTU and GANV vOTU both possess notable activity for K48 and K63 di-Ub, there appears to be more substantial activity towards K11. TAGV vOTU, on the other hand, prefers K63 and K11 to a greater extent, while not possessing as much activity towards K48. For FARV vOTU, the opposite is observed, with K48 being preferred. DGKV vOTU, consistent with its low Ub-AMC activity, possesses very low activity for the di-Ub FRET substrates, regardless of the linkage. Similar to the pattern observed for HAZV and GANV, QYBV vOTU shows the most activity towards K11, though at lower overall levels. Additionally, QYBV vOTU shows a more pronounced difference in the relative preference for K48 versus K63 linkages, with substantially more activity towards K48.

Regrettably, the commercial availability of FRET-TAMRA di-Ub substrates is restricted to these tested linkages. Additionally, limitations are known to exist due to how the positions of the donor-quencher pairs affects binding of these substrates with the proteases. To gain a more complete and natural perspective of di-Ub linkage preferences, these vOTUs were also assessed by SDS-PAGE for the ability to cleave unlabeled di-Ub

substrates of all eight linkage types (Fig 3.3B). As expected, the vOTUs did not show equal preferences for the different linkages. Intriguingly, some of the results appeared to differ from the FRET analysis. Specifically, for both HAZV vOTU and FARV vOTU the gel cleavage assay would suggest the K63 activity to be the highest with K48 and K11 roughly equal, suggesting that the positions of the donor-quencher pairs may have hindered binding to some of the substrates. As expected, the HAZV, GANV, and TAGV vOTU showed substantial cleavage of several di-Ub substrates that is consistent with their high Ub-AMC activity, while the DGKV and QYBV vOTUs showed low level of substrate cleavage over the same time course. Intriguingly, FARV vOTU showed substantial cleavage of some of the substrates, despite not possessing high Ub-AMC activity. This may be reflective of differences in the assays in measuring DUB activity. Alternatively, it may also suggest the existence of an additional site of interaction with the proximal Ub that enhances the efficiency of di-Ub cleavage.

Assimilation with previously reported data reveals interesting trends and points of divergence between the vOTUs ([32]; Fig 3.3C). Linear and K29-linked di-Ub does not show any sign of cleavage with any vOTU. vOTUs demonstrate varying levels of low/detectable activity on K27-linked and K33-linked di-Ub. In contrast, vOTUs show a consistent pattern of higher activity towards K6, K11, K48, and K63 di-Ub. While most of the vOTUs show some level of enhanced activity towards these linkages, the specific linkage most preferred can differ. The CCHFV, HAZV, TAGV, and FARV vOTUs all show a distinct preference for K63 over K48 linkages, while DUGV and QYBV vOTU show more activity towards K48. GANV vOTU shows approximately equal preference for these linkages. Interestingly, GANV vOTU also shows more activity towards both K6

and K11 di-Ub at approximately equal levels. The high degree of preference towards these substrates extends to the majority of the vOTUs, as even for DGKV vOTU, which shows minimal or no cleavage of most of the substrates, cleavage of K6-linked di-Ub can be identified within an hour (Fig 3.3B). The other vOTUs, with the exception of ERVEV, all show detectable levels of K6 cleavage, with most also cleaving K11. The CCHFV, HAZV, DUGV, and FARV vOTUs all showed a greater relative preference for K6 over K11, while TAGV vOTU was the opposite. QYBV vOTU, similar to GANV, showed approximately equivalent activity towards K6 and K11, though overall activity was lower. Overall, these patterns of activity suggest that vOTUs do not merely cut any Ub moiety, but that they are specific to a subset of linkages that may influence specific aspects of cellular biology.

Nairovirus vOTUs possess shared, but distinct structural characteristics.

To gain a better understanding of how sequence diversity translates into structural differences, X-ray crystal structures were sought of vOTUs from divergent species. The vOTUs from DGKV, QYBV, and TAGV readily crystallized and were solved to 1.62 Å, 1.65 Å, and 2.05 Å, respectively (Table 3.1). These vOTUs represent diverse nairovirus species, and possess extensive variation in Ub activity with the DGKV, QYBV, and TAGV vOTUs possessing low, medium, and high activity towards Ub-AMC, respectively (Fig 3.2). TAGV provides a glimpse into the *Sakhalin orthonairovirus* species, a taxon that is more closely related to the ERVEV and CCHF/NSD/Dugbe/Hazara cluster, while DGKV and QYBV are from the *Dera Ghazi Khan* and *Qalyub orthonairovirus* species, respectively, and are much more distantly related (Fig 3.1).

These structures reveal global similarities among the vOTUs (Fig 3.4 and 3.S2 Fig). Each vOTU possesses a seven-stranded beta sheet as the core feature, with five major alpha

Table 3.1. Data collection and refinement statistics for vOTU crystal structures.

	Se-SAD QYBV vOTU (PDB entry 6DWX)	QYBV vOTU (PDB entry 6DX1)	DGKV vOTU (PDB entry 6DX2)	TAGV vOTU (PDB entry 6DX3)	FARV vOTU (PDB entry 6DX5)
Data collection					
Space group	P3 ₂ 21	P3 ₂ 21	P4 ₁	P1	P4 ₁ 2 ₁ 2
Wavelength (Å)	0.9795	1	1	1	1
Cell dimensions					
<i>a, b, c</i> (Å)	110.5, 110.5, 106.2	110.5, 110.5, 106.2	68.4, 68.4, 69.8	47.2, 60.9, 66.5	70.28, 70.28, 176.26
α, β, γ (°)	90, 90, 120	90, 90, 120	90, 90, 90	64.9, 89.8, 84.3	90, 90, 90
Resolution (Å)	50.00–2.40 (2.44–2.40) [†]	50.00–1.65 (1.68–1.65) [†]	50.00–1.62 (1.65–1.62) [†]	50.00–2.05 (2.09–2.05) [†]	50.00–2.22 (2.26–2.22) [†]
<i>R</i> _{merge}	0.038 (0.118)	0.106 (0.821)	0.064 (1.071)	0.102 (0.450)	0.116 (0.874)
<i>CC</i> _{1/2}	0.999 (0.996)	0.998 (0.719)	0.994 (0.568)	0.990 (0.847)	0.992 (0.890)
<i>I</i> / σ <i>I</i>	80.6 (29.9)	21.6 (1.8)	24.8 (1.1)	17.3 (2.3)	18.9 (2.9)
Completeness (%)	100.0 (100.0)	100.0 (100.0)	99.0 (99.5)	97.4 (97.7)	99.6 (100.0)
Redundancy	14.9 (15.0)	9.3 (6.2)	4.9 (4.3)	3.6 (3.4)	6.9 (6.8)
Phasing statistics					
No. of Se sites found	6				
Phasing Fig of merit	0.546				
Refinement					
Resolution (Å)	36.20–2.40 (2.48–2.40)	36.16–1.65 (1.71–1.65)	28.02–1.62 (1.67–1.62)	36.23–2.05 (2.13–2.05)	35.14–2.22 (2.30–2.22)
No. reflections	29,862	89,728	40,773	40,235	22,454
<i>R</i> _{work} (%) / <i>R</i> _{free} (%)	0.174/0.195	0.171/0.186	0.180/0.212	0.227/0.250	0.163/0.203
No. atoms					
Protein	3843	3841	2492	5379	2730
Ligand/ion [‡]	0	0	0	2	24
Water	123	498	183	394	169
<i>B</i> -factors					
Protein	34.88	25.30	45.62	35.16	43.92
Ligand/ion [‡]	- -	- -	- -	55.16	103.21
Water	37.35	37.28	53.31	39.09	42.17
R.m.s. deviations					
Bond lengths (Å)	0.008	0.006	0.014	0.005	0.015
Bond angles (°)	0.83	0.76	1.26	0.71	1.24

[†]Values in parentheses denote the highest resolution shell

[‡]Includes Mg and DTT

<https://doi.org/10.1371/journal.ppat.1007515.t001>

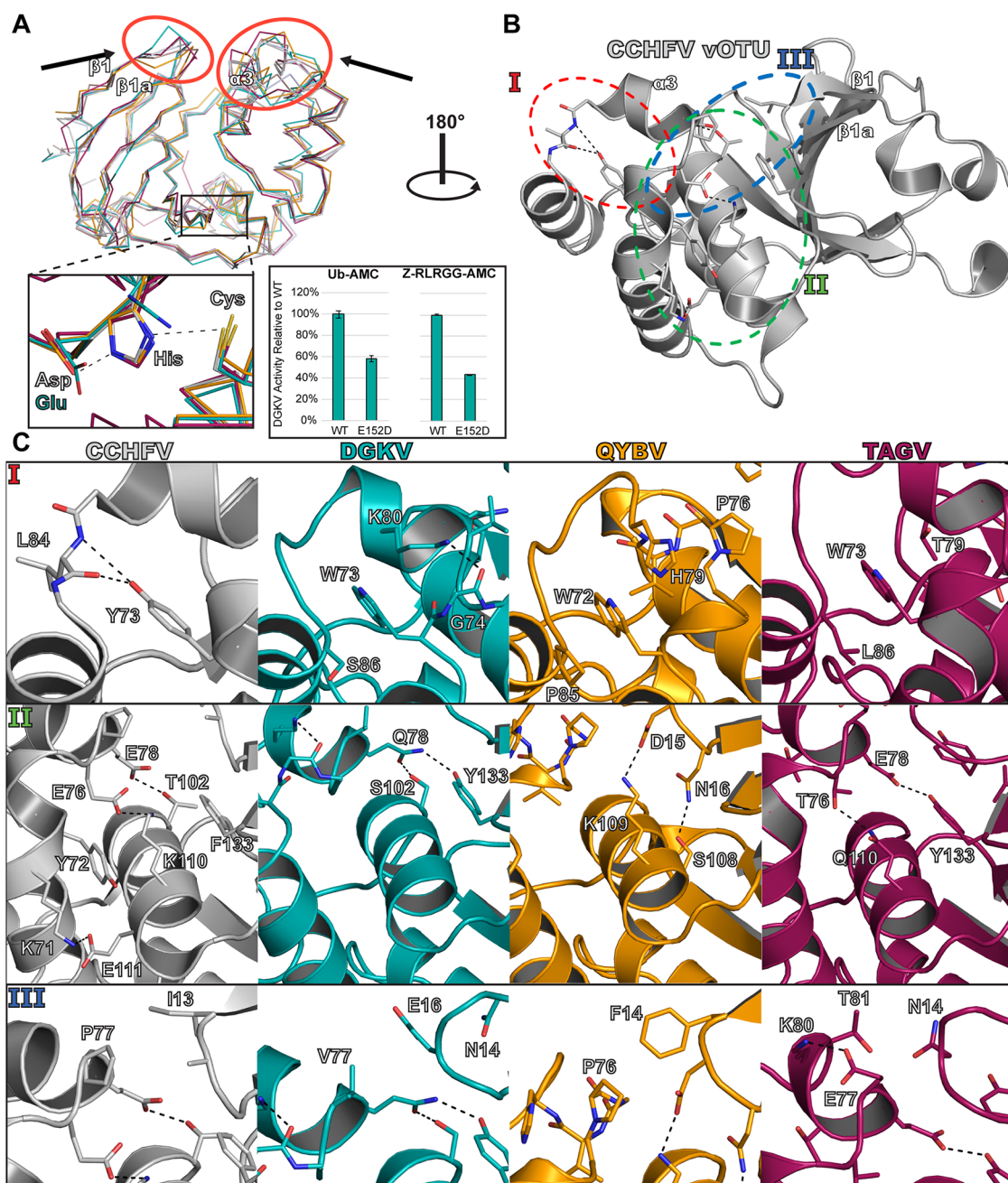


Fig 3.4. Structural comparison of new vOTU structures. (A) Secondary structure overlay of the vOTUs from CCHFV, DGKV, QYBV, and TAGV. The red circles highlight areas of the binding interface that show large structural divergence. The region of the active site is denoted by a black box, with a closeup shown. The relative activities of the DGKV vOTU WT and E152D mutant for Ub-AMC and the peptide Z-RLRGG-AMC are shown, with error bars representing the standard deviation of two independent experiments. (B-C) Specific molecular interactions accounting for these differences can be identified in distinct regions of the vOTUs. CCHFV vOTU is colored gray, DGKV vOTU in teal, QYBV vOTU in orange, and TAGV vOTU in magenta. Black dashed lines denote atom pairs that are within hydrogen bonding distance.

helices framing the rest of the structure. The catalytic triads perfectly superimpose over each with the exception of DGKV vOTU (Fig 3.4A). In DGKV vOTU, aspartate is replaced by a glutamate that alters the spatial dynamics of the catalytic triad, possibly contributing to a less rigid structure that allows the histidine to adopt the alternate conformation. While atypical for the vOTUs, it does not appear to be the cause of DGKV's low DUB activity, as mutating the glutamate to an aspartate only further diminished activity. Looking beyond the catalytic triad, a structural overlay of the vOTUs highlights a point of difference in the overall structure that distinguishes the proteases from each other. Specifically, there appears to be substantial variability in the region encompassing the $\alpha 3$ ("selectivity") helix that has been associated with substrate preference, and the loop between the $\beta 1$ and $\beta 1a$ strands (Fig 3.4A; [32, 33]). Comparing the root mean square deviation (R.m.s.d.) for the positions of the main chain atoms of these different structures further emphasizes how they deviate from structure to structure (3.S2 Fig).

Closer examination of the structures reveals distinct molecular interactions that account for these observed structural differences within the vOTUs. Specifically, particular amino acid differences can be identified that form interactions that would promote the observed conformation of each protease, suggesting these differences to not merely be a consequence of dynamics or crystal packing. Intriguingly, these residues are not limited to just the selectivity helix and $\beta 1$ - $\beta 1a$ loop but extend to other secondary structural elements in local proximity, forming an ensemble of interactions that drive the noticeable variability of the $\alpha 3$ region (Fig 3.4B and C). The first area of prominent influence centers around position 73 of CCHFV vOTU (Fig 3.4C, Panel I). This position is strongly conserved in possessing an aromatic residue, consisting of a phenylalanine or a

tyrosine in CCHFV and more closely related viruses, while consisting of a tryptophan in the rest of the vOTUs studied (Fig 3.1B). While subtle, this change results in distinctly different local interactions that influence the positioning of the selectivity helix. In the CCHFV vOTU, Tyr73 forms hydrogen bonds with the backbone of Leu84 within the α 3- α 4 loop. In contrast, the tryptophan residues in the other vOTUs fill into a hydrophobic cleft that involves residues within the selectivity helix. In DGKV vOTU, Trp73 packs with the methylene group of Ser86 on one side and the aliphatic portion of Lys80's side chain on the other. Lys80 itself is stabilized in this permissive conformation by hydrogen bond pairing with the carbonyl of Gly74. In QYBV vOTU, Trp72 packs with Pro85. Additionally, it is in proximity to His79, suggesting potential stacking of the rings. Such an interaction could have an indirect effect on the positioning of Pro76 at the surface of the vOTU-substrate interface. In TAGV vOTU, Trp73 fits between Leu86 and Thr79.

The second area centers around helix α 5 and shows a great degree of variation between the vOTUs (Fig 3.4C, Panel II). It can encompass interactions that can extend to the α 2 and α 3 helices as well as the β 1a sheet with the potential to influence the local structural architecture. CCHFV vOTU possesses a number of interactions within this region, including unique lysine pairings consisting of Lys71, Glu111, Lys110, and Glu76 that accommodate hydrophobic packing with Tyr72 and Phe133. Along with hydrogen bond pairing of Glu78 with Thr102, these work in conjunction in orienting the position of the selectivity helix, a region that has been implicated in substrate preference [32, 34]. The other vOTUs, in contrast, possess fewer interactions but still could influence the structure. In DGKV vOTU, Gln78 within the selectivity helix is central to the interaction, pairing with both Ser102 and Tyr133 by hydrogen bonding. Similarly, for TAGV vOTU Thr76

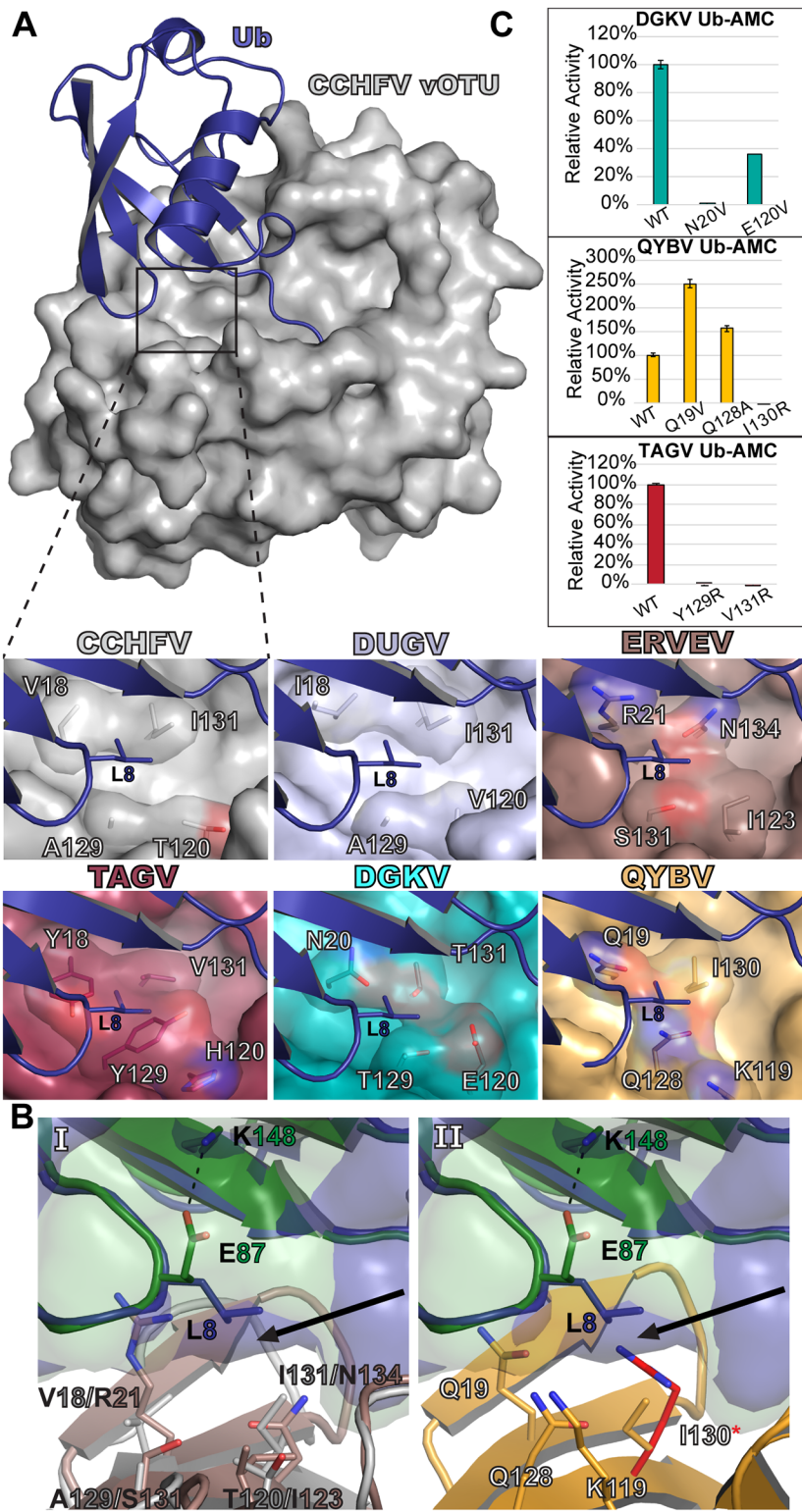
and Glu78 form electrostatic interactions with Gln110 and Tyr133, respectively. In contrast, for QYBV vOTU there do not appear to be any direct interactions with the selectivity helix. Instead, Lys109 and Ser108 form electrostatic interactions with Asp15 and Asn16, respectively, suggesting a role in manipulating the positioning of the β 1- β 1a loop.

The third region consists of the selectivity helix and β 1- β 1a loop themselves (Fig 3.4C, Panel III). Specifically, direct interactions, or the lack thereof, work in conjunction with the other interactions to complete the structural features. This is most notable in QYBV vOTU, in which Phe14 appears to pack with Pro76. In CCHFV vOTU, the corresponding residue is Ile13, which does not appear to be able to bridge the distance and form an interaction. In TAGV vOTU, Asn14 and Thr81 are in general proximity, but appear to be too distant to form a strong interaction with each other. Similarly, DGKV vOTU appears to lack any direct interactions. Overall, these interactions contribute to structural features that influence spatial and chemical presentation of the vOTU interface, potentially affecting how these vOTUs engage substrates.

General deubiquitinating activity can be correlated to a “selectivity pocket”

Binding with Ub often centralizes around the specific hydrophobic residues Leu8, Ile44, and Val70 [41]. Looking at X-ray crystal structures of the CCHFV and DUGV vOTUs bound to Ub reveals that Leu8 in particular has to be spatially accommodated in a pocket deep within the interaction interface (Fig 3.5A). To confirm that this interaction with Leu8 is likewise involved in Ub binding with these other vOTUs, isothermal titration calorimetry (ITC) was performed using the TAGV vOTU to determine the relative binding efficiency of alanine and asparagine Ub mutants (Ub-L8A and Ub-L8N) compared to WT

Fig 3.5. Selectivity pocket of nairovirus vOTUs. (A) The CCHFV vOTU Ub bound structure (PDB ID 3PRP) is shown with the location of the selectivity pocket indicated with a box. The selectivity pockets of the other vOTUs are shown, with the Ub (purple) modeled in from the CCHFV structure based on a secondary alignment of the vOTUs. DUGV vOTU (PDB ID 4HXD) is colored silver and ERVEV vOTU (PDB ID 5JZE) is colored brown. The other vOTUs are colored as in Fig 3.3. All models were generated by aligning the vOTUs with the CCHFV vOTU Ub bound structure in Coot. (B) The extra space (black arrow) existing in the ERVEV-mouse ISG15 structure (PDB ID 5JZE), with the CCHFV vOTU bound to Ub included for comparison (Panel I). QYBV vOTU with Ub and mouse ISG15 (green) modeled in based on vOTU secondary structure alignments, with an arginine also modeled into the space opened up by the mouse ISG15 conformation (Panel II). (C) Activities for Ub-AMC for mutant DGKV, QYBV, and TAGV vOTUs relative to WT. Error bars represent the standard deviation of two independent experiments.



Ub (Table 3.2, 3.S3A Fig). This revealed a stark difference in the affinity. While WT Ub bound strongly with a dissociation constant (K_D) of $11.5 \pm 2.5 \mu\text{M}$, Ub-L8A showed no detectable binding under similar conditions. The Ub-L8N mutant fared only slightly better than the Ub-L8A mutant with a 20 times weaker dissociation constant, K_D of $295.3 \pm 39.7 \mu\text{M}$, compared to WT. These results further underscore the importance of vOTUs being able to accommodate Ub Leu8 in order to have robust deubiquitinating activity. Examining the analogous residues in the other vOTUs reveals a diverse composition for this pocket that could influence how well Leu8 can be accommodated. In TAGV vOTU, this pocket is largely hydrophobic possessing two tyrosines as well as a valine. In contrast, the DGKV and QYBV vOTUs possess more polar residues, including asparagine, glutamate, and threonine for DGKV and glutamine and lysine in QYBV. When considering the activity towards Ub based on the AMC assay, a general trend emerges that correlates the degree of an enzyme's ability to engage mono-Ub with the hydrophobicity of this pocket.

Looking more closely at this interface suggests an additional nuance to the ability to accommodate particular substrates. Specifically, spatio-chemical characteristics could largely influence what defines a good or acceptable pocket composition for binding a given substrate. In the vOTUs that most effectively engage with Ub, such as CCHFV, HAZV, NSDV/GANV, and TAGV, the residue that most directly interfaces with Ub's Leu8 is an isoleucine, valine, or threonine that corresponds to position 131 in CCHFV vOTU (Fig 3.1B, Fig 3.2, Fig 3.5A). This correlation is consistent across the *Nairoviridae* family. Despite being phylogenetically distant from CCHFV and the other robust vOTU DUBs, QYBV demonstrates substantial Ub activity and possesses Ile130 that could pack with Ub's Leu8.

Table 3.2. Isothermal Titration Calorimetry of TAGV-Ub binding.

Protein	N ^a (sites)	K _D (μ M)	ΔH^b (kJ/mol)	ΔG^c (kJ/mol)	-T ΔS^d (kJ/mol)
Ub ^c	1.34 \pm 0.09	11.5 \pm 2.5	-19.6 \pm 1.5	-28.3 \pm 0.6	-8.6 \pm 2.0
Ub-L8A ^e		>1 mM			
Ub-L8N ^e	0.99 \pm 0.14	295.3 \pm 39.7	-11.0 \pm 2.5	-20.2 \pm 0.3	-9.2 \pm 2.9

^a Binding stoichiometry.

^b Binding enthalpy.

^c Gibb's free energy.

^d Entropy factor.

^e Average from n = 3 with error calculated using the standard deviation

<https://doi.org/10.1371/journal.ppat.1007515.t002>

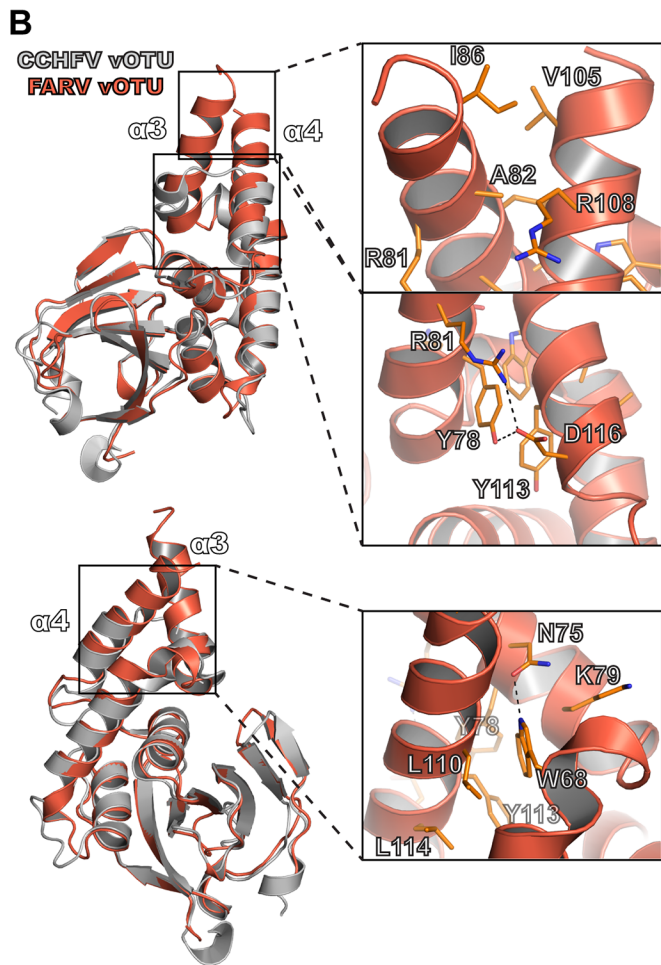
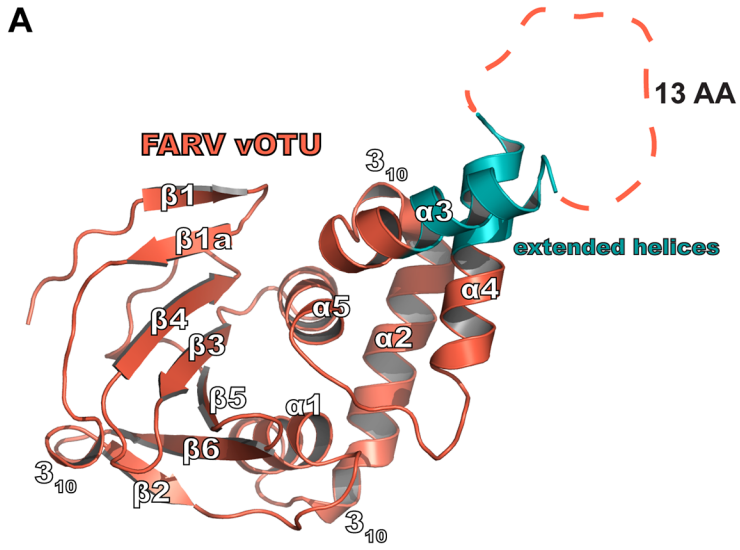
In other vOTUs that have poor Ub activity this residue is typically polar, such as ERVEV's Asn134 (Fig 3.5B, Panel I). This creates an environment that would discourage binding with Ub. Mutation of this residue in ERVEV to the corresponding hydrophobic residues in CCHFV has been observed to generate robust Ub activity [33]. The FARV and ISKV vOTUs appear to have similar characteristics, with both encoding a glutamine at this position. Intriguingly, other vOTUs may go even further in discouraging Ub binding. These include LPHV and HTV-1, which possess an arginine and lysine, respectively, at their equivalent positions to Asn134. Modeling in an arginine at this position, such as what LPHV vOTU possesses, reveals that this type of change would be prohibitive for Ub binding (Fig 3.5B, Panel II).

To test the central role of this pocket for Ub activity, a series of mutants were made in the DGKV, QYBV, and TAGV vOTUs and tested against Ub-AMC (Fig 3.5C). As expected, the disruptive mutants I130R in QYBV and Y129R and V131R in TAGV completely knocked out the ability to process Ub-AMC, in keeping with a previous report demonstrating that the presence of arginine hindered ERVEV vOTU Ub activity [33]. Further, increasing the hydrophobicity of the pocket in QYBV vOTU was able to enhance Ub-AMC cleavage, boosting activity by 150% and 50% for the Q19V and Q128A mutants, respectively. Interestingly, changing the pocket in DGKV vOTU failed to improve activity. This suggests that some vOTUs lacking any outright DUB activity may have evolved to a degree that prevents the generation of this activity through simple changes to better accommodate Leu8 in Ub. This leaves the presence of a Ub Leu8 accommodating pocket in vOTUs as a major marker for deubiquitinating activity and, if present, the ability to dictate variable levels of activity based on the hydrophobicity.

Hughes orthonairovirus vOTUs possess a unique coiled-coil structural feature

While the vOTUs show a range of sequence diversity, most of them possess domains of approximately the same size with one notable exception. Viruses in the *Hughes orthonairovirus* species possess an additional 26-30 amino acids in the middle of the vOTU. When aligned with the other vOTUs, this extra sequence corresponds to the region of the $\alpha 3/\alpha 4$ helices. To assess how this additional sequence influences the structure of vOTUs in this subset of nairoviruses, a crystal structure of FARV vOTU was solved to 2.22 Å (Table 3.1). Inspection of the structure immediately revealed the impact of this additional sequence on the protease's structure (Fig 3.6A). While possessing the familiar core domain and secondary structure features, the protease possesses extended $\alpha 3/\alpha 4$ helices that are connected by several intervening residues. Thirteen residues could not be built due to a lack of well-defined electron density in the crystal structure, and those that could be modeled possess high B factors, suggesting this region to have a high degree of flexibility. This contrasts with the vOTUs from CCHFV and other nairoviruses that possess relatively small $\alpha 3/\alpha 4$ helices connected by a short loop (Fig 3.6B). Additionally, the $\alpha 3/\alpha 4$ helices of FARV vOTU appear to interact with each other in a manner resembling a coiled-coil motif. This is facilitated by hydrophobic packing between Ile86, Val105, Ala82, and the aliphatic portion of the Arg108 sidechain. This relationship between the helices is further promoted by electrostatic interactions, including a salt bridge between Arg81 and Asp116, as well as a hydrogen bond between Tyr78 and Asp116. Beyond this interaction, Tyr78 is also positioned to hydrophobically interact with Tyr113, which together create an environment in which Trp68 can insert. Trp68 further promotes the

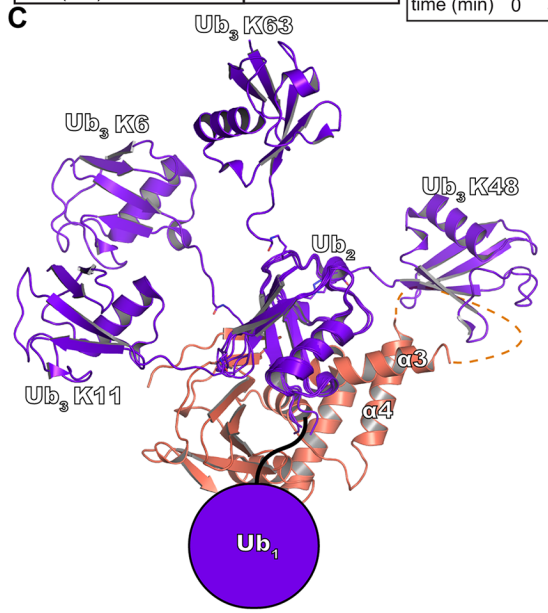
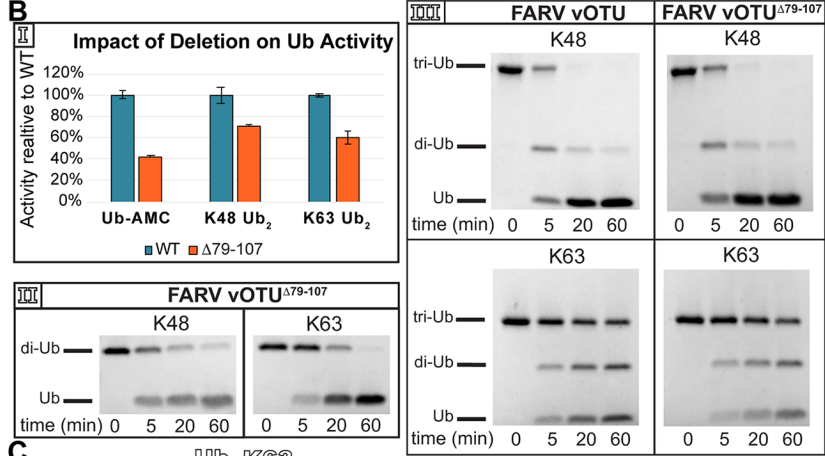
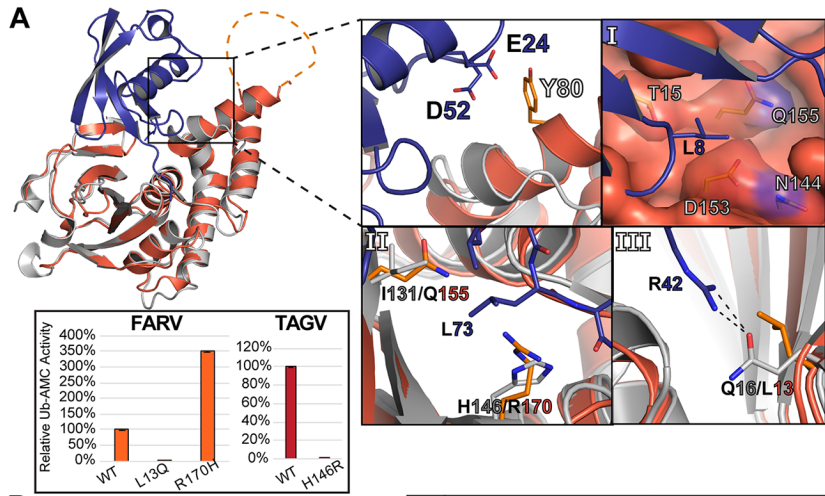
Fig 3.6. Structure of the FARV vOTU. (A) Overall structure of the FARV vOTU with the secondary structure denoted based on DSSP. The extended regions of the $\alpha 3$ and $\alpha 4$ helices are colored in teal. Intervening amino acids lacking electron density are represented by an orange dashed line. (B) Molecular features of the extended $\alpha 3$ - $\alpha 4$ helices of FARV vOTU, with CCHFV vOTU included for comparison. Atom pairs within hydrogen bonding distance are denoted by black dashes.



interaction between these helices through a hydrogen bond with Asn75, as well as through additional hydrophobic packing with Lys79 and Leu110.

The presence of the extra sequence/structural motif in the *Hughes orthonairovirus* species raises the question of whether it could be involved in substrate interaction. A model of how FARV vOTU could interact with Ub further accentuates this possibility, suggesting the $\alpha3/\alpha4$ helices to be in close enough proximity to participate in binding (Fig 3.7). Such an interaction could potentially offset other factors in FARV vOTU are not ideal for binding. Looking at the selectivity pocket of FARV vOTU reveals it to possess more of a hydrophilic character and contains a relatively bulky Gln155 residue in the equivalent site to position 131 in CCHFV (Fig 3.7A, Panel I). Additionally, FARV vOTU possesses a potential steric hindrance to efficient binding with the presence of Arg170 (Fig 3.7A, Panel II). This residue may be less accommodating for the Leu73 in Ub than other vOTUs, such as CCHFV and TAGV which contain a histidine at this site. Further, FARV vOTU may lack a significant interaction that CCHFV vOTU possesses with Arg42 of Ub (Fig 3.7A, Panel III). In contrast to Gln16 in CCHFV vOTU that is able to form a hydrogen bond, FARV vOTU possesses a leucine that is unable form this interaction. To test the influence of these sites on DUB activity, mutations were made to Arg170 and Leu13 in FARV vOTU to histidine and glutamine, respectively. As anticipated, R170H was able to improve Ub-AMC activity, boosting it by ~250%. Making the reverse mutation in TAGV vOTU, H146R, essentially knocked out this activity suggesting this residue to have a key impact in diminishing FARV vOTU's activity compared to other vOTUs. Interestingly, the L13Q mutation in FARV vOTU led to a large reduction in Ub-AMC cleavage. Looking more closely at this region shows that Leu13 is in the middle of a large hydrophobic region in

Fig 3.7. Model of molecular contributors to FARV mono- and poly-Ub activity. (A) FARV vOTU (reddish orange) in a Coot-calculated secondary structure overlay with CCHFV vOTU (gray) bound to Ub (PDB ID 3PRP). The selectivity pocket of FARV vOTU is shown in Panel I, with other elements potentially diminishing FARV vOTU Ub activity in Panels II and III. Black dashes show hydrogen bond interactions. Inset shows the Ub-AMC activity relative to WT of FARV and TAGV vOTU mutants. Error bars represent the standard deviation of two independent experiments. (B) Enzymatic activity of FARV vOTU^{Δ79-107} compared to WT for Ub-AMC and K48/K63 FRET-TAMRA (Panel I), gel cleavage assays of K48/K63 di-Ub with FARV vOTU^{Δ79-107} (Panel II), and gel cleavage assays of K48/K63 tri-Ub with WT FARV vOTU and FARV vOTU^{Δ79-107} (Panel III). (C) Model of tri-Ub binding with FARV vOTU. The proximal Ub of K6 linked (PDB ID 5OHP), K11 linked (PDB ID 5LRV), K48 linked (PDB ID 5E6J), and K63 linked (PDB ID 2JF5) di-Ub was anchored to bound mono-Ub based on a secondary structure alignment in Coot. The filled circle indicates the common space that would likely be occupied by the Ub interacting with the second site of interaction of FARV vOTU.



FARV vOTU (3.S3B Fig). The swap to a large polar residue may impact the structural integrity of the $\beta 1$ - $\beta 1a$ region, further underscoring the nuances created by the variability of this region.

To probe the potential significance of the $\alpha 3/\alpha 4$ motif in offsetting these other effects in FARV vOTU, a construct was synthesized lacking residues 79-107 (“FARV vOTU $\Delta 79-107$ ”) and assessed for activity against Ub substrates (Fig 3.7B). Removing this region reduced activity towards Ub-AMC by almost 60%, suggesting that this motif could play a significant role in Ub binding (Fig 3.7B, Panel I). Interestingly, when tested against K48 and K63 FRET di-Ub substrates a more modest reduction in activity is observed, with only about a 30% and 40% reduction in activity, respectively. This is further borne out with unlabeled di-Ub, with there being no substantial difference between the WT and $\Delta 79-107$ vOTUs over the longer reaction time course (Fig 3.3B and Fig 3.7B, Panel II).

Although the di-Ub cleavage assays are able to differentiate linkage preference, the structural architecture is still relatively simple. To gauge whether this motif can engage with more complex poly-Ub structures, the WT and $\Delta 79-107$ FARV vOTUs were tested with K48 and K63 linked tri-Ub (Fig 3.7B, Panel III). Interestingly, both constructs showed a clear preference for K48 over K63 tri-Ub. This is in contrast to the gel cleavage assay for di-Ub, which showed a slight preference for K63 di-Ub (Fig 3.3B and Fig 3.7B, Panel II). Beyond this, both constructs showed similar patterns of activity for these substrates.

Activity towards di-Ub is influenced by residues outside the central Ubiquitin Interacting Motif.

Despite possessing low to moderate activity towards Ub-AMC, FARV vOTU possesses substantial activity towards some di-Ub linkages (Fig 3.2 and Fig 3.3). This suggests an additional site of interaction with the proximal Ub molecule that substantially increases the overall efficiency. To ascertain where this site may be located, a model of how FARV vOTU may bind di-Ub was generated (Fig 3.8). Examining the potential interface with the proximal Ub, two residues in FARV vOTU, Arg30 and Lys32, immediately stand out as potential contributors. These residues are just beyond the active site, and are part of a region that likely forms the closest contact with the proximal Ub. Beyond these two residues, Thr147 of FARV vOTU also stands out as being in an area with a higher R.m.s.d. between the vOTU structures, which in FARV vOTU positions it closer to the general area of the proximal Ub (Fig 3.1B and 3.S2 Fig).

To assess whether these sites could play a role in the FARV vOTU's interaction with di-Ub, mutations at these positions were designed in an attempt to alter activity towards K48 and K63 FRET di-Ub substrates. As a control, each mutant was also run with mono-Ub substrates. Due to the proximity of Arg30 and Lys32 to the space that would be occupied by the fluorogenic molecule, assays were performed with both Ub-AMC and Ub-Rhodamine110 (Rh110) to mitigate artifacts. Excitingly, these mutations substantially altered the rate of di-Ub cleavage, often towards both substrates (Fig 3.8). Individually mutating Arg30 and Lys32 to leucine reduces activity towards K48 di-Ub to 43-55% of wildtype and activity towards K63 to 56-70%. Although the mono-Ub activity appears to suffer as well in the case of R30L, the ~30% difference in the Ub-AMC versus Ub-Rh110

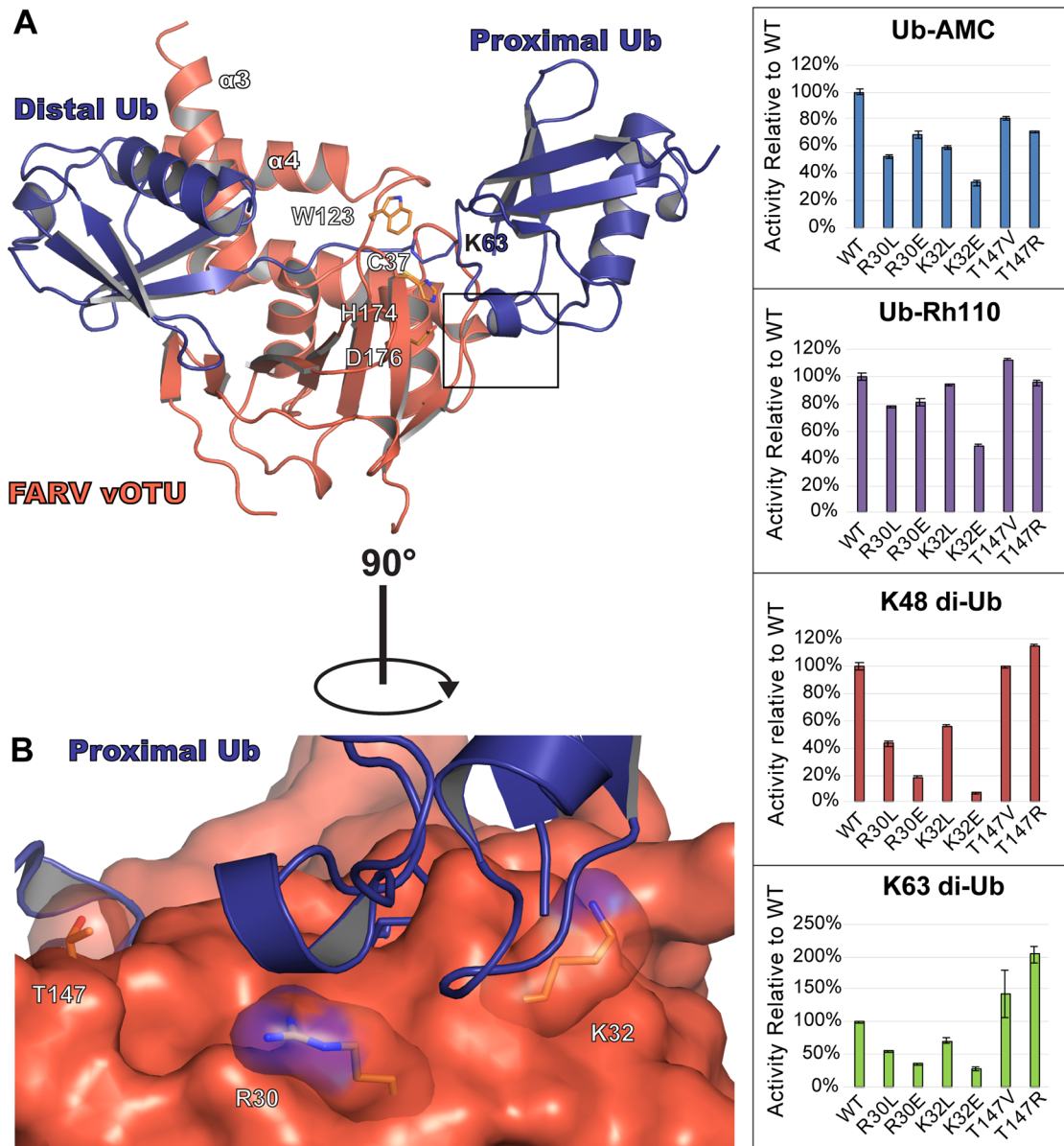


Fig 3.8. Second site of FARV vOTU interaction with di-Ub. (A) Model of FARV vOTU (reddish orange) bound to K63-linked di-Ub (purple; PDB ID 2JF5). FARV vOTU was overlaid with CCHFV vOTU bound to Ub (PDB ID 3PRP; not rendered) based on secondary structure alignment of the vOTUs. The distal Ub was anchored to the bound mono-Ub by aligning the secondary structure in Coot, followed by manual bond rotations within Lys63 of the proximal Ub in PyMol to model a plausible fit with minimal clashes based on the CCHFV vOTU active site and protease surface. The predicted region of FARV vOTU engagement with the proximal Ub is indicated by a black box. (B) Closeup view of the predicted region, with the residues selected for mutation shown as sticks. Activity of the mutants relative to WT is shown for Ub-AMC, Ub-Rh110, K48 di-Ub FRET-TAMRA, and K63 di-Ub FRET-TAMRA (right).

mono-Ub substrates suggests this to be an artifact of interactions with the AMC fluorophore. Otherwise, these mutants had little or no effects on mono-Ub activity. When a charge flip was introduced at position 30, activity was reduced to 18% for K48 and 35% for K63 while not substantially altering the activity for mono-Ub. A charge flip at position 32 had the most pronounced effect, driving it down to 7% for K48 and 38% for K63. However, there is also a substantive corresponding reduction in both the AMC and Rh110 mono-Ub substrates, indicating a potentially large disruptive interaction with the hydrophobic fluorophores or possible influence on the local fold. Interestingly, while mutating Thr147 to valine did not appreciably change the activity, introducing an arginine at this position increased the activity by 15% for K48 and doubled it for K63, suggesting the longer sidechain may be able to form a new interaction.

Discussion

Taking advantage of Ub conservation

Ub is among the most conserved and important cellular regulatory components, influencing almost every key aspect of cell biology. Ub itself is tightly regulated by an array of endogenous DUB enzymes that specifically curb and tailor its effects. The realization that viruses also possessed enzymes with DUB activity introduced a paradigm in which these normal regulatory mechanisms could be manipulated to suppress immune responses and enhance viral propagation [19, 42-45]. Further investigation into these mechanisms continues to uncover how these viral DUBs disrupt cellular responses to infection. In particular, the role of robust DUB activity in promoting viral replication and conferring virulence in CCHFV and SARS-CoV emphasizes the impact of the respective

proteases and highlights the emerging importance of understanding their effects when considering potential pathogenicity and therapeutic strategies.

With the almost perfectly conserved sequence of Ub, it is not surprising that tick-borne nairoviruses from disparate taxa possess notable DUB activity. Such a mechanism could provide broad utility in infecting hosts beyond the primary arthropod reservoir by enabling a route of horizontal as well as vertical transmission that amplifies viral replication. The diversity in the observed activity, however, raises questions as to the specific effects relating to arthropod versus vertebrate hosts. In general, the vOTUs from viruses most closely related to CCHFV appear to have the most substantial DUB activity based on the Ub-AMC assay (Figs 3.1 and 3.2). These viruses are known to cause viremia in vertebrate hosts, including mammals. This raises the prospect that increased Ub activity may be an adaptive mechanism allowing these nairoviruses to infect a wider host range. While ticks are known to possess RNAi and Toll sensing-mediated antiviral responses, there is little information pertaining to whether Ub plays a significant role in arthropod responses to viral infection [46-48]. Further characterization of Ub systems in arthropods will be needed to shed light into these questions and would clarify the significance of vOTU enzymatic diversity in nairovirus adaptation for arthropod versus vertebrate hosts.

Nairovirus vOTUs have activity towards poly-Ub linkages involved in significant immune signaling processes

In contrast to some mammalian DUBs, OTU proteases generally show poly-Ub linkage specificity that ranges from moderate to highly specific [38]. Nairovirus vOTUs reflect this tendency, possessing activity towards poly-Ub linkages that is neither highly promiscuous nor completely selective for a single linkage type with each vOTU

possessing its own respective preferences for the different linkages. While showing individual variation, the vOTUs consistently show the ability to process K6, K11, K48, and K63 linked di-Ub. The fact that nairovirus vOTUs generally show activity towards K48 and K63 di-Ub is significant. These well-studied forms of di-Ub have clearly established roles for cellular processes in general, as well as in antiviral responses specifically. It can be easily envisioned how disruption of K48 and K63-mediated functions could dampen antiviral responses. It is intriguing, however, that vOTUs as a whole also possess substantial activity towards K6 and K11 linkages. These forms of Ub have been studied much less extensively, with roles that have typically been associated with DNA damage responses and cell cycle regulation [49, 50]. As part of the L protein, vOTU activity would be restricted to the cytosol, raising questions as to whether these observed activities of vOTUs are incidental, or if there are important cytosolic functions of K6 and K11 linkages that could be manipulated. Recent studies have begun to expand knowledge of these linkages. Specifically, K11 poly-Ub has been associated with TNF signaling, providing a direct link to the innate immune response [51]. Even more recently, K6 has emerged as a key component in regulating mitophagy [52, 53]. Given the key role of mitochondria in innate immunity, this raises an interesting question of how vOTU activity could impact this process, and whether such manipulation could provide benefits for the virus [54]. What other functions remain to be identified for these linkages is still an open question, as well as how vOTUs may engage with them to modify cellular responses. The differences in linkage preferences between vOTUs implies potential differences in the degree to which specific viruses may influence these pathways. Alternatively, it's possible that the relative

importance of the linkages may differ in different hosts, and that different vOTU preferences reflects virus adaptation to their specific preferred hosts.

Influence of genomic diversity on the Nairovirus vOTU fold

The new vOTU structures reveal an array of conserved and divergent features. The conserved elements of Nairovirus vOTU structure distinguishes these from other OTU proteases, as highlighted by how they cluster together in a structure-based phylogenetic tree (Fig 3.1A, inset; [34, 55, 56]). Most notably, this includes the presence of two additional beta sheets and a helix at the N-terminus of vOTUs that are absent from eukaryotic OTUs. While possessing these characteristic features of the vOTU fold, the nairoviruses show distinguishable differences from each other that can be traced to specific residue differences. This is particularly noteworthy when looking at the relationship between the selectivity pocket and the observed Ub activity by a given protease. It is significant that vOTUs possessing the highest activity for Ub all possess highly hydrophobic residues in this region. While many of the vOTUs possessing robust DUB activity are closely related phylogenetically, the presence of substantial activity in the more distantly related QYBV vOTU demonstrates that it is not exclusive to this subset of viruses. This suggests the vOTU fold to be a flexible platform that has allowed DUB activity to evolve independently to the benefit of each virus. Beyond the central role of this pocket that is deep in the binding interface, the vOTUs also display structural diversity in more peripheral regions. This includes areas that have been observed to influence substrate binding in vOTUs, such as the $\alpha 3$ selectivity helix, suggesting a potential impact on how vOTUs engage with other proteins.

Possible functions of the structural motif in the Hughes orthonairovirus species

Viruses in the *Hughes orthonairovirus* species possess a motif previously unobserved for OTU domains. This raises the question of whether this structural feature could have a functional impact. In particular, whether this motif could impact engagement with substrate. The effect of removing this motif from the FARV vOTU on Ub-AMC activity suggests that it can at least contribute to mono-Ub binding. This is consistent with what is observed when comparing FARV vOTU to a Ub-bound structure of CCHFV vOTU, where elements of this motif are in proximity for potential interactions with Ub (Fig 3.7A). This additional interface provided by the motif likely compensates for the presence of other less optimal factors for Ub binding, including an arginine that hinders interaction with the tail of Ub. Overall, these structural features suggest a mixture of elements that either promote or hinder interaction, with some that may carry a more dominant effect. The involvement of the structural motif in FARV vOTU formed by the two helices and intervening loop, which we also refer to as a substrate interacting bundle (SIB), suggests it may form a region that introduces potential to engage with otherwise inaccessible surfaces.

Interestingly, removing the SIB motif from FARV vOTU appears to have a lesser impact on di-Ub activity compared to mono-Ub (Fig 3.7B). This could be accounted for by the presence of an additional site of interaction in FARV vOTU that interacts with the proximal Ub. The existence of one or more subsites has been postulated as a mechanism for discriminating different di-Ub linkages based on the proximal Ub, and has been demonstrated in several mammalian OTUs [38, 39]. While not definitively observed in vOTUs, the ability to distinguish between different linkages implies a similar mechanism.

The FARV vOTU mutants provide the first reported direct evidence identifying such a site in a vOTU, confirming that vOTUs can utilize this mechanism to distinguish various linkages. In addition to supplying potential leads for elucidating such sites in other vOTUs, it also demonstrates a case where this site can have a major impact on activity towards substrate, even when factors hindering binding with the distal Ub are present.

Although di-Ub wouldn't directly interact with the SIB motif in a manner that would directly influence cleavage, it is possible that a more complex poly-Ub structure could engage with it. Modeling how tri-Ub might bind suggests that a K48 linkage could place one of the Ub molecules in close proximity to the structural motif (Fig 3.7C). In contrast, for the other linkages FARV vOTU most readily cleaves—K6, K11, and K63—this Ub would likely be too distant to form any interaction. Surprisingly, removal of the SIB motif has no noticeable impact on K48 tri-Ub cleavage, despite the apparent proximity the tri-Ub could have. It's possible that tri-Ub may not possess a large enough architecture to be influenced by the SIB motif, and that a longer poly-Ub may interact with it. Additionally, Ub is able to form complex chains consisting of multiple linkage types [57]. It may be that the SIB motif can engage more effectively with these “heterotypic” Ub chains. Alternatively, the primary role of the SIB motif may go beyond Ub and facilitate interactions with other binding partners. The vOTU domain exists in the context of the multifunctional L protein. Apart from the vOTU domain, the structural features and dynamics of the nairovirus L protein are currently unknown. This leaves open the possibility that the SIB motif could be involved in binding another feature of the L protein to stabilize the overall architecture, or in facilitating interactions with other proteins. In addition, the SIB motif could potentially bind to other host factors in the innate immune

system. Viruses in the *Hughes orthonairovirus* species have been isolated from birds or from ticks that infest them. The immune system of birds, including antiviral responses, possesses considerable differences from mammals in terms of what elements are present and how they are regulated (reviewed in [58] and [59]). This includes the apparent absence of an ISG15 homologue in birds. These differences from mammals raises the possibility that the SIB motif could play a role in adaptation to the avian innate immune system, perhaps by facilitating interactions with proteins other than Ub. In addition, the lack of ISG15 in birds leaves open the possibility that the motif could engage with other Ub-like entities that are involved in regulating the innate immune response.

Challenges to defining vOTU function

While divergent vOTUs possess the ability to engage with Ub, it is possible that this may not be the only, or even predominant function of all vOTUs. In the case of ERVEV, it has been observed that it possesses poor activity towards Ub, while showing potent ability to engage with ISG15 (Fig 3.2; [32, 33]). This raises the possibility that other vOTUs that possess poor Ub activity may be able to engage with other Ub-like entities. While none of the new vOTUs assessed possess notable deISGylase activity, the availability of AMC-derived substrates is limited to human ISG15 (hISG15). In contrast to Ub, ISG15 shows considerable species-species variances that have been shown to impact binding with viral proteins, including vOTUs from nairoviruses [33, 60, 61]. This leaves open the possibility that vOTUs, while not engaging with hISG15, may still possess the ability to interact with ISG15 from species they productively infect. The presence of arginine, lysine, or glutamine in the selectivity pocket of several of the vOTUs, while not ideal for Ub, may still allow them to engage with other substrates. The structure of the

ERVEV vOTU bound to mouse ISG15 (mISG15) has a gap in the area that Ub's Leu8 would typically occupy (Fig 3.5B, Panel I). Modeling suggests that this feature would also be more permissive of binding with vOTUs possessing a bulky residue such as arginine at position 131 (Fig 3.5B, Panel II). This gap is caused by a pairing of Glu87 with Lys148 in mISG15 that pulls the sidechain of Glu87 away from the interface, and suggests a possible mechanism that could allow vOTUs with hydrophilic or bulky residues to effectively engage with non-Ub moieties. As highlighted by the lack of ISG15 in birds, however, it's also possible that vOTUs, particularly in the *Hughes orthonairovirus* species, may engage with other Ub-like entities that can modulate the immune response. The lack of either Ub or ISG15 activity in a number of vOTUs further accentuates this possibility, implying possible biochemical functions that have yet to be characterized among vOTUs. Further developments shedding light on these questions could yield key insights into these influential virus-host interactions.

Conclusion

The recent increase in genomic characterization of nairoviruses has uncovered a wealth of diversity among them. While our knowledge of nairoviral sequence diversity has expanded, much is still unknown on how this variability affects virus-host relationships. The exact range of vertebrate hosts and their disease state upon infection is not presently known for all members of the *Nairoviridae* family. This novel characterization of nairovirus vOTUs reveals a diversity in the ability to engage mono- and poly-Ub that mirrors the genomic diversity. Additionally, this study uncovers motifs that appear to play a predominant role in determining these preferences, making it feasible to begin predicting DUB activity in uncharacterized or newly discovered nairoviruses. Given

the presence of robust DUB activity in nairoviruses known to infect humans, including CCHFV and NSDV, this could serve as an early flag for assessing the risk posed by emerging viruses, and may shed light on the evolutionary trends leading to some viruses to having this capability over others. Further, these new structure and activity insights provide a platform to continue the development of robust tools, such as poly-Ub specific vOTUs, that can be paired with reverse genetics systems to better understand the role of the vOTU in the course of a viral infection and how differences in certain activities impact nairoviruses. Such knowledge could help propel the field in fully elucidating the detailed functional mechanism of the vOTU in the viral life cycle, potentially aiding in the development of better disease model systems. In addition, it provides insight that will further gauge the prospects of the vOTU as a therapeutic target for nairovirus-caused diseases such as CCHF, either through the development of specific inhibitors or live attenuated virus vaccines. Further, the diversity of the vOTU suggests a potential relationship with viral host adaptation, and that the role of the vOTU may extend beyond its well-known function in engaging with Ub and/or ISG15.

Methods

Construction, expression, and purification of vOTUs

The vOTUS were constructed and expressed as previously described in published methods [32, 55]. Purification of QYBV, TAGV, and DGKV were carried out as previously described. For FARV, a slightly different approach altered from the previously described method was used to optimize the expression. *E. coli* strains with vOTUs from FARV were grown at 37°C in 6 L of Luria-Bertani broth with 100 µg/ml ampicillin. Once the optical density reached 0.6-0.8, 0.8 mM isopropyl-β-D-thiogalactopyranoside (IPTG)

was added to induce gene expression. The temperature was then dropped to 25°C and expression continued overnight. The culture was subsequently centrifuged at 5000xg for 10 minutes and the pelleted cells stored at -80°C.

Enzymatic assays

Assays were carried out as described previously [32, 33]. Briefly, assays were run in 100 mM NaCl, 50 mM HEPES [pH 7.5], 0.01 mg/mL BSA, 5 mM dithiothreitol (DTT) at 25°C. Reactions were run in 96-well plates with a 50 µl reaction volume using a CLARIOstar plate reader (BMG Labtech, Inc.). For Ub-AMC, all vOTUs were assessed at a final enzyme concentration of 4 nM. For ISG15-AMC, vOTUs were assessed at a final enzyme concentration of 20 nM with the exception of NSDV, GANV, and ERVEV, which were run at a final enzyme concentration of 4 nM due to the high activity towards the substrate. Both Ub-AMC and ISG15-AMC assays were run at a final substrate concentration of 1 µM. Assays with Ub-Rh110 were run under the same reaction conditions as Ub-AMC with instrument settings adjusted to optimize detection of the fluorophore. For DGKV vOTU additional assays were run with the WT and E152D mutant using the peptide Z-RLRGG-AMC (Bachem) substrate with protease concentrations of 4 µM and a substrate concentration of 50 µM.

Poly-Ub cleavage assays

Assays with FRET TAMRA/QXL pair tagged K11, K48, and K63 di-Ub substrates were performed as previously described with 4 nM vOTU and 1 µM substrate [32]. Untagged poly-Ub cleavage assays were adapted from the previously published method. Briefly, 4 nM of each vOTU was tested against 10 µM Linear (M1), K6, K11, K27, K29, K33, K48, and K63 linked di-Ub (Boston Biochem, MA). Reactions were initiated by the

addition of vOTU and incubated at 37°C in reaction buffer (100 mM NaCl, 5 mM HEPES [pH 7.5], 2 mM DTT). The reactions were stopped at the time points indicated by mixing 5 µl of each reaction with 2x Laemmli sample buffer and heat killed by boiling at 98°C for 5 minutes. The cleavage over time was visualized using 8-16% Mini-Protean TGX precast gels (Bio-Rad) by Coomassie staining. Assays with K48 and K63 linked tri-Ub were run in the same manner except that tri-Ub was present at 20 µM.

Crystallization of vOTUs

All four vOTUs were screened against a series of Qiagen NeXtal suites in a 96-well hanging drop format with a TTP LabTech Mosquito (TTP Labtech, Herfordshire, United Kingdom). QYBV vOTU was screened at 11.36 mg/ml, TAGV vOTU at 12.70 mg/ml, DGKV vOTU at 10.96 mg/ml, and FARV vOTU at 10.96 mg/ml. Initial hits were optimized along salt, precipitant, and pH gradients as applicable. The TAGV and FARV vOTU hits were also optimized with an Additive HT Screen from Hampton Research. Final optimized crystals for all four vOTUs were flash frozen in cryoprotective solutions. For QYBV vOTU, the final optimized crystals were in 0.3 M magnesium acetate and 16% PEG 3350, with 0.3 M magnesium acetate, 20% PEG 3350, and 18% of a 1:1:1 solution of ethylene glycol, dimethyl sulfoxide, and glycerol (EDG) as the cryoprotectant. The final crystals for TAGV vOTU were grown in 0.15 M magnesium formate, 22% PEG 3350, with 0.25 M TCEP as an additive, with a cryoprotectant solution consisting of 0.15 M magnesium formate, 22% PEG 3350, 18% EDG. Final optimized crystals for DGKV vOTU were found in the condition with 0.1 M citric acid pH 3.5, 13% PEG 6000 and were flash frozen in 0.1 M citric acid pH 3.5, 20% PEG 6000, 18% EDG. For FARV vOTU, the final optimized crystals were grown in 0.3 M magnesium chloride, 0.1 M MES pH 6.5, and

8% PEG 4000, and flash frozen in 0.3 M magnesium chloride, 0.1 M MES pH 6.5 and 20% PEG 4000 as the cryoprotectant. For selenomethionyl (Se-Met) derivative QYBV vOTU crystals, bacterial cells were grown in minimal media to OD 0.6 and induced with 0.8 mM IPTG at 37°C for 4 hrs. Prior to induction, the cultures were supplemented with eight amino acids (Leu, Ile, Val, and Trp at 0.05 g/L; Thr, Lys, Phe, and Cys at 0.1 g/L) as well as selenomethionine (0.12 g/L). Cells were harvested and protein purified as previously described. Final crystals were grown in 0.3 M magnesium acetate, 16% PEG 3350, in drops formed from 1 μ l of solution and 2 μ l of 9.45 mg/ml protein. Native datasets of the QYBV, DGKV, TAGV, and FARV vOTUs were collected at a wavelength of 1 Å. A Se-Met single anomalous dispersion (SAD) dataset for QYBV vOTU was collected at the absorption edge of Se at 0.9792 Å.

Structural solutions of vOTUs

The data sets were indexed, integrated and scaled with HKL-2000 [62]. Experimental phasing of the Se-Met-SAD dataset was performed using the Phenix suite of programs [63]. HySS was utilized to locate the Se-Met sites, with Phaser solving the experimental phases [64-66]. Initial model building was performed using AutoBuild, with subsequent cycles of Refinement and model building carried out in Phenix and Coot ([63, 67, 68]. This structure was then used as a search model to solve the QYBV vOTU native dataset by Molecular Replacement in Phaser [66]. The other vOTUs were solved by Molecular Replacement. A QYBV vOTU-based homology model was used to solve DGKV vOTU, while homology models based on DUGV vOTU (PDB entry 4HXD) were used to solve TAGV vOTU and FARV vOTU. All the structures were built with

Autobuild, followed by alternating manual building and refinement in Coot and Phenix. Structures were validated using the MolProbity server [69].

Generation of vOTU and Ub mutants

Mutations were made using the QuikChange Lightning Kit according to the manufacturer's protocol (Agilent Technologies, Inc.). The PCR-generated plasmids were transformed into *Escherichia coli* NEB-5 α cells by heat shock. The mutant plasmids were confirmed by sequencing and transformed into T7 Express cells (New England Biolabs).

Isothermal Titration Calorimetry of TAGV vOTU binding with Ub, Ub-L8A, and Ub-L8N

T7 Express cells expressing Ub, Ub-L8A, and Ub-L8N in pET-15b were grown to OD 0.6-0.8 at 37°C. Expression was induced with 0.5 mM IPTG and continued at 18°C overnight. The cells were pelleted and stored as described above. The pellet was resuspended in 500 mM NaCl, 50 mM Tris [pH 7.5] supplemented with lysozyme at 4°C for 30 minutes. The cells were sonicated on ice at 70% power with a 50% duty cycle for a total of 6 minutes, followed centrifugation at 48,000xg for 45 minutes. The supernatant was filtered through a 0.8 μ m and applied to a gravity flow Ni-NTA column (GoldBio) pre-equilibrated with 500 mM NaCl, 50 mM Tris [pH 7.5]. The column was washed with the same buffer containing 30 mM imidazole, followed by elution with 300 mM imidazole. Thrombin was added to cleave the 6X His-tag and the elution dialyzed overnight in 250 mM NaCl, 25 mM HEPES [pH 7.5], 2 mM DTT at 4°C. After dialysis the protein was filtered through a 0.22 μ m membrane and run over a Superdex 200 column (GE Healthcare) equilibrated with 100 mM NaCl, 5 mM HEPES [pH 7.5], 2 mM DTT. The fractions were pooled based on the chromatogram and concentrated to ~2-2.5 mM, supplemented with

5% glycerol, and flash frozen in liquid nitrogen followed by storage at -80°C until further use. TAGV vOTU was purified as previously described and dialyzed alongside Ub and Ub-L8N in 150 mM NaCl, 50 mM HEPES [pH 7.5], 1 mM TCEP overnight at 4°C. ITC was performed with a Microcal PEAQ-ITC (Malvern, Worcestershire, UK). Ub or Ub-L8N were titrated into the cell in series of 19 injections, 2 μ L each with a spacing of 180 seconds. The temperature was kept constant at 25°C with a reference power ranging from 6-10 μ cal/s. For the TAGV vOTU binding with WT Ub the vOTU was present in the cell at 114-134 μ M with Ub at 1.26-1.29 mM in the syringe. For TAGV vOTU binding with Ub-L8A the vOTU was present in the cell at 111-114 μ M with Ub-L8A at 1.32-1.35 mM in the syringe. For TAGV vOTU binding with Ub-L8N the vOTU was present in the cell at 234-235 μ M in the cell and Ub-L8N at 4.67-4.74 mM in the syringe. The data was processed in the Microcal PEAQ-ITC Analysis Software and fit to an independent model. Values for Ub and Ub-L8N represent the average and standard deviation of three independent runs for each experiment.

Accession numbers

Final protein structures were deposited in the Protein Data Bank with IDs 6DWX, 6DX1, 6DX2, 6DX3, and 6DX5 for Se-Met QYBV vOTU, native QYBV vOTU, DGKV vOTU, TAGV vOTU, and FARV vOTU respectively.

Acknowledgments

Data were collected at Southeast Regional Collaborative Access Team (SER-CAT) 22-ID beamline at the Advanced Photon Source, Argonne National Laboratory and the University of Georgia X-ray diffraction Core Facility (XRDC). The findings and

conclusions in this report are those of the authors and do not necessarily represent the official position of the Centers for Disease Control and Prevention.

References

1. Alkhovsky SV, Lvov DK, Shchetinin AM, Deriabin PG, Shchelkanov MY, Aristova VA, et al. Complete Genome Coding Sequences of Artashat, Burana, Caspiy, Chim, Geran, Tamdy, and Uzun-Agach Viruses (Bunyavirales: Nairoviridae: Orthonairovirus). *Genome Announc.* 2017;5(40). Epub 2017/10/07. doi: 10.1128/genomeA.01098-17. PubMed PMID: 28983005; PubMed Central PMCID: PMC5629062.
2. Kuhn JH, Wiley MR, Rodriguez SE, Bao Y, Prieto K, Travassos da Rosa AP, et al. Genomic Characterization of the Genus Nairovirus (Family Bunyaviridae). *Viruses.* 2016;8(6). Epub 2016/06/15. doi: 10.3390/v8060164. PubMed PMID: 27294949; PubMed Central PMCID: PMC4926184.
3. Maes P, Alkhovsky SV, Bao Y, Beer M, Birkhead M, Briese T, et al. Taxonomy of the family Arenaviridae and the order Bunyavirales: update 2018. *Arch Virol.* 2018;163(8):2295-310. doi: 10.1007/s00705-018-3843-5. PubMed PMID: 29680923.
4. Walker PJ, Widen SG, Firth C, Blasdel KR, Wood TG, Travassos da Rosa AP, et al. Genomic Characterization of Yogue, Kasokero, Issyk-Kul, Keterah, Gossas, and Thiafora Viruses: Nairoviruses Naturally Infecting Bats, Shrews, and Ticks. *Am J Trop Med Hyg.* 2015;93(5):1041-51. Epub 2015/09/02. doi: 10.4269/ajtmh.15-0344. PubMed PMID: 26324724; PubMed Central PMCID: PMC4703270.
5. Walker PJ, Widen SG, Wood TG, Guzman H, Tesh RB, Vasilakis N. A Global Genomic Characterization of Nairoviruses Identifies Nine Discrete Genogroups with Distinctive Structural Characteristics and Host-Vector Associations. *Am J Trop Med Hyg.* 2016;94(5):1107-22. Epub 2016/02/24. doi: 10.4269/ajtmh.15-0917. PubMed PMID: 26903607; PubMed Central PMCID: PMC4856612.
6. Bente DA, Forrester NL, Watts DM, McAuley AJ, Whitehouse CA, Bray M. Crimean-Congo hemorrhagic fever: history, epidemiology, pathogenesis, clinical syndrome and genetic diversity. *Antiviral Res.* 2013;100(1):159-89. Epub 2013/08/03. doi: 10.1016/j.antiviral.2013.07.006. PubMed PMID: 23906741.
7. Burt FJ, Spencer DC, Leman PA, Patterson B, Swanepoel R. Investigation of tick-borne viruses as pathogens of humans in South Africa and evidence of Dugbe virus infection in a patient with prolonged thrombocytopenia. *Epidemiol Infect.* 1996;116(3):353-61. Epub 1996/06/01. PubMed PMID: 8666081; PubMed Central PMCID: PMC2271429.

8. Dandawate CN, Work TH, Webb JK, Shah KV. Isolation of Ganjam virus from a human case of febrile illness: a report of a laboratory infection and serological survey of human sera from three different states of India. *Indian J Med Res.* 1969;57(6):975-82. Epub 1969/06/01. PubMed PMID: 5823182.
9. L'Vov D K, Kostiukov MA, Daniyarov OA, Tukhtaev TM, Sherikov BK. [Outbreak of arbovirus infection in the Tadzhik SSR due to the Issyk-Kul virus (Issyk-Kul fever)]. *Vopr Virusol.* 1984;29(1):89-92. Epub 1984/01/01. PubMed PMID: 6143452.
10. Rao CV, Dandawate CN, Rodrigues JJ, Rao GL, Mandke VB, Ghalsasi GR, et al. Laboratory infections with Ganjam virus. *Indian J Med Res.* 1981;74:319-24. Epub 1981/09/01. PubMed PMID: 6797936.
11. Treib J, Dobler G, Haass A, von Blohn W, Strittmatter M, Pindur G, et al. Thunderclap headache caused by Erve virus? *Neurology.* 1998;50(2):509-11. Epub 1998/03/04. PubMed PMID: 9484383.
12. Kalunda M, Mukwaya LG, Mukuye A, Lule M, Sekyalo E, Wright J, et al. Kasokero virus: a new human pathogen from bats (*Rousettus aegyptiacus*) in Uganda. *Am J Trop Med Hyg.* 1986;35(2):387-92. Epub 1986/03/01. PubMed PMID: 3082234.
13. Davies FG. Nairobi sheep disease. *Parassitologia.* 1997;39(2):95-8. Epub 1997/06/01. PubMed PMID: 9530691.
14. Ishii A, Ueno K, Orba Y, Sasaki M, Moonga L, Hang'ombe BM, et al. A nairovirus isolated from African bats causes haemorrhagic gastroenteritis and severe hepatic disease in mice. *Nat Commun.* 2014;5:5651. Epub 2014/12/03. doi: 10.1038/ncomms6651. PubMed PMID: 25451856; PubMed Central PMCID: PMC4268697.
15. Begum F, Wisseman CL, Jr., Casals J. Tick-borne viruses of West Pakistan. II. Hazara virus, a new agent isolated from *Ixodes redikorzevi* ticks from the Kaghan Valley, W. Pakistan. *Am J Epidemiol.* 1970;92(3):192-4. Epub 1970/09/01. PubMed PMID: 5458947.
16. Dowall SD, Findlay-Wilson S, Rayner E, Pearson G, Pickersgill J, Rule A, et al. Hazara virus infection is lethal for adult type I interferon receptor-knockout mice and may act as a surrogate for infection with the human-pathogenic Crimean-Congo hemorrhagic fever virus. *J Gen Virol.* 2012;93(Pt 3):560-4. Epub 2011/11/18. doi: 10.1099/vir.0.038455-0. PubMed PMID: 22090213.
17. Converse JD, Hoogstraal H, Moussa MI, Feare CJ, Kaiser MN. Soldado virus (Hughes group) from *Ornithodoros (Alectorobius) capensis* (Ixodoidea: Argasidae) infesting Sooty Tern colonies in the Seychelles, Indian Ocean. *Am J Trop Med Hyg.* 1975;24(6 Pt 1):1010-8. Epub 1975/11/01. PubMed PMID: 1200252.
18. Bergeron E, Albarino CG, Khristova ML, Nichol ST. Crimean-Congo hemorrhagic fever virus-encoded ovarian tumor protease activity is dispensable for virus

RNA polymerase function. *J Virol.* 2010;84(1):216-26. Epub 2009/10/30. doi: 10.1128/JVI.01859-09. PubMed PMID: 19864393; PubMed Central PMCID: PMC2798392.

19. Frias-Staheli N, Giannakopoulos NV, Kikkert M, Taylor SL, Bridgen A, Paragas J, et al. Ovarian tumor domain-containing viral proteases evade ubiquitin- and ISG15-dependent innate immune responses. *Cell Host Microbe.* 2007;2(6):404-16. Epub 2007/12/15. doi: 10.1016/j.chom.2007.09.014. PubMed PMID: 18078692; PubMed Central PMCID: PMC2184509.

20. Holzer B, Bakshi S, Bridgen A, Baron MD. Inhibition of interferon induction and action by the nairovirus Nairobi sheep disease virus/Ganjam virus. *PLoS One.* 2011;6(12):e28594. Epub 2011/12/14. doi: 10.1371/journal.pone.0028594. PubMed PMID: 22163042; PubMed Central PMCID: PMC3230622.

21. Bakshi S, Holzer B, Bridgen A, McMullan G, Quinn DG, Baron MD. Dugbe virus ovarian tumour domain interferes with ubiquitin/ISG15-regulated innate immune cell signalling. *J Gen Virol.* 2013;94(Pt 2):298-307. Epub 2012/11/09. doi: 10.1099/vir.0.048322-0. PubMed PMID: 23136361; PubMed Central PMCID: PMC3709621.

22. Bowie AG, Unterholzner L. Viral evasion and subversion of pattern-recognition receptor signalling. *Nat Rev Immunol.* 2008;8(12):911-22. Epub 2008/11/08. doi: 10.1038/nri2436. PubMed PMID: 18989317.

23. Sadler AJ, Williams BR. Interferon-inducible antiviral effectors. *Nat Rev Immunol.* 2008;8(7):559-68. Epub 2008/06/26. doi: 10.1038/nri2314. PubMed PMID: 18575461; PubMed Central PMCID: PMC2522268.

24. Rodriguez MR, Monte K, Thackray LB, Lenschow DJ. ISG15 functions as an interferon-mediated antiviral effector early in the murine norovirus life cycle. *J Virol.* 2014;88(16):9277-86. Epub 2014/06/06. doi: 10.1128/JVI.01422-14. PubMed PMID: 24899198; PubMed Central PMCID: PMC4136287.

25. Werneke SW, Schilte C, Rohatgi A, Monte KJ, Michault A, Arenzana-Seisdedos F, et al. ISG15 is critical in the control of Chikungunya virus infection independent of UbE1L mediated conjugation. *PLoS Pathog.* 2011;7(10):e1002322. Epub 2011/10/27. doi: 10.1371/journal.ppat.1002322. PubMed PMID: 22028657; PubMed Central PMCID: PMC3197620.

26. Zhang X, Bogunovic D, Payelle-Brogard B, Francois-Newton V, Speer SD, Yuan C, et al. Human intracellular ISG15 prevents interferon-alpha/beta over-amplification and auto-inflammation. *Nature.* 2015;517(7532):89-93. Epub 2014/10/14. doi: 10.1038/nature13801. PubMed PMID: 25307056; PubMed Central PMCID: PMC4303590.

27. Zhao C, Denison C, Huibregtse JM, Gygi S, Krug RM. Human ISG15 conjugation targets both IFN-induced and constitutively expressed proteins functioning in

diverse cellular pathways. *Proc Natl Acad Sci U S A.* 2005;102(29):10200-5. Epub 2005/07/13. doi: 10.1073/pnas.0504754102. PubMed PMID: 16009940; PubMed Central PMCID: PMCPMC1177427.

28. Zhao C, Hsiang TY, Kuo RL, Krug RM. ISG15 conjugation system targets the viral NS1 protein in influenza A virus-infected cells. *Proc Natl Acad Sci U S A.* 2010;107(5):2253-8. Epub 2010/02/06. doi: 10.1073/pnas.0909144107. PubMed PMID: 20133869; PubMed Central PMCID: PMCPMC2836655.

29. Swaim CD, Scott AF, Canadeo LA, Huibregtse JM. Extracellular ISG15 Signals Cytokine Secretion through the LFA-1 Integrin Receptor. *Mol Cell.* 2017;68(3):581-90 e5. Epub 2017/11/04. doi: 10.1016/j.molcel.2017.10.003. PubMed PMID: 29100055; PubMed Central PMCID: PMCPMC5690536.

30. Scholte FEM, Zivcec M, Dzimianski JV, Deaton MK, Spengler JR, Welch SR, et al. Crimean-Congo Hemorrhagic Fever Virus Suppresses Innate Immune Responses via a Ubiquitin and ISG15 Specific Protease. *Cell Rep.* 2017;20(10):2396-407. Epub 2017/09/07. doi: 10.1016/j.celrep.2017.08.040. PubMed PMID: 28877473; PubMed Central PMCID: PMCPMC5616139.

31. Niemeyer D, Mosbauer K, Klein EM, Sieberg A, Mettelman RC, Mielech AM, et al. The papain-like protease determines a virulence trait that varies among members of the SARS-coronavirus species. *PLoS Pathog.* 2018;14(9):e1007296. doi: 10.1371/journal.ppat.1007296. PubMed PMID: 30248143; PubMed Central PMCID: PMCPMC6171950.

32. Capodagli GC, Deaton MK, Baker EA, Lumpkin RJ, Pegan SD. Diversity of ubiquitin and ISG15 specificity among nairoviruses' viral ovarian tumor domain proteases. *J Virol.* 2013;87(7):3815-27. Epub 2013/01/25. doi: 10.1128/JVI.03252-12. PubMed PMID: 23345508; PubMed Central PMCID: PMCPMC3624237.

33. Deaton MK, Dzimianski JV, Dackowski CM, Whitney GK, Mank NJ, Parham MM, et al. Biochemical and Structural Insights into the Preference of Nairoviral DeISGylases for Interferon-Stimulated Gene Product 15 Originating from Certain Species. *J Virol.* 2016;90(18):8314-27. Epub 2016/07/15. doi: 10.1128/JVI.00975-16. PubMed PMID: 27412597; PubMed Central PMCID: PMCPMC5008091.

34. Akutsu M, Ye Y, Virdee S, Chin JW, Komander D. Molecular basis for ubiquitin and ISG15 cross-reactivity in viral ovarian tumor domains. *Proc Natl Acad Sci U S A.* 2011;108(6):2228-33. Epub 2011/01/27. doi: 10.1073/pnas.1015287108. PubMed PMID: 21266548; PubMed Central PMCID: PMCPMC3038727.

35. Komander D, Rape M. The ubiquitin code. *Annu Rev Biochem.* 2012;81:203-29. Epub 2012/04/25. doi: 10.1146/annurev-biochem-060310-170328. PubMed PMID: 22524316.

36. Bremm A, Freund SM, Komander D. Lys11-linked ubiquitin chains adopt compact conformations and are preferentially hydrolyzed by the deubiquitinase Cezanne.

Nat Struct Mol Biol. 2010;17(8):939-47. Epub 2010/07/14. doi: 10.1038/nsmb.1873. PubMed PMID: 20622874; PubMed Central PMCID: PMCPMC2917782.

37. Licchesi JD, Mieszczanek J, Mevissen TE, Rutherford TJ, Akutsu M, Virdee S, et al. An ankyrin-repeat ubiquitin-binding domain determines TRABID's specificity for atypical ubiquitin chains. *Nat Struct Mol Biol.* 2011;19(1):62-71. Epub 2011/12/14. doi: 10.1038/nsmb.2169. PubMed PMID: 22157957; PubMed Central PMCID: PMCPMC5260945.

38. Mevissen TE, Hospenthal MK, Geurink PP, Elliott PR, Akutsu M, Arnaudo N, et al. OTU deubiquitinases reveal mechanisms of linkage specificity and enable ubiquitin chain restriction analysis. *Cell.* 2013;154(1):169-84. Epub 2013/07/06. doi: 10.1016/j.cell.2013.05.046. PubMed PMID: 23827681; PubMed Central PMCID: PMCPMC3705208.

39. Mevissen TET, Kulathu Y, Mulder MPC, Geurink PP, Maslen SL, Gersch M, et al. Molecular basis of Lys11-polyubiquitin specificity in the deubiquitinase Cezanne. *Nature.* 2016;538(7625):402-5. Epub 2016/10/21. doi: 10.1038/nature19836. PubMed PMID: 27732584; PubMed Central PMCID: PMCPMC5295632.

40. Wang T, Yin L, Cooper EM, Lai MY, Dickey S, Pickart CM, et al. Evidence for bidentate substrate binding as the basis for the K48 linkage specificity of otubain 1. *J Mol Biol.* 2009;386(4):1011-23. Epub 2009/02/13. doi: 10.1016/j.jmb.2008.12.085. PubMed PMID: 19211026; PubMed Central PMCID: PMCPMC2682458.

41. Dikic I, Wakatsuki S, Walters KJ. Ubiquitin-binding domains - from structures to functions. *Nat Rev Mol Cell Biol.* 2009;10(10):659-71. Epub 2009/09/24. doi: 10.1038/nrm2767. PubMed PMID: 19773779.

42. Balakirev MY, Jaquinod M, Haas AL, Chroboczek J. Deubiquitinating function of adenovirus proteinase. *J Virol.* 2002;76(12):6323-31. Epub 2002/05/22. PubMed PMID: 12021365; PubMed Central PMCID: PMCPMC136223.

43. Barretto N, Jukneliene D, Ratia K, Chen Z, Mesecar AD, Baker SC. The papain-like protease of severe acute respiratory syndrome coronavirus has deubiquitinating activity. *J Virol.* 2005;79(24):15189-98. Epub 2005/11/25. doi: 10.1128/JVI.79.24.15189-15198.2005. PubMed PMID: 16306590; PubMed Central PMCID: PMCPMC1316023.

44. Lindner HA, Fotouhi-Ardakani N, Lytvyn V, Lachance P, Sulea T, Menard R. The papain-like protease from the severe acute respiratory syndrome coronavirus is a deubiquitinating enzyme. *J Virol.* 2005;79(24):15199-208. Epub 2005/11/25. doi: 10.1128/JVI.79.24.15199-15208.2005. PubMed PMID: 16306591; PubMed Central PMCID: PMCPMC1316033.

45. Sulea T, Lindner HA, Purisima EO, Menard R. Deubiquitination, a new function of the severe acute respiratory syndrome coronavirus papain-like protease? *J Virol.* 2005;79(7):4550-1. Epub 2005/03/16. doi: 10.1128/JVI.79.7.4550-4551.2005. PubMed PMID: 15767458; PubMed Central PMCID: PMCPMC1061586.

46. Johnson N. Tick-Virus Interactions: Toll Sensing. *Front Cell Infect Microbiol.* 2017;7:293. Epub 2017/07/18. doi: 10.3389/fcimb.2017.00293. PubMed PMID: 28713778; PubMed Central PMCID: PMC5492658.
47. Ruckert C, Bell-Sakyi L, Fazakerley JK, Fragkoudis R. Antiviral responses of arthropod vectors: an update on recent advances. *Virusdisease.* 2014;25(3):249-60. Epub 2015/02/13. doi: 10.1007/s13337-014-0217-9. PubMed PMID: 25674592; PubMed Central PMCID: PMC4188209.
48. Schnettler E, Tykalova H, Watson M, Sharma M, Sterken MG, Obbard DJ, et al. Induction and suppression of tick cell antiviral RNAi responses by tick-borne flaviviruses. *Nucleic Acids Res.* 2014;42(14):9436-46. Epub 2014/07/24. doi: 10.1093/nar/gku657. PubMed PMID: 25053841; PubMed Central PMCID: PMC4132761.
49. Morris JR, Solomon E. BRCA1 : BARD1 induces the formation of conjugated ubiquitin structures, dependent on K6 of ubiquitin, in cells during DNA replication and repair. *Hum Mol Genet.* 2004;13(8):807-17. Epub 2004/02/21. doi: 10.1093/hmg/ddh095. PubMed PMID: 14976165.
50. Wickliffe KE, Williamson A, Meyer HJ, Kelly A, Rape M. K11-linked ubiquitin chains as novel regulators of cell division. *Trends Cell Biol.* 2011;21(11):656-63. Epub 2011/10/08. doi: 10.1016/j.tcb.2011.08.008. PubMed PMID: 21978762; PubMed Central PMCID: PMC3205209.
51. Dynek JN, Goncharov T, Dueber EC, Fedorova AV, Izrael-Tomasevic A, Phu L, et al. c-IAP1 and UbcH5 promote K11-linked polyubiquitination of RIP1 in TNF signalling. *EMBO J.* 2010;29(24):4198-209. Epub 2010/11/30. doi: 10.1038/emboj.2010.300. PubMed PMID: 21113135; PubMed Central PMCID: PMC3018797.
52. Durcan TM, Fon EA. USP8 and PARK2/parkin-mediated mitophagy. *Autophagy.* 2015;11(2):428-9. Epub 2015/02/24. doi: 10.1080/15548627.2015.1009794. PubMed PMID: 25700639; PubMed Central PMCID: PMC4502724.
53. Durcan TM, Tang MY, Perusse JR, Dashti EA, Aguilera MA, McLelland GL, et al. USP8 regulates mitophagy by removing K6-linked ubiquitin conjugates from parkin. *EMBO J.* 2014;33(21):2473-91. Epub 2014/09/14. doi: 10.15252/embj.201489729. PubMed PMID: 25216678; PubMed Central PMCID: PMC4283406.
54. Kim SJ, Ahn DG, Syed GH, Siddiqui A. The essential role of mitochondrial dynamics in antiviral immunity. *Mitochondrion.* 2018;41:21-7. Epub 2017/12/17. doi: 10.1016/j.mito.2017.11.007. PubMed PMID: 29246869; PubMed Central PMCID: PMC5988924.
55. Capodagli GC, McKercher MA, Baker EA, Masters EM, Brunzelle JS, Pegan SD. Structural analysis of a viral ovarian tumor domain protease from the Crimean-Congo hemorrhagic fever virus in complex with covalently bonded ubiquitin. *J Virol.*

2011;85(7):3621-30. Epub 2011/01/14. doi: 10.1128/JVI.02496-10. PubMed PMID: 21228232; PubMed Central PMCID: PMCPMC3067871.

56. James TW, Frias-Staheli N, Bacik JP, Levingston Macleod JM, Khajehpour M, Garcia-Sastre A, et al. Structural basis for the removal of ubiquitin and interferon-stimulated gene 15 by a viral ovarian tumor domain-containing protease. *Proc Natl Acad Sci U S A*. 2011;108(6):2222-7. Epub 2011/01/20. doi: 10.1073/pnas.1013388108. PubMed PMID: 21245344; PubMed Central PMCID: PMCPMC3038750.

57. Yau R, Rape M. The increasing complexity of the ubiquitin code. *Nat Cell Biol*. 2016;18(6):579-86. Epub 2016/05/28. doi: 10.1038/ncb3358. PubMed PMID: 27230526.

58. Magor KE, Miranzo Navarro D, Barber MR, Petkau K, Fleming-Canepa X, Blyth GA, et al. Defense genes missing from the flight division. *Dev Comp Immunol*. 2013;41(3):377-88. Epub 2013/04/30. doi: 10.1016/j.dci.2013.04.010. PubMed PMID: 23624185.

59. Santhakumar D, Rubbenstroth D, Martinez-Sobrido L, Munir M. Avian Interferons and Their Antiviral Effectors. *Front Immunol*. 2017;8:49. Epub 2017/02/16. doi: 10.3389/fimmu.2017.00049. PubMed PMID: 28197148; PubMed Central PMCID: PMCPMC5281639.

60. Daczkowski CM, Dzimianski JV, Clasman JR, Goodwin O, Mesecar AD, Pegan SD. Structural Insights into the Interaction of Coronavirus Papain-Like Proteases and Interferon-Stimulated Gene Product 15 from Different Species. *J Mol Biol*. 2017;429(11):1661-83. Epub 2017/04/26. doi: 10.1016/j.jmb.2017.04.011. PubMed PMID: 28438633; PubMed Central PMCID: PMCPMC5634334.

61. Sridharan H, Zhao C, Krug RM. Species specificity of the NS1 protein of influenza B virus: NS1 binds only human and non-human primate ubiquitin-like ISG15 proteins. *J Biol Chem*. 2010;285(11):7852-6. Epub 2010/01/23. doi: 10.1074/jbc.C109.095703. PubMed PMID: 20093371; PubMed Central PMCID: PMCPMC2832935.

62. Otwinowski Z, Minor W. Processing of X-ray diffraction data collected in oscillation mode. *Methods Enzymol*. 1997;276:307-26. Epub 1997/01/01. PubMed PMID: 27754618.

63. Adams PD, Afonine PV, Bunkoczi G, Chen VB, Davis IW, Echols N, et al. PHENIX: a comprehensive Python-based system for macromolecular structure solution. *Acta Crystallogr D Biol Crystallogr*. 2010;66(Pt 2):213-21. Epub 2010/02/04. doi: 10.1107/S09074444090052925. PubMed PMID: 20124702; PubMed Central PMCID: PMCPMC2815670.

64. Grosse-Kunstleve RW, Adams PD. Substructure search procedures for macromolecular structures. *Acta Crystallogr D Biol Crystallogr*. 2003;59(Pt 11):1966-73. Epub 2003/10/24. PubMed PMID: 14573951.

65. McCoy AJ, Storoni LC, Read RJ. Simple algorithm for a maximum-likelihood SAD function. *Acta Crystallogr D Biol Crystallogr*. 2004;60(Pt 7):1220-8. Epub 2004/06/24. doi: 10.1107/S0907444904009990. PubMed PMID: 15213383.
66. McCoy AJ, Grosse-Kunstleve RW, Adams PD, Winn MD, Storoni LC, Read RJ. Phaser crystallographic software. *J Appl Crystallogr*. 2007;40(Pt 4):658-74. Epub 2007/08/01. doi: 10.1107/S0021889807021206. PubMed PMID: 19461840; PubMed Central PMCID: PMC2483472.
67. Terwilliger TC, Grosse-Kunstleve RW, Afonine PV, Moriarty NW, Zwart PH, Hung LW, et al. Iterative model building, structure refinement and density modification with the PHENIX AutoBuild wizard. *Acta Crystallogr D Biol Crystallogr*. 2008;64(Pt 1):61-9. Epub 2007/12/21. doi: 10.1107/S090744490705024X. PubMed PMID: 18094468; PubMed Central PMCID: PMC2394820.
68. Emsley P, Cowtan K. Coot: model-building tools for molecular graphics. *Acta Crystallogr D Biol Crystallogr*. 2004;60(Pt 12 Pt 1):2126-32. Epub 2004/12/02. doi: 10.1107/S0907444904019158. PubMed PMID: 15572765.
69. Chen VB, Arendall WB, 3rd, Headd JJ, Keedy DA, Immormino RM, Kapral GJ, et al. MolProbity: all-atom structure validation for macromolecular crystallography. *Acta Crystallogr D Biol Crystallogr*. 2010;66(Pt 1):12-21. Epub 2010/01/09. doi: 10.1107/S0907444909042073. PubMed PMID: 20057044; PubMed Central PMCID: PMC2803126.
70. Kumar S, Stecher G, Tamura K. MEGA7: Molecular Evolutionary Genetics Analysis Version 7.0 for Bigger Datasets. *Mol Biol Evol*. 2016;33(7):1870-4. Epub 2016/03/24. doi: 10.1093/molbev/msw054. PubMed PMID: 27004904.
71. Roberts E, Eargle J, Wright D, Luthey-Schulten Z. MultiSeq: unifying sequence and structure data for evolutionary analysis. *BMC Bioinformatics*. 2006;7:382. Epub 2006/08/18. doi: 10.1186/1471-2105-7-382. PubMed PMID: 16914055; PubMed Central PMCID: PMC21586216.
72. Notredame C, Higgins DG, Heringa J. T-Coffee: A novel method for fast and accurate multiple sequence alignment. *J Mol Biol*. 2000;302(1):205-17. Epub 2000/08/31. doi: 10.1006/jmbi.2000.4042. PubMed PMID: 10964570.

CHAPTER 4

DETERMINING THE MOLECULAR DRIVERS OF SPECIES-SPECIFIC INTERFERON-STIMULATED GENE PRODUCT 15 INTERACTIONS WITH NAIROVIRUS OVARIAN TUMOR DOMAIN PROTEASES ¹

¹ Dzimianski, J.V, I.L. Williams, C. Langley, B.T. Freitas, F.E.M. Scholte, J.R. Spengler, É. Bergeron, and S.D. Pegan. 2019. Submitted to *PLOS Pathogens*, 03/21/19.

Abstract

Tick-borne nairoviruses (order *Bunyavirales*) encode an ovarian tumor domain protease (OTU) that suppresses the innate immune response by reversing the post-translational modification of proteins by ubiquitin (Ub) and interferon-stimulated gene product 15 (ISG15). Ub is almost perfectly conserved across eukaryotes, whereas ISG15 is only present in vertebrates and shows substantial sequence diversity. This diversity can impact the ability of viral proteins to engage different species' ISG15, potentially contributing to host tropism. Prior attempts to address this effect have focused on only a single species' ISG15 or a limited selection of nairovirus OTUs. To gain a more complete perspective of OTU-ISG15 interactions, we biochemically assessed the relative activities of diverse nairovirus OTUs for 12 species' ISG15. This revealed that ISG15 activity is predominantly restricted to particular nairovirus lineages reflecting, in general, known virus-host associations. To uncover the underlying molecular factors, X-ray crystal structures of Kupe virus and Ganjam virus OTUs bound to sheep ISG15 were solved and compared to complexes of Crimean-Congo hemorrhagic fever virus and Erve virus OTUs bound to human and mouse ISG15, respectively. Seven residues in ISG15 were identified that predominantly influence species specificity, with mutational analysis producing controllable shifts in susceptibility to OTUs. Additionally, residues in the OTU were identified that influence ISG15 preference, suggesting the potential for OTUs to adapt to different ISG15s. These findings provide a foundation to further develop research methods to trace nairovirus-host relationships and delineate the full impact of ISG15 diversity on nairovirus infection.

Author Summary

Virus-host relationships are multilayered, often involving interactions between numerous viral and host proteins. As a result, host tropism involves adaptation of these interactions, which may vary greatly between hosts. One example of this is the interaction of nairovirus ovarian tumor domain proteases (OTUs) with the host protein interferon-stimulated gene product 15 (ISG15). It is known that interspecies diversity in ISG15 can influence the ability of viral proteins to engage it. However, an overall picture has been lacking regarding possible connections between variability of OTU-ISG15 interactions and nairovirus host range, as well as the specific factors dictating this variability. Here we sought to obtain a more comprehensive understanding of the relationship between preferences in OTU-ISG15 interactions and nairovirus host tropism, and to identify the molecular factors governing these preferences. Combining biochemical and structural approaches we were able to ascertain the primary drivers of OTU-ISG15 interactions and design proteins with specifically altered interaction profiles. These studies provide a basis to design predictive models for nairovirus-host associations and develop tools to further elucidate the role of ISG15 in combating nairovirus infection.

Introduction

Viruses within the *Nairoviridae* family, which number ~40 divided between 16 species, have been detected from every major continent, giving this group of viruses a global geographic distribution [1, 2]. Nairoviruses are predominantly tick-associated arthropod-borne viruses (arboviruses), several of which are known causative agents of human disease, most notably Crimean-Congo hemorrhagic fever virus (CCHFV). CCHFV is one of the most widespread hemorrhagic fever viruses [3]; infections have been reported across Africa, the Middle East, Asia, and Eastern and Southern Europe, with outbreak associated case-fatality rates ranging from 5-40%. CCHFV initially causes a mild, nonspecific febrile illness that may progress to severe or fatal disease resulting from hemorrhage, multi-organ failure and shock [3]. Other nairoviruses known to cause human disease include Nairobi Sheep Disease virus (NSDV) in Africa and Asia (Asian variant Ganjam virus, GANV), Dugbe virus (DUGV) and Kasokero virus (KASV) in Africa, Erve virus (ERVEV) in Western Europe, and Issyk-kul virus (ISKV) in northeast Europe. These viruses typically cause mild fever, headache, or diarrhea [4-9]. In addition to infecting humans, many nairoviruses have been directly associated with other vertebrate hosts. CCHFV, for example, is reported to infect a wide array of mammalian species [10, 11], however disease is restricted to humans. Importantly, CCHFV maintenance and transmission relies on asymptomatic circulation among a number of hosts, including small mammals, reptiles, and livestock (Reviewed in [10, 11]). NSDV and DUGV have both been detected in livestock, with NSDV causing severe gastroenteritis in sheep and goats, and other nairoviruses, including KASV and the related Leopards Hill virus (LPHV), were isolated from bats [4, 6, 12-14]. In addition to these direct isolates, other nairoviruses have

been discovered in close proximity to vertebrate hosts. Kupe virus (KUPEV), for example, was isolated from ticks infesting cattle, sheep, and goats, while viruses in the *Hughes orthonairovirus* species, such as Farallon virus (FARV), were found in ticks infesting gull nests [15-17].

Nairoviruses possess a negative sense, single-stranded RNA ((-)ssRNA) genome consisting of three segments denoted as small (S), medium (M), and large (L), that encode the viral nucleoprotein, glycoproteins, and the multifunctional L protein, respectively. The L protein contains the RNA-dependent RNA polymerase (RdRp). In addition, the L protein also contains a viral homologue of the ovarian tumor domain protease (OTU) at the N-terminus that reverses posttranslational modifications by ubiquitin (Ub) and interferon (IFN) stimulated gene product 15 (ISG15) (Fig 4.1A). Ub and ISG15 are conjugated to proteins (ubiquitination/ISGylation) in a process involving activating (E1), conjugating (E2), and ligating (E3) enzymes. Ubiquitination plays a key role in activation of the innate immune response, while ISGylation primarily occurs on newly synthesized proteins in response to IFN induction, making viral proteins a predominant target [18]. It is therefore not surprising that the function of the OTU as a deubiquitinase (DUB) and deISGylase has been found to have an important role in immune suppression [19-22]. Recent studies have provided greater clarity to this mechanism. In particular, reverse genetics experiments with CCHFV have demonstrated a clear connection of DUB activity with enhanced viral replication through suppression of the type I IFN response [22]. The role of deISGylase activity, while not as clear-cut, appears to be involved in promoting higher levels of L protein during later stages of CCHFV infection. Similar results linking DUB activity with immune suppression have been observed in the severe acute respiratory syndrome

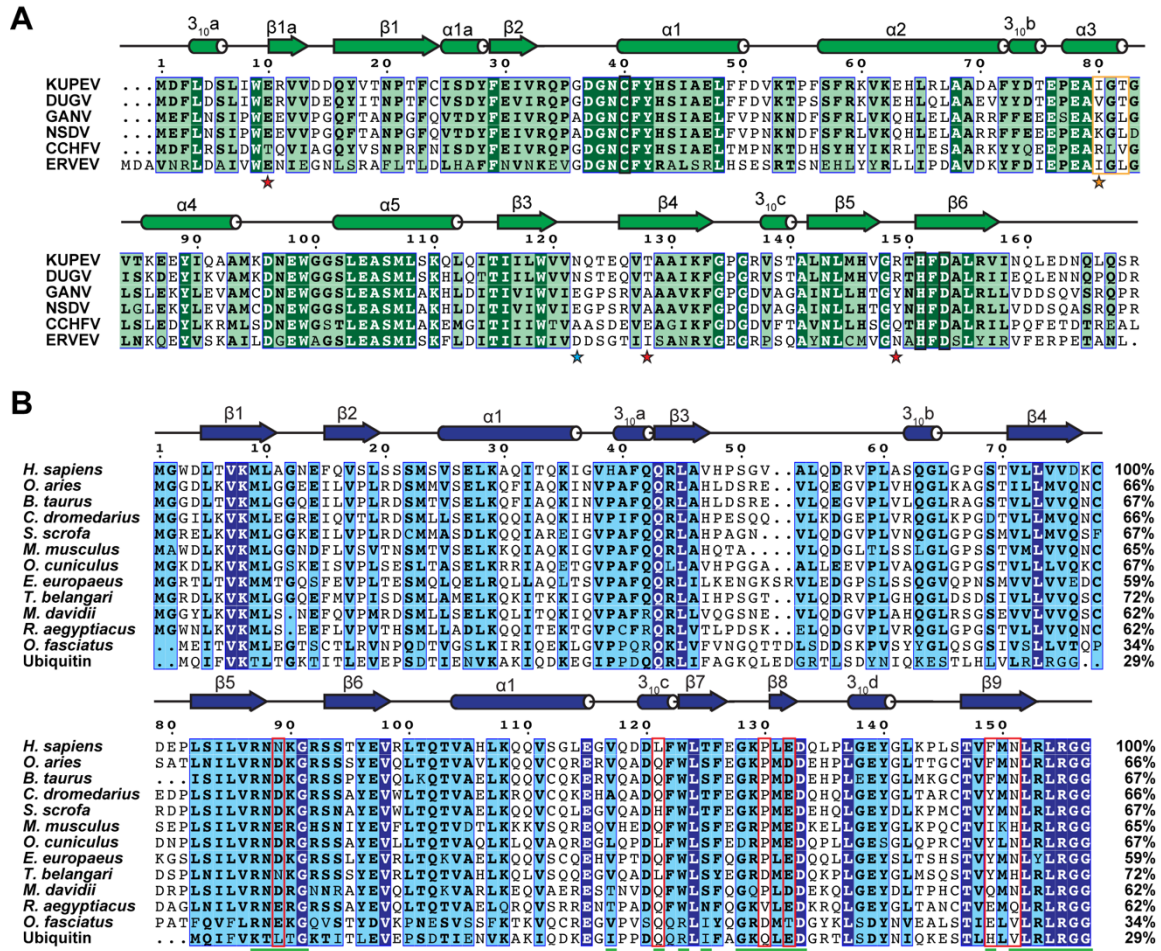


Fig. 4.1. Sequence alignment of OTUs and ISG15. (A) Sequence alignment of the OTUs from KUPEV, DUGV, GANV, NSDV, CCHFV, and ERVEV. A generic secondary structure of the nairovirus OTUs is shown. Residue numbering is based in the KUPEV OTU. Residues forming the catalytic triad are boxed in black. Mutation sites targeted to influence overall activity is indicated by a blue star, sites to influence shISG15 activity with an orange star/orange box, and sites to influence mISG15 activity with red stars. An expanded sequence alignment with the remaining OTUs is included in the 4.S2 Fig. (B) Alignment of ISG15s from human (*Homo sapiens*), sheep (*Ovis aries*), cow (*Bos taurus*), camel (*Camelus dromedaries*), pig (*Sus scrofa*), mouse (*Mus musculus*), rabbit (*Oryctolagus cuniculus*), hedgehog (*Erinaceus europaeus*), northern tree shrew (*Tupaia belangeri*), vesper bat (*Myotis davidii*), Egyptian fruit bat (*Rousettus aegyptiacus*), and fish (*Oplegnathus fasciatus*) with human ubiquitin for comparison. A generic secondary structure of ISG15 is shown. Percent identity relative to hISG15 is indicated. The residue numbering is based on human ISG15. The residues in ISG15 forming the binding interface with KUPEV OTU are indicated by green bars. Residues focused on in this study related to differential interactions with OTUs are boxed in red. Sequence alignments were generated using CLUSTALW followed by visual inspection and adjustment [68, 69]. Initial graphics for the sequence alignments were created using the ESPrnt server [70].

coronavirus (SARS-CoV), which possesses a papain-like protease (PLP) that also serves as a DUB/deISGylase [23]. Overall, the ability of proteases possessing DUB/deISGylase activity to promote viral replication has led to it being considered a distinguishing virulence trait [23].

Intriguingly, ISG15 possesses a large degree of functional and interspecies diversity. In addition to mediating effects through ISGylation, it has also been observed to function in a free form extracellularly as a cytokine and intracellularly in the cytosol to modulate immune responses [24-34]. Interestingly, ISG15 has also been suggested to have differing roles between species, with a more pronounced antiviral effect in mice compared to humans [32]. In addition to potential differences at the overall species level, ISG15 also shows a great degree of diversity in its protein sequence between species. In contrast to Ub, which is almost perfectly conserved among eukaryotes, ISG15 shows a much greater degree of diversity with sequence identities that can drop below 60% among mammals (Fig. 4.1B). These primary structure differences may translate into tertiary ones, with ISG15s from different species potentially possessing different preferred orientations of its two Ubl domains [35-37]. Such positional differences in the domains could result in different surface and steric environments for potential protein-protein interactions. In addition, the sequence differences occur within specific regions known to form interfaces with viral proteins, leading to potential species-specific effects in these interactions [38]. This has already been illustrated with the Influenza B nonstructural protein 1 (NS1B). NS1B has a high affinity for human ISG15, resulting in the sequestration of ISGylated viral proteins and preventing their dominant negative effect on the formation of the ribonucleoprotein (RNP) [39]. In contrast, NS1B is unable to efficiently bind mouse ISG15

(mISG15), preventing a similar effect in mice [36, 40-42]. This has been suggested to contribute to Influenza B's limited host tropism. Along similar lines, nairovirus OTUs and coronavirus PLPs also show biochemical sensitivity to ISG15 species-species differences, which has been suggested to potentially contribute to the preferred host ranges of these viruses [35, 43].

Interestingly, a previous study reported an apparent lack of activity in many nairovirus OTUs for ISG15 [44]. However, the authors point out that the assays were limited to a hISG15 substrate and could not preclude the possibility that OTUs might still interact with ISG15s from other species. Previous structural studies have identified some specific elements in OTU-ISG15 interactions that might be involved in defining ISG15 substrate specificity [43]. However, a complete picture is still lacking regarding the importance of these and potentially other factors in driving ISG15 species preferences. This includes how they may differ among nairovirus OTUs. To address this gap in understanding about nairovirus OTU-ISG15 interactions, diverse OTUs were assessed for their ability to interact with a broad set of different species' ISG15s to obtain a more global perspective of the trends among OTUs. This revealed that deISGylase activity may be a feature specific to particular lineages of nairoviruses. Within these viruses possessing deISGylase activity, a range of preferences are observed with some OTUs apparently lacking hISG15 activity possessing substantial activity towards other species' ISG15s. Further insights were obtained through novel structures of the KUPEV and GANV OTUs bound to sheep ISG15, revealing not only the first structure of sheep ISG15 but also the key features of its interface with OTUs. Comparison with other OTU-ISG15 structures yielded additional insight into the OTU-ISG15 interface. This coupled with mutational

analysis led to the identification of key features that can permit or prevent ISG15 interaction with certain OTUs. These insights into the molecular underpinnings of OTU-ISG15 interactions provide an opportunity to further assess ISG15 species-specific effects in cellular systems, particularly in the context of viral infections. In addition, it provides a foundation to develop molecular probes as biosurveillance tools to evaluate the potential host associations of emerging viruses.

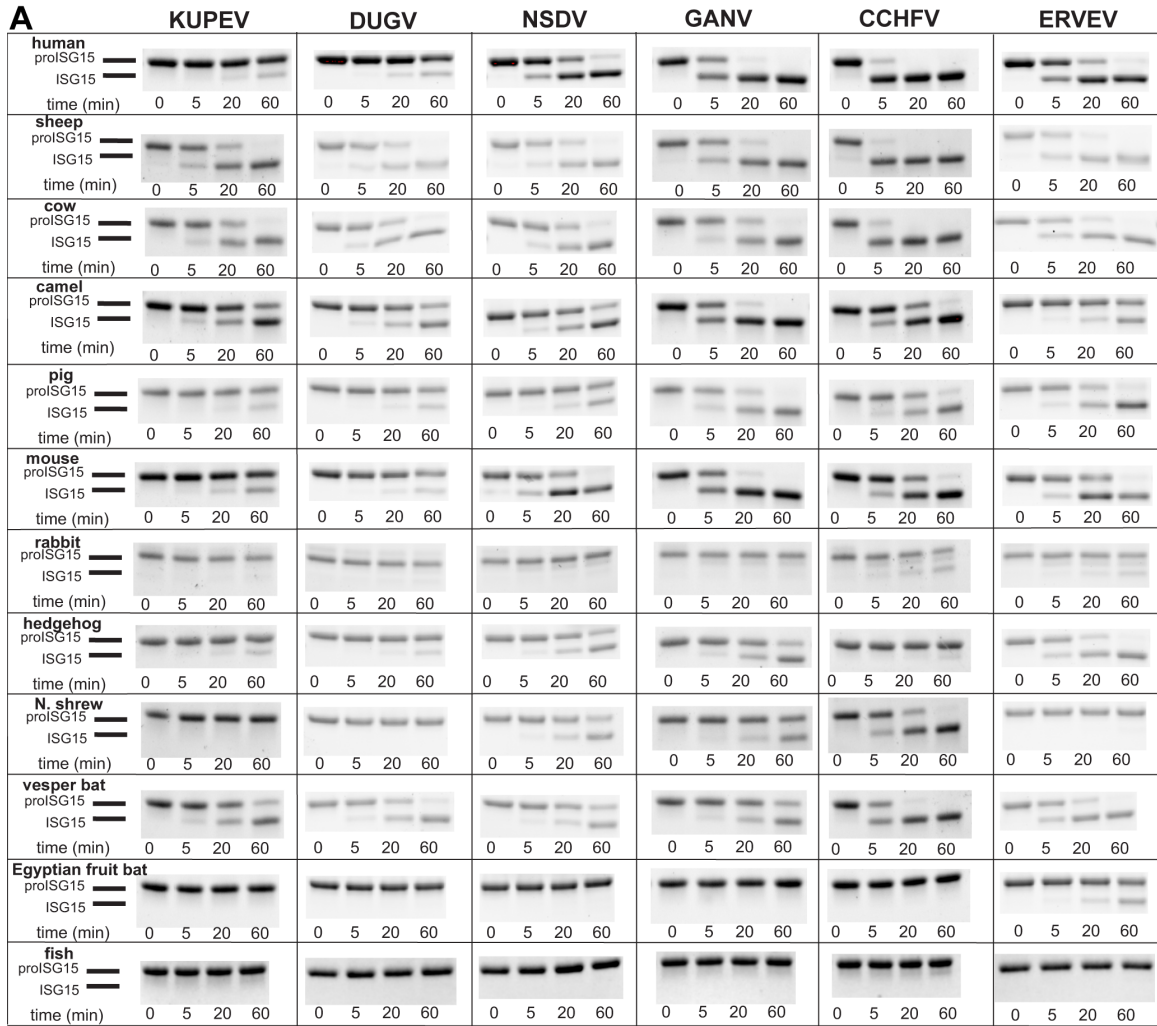
Results

Species-specific cleavage of proISG15s by nairovirus OTUs

To assess the patterns of ISG15 species preference by nairovirus OTUs, we took advantage of the ability of viral DUBs to cleave precursor proISG15 into mature ISG15 [35, 43, 45, 46]. The proISG15 substrates were derived from 12 species, including human (pro-hISG15), sheep (pro-shISG15), cow (pro-cwISG15), camel (pro-clISG15), porcine (pro-pISG15), mouse (pro-mISG15), rabbit (pro-rISG15), hedgehog (pro-hhISG15), northern tree shrew (pro-nsISG15), vesper bat (pro-bISG15), Egyptian fruit bat (pro-raISG15), and fish (pro-fiISG15), and were tested against a panel of diverse nairovirus OTUs. Time points were taken over the course of an hour and the relative quantities of pro- versus mature ISG15 resolved by SDS-PAGE.

Comparing the different cleavage profiles immediately reveals global trends among the OTUs. Interestingly, the OTUs possessing the most prominent proISG15 activity correlate to viruses that are closely related phylogenetically to CCHFV (Fig 4.2 and 4.S2 Fig, [44]). This is not entirely surprising as robust hISG15 activity has been previously observed in several of these viruses, such as CCHFV, NSDV/GANV, and ERVEV [43, 44, 47]. In contrast, no cleavage is observed with the OTUs for many of the viruses outside of

Fig 4.2. Activity of nairovirus OTUs for proISG15 from different species. (A) Each OTU was present at a 20 nM concentration was run against 10 μ M of each ISG15 at 37°C. Time points were taken at the indicated timepoints and the reaction quenched in 2x laemmli and boiling at 98°C for five minutes. SDS-PAGE analysis was performed using Mini-PROTEAN® TGX Stain-Free™ as described in the Materials and Methods. (B) Summary of proISG15 cleavage assays for 14 OTUs (data for HAZV, TAGV, FARV, DGKV, HpTV-1, LPHV, QYBV, and ISKV included in 4.S2 Fig). Colors range from green (robust cleavage) to dark red (no cleavage).



B

	KUPEV	DUGV	NSDV	GANV	CCHFV	ERVEV	HAZV	TAGV	FARV	DGKV	HpTV-1	LPHV	QYBV	ISKV
human	--	--	+	++	+++	+	---	---	---	---	---	---	---	---
sheep	++	++	++	++	+++	++	---	---	---	---	---	---	---	---
cow	++	++	++	++	+++	++	---	---	---	---	---	---	---	---
camel	-	-	+	++	+	-	---	---	---	---	---	---	---	---
pig	--	--	-	++	+	+	---	---	---	---	---	---	---	---
mouse	--	--	+	++	+	++	---	---	---	---	---	---	---	---
rabbit	---	---	---	---	-	--	---	---	---	---	---	---	---	---
hedgehog	--	--	-	-	--	+	---	---	---	---	---	---	---	---
N. shrew	---	---	-	-	+	---	---	---	---	---	---	---	---	---
vesper bat	+	+	-	-	++	+	---	---	---	---	---	---	---	---
Egyptian fruit bat	---	---	---	---	---	-	---	---	---	---	---	---	---	---
fish	---	---	---	---	---	---	---	---	---	---	---	---	---	---

these lineages, such as Taggert (TAGV), FARV, and Dera Ghazi Khan virus (DGKV). Although very weak cleavage can be observed in a few cases, such as the Issyk-kul virus (ISKV) with pro-hISG15 and pro-bISG15 or Leopards Hill virus (LPHV) with pro-shISG15, pro-cISG15, and pro-hhISG15, activity for ISG15 appears to be primarily restricted to a defined subset of nairoviruses.

Looking more closely at the cluster of OTUs that possess pronounced proISG15 activity yields intriguing observations. Some OTUs that possess weak or undetectable activity for pro-hISG15 possess substantial activity for that of other species. This is specifically apparent in the KUPEV and DUGV OTUs, which are able to cleave sheep- and cow-derived proISG15s efficiently and show moderate activity towards camel and vesper bat. In addition, interesting contrasts with some of the ISG15s come to light. The vesper bat and Egyptian fruit bat ISG15s share 64% sequence identity but have completely different interaction profiles. While the proISG15 from vesper bat is processed by several of the OTUs, the Egyptian fruit bat proISG15 is only detectably cleaved by ERVEV. Similarly, pro-nsISG15 ranges from no cleavage by KUPEV, DUGV, or ERVEV to relatively efficient cleavage by CCHFV. With the exception of fish proISG15, which shows no sign of cleavage by any of the OTUs, most of the other proISG15s show susceptibility to processing that varies between the different nairovirus OTUs they are tested against. Comparing the OTUs to each other reveals another intriguing feature. While KUPEV and DUGV, which belong the same nairovirus species, possess almost identical cleavage profiles, the same cannot be said for NSDV and GANV. Despite being a variant of the same virus, GANV possesses enhanced activity towards pro-hISG15, pro-cISG15, pro-pISG15, and pro-mISG15. This suggests that even apparently small

differences may play a role in tuning OTU activity, resulting in the wide range of OTU-ISG15 interaction profiles.

Structures of KUPEV OTU and GANV OTU bound to shISG15

The results yielded by the proISG15 cleavage assay produce questions regarding the molecular determinants of ISG15 species specificity in OTUs. A particularly intriguing point is why shISG15 and cwISG15 seem to be broadly engaged while hISG15 is more restricted. While the OTU from KUPEV, for example, highly prefers pro-shISG15, GANV has a roughly equal preference for both pro-shISG15 and pro-hISG15. Although both viruses are associated with livestock, only GANV is known to cause human illness raising the prospect that differences in ISG15 preference could be related to this divergence. To delve into these questions, complex structures of these OTUs bound to shISG15 were sought by X-ray crystallography. This yielded an atomic resolution structure of KUPEV OTU bound to the C-terminal domain of shISG15 (CshISG15) solved to 2.06 Å and a low resolution structure of GANV OTU bound to full length ISG15 to 3.2 Å (Table 4.1).

Examination of the high resolution KUPEV OTU-CshISG15 structure reveals it to possess the familiar overall mode of binding of OTUs with substrate (Fig 4.3A). Looking more closely at the interface uncovers a mix of hydrophobic and electrostatic interactions that is reminiscent of other nairovirus OTUs [43, 47-50]. The main areas of interaction can be divided into three major regions of the OTU surface (Fig 4.3B) [48-50]. The first region surrounds the OTU active site and interacts with portions of the tail of CshISG15 through electrostatic interactions (Fig 4.3B, Panel I). This includes direct interactions between the sidechain of CshISG15's Arg155 with the sidechain of Glu98 and the backbone carbonyl of Trp99 in KUPEV OTU, the backbone amide of Leu154 with the hydroxyl of Ser102,

Table 4.1. Data collection and refinement statistics

	KUPEV OTU-CshISG15 (PDB entry 6OAR)	GANV OTU-shISG15 (PDB entry 6OAT)
Data collection		
Space group	P2 ₁ 2 ₁ 2 ₁	P6 ₁
Wavelength (Å)	1	1
Cell dimensions		
<i>a</i> , <i>b</i> , <i>c</i> (Å)	41.8, 158.8, 171.0	55.0, 55.0, 494.8
α , β , γ (°)	90, 90, 90	90, 90, 120
Resolution (Å)	50.00-2.06 (2.11-2.06) [†]	50.00-3.2 (3.26-3.2) [†]
<i>R</i> _{merge}	0.100 (0.876)	0.184 (1.136)
<i>CC</i> _{1/2}	0.994 (0.699)	0.938 (0.720)
<i>I</i> / σ <i>I</i>	15.9 (1.51)	11.2 (1.3)
Completeness (%)	99.8 (99.9)	85.0 (87.6)
Redundancy	5.1 (4.6)	6.7 (6.4)
Refinement		
Resolution (Å)	41.29-2.06 (2.14-2.06)	39.51-3.20 (3.32-3.20)
No. reflections	70,367	11,664
<i>R</i> _{work} (%) / <i>R</i> _{free} (%)	17.7/21.7	26.0/33.0
No. atoms		
Protein	7532	4912
Ligand/ion [‡]	16	8
Water	359	0
<i>B</i> -factors		
Protein	45.79	121.61
Ligand/ion [‡]	38.02	62.77
Water	45.26	---
R.m.s. deviations		
Bond lengths (Å)	0.005	0.005
Bond angles (°)	0.55	0.74

[†]Values in parentheses denote the highest resolution shell

[‡]Includes the propargylamine linker

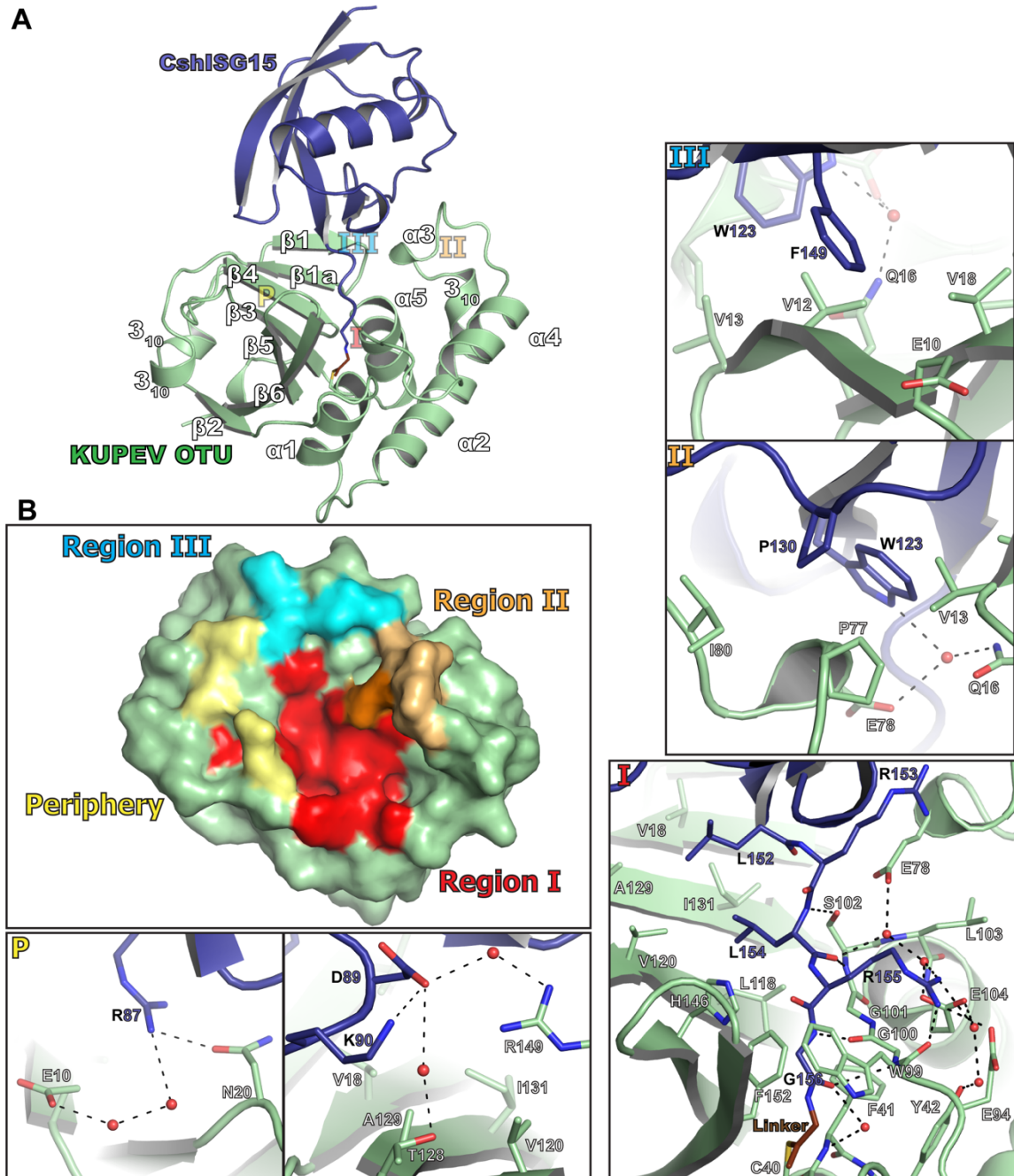


Fig 4.3. Structure of KUPEV OTU in complex with CshISG15. (A) Overall crystal structure of the KUPEV OUT (green) bound to CshISG15 (purple) with the propargylamine linker shown in brown. The secondary structure for KUPEV OTU as calculated by the DSSP server is indicated [71]. (B) Surface rendering of KUPEV OTU highlighting the three regions of OTUs that have been described as forming a binding interface with ISG15, as well as peripheral residues that also contribute to binding. Closeup views of each region are shown revealing the predominant contributors to hydrophobic and electrostatic interactions between KUPEV OTU and shISG15. Black dashes indicate interatomic distances ≤ 3.5 Å between atoms capable of forming electrostatic pairs.

and hydrogen bond interactions between the amide of Gly156 with the carbonyl of Gly100. In addition, there are also water-mediated interactions that facilitate binding in this region. This includes a network bridging Arg155 with Tyr42 and Glu104, Leu154 with Leu103, Glu78, and Glu104, and Gly156 with Phe41. In addition to electrostatic interactions, this region also provides a hydrophobic floor consisting primarily of Leu118, Val120, Ile131, His146, and Phe152 that facilitates the accommodation of Leu152 and Leu154 of CshISG15.

The second and third major regions of the KUPEV OTU surface encompass the α 3 “selectivity helix” and beta sheets 1, 3, and 4, respectively, and work in tandem to create the major hydrophobic interface with CshISG15 outside of the C-terminal tail (Fig 4.3B, Panels II and III). On the CshISG15 side, the interface is formed by Trp123, Pro130, and Phe149. Trp123 forms the central component of this hydrophobic patch, and is accommodated by components of both regions. On one side Trp123 rests against Pro77 and aliphatic portion of Glu78 in Region 2. This is further stabilized by water mediated interactions between the indole nitrogen of Trp123 with Glu78 and Gln16. On the other side Val12 and Val13 in Region 3 form a wall securing the tryptophan interaction. Pro130 primarily interacts with Region 2, fitting into a hydrophobic cleft formed by Pro77 and Ile80 that is supported by Val13. In Region 3, Phe149 is accommodated by Val12, Val18, and the aliphatic section of the Glu10 sidechain.

In addition to these central hydrophobic interactions, there are also some peripheral electrostatic interactions that also contribute, including both direct and water-mediated components (Panel P). In Region 3, Arg87 interacts directly with Asn20 and indirectly with Glu10 and Thr19. Asp89 is able to form water-mediated interactions with both T128

and Arg149. Interestingly, Asp89 points away from the interface. This contrasts with what has been observed for this residue position in OTU-Ub structures and CCHFV OTU-hISG15 structures where the sidechain is buried into interface. In the case of Ub, the analogous residue is a leucine that inserts into a “selectivity pocket” (residues Val18, Val120, Ala129, and Ile131 in KUPEV OTU) and is critical for efficient Ub binding [44]. Considering the hydrophobicity of this pocket in KUPEV, it is not surprising that the charged aspartate would adopt a more solvent-exposed conformation. For the CCHFV OTU-hISG15 complex, on the other hand, position 120 is occupied by a threonine that is able to hydrogen bond with Asn89. In addition, CCHFV encodes a glutamate at position 128 that would likely restrict the conformational freedom of residue 89 due to steric and charge repulsion effects. These differences suggest that while this pocket is critical and generally predictive for Ub binding to nairovirus OTUs, an analogous role for ISG15 binding is not likely to be as pervasive.

Differences between nairovirus OTU-ISG15 interfaces

Comparison of the lower resolution GANV OTU-shISG15 with KUPEV OTU-CshISG15 reveals many commonalities in the interface. Similar to KUPEV, GANV OTU binding to shISG15 involves a mixture of electrostatic and hydrophobic components. One point of difference involves Region 2, where GANV possesses Ser77 and Lys80 instead of proline and isoleucine, respectively (Fig 4.4A). While different, the residues orient in a way that is still accommodating of a hydrophobic interaction. Another commonality with the KUPEV OTU-CshISG15 structure is that Asp89 points away from the GANV surface and is oriented in a way that may allow it to interact with residue 149 (a tyrosine in GANV versus arginine in KUPEV). The largest point of difference between the two OTUs occurs

peripherally at residue 122. In GANV, this position is occupied by a glutamate that is in proximity to interact with shISG15's Lys90. In other ISG15s this position is universally lysine/arginine, and in Ub a threonine. In KUPEV residue 122 is an asparagine residue, while in CCHFV it is an alanine (Fig 4.1A). These residues would not have the same potential to interact with ISG15 or ubiquitin substrates as Glu122 in GANV, suggesting this may partially account for the enhanced activity that has been observed for GANV OTU towards Ub and hISG15-7-amido-4-methylcoumarin (AMC) substrates [44]. To confirm this, Glu122 in GANV OTU was mutated to an asparagine, and the corresponding positions in the KUPEV and CCHFV OTUs to glutamate. As anticipated, the GANV OTU E122N mutant reduced activity for hISG15-AMC to almost a tenth of WT levels, while KUPEV OTU N122E boosted activity by more than a factor of six relative to WT (Fig 4.4B). The CCHFV OTU A122E mutant had a modest effect with just a marginal increase in activity, suggesting that other structural features may dictate the relative importance of this residue.

Identifying the residues driving ISG15 species preference

Nairovirus OTU interactions with ISG15 are confined to a well-defined region of the ISG15 surface (Fig 4.1B, Fig 4.5, [38, 43, 48, 50]). Within this surface, there are several components that are highly conserved across ISG15s. Particularly noteworthy are Trp123 and the LRLRGG terminal tail that form major interactions and are almost universally conserved among ISG15s. Other residues that form a part of the interface and are likewise highly conserved include Arg87 and Lys/Arg90. This restricts the probable contributors of species variation to just a handful of variable residues. Analysis of CCHFV OTU-hISG15 and ERVEV OTU-CmISG15 structures identified residues 89 and 149-151 (87 and 147-149 in mISG15) as key components of interface variability [43]. While Asn89 in

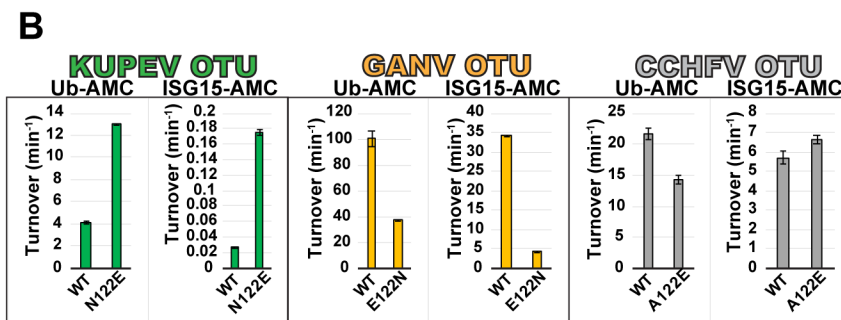
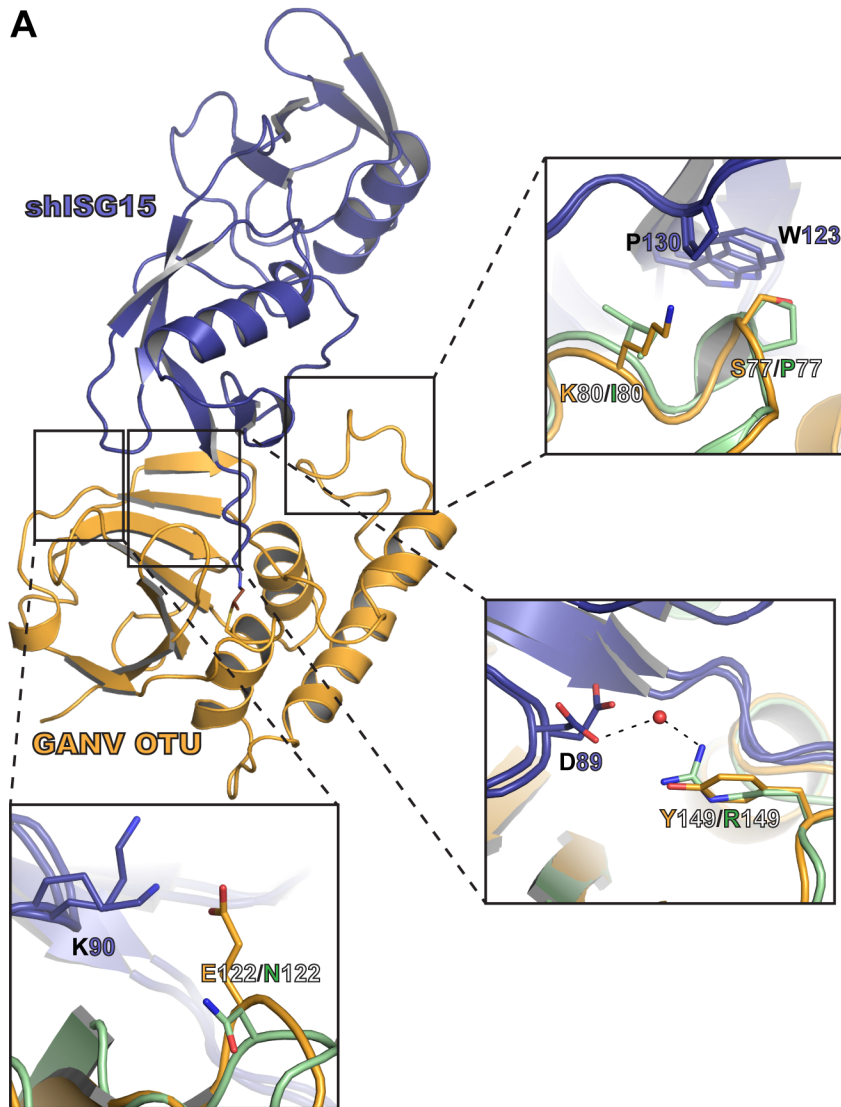


Fig 4.4. Structure of GANV OTU in complex with shISG15. A cartoon rendering of the GANV OTU (orange) bound in complex with shISG15 (purple) with the propargylamine linker shown in brown. The three major areas of difference between GANV OTU-shISG15 and KUPEV OTU-CshISG15 are indicated with boxes. Activities of mutant KUPEV, GANV, and CCHFV OTUs relative to WT towards Ub-AMC and hISG15-AMC are shown. Values are the mean \pm standard deviation of two independent experiments.

hISG15 inserts into the selectivity pocket of CCHFV, in the ERVEV OTU-CmISG15 structure Glu87 points away from the interface in an orientation that is facilitated by an internal salt bridge formed with Lys148 (Fig 4.5B, Panel I). In most ISG15s, the 148/150 position is typically a methionine or leucine, making this pairing unique for mouse ISG15. At position 147/149, the location within the interface results in factors that could be heavily influenced by spatial characteristics (Fig 4.5B Panel II). For example, a phenylalanine compared to isoleucine, as seen in hISG15 versus mISG15, could impact the degree to which this residue can pack in the interface, as could the presence of a polar or charged residue as seen in other ISG15s, such as northern tree shrew and fish (Fig 4.1B). In the case of the 149/151, this residue is buried in the interface, making it a potentially sterically-sensitive position (Fig 4.5B Panel III). Interestingly, this position is almost always occupied by a polar residue in ISG15s despite localizing to an area that is predominantly hydrophobic. For relatively small residues such as asparagine this appears to be accommodated, but suggests that bulkier sidechains, such as the glutamine present in raISG15, could be prohibitive for binding.

To test the influence of these positions on ISG15 species preference, mutations were introduced to the proISG15 constructs and assessed for their impact on cleavage by the OTUs (Fig 4.5C). When pro-hISG15 is mutated at these positions to resemble what is seen in shrew (F149Y/N151H), fish (N89E/F149E/N151V), and mouse (N89E/F149Y/M150K/N151H) this has a major effect when assessed for cleavage by CCHFV OTU. In each case, the cleavage is reduced in a way that largely reflects what would be expected, with moderate impact on the shrew-like mutant and a great diminishment of activity for the fish-like and mouse-like mutants. This is similarly seen

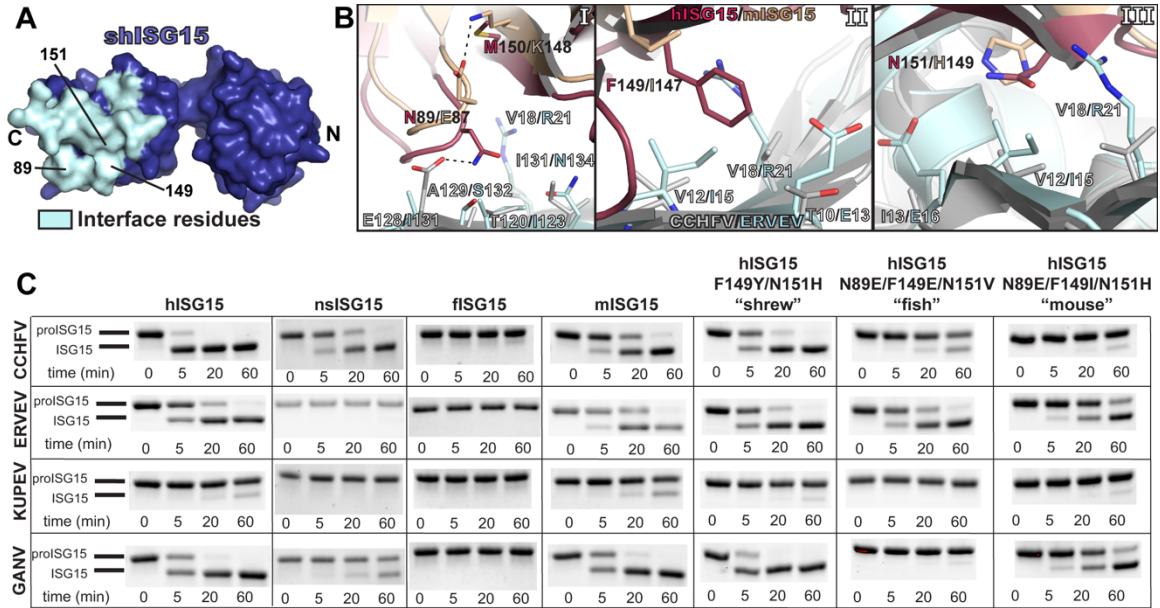


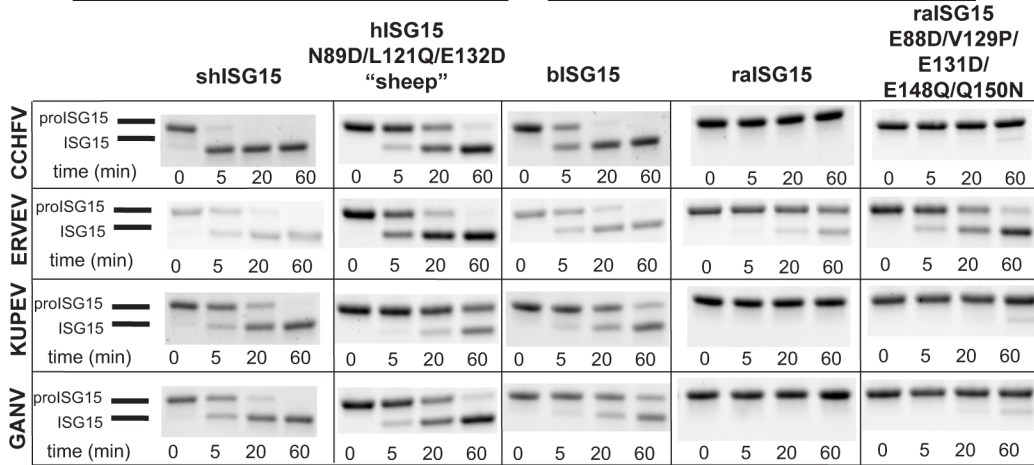
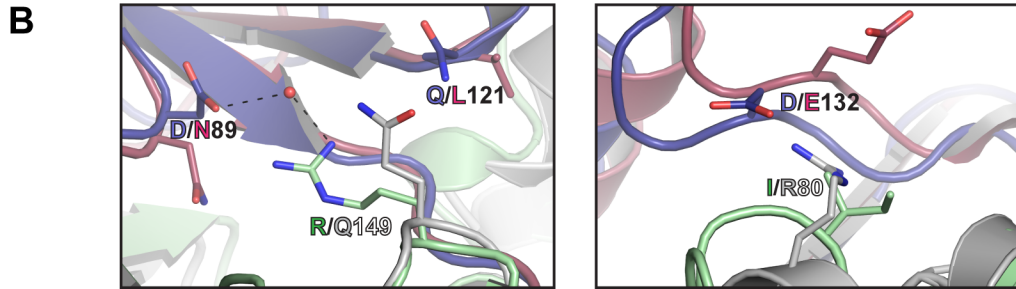
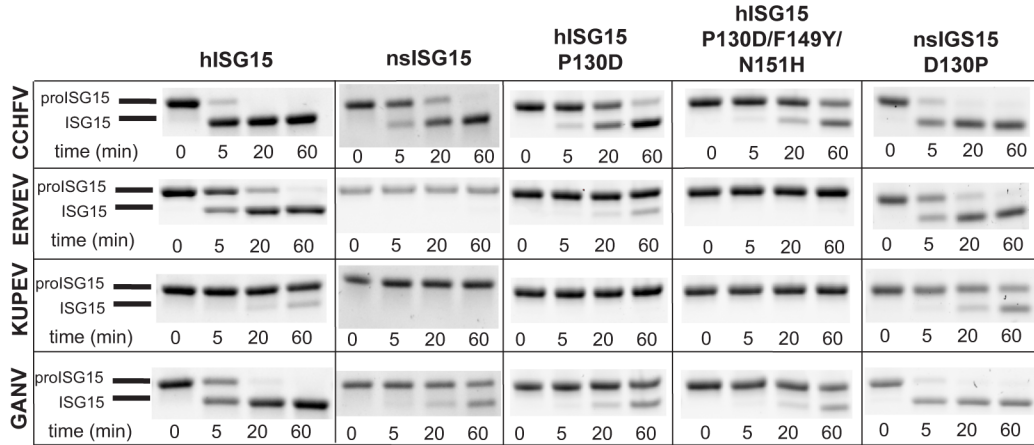
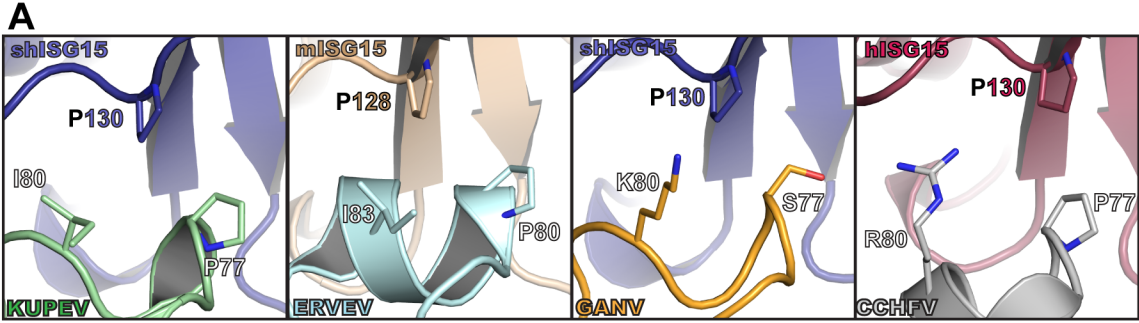
Fig 4.5. Molecular contributors to species-variable ISG15 interactions with nairovirus OTUs. (A) Surface rendering of shISG15 (purple) with the residues forming the interface shown in light teal. The locations of residues 89, 149, and 151 that have been previously suggested as responsible for species-specific interactions are indicated (B) Molecular environment of the CCHFV OTU-ChISG15 (PDB ID 3PHX) and ERVEV OTU-CmISG15 (PDB ID 5JZE) structures surrounding residues 89 and 149-151 (87 and 147-149 in mISG15). CCHFV is colored gray, ERVEV light teal, hISG15 light burgundy, and mISG15 wheat. (C) Cleavage assays of the CCHFV, ERVEV, KUPEV, GANV OTUs with mutant pro-hISG15 constructs. Mutations were introduced to pro-hISG15 at residues 89, 149, and 151 to match the composition present in northern tree shrew, fish, or mouse. Samples from each timepoint were run on BioRad Mini-PROTEAN® TGX Stain-Free™ gels and visualized as described in the Materials and Methods.

for the KUPEV and GANV OTUs when assessed against the hISG15-fish hybrid, which completely eliminates activity.

Interestingly, these positions do not exert the expected effects for every OTU. In particular, the mutations appear to have no impact on ERVEV binding for either the hISG15-shrew or hISG15-fish hybrids. In the same way, KUPEV and GANV seem to be unaffected by the hISG15-shrew hybrid. This suggested that other factors may be at play that have a more important role in some OTU-ISG15 interactions. Re-examination of the structures revealed aspects of the ERVEV and KUPEV OTUs that may account for these observations. Specifically, the hydrophobic cleft formed by Pro77/80 and Ile80/83 may be critical in ISG15 binding via Pro128/130 (Fig 4.6A). Although proline is the most common residue at this position in ISG15s, in the case of northern tree shrew and fish this residue is an aspartate. This likely accounts for the lack of activity for these ISG15s by the ERVEV and KUPEV OTUs. On the other hand, the CCHFV and GANV OTUs encode an arginine and lysine at position 80, respectively, creating a less stringent environment for binding that still permits cleavage, though perhaps not as optimally. To test the importance of this site, pro-hISG15 and pro-nsISG15 were both mutated to assess the effects of a residue swap (pro-hISG15-P130D and pro-nsISG15-D130P). Mutating this site alone is able to reduce or eliminate cleavage of pro-hISG15 by all the OTUs tested. Conversely, the opposite mutation in pro-nsISG15 introduced or enhanced cleavage. Combination of this mutation with the others in pro-hISG15 creates a range of cleavage efficiencies that can be used to match that of a particular OTU-pro-nsISG15 profile.

The influence of this position in pro-nsISG15 raised the question of whether there may be other less obvious residues in ISG15 that also influence the interface. This is

Fig 4.6. Additional residues influencing species-specific OTU-ISG15 interactions. (A) Comparison of KUPEV OTU-shISG15, ERVEV OTU-mISG15 (PDB ID 5JZE), GANV OTU-shISG15, and CCHFV OTU-hISG15 (PDB ID 3PHX) interactions between residue 130/128 of ISG15 and residues 77-80 of the OTU highlighting the variable sensitivity of this region. Structures colored as in Figs 4.3-4.5. Cleavage assays show the relative impact of mutations in pro-hISG15 and pro-nsISG15 on reactions with the CCHFV, ERVEV, KUPEV, and GANV OTUs. (B) KUPEV OTU-CshISG15 and CCHFV OTU-ChISG15 interactions at points that differ between shISG15 and hISG15. Cleavage assays show the impact of performing residue swaps in pro-hISG15 and pro-raISG15 on reactions with CCHFV, ERVEV, KUPEV, and GANV. Samples from each timepoint were run on BioRad Mini-PROTEAN[®] TGX Stain-Free[™] gels and visualized as described in the Materials and Methods.



particularly the case for shISG15, which despite being highly similar to hISG15 at the five positions tested can show a different cleavage profile, particularly in the case of KUPEV OTU. Examination suggested two other residues that could potentially contribute: Leu121 in hISG15 versus glutamine in shISG15, and Glu132 versus aspartate (Fig 4.6B). The location of residue 121 suggests that transient interactions might be possible if Arg149 were to adopt an alternate rotamer, while having a glutamate at position 132 could potentially add a steric component that might interfere with Ile80. Running assays with pro-hISG15-N89D/L121Q/E132D yielded variable results. For KUPEV OTU this modestly increased the cleavage, but for GANV and CCHFV it may have hindered it while leaving ERVEV unaffected. This suggests that residues other than those in the direct surface interface may have the ability to influence interaction.

As a further test of the utility of changing these residues to alter the suitability of a particular species' ISG15 as an OTU substrate, these sites were compared between vesper bat ISG15 versus Egyptian fruit bat ISG15. These two ISG15s provide a stark contrast in the activity that OTUs generally exhibit towards them, with moderate to high cleavage observed for vesper bat while only ERVEV is able to cleave Egyptian fruit bat proISG15 (Fig 4.2). As would be expected, these two ISG15s differ at five out of the seven identified residue positions (Fig 4.1B). To test the influence of these residues in distinguishing the two bat species, these sites were mutated in pro-raISG15 to match the composition with the corresponding residues in pro-bISG15. Excitingly, these mutations were able to introduce cleavage of pro-raISG15 by KUPEV, GANV, and CCHFV, and enhanced the cleavage by ERVEV (Fig. 4.6B). Overall, these assays demonstrate that shifting ISG15

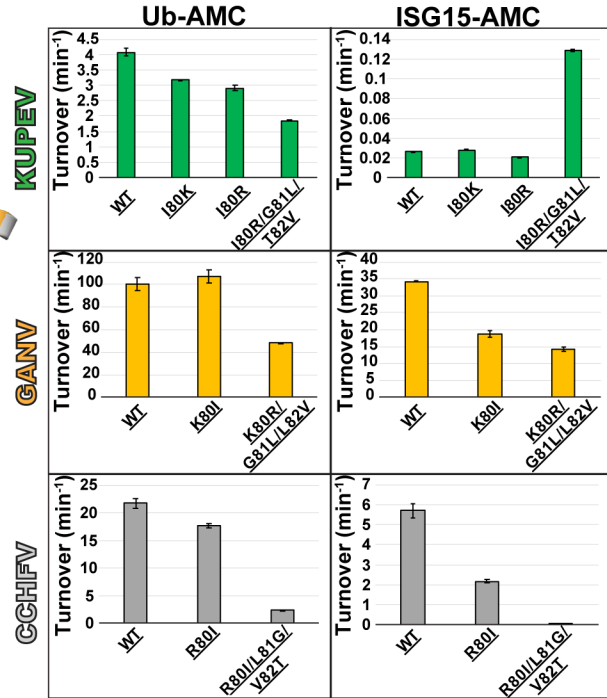
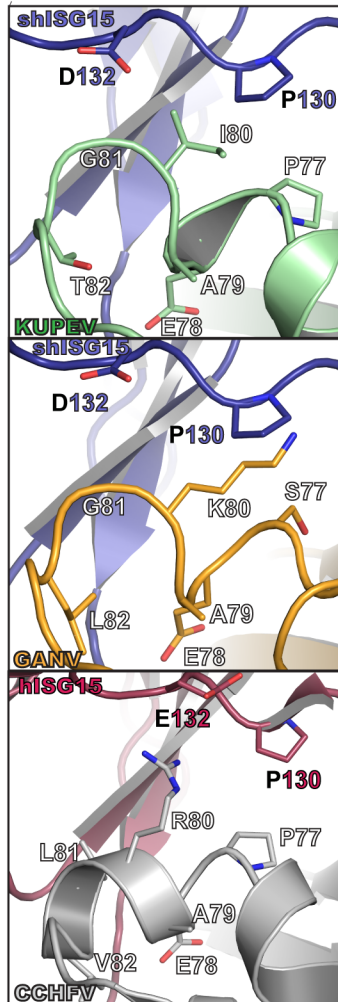
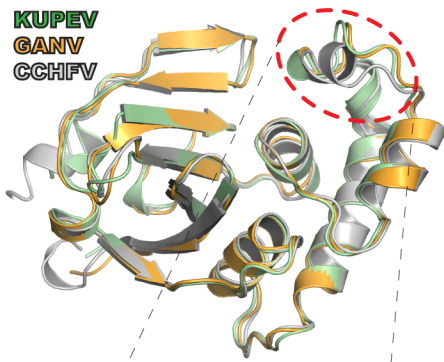
substrate preferences can be accomplished through specifically mutating a particular set of residues, and that this can have a key role in species-specific patterns.

Shifting OTU specificity for ISG15s from different species

The ability to shift species-specific preferences from an ISG15-directed approach led us to ask whether similar results could be achieved by mutating the OTU. From a virus-host adaptation standpoint, the OTU is the more likely of the two proteins to be subject to selective pressure, and would also be subject to a higher mutation rate from the viral RdRp compared to the host machinery. The wide divergence in activity observed in some OTUs towards different ISG15s, could be driven by specific residues that form the focal point of species-specificity. For example, while KUPEV OTU possesses low versus high activity for pro-hISG15 and pro-shISG15, respectively, the GANV and CCHFV OTUs possess activities for each that are close to equal (Fig 4.2). Similarly, KUPEV and GANV possess activity for pro-mISG15 that is close to their respective activity levels for pro-hISG15, while for CCHFV the activity is lower for pro-mISG15. This led us to assess the potential structural features that delineate these differences.

Examination of the OTU surface in KUPEV, GANV, and CCHFV that would interact with the variable regions of hISG15 and shISG15 suggested that the $\alpha 3$ “selectivity” helix of OTUs could play a role in differential specificity (Fig 4.7). This helix, particularly residue 80, is positioned where interactions with residue 132 in ISG15, a glutamate in human versus aspartate in sheep, may be able to influence binding. In GANV and CCHFV residue 80 is a lysine and arginine, respectively, which are both flexible and capable of forming an electrostatic interaction. In KUPEV OTU this residue is an isoleucine, potentially making it less conducive for the longer glutamate compared to

Fig 4.7. Targeting the OTU “selectivity helix” to alter ISG15 preference. (Upper left) Overlay of the KUPEV, GANV, and CCHFV OTUs colored as in Figs 4.3-4.5. The helix is indicated by a red oval, with closeup views of the helix in each structure shown on the lower left. (Upper right) Impact of single or multiple mutations within the helix on the activity of the KUPEV, GANV, and CCHFV OTUs. Values represent the mean \pm standard deviation of two independent experiments. (Lower right) Cleavage assays of OTU mutants with pro-hISG15 and pro-shISG15. Samples from each timepoint were run on BioRad Mini-PROTEAN[®] TGX[™] gels and visualized by Coomassie staining.



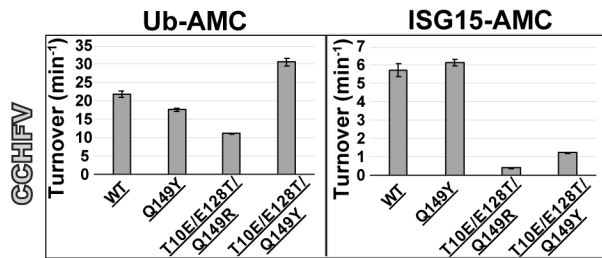
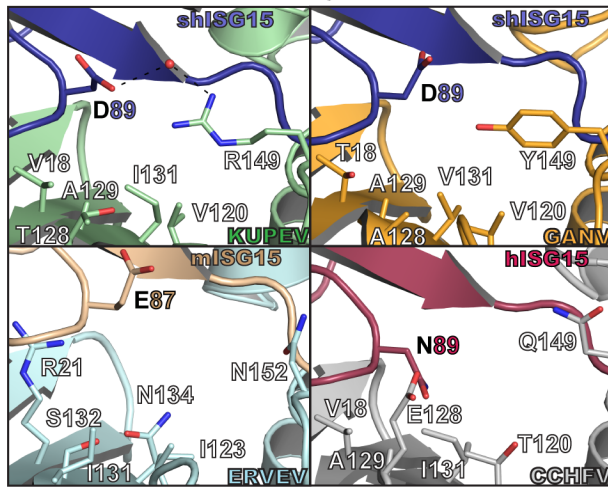
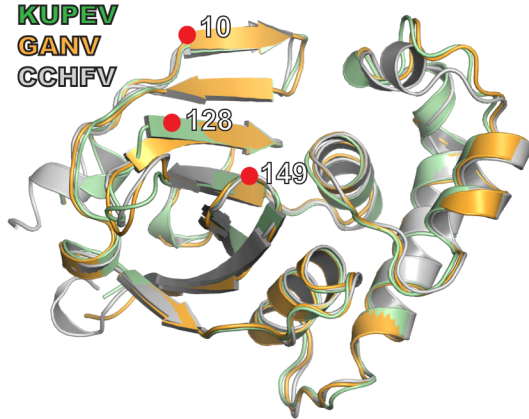
	hISG15	shISG15
KUPEV WT		
KUPEV I80K		
KUPEV I80R		
KUPEV I80R/G81L/T82V		
GANV WT		
GANV K80I		
GANV K80R/G81L/L82V		
CCHFV WT		
CCHFV R80I		
CCHFV R80I/L81G/V82T		

aspartate. To test whether the selectivity helix might be responsible for differentiating human and sheep ISG15, mutations were introduced to each OTU at residue 80 and assessed for their activity. In KUPEV OTU the isoleucine was changed to either a lysine or aspartate, and GANV and CCHFV to an isoleucine. Additionally, due to the difference in the position of the helix as a result of a glycine at position 81 in KUPEV and GANV versus a leucine in CCHFV, additional mutants were made to examine the impact of this helix's localization by converting residues 80-82 in KUPEV and GANV to the corresponding ones in CCHFV and CCHFV to the ones in KUPEV. To assess the impact of these changes, each mutant was tested for activity towards hISG15-AMC, pro-hISG15, and pro-shISG15 as well as Ub-AMC to gauge the effect on activity beyond ISG15. In KUPEV OTU it appears that residue 80 alone does not have a significant impact on ISG15 interaction, as I80K and I80R had no effect or a slight decrease, respectively, for hISG15-AMC. This is further borne out by the cleavage assays as there is no detectable difference from WT, and Ub-AMC is only slightly decreased in each case. The KUPEV helix mutant (I80R/G81L/T82V), on the other hand showed an increase in hISG15-AMC activity by a factor of five while reducing Ub-AMC activity by half. This increase in ISG15 activity is reflected in both pro-hISG15 and pro-shISG15 cleavage, suggesting that this helix plays an important role for ISG15 activity in general. For GANV OTU, the K80I mutant reduces hISG15-AMC activity by half but does not affect Ub-AMC, while the helix mutant reduces both by approximately half. Interestingly, this doesn't seem to be completely reflected in the proISG15 assay, as only the GANV helix mutant's ability to cleave pro-hISG15 appears to be affected. This may reflect the different levels of sensitivity and innate differences in the nature of the assays, possibly in relation to the high GANV turnover rate for ISG15-

AMC. In contrast, the CCHFV mutants revealed clear differences between different substrates. The helix mutant obliterated hISG15-AMC activity while reducing the activity towards Ub-AMC to almost a tenth of wildtype levels. This carried over into the proISG15 assay, with almost no cleavage observed. The R80I mutant, on the other hand, was more selective, reducing hISG15-AMC activity by more than half while only lowering Ub-AMC activity by a fifth. In addition, this mutant showed a differential impact in the proISG15 assay, with a noticeable reduction in pro-hISG15 cleavage while pro-shISG15 was not detectably impacted. This indicates that the relative preference for hISG15 versus shISG15 can be influenced by the selectivity helix and specifically residue 80. However, it appears that the relative impact of this region may not be universal for OTUs, or that it cannot be reduced to only these residues.

In the case of mISG15 specificity, analysis of the structures suggested that mISG15 residue 87/89 may play an important role (Fig 4.8). In both the KUPEV/GANV OTU-shISG15 and ERVEV OTU-CmISG15 structures, this residue is pointed away from the interface. Both KUPEV and GANV are able to interact with Asp89 in shISG15 through water-mediated electrostatic interactions with an arginine or tyrosine residue at position 149. Given this, it's possible that the longer Glu87 in mISG15 could form a direct electrostatic interaction with these residues. CCHFV, on the other hand, possesses a glutamine at residue 149 that would have a lower propensity to form this interaction. To assess the impact of this residue position, a Q149Y mutant of CCHFV OTU was generated (Fig. 4.8). This mutant had a modest decrease in Ub-AMC activity while leaving hISG15-AMC unaffected. In the cleavage assay, on the other hand, although pro-hISG15 cleavage remains unchanged, the activity towards pro-mISG15 is noticeably improved with

Fig 4.8. Selectively altering CCHFV OTU interactions with hISG15 and mISG15. (Top) Overlay of the KUPEV, GANV, and CCHFV OTUs with the targeted sites shown by red circles. Closeup views of the structural environment encompassing residues 128 and 149 (131/152 in ERVEV) of the OTUs is shown. Colored as in Figs 4.3-4.5. (Bottom) Impact of mutations on the activity of CCHFV OTU towards Ub-AMC, ISG15-AMC, pro-hISG15, and pro-mISG15. Values shown for the AMC assays represent the mean \pm standard deviation of two independent experiments. Samples from each proISG15 assay timepoint were run on BioRad Mini-PROTEAN[®] TGX[™] gels and visualized by Coomassie staining.



CCHFV	hISG15				mISG15					
	proISG15	ISG15	time (min)		proISG15	ISG15	time (min)			
WT	—	—	0	5	20	60	0	5	20	60
Q149Y	—	—	0	5	20	60	0	5	20	60
T10E/E128T/Q149R	—	—	0	5	20	60	0	5	20	60
T10E/E128T/Q149Y	—	—	0	5	20	60	0	5	20	60

increased product formation at 5 minutes and complete cleavage in an hour. This suggests that residue 149 plays a greater role in dictating mISG15 preference compared to hISG15. To assess whether a reversal in ISG15 specificity might be feasible, additional residues were also targeted for mutation in conjunction with position 149. Glu128 in CCHFV is an important contributor to hISG15 binding by interaction with Asn89, however this would likely present an obstacle to mISG15 binding due to the charge and larger size of Glu87. This residue was mutated to threonine to remove this obstacle and dampen hISG15 activity and combined with either a Q149R or Q149Y mutation to promote mISG15 activity. Due to the documented impact of the E128T in reducing Ub activity as well, an additional mutation was added (T10E) that is favorable for Ub in an attempt to compensate [47]. Analysis of the T10E/E128T/Q149R triple mutant revealed that Ub-AMC activity was still reduced by half, however, hISG15-AMC was reduced by more than 90%. This carried over in the proISG15 cleavage assay, where CCHFV goes from cleaving pro-hISG15 completely within 20 minutes to substrate still remaining for the triple mutant after an hour. Activity towards pro-mISG15 also suffers a small reduction, but not to the same degree as pro-hISG15. This produces an OTU with comparable, or slightly weaker, overall activity for mISG15 compared to hISG15, indicating that these mutants had a differential impact between ISG15 species. In the T10E/E128T/Q149Y mutant, on the other hand, Ub-AMC activity is actually boosted by ~40%, while activity for hISG15-AMC is reduced by almost 80%. This is reflected in the proISG15 assay with reduced cleavage observed with pro-hISG15, with some substrate still remaining after 20 minutes. Cleavage of pro-mISG15, however, is boosted relative to the wildtype OTU and closely resembles what is achieved by the Q149Y mutation alone. This puts the activity of this triple mutant towards pro-

mISG15 to levels slightly weaker than the activity shown with pro-hISG15, again showing a clear differential effect between the two species' ISG15. Overall, these analyses reveal important factors within the OTU that influence ISG15 species preference, and that the specific ones driving it most can differ between different OTUs.

Discussion

The implications of OTU-ISG15 specificity

The spectrum of activity of nairovirus OTUs on ISG15 from different host species raises interesting questions regarding host tropism. Apart from the better-known CCHFV, NSDV/GANV, and DUGV/KUPEV, for most nairoviruses it is unclear which are the preferred vertebrate hosts for virus maintenance and transmission in nature. The presence of general deISGylating activity among only about half of the currently characterized nairovirus species broadly known to infect mammals indicates that this could have been a particular adaptation to support replication of this subset of virus lineages. This suggests that the other virus species that do not demonstrate deISGylating activity may preferentially infect other vertebrates lacking ISG15, such as birds, or that they are primarily restricted to arthropod hosts. It could also be that the general function of the OTU in immune antagonism differs between nairoviruses, and that the presence of deISGylating activity among some of them represents an overall enhanced function of the OTU in co-adapting to mammalian species.

Consideration of the nairoviruses that do possess deISGylating activity raises additional questions on the adaptive nature of the OTU. Specifically, what is driving the specificity of OTUs for particular species' ISG15? Two general scenarios present themselves: (1) direct adaption to particular vertebrate hosts, or; (2) an indirect result of

the lifecycle of the tick vector/reservoir (i.e., the vertebrates preferred by the tick). In the case of the former, the preference for a particular ISG15 supports individual virus-host relationships, with the fine-tuning of OTU activity driven by the need for enhanced viral replication in one (or more) vertebrate hosts. This model is consistent with CCHFV which is known to replicate in diverse vertebrate species, and was shown here to interact with several species' ISG15 efficiently. However, a limiting factor for maintenance of endemic foci of CCHFV is reported to be the presence of the preferred *Hyalomma* spp. tick vector and reservoir [3, 51]. This suggests adaption to ticks as the primary factor driving virus evolution. Ticks lack ISG15 but possess other Ub-like proteins, such as SUMO and Nedd8 [52], that could present opportunities for OTU evolution in adaptation to some arthropods. In this model, the presence of deISGylating activity for ISG15 of differing vertebrate origin may be incidental. Many ticks infest livestock, including sheep and cattle, fitting nicely with the increased prevalence of activity towards these ISG15s among OTUs (Fig 4.2). Naturally the two hypotheses for the patterns of ISG15 specificity are not mutually exclusive and do not preclude the possibility that nairovirus co-adaptation could occur with both tick and vertebrate hosts. In particular, increased levels of viremia within the vertebrate host could enhance transmission to other ticks, presenting an overall selective advantage. It could be envisioned, then, that nairovirus host adaptation could be driven at two levels, with the primary level driven by the tick host, and the secondary level driven by the vertebrate host. Interestingly, only viruses of the tick-associated *Orthonairovirus* genus of the *Nairoviridae* family possess an OTU, with other nairovirus genera associated with millipedes and spiders apparently lacking this domain. This generally supports the notion of the OTU playing a role for exposure to multiple hosts.

As both direct and indirect vertebrate host adaptation may be the most advantageous for tick-borne nairoviruses, it is not surprising that the specific OTU-ISG15 preferences shown here largely correlate with the reported host circulation patterns of nairoviruses. For example, CCHFV has been serologically associated with a wide range of domestic and wild animals. While CCHFV displays broad deISGylating activity, enhanced activity is observed for hISG15, shISG15, and cwISG15. This enhanced activity in humans, sheep, and cows corresponds well with the observation that CCHFV not only causes viremia in these hosts, but also that the adult stage of *Hyalomma* ticks prefer members of the ruminant family *Bovidae* [51]. Though less comprehensive information is available for other nairoviruses, this trend is also apparent with NSDV/GANV, DUGV, and KUPEV. In each of these cases there is a known association with livestock, either by causing viremia or residence in ticks that infest these animals. As would be expected based on these known virus-host associations, all of these viruses show enhanced activity for shISG15 and cwISG15.

How variation in nairovirus OTU activity on ISG15 may relate to disease susceptibility in a particular host is unclear. Despite showing approximately equivalent preferences for hISG15, shISG15, and cwISG15, CCHFV causes severe disease in humans but is asymptomatic in livestock. A similar phenomenon occurs with NSDV/GANV, in which some sheep and goat populations contract deadly illness while cattle and other livestock are refractory to infection [14]. One possible explanation for this is that ISG15 represent only one aspect of the virus-host interface, and that other factors contribute to variable clinical outcomes. Alternatively, there could also be differences in the function of ISG15 between different species that influence the susceptibility to disease, as is

observed in the case comparing mice and humans [32]. Due to a more potent antiviral role of ISG15 in mice, it is possible that highly adapted OTU-ISG15 interactions merely facilitate successful and asymptomatic viral replication, whereas in humans they result in severe disease. Thus, while OTU preferences for particular species' ISG15 could serve as a marker for its host range, it cannot be assumed that equivalent biochemical activities always translate to equivalent presentations of illness between species.

Insights from the structural characterization of OTU-ISG15 interactions

The new structures of the KUPEV and GANV OTUs bound to shISG15 brings the total number of unique OTU-ISG15 interfaces to four, with CCHFV and ERVEV having been solved bound to hISG15 and mISG15, respectively [43, 48, 50]. This combination of four viral OTUs and three different species' ISG15 provides a breadth of knowledge on the factors that drive species-specificity. Here we have been able to identify and validate the molecular features of ISG15 that are primarily responsible for the species-variable patterns that are displayed. Specifically, there are seven residues in ISG15 that are predominant in determining species variability at the OTU binding interface, and making targeted mutations at these sites alters the interaction profile with OTUs. The trends observed provide a strong foundation for assessing virus-host interactions. For example, the data presents opportunities to predict virus-host interactions from ISG15 sequence alone, possibly allowing for the identification of previously unknown hosts involved in the enzootic maintenance of nairoviruses. In addition, these new structures and biochemical data may provide insights into the direction in which a given nairovirus is adapting. In one vein, this includes whether there are lineage-specific structural features of ISG15 that an OTU prefers. Perhaps more prescient, however, is the fact that simple point mutations in

the nairovirus are able to shift the species specificity of the OTU. This suggests that only a few changes may be necessary for a virus to shift its vertebrate host range, with possible additional implications for manifestation of disease depending on host-specific features with ISG15. Testing mutant variants of nairovirus OTUs may help anticipate the degree to which it would have to adapt to human hosts and provide insights into the potential threat posed by the virus.

Potential applications for OTU-ISG15 diversity

In addition to analytical approaches to assessing virus-host interactions, the diversity in OTU-ISG15 interactions also presents opportunities for empirical methods. Given the relationship between ISG15 preference and nairovirus host association, development of high throughput methods would present a time and cost-efficient way to screen for putative virus-host interactions and identify potentially unknown vertebrate hosts. In addition, it would provide a more complete picture of how host diversity impacts these relationships.

Knowledge of the key residues impacting OTU-ISG15 interactions may also create opportunities to explore what is currently unknown about ISG15 function. Altering the susceptibility of the ISG15 to viral DUBs could help decipher whether species differences are primarily mediated at the level of this protein-protein interaction, or if there are differences in ISG15's role on a larger scale. On a practical level, it could also contribute to the development of novel animal models of disease. Animal models to study nairovirus disease, specifically CCHFV, have been largely limited due to the need to use immunocompromised animals such as Stat-1^{-/-} or IFNAR^{-/-} mice [53, 54]. While a non-human primate model has been recently described for CCHFV [55], the field would benefit

from an immunocompetent small animal model system to study disease and potential treatments. Perhaps modification of ISG15 could be a more conservative and specific route to make an animal more susceptible to particular nairoviruses for the purposes of such studies. Alternatively, it could be envisioned how ISG15 could be modified in agriculturally important animals to make them more resistant to disease, for example genetically engineering a strain of sheep to be less susceptible to NSDV. From the virus side, in principle the potential exists to either abrogate activity, as might be done in the development of an attenuated vaccine, or selectively enhance activity to make a specific variant for animal studies.

Conclusion

The role of OTU-ISG15 interactions during nairovirus infection have remained largely in obscurity. This is in part due to the mystery that has enshrouded ISG15 function, including the potential that it differs between species, and the lack of clarity on the full impact of the OTU in nairovirus infections. Here we expand the knowledge of OTU interactions, revealing that strong ISG15 interactions are associated with particular virus lineages and uncovering a relationship between preferred species' ISG15 and reported host tropism. Leveraging novel structures, specific residues in both OTUs and ISG15 were identified that primarily drive these preferences. This yields insights that can be used to inform further developments into studying the role of ISG15 and possible ways to utilize its diversity. Overall, this presents exciting opportunities to better understand ISG15's functional impact in countering viral infections.

Materials and methods

Constructs, Expression and purification of OTUs and ISG15s

The OTUs of CCHFV, DUGV, ERVEV, NSDV, GANV, TAGV, QYBV, FARV, and KUPV were constructed, expressed, and purified as previously described [43, 44, 47, 49]. For ISG15s, those in the pro form from human (*Homo sapiens*; Accession: AAH09507.1), mouse (*Mus musculus*; Accession: AAB02697.1), sheep (*Ovis aries*; Accession: AF152103.1), dromedary camel (*Camelus dromedarius*; Accession: XP_010997700.1), northern tree shrew (*Tupaia belangeri*; Accession: AFH66859.1), vesper bat (*Myotis davidii*; Accession: ELK23605.1), and fish (*Oplegnathus fasciatus*; Accession: BAJ16365.1) were constructed, expressed and purified as previously described [43].

Similarly to the previously reported pro-ISG15s, the constructs of pro-ISG15s originating from porcine (*Sus scrofa*; Accession ACB87600.1) rabbit (*Oryctolagus cuniculus*; Accession XP_017195918), Egyptian fruit bat (*Rousettus aegyptiacus*; XP_015999857.1), cow (*Bos taurus*; NP_776791.1), and hedgehog (*Erinaceus europaeus*; XP_007525810.2) were comprised of their species mature ISG15 sequence identified by sequence homology, codon optimized, and had additional amino acid sequence GTEPGGRSGHHHHHH added to the C-terminal end. These constructs were placed into a pET-15b plasmid using the NdeI/BamHI restriction sites. The expression and purification of these pro-ISG15s mirrored that of previously reported pro-ISG15s [43]. In short, *E. coli* BL21 (DE3) cells containing these pro-ISG15 constructs were grown in 6 L of LB broth containing 100 µg/mL ampicillin until an OD₆₀₀ of 0.6 was reached. Expression was induced by the addition of IPTG to a final concentration of 0.5 mM then the culture was

grown overnight at 18°C. Subsequently, bacterial cells were isolated via centrifugation at 6,000 x g for 10 min and stored at -80°C until purification. For purification, the cell pellets containing these ISG15s were suspended in Buffer A [500 mM NaCl, 50 mM Tris (pH 7.0), 1 mM Tris (2-carbozyethyl) phosphine hydrochloride (TCEP-HCl)]. The addition of 5 mg of chicken lysozyme per 500 mL of Buffer A was used to initiate lysis for 30 minutes at 4°C then sonicated on ice at 50% power with 5-second pulse increments for 6 minutes. The insoluble cell debris was separated via centrifugation for 30 min at 48,000 x g. The resulting supernatant was filtered with a 0.80 µm filter prior to flowing it over a high-density nickel agarose beads (GoldBio) equilibrated with Buffer A. The column was then washed using Buffer A supplemented with 30 mM imidazole prior to eluting the protein of the column using Buffer A supplemented with 300 mM imidazole. The eluted protein was further purified using a Superdex-S75 column equilibrated with Buffer B [200 mM NaCl, 50 mM HEPES (pH 7.0), 2 mM DTT]. These purified pro-ISG15s were concentrated to ~1-4 mg/mL for storage at -80°C until use. All OTU and ISG15 protein concentrations were determined through UV-visible spectroscopy at 280 nm using molar extinction coefficients experimentally derived by the method of Gill and von Hippel [56].

To generate the propargylamine derivatized shISG15 and its C-terminal variant containing amino acids 79-156, sequence with codon for last glycine removed was inserted into pTYB2 using the NdeI/SmaI restrictions sites. As previously described [57], subsequent mutation was performed to alter the SmaI site to create the desired the RLRG sequence at the C-terminus of the two ISG15 constructs. These constructs were expressed and initially purified in the same way as the other ISG15 constructs. For purification, the only difference in the initial steps were the use of buffer C [75 mM NaCl, 50 mM Na

Acetate, and 25 mM HEPES (pH 6.8)] augmented with 0.16% Triton X-100). Once the clarified supernatant was obtained, it was flowed over a chitin resin column pre-equilibrated with buffer C. The chitin resin was subsequently washed with 2 column volumes of buffer C and resuspended in 50 ml of buffer C supplemented with 260 mM sodium 2-mercaptoethanesulfonate (MESNA). The solution was then rotated gently overnight 4°C, and the chitin beads were recollected by gravity flow. The volume of the solution containing the thioester forms of shISG15 and CshISG15 was reduced to 10 mL. To generate the final derivatized product of shISG15-PA, or CshISG15-PA, 0.92 g of propargylamine and 240 µL of 5 M NaOH were added to the ISG15 thioester containing solutions and left to incubate overnight at 4°C.

ISG15 Protease Activity Assay

Activity assays of OTUs originating from CCHFV, DUGV, ERVEV, NSDV, GANV, TAGV, QYBV, FARV, and KUPEV with purified Egyptian fruit bat proISG15 (pro-raISG15), northern tree shrew proISG15 (pro-nsISG15), rabbit proISG15 (pro-rISG15), sheep proISG15 (pro-shISG15), cow proISG15 (pro-cwISG15), fish proISG15 (pro-fISG15), mouse proISG15 (pro-mISG15), hedgehog proISG15 (pro-hhISG15), camel proISG15 (pro-clISG15), vesper bat proISG15 (pro-bISG15), and human proISG15 (pro-hISG15) were adapted from the previously reported methods [58]. Briefly, 20 nM OTU was tested for the ability to cleave 10 µM of each proISG15. Timepoints were taken over the course of an hour and the reactions quenched in 2x Laemmli buffer and boiling at 98°C for 5 minutes. Samples were run on BioRad Mini-PROTEAN® TGX™ (OTU mutants with proISG15) or Mini-PROTEAN® TGX Stain-Free™ pre-cast gels (wildtype proISG15 assays and mutant proISG15 assays). All the OTU mutant assays with proISG15 and

assays involving pro-fISG15 were visualized by Coomassie staining. Visualization of the remaining assay timepoints relied on Stain-Free technology that enhances the fluorescence of endogenous tryptophan. The gels were UV-activated for two minutes and subsequently imaged in a BioRad ChemiDoc™ Imaging system according to the manufacturer's recommendations.

KUPEV OTU-CshISG15 and GANV OTU-shISG15 Complex Formation

The procedure to form the KUPEV OTU-CshISG15 and GANV OTU-shISG15 complexes was adapted from previously described methods [43]. In short, purified KUPEV OTU and GANV OTU was added directly to the CshISG15-PA and shISG15-PA mixtures respectively in a 1:4 ratio. The solutions were then dialyzed in buffer D [250 mM NaCl, 25 mM HEPES (pH 7.0)] and buffer E [100 mM NaCl, 50 mM Tris (pH 8.0)] respectively overnight at 4°C. The dialyzed complex solution was then flowed through high-density nickel agarose beads pre-equilibrated with buffer D and buffer E respectively. The KUPEV OTU-CshISG15 complex was washed with buffer D supplemented with 30 mM imidazole and eluted with buffer D supplemented with 300 mM imidazole. The GANV OTU-shISG15 complex was washed with buffer E supplemented with 10 mM imidazole and eluted with 300 mM imidazole. To further purify the GANV complex, the solution, dialyzed in 50 mM Tris (pH 8.0), underwent anion exchange chromatography, eluting from a MonoQ 10/100 column using a linear gradient from 0 to 1 M NaCl with 50 mM Tris (pH 8.0). To further purify the complexes, size exclusion was performed on a Superdex 75 column pre-equilibrated with buffer F [100 mM NaCl, 5 mM HEPES (pH 7.0), and 5 mM DTT] for KUPEV OTU-CshISG15 and buffer G [100 mM NaCl, 5 mM HEPES (pH 7.5), and 10 mM DTT] for GANV OTU-shISG15. The KUPEV OTU-CshISG15 and GANV

OTU-shISG15 complexes were then concentrated to 12 mg/ml and 12.5 mg/ml respectively.

Crystallization of KUPEV OTU-CshISG15 and GANV OTU-shISG15

The Kupe OTU-CoISG15 and GANV OTU-shISG15 complexes were screened against a series of Qiagen NeXtal suites by hanging drop using a TTP Labtech Mosquito (TTP Labtech, Herfordshire, United Kingdom). For the Kupe OTU-CshISG15 complex, the initial screens yielded small, cube-shaped crystals from a condition containing 0.1 M Sodium Acetate (pH 4.6) and 2.0 M Potassium Acetate. This condition was optimized using a follow up screen, varying concentrations from 2.1 M to 2.6 M Potassium Acetate and varying pH from 3.6 to 5.1. The final optimized crystals were grown in hanging drops with 2 ul of protein complex solution mixed 2:1 with mother liquor containing 0.1 M Sodium acetate (pH 4.1) and 2.2 M Potassium acetate. The crystals were flash cooled in a cryoprotective solution containing 0.1 M sodium acetate (pH 4.1), 3 M Potassium acetate, and 30% glycerol. For the GANV OTU-shISG15 complex, the initial screens yielded flat, hexagonal crystals from a condition containing 0.1 M MES (pH 6.5) and 15% PEG 20,000. This condition was optimized using a follow up screen, varying concentrations from 8% to 19% PEG 20,000. The final optimized crystals were grown in hanging drops with 1 ul of protein complex solution mixed 1:1 with mother liquor containing 0.1 M MES (pH 5.5) and 15% PEG 20,000. The crystals were flash cooled in a cryoprotective solution containing 15% PEG 20,000 and an 18% solution consisting of ethylene glycol, DMSO, and glycerol present in a 1:1:1 ratio (EDG).

All crystals were mounted under a dry N₂ stream at 100 K. A data set for KUPEV OTU-CshISG15 was collected at the National Synchrotron Light Source II (Brookhaven

National Laboratory, Upton, NY) on Life Science Biomedical Technology Research AMX beamline 17-ID-1 using a Eiger9M detector. Data were collected using wavelength 1 Å. Similarly, a data set for GANV OTU-shISG15 was collected at the Advanced Photon Source (Argonne National Labs, Argonne, IL) on SBC-CAT beamline ID-18 using a Pilatus3 X 6M detector. Data were collected using wavelength 1 Å.

Data Processing and Structure Solutions

All X-ray images were indexed, strategized, integrated, and scaled using HKL2000 [59]. To create a cross-validation set from a random 5% of the reflections to be used throughout refinement, the CCP4 software suite was employed [60]. The initial phase solutions for the structures of KUPEV OTU-CshISG15 and GANV OTU-shISG15 were obtained using molecular replacement via Phaser [61]. The search models for both KUPEV OTU-CshISG15 and GANV OTU-shISG15 were homology models created by MODELLER[62] using the structures of CCHFV OTU-hISG15 (PDB entries 3PHX and 3PSE)[63], DUGV OTU-Ub (PDB entry 4HXD) [47], and ERVEV OTU-mISG15 (PDB entry 5JZE) [43] as templates. The structures were refined initially using Autobuild [64] then iterative cycles of model building with Coot [65] and refinement with Phenix [66]. The Find Water COOT program function was used to initially add water molecules to $2F_o - F_c$ density peaks greater than 1σ and subsequently were assessed individually [67]. Molprobit was used to examine the final model of each structure to confirm the quality of the structures. The data collection and refinement statistics for each structure along are listed in Table 4.1. KUPEV vOTU-CshISG15 (PDB entry 6OAR) and GANV vOTU-shISG15 (PDB entry 6OAT) have been deposited in the protein data bank.

Mutant Generation and Enzymatic Assays

Mutants of proISG15 and nairovirus OTUs were generated by the QuikChange approach using the manufacturer's protocol (Agilent Technologies, Inc). The resulting PCR product was transformed into NEB-5 α cells by heat shock (New England Biolabs), followed by plasmid purification and confirmation of mutants by sequencing. Confirmed mutant plasmids were transformed into BL21(DE3) or T7 Express cells by heat shock (New England Biolabs). The proISG15 cleavage assays were run as described above. Assays with Ub- and ISG15-AMC for the OTU mutants were run in duplicate as previously described [43, 44, 47]. Confirmation of Ub-AMC activity for HAZV, TAGV, FARV, DGKV, HpTV-1, LPHV, QYBV, and ISKV were run with an adapted protocol (4.S2 FigB). Assays were run in triplicate with 4 nM OTU against 1 μ M Ub-AMC in a 30 μ L reaction volume.

Acknowledgements

For the KUPEV OTU-CshISG15 structure this research used the Life Science Biomedical Technology Research AMX beamline 17-ID-1 of the National Synchrotron Light Source II, a U.S. Department of Energy (DOE) Office of Science User Facility operated for the DOE Office of Science by Brookhaven National Laboratory under Contract No. DE-SC0012704. The Life Science Biomedical Technology Research resource is primarily supported by the National Institute of Health, National Institute of General Medical Sciences (NIGMS) through a Biomedical Technology Research Resource P41 grant (P41GM111244), and by the DOE Office of Biological and Environmental Research (KP1605010). Results for the GANV OTU-shISG15 X-ray crystal structure shown in this report are derived from work performed at Argonne National Laboratory,

Structural Biology Center (SBC) at the Advanced Photon Source. SBC-CAT is operated by UChicago Argonne, LLC, for the U.S. Department of Energy, Office of Biological and Environmental Research under contract DE-AC02-06CH11357. The work was supported partly by NIH/NIAID application number 1R01AI109008 (SDP, EB). The findings and conclusions in this report are those of the authors and do not necessarily represent the official position of the Centers for Disease Control and Prevention.

References

1. Maes P, Adkins S, Alkhovsky SV, Avsic-Zupanc T, Ballinger MJ, Bente DA, et al. Taxonomy of the order Bunyavirales: second update 2018. *Arch Virol.* 2019;164(3):927-41. Epub 2019/01/22. doi: 10.1007/s00705-018-04127-3. PubMed PMID: 30663021.
2. Maes P, Alkhovsky SV, Bao Y, Beer M, Birkhead M, Briese T, et al. Taxonomy of the family Arenaviridae and the order Bunyavirales: update 2018. *Arch Virol.* 2018;163(8):2295-310. doi: 10.1007/s00705-018-3843-5. PubMed PMID: 29680923.
3. Bente DA, Forrester NL, Watts DM, McAuley AJ, Whitehouse CA, Bray M. Crimean-Congo hemorrhagic fever: history, epidemiology, pathogenesis, clinical syndrome and genetic diversity. *Antiviral Res.* 2013;100(1):159-89. Epub 2013/08/03. doi: 10.1016/j.antiviral.2013.07.006. PubMed PMID: 23906741.
4. Burt FJ, Spencer DC, Leman PA, Patterson B, Swanepoel R. Investigation of tick-borne viruses as pathogens of humans in South Africa and evidence of Dugbe virus infection in a patient with prolonged thrombocytopenia. *Epidemiol Infect.* 1996;116(3):353-61. Epub 1996/06/01. PubMed PMID: 8666081; PubMed Central PMCID: PMCPMC2271429.
5. Dandawate CN, Work TH, Webb JK, Shah KV. Isolation of Ganjam virus from a human case of febrile illness: a report of a laboratory infection and serological survey of human sera from three different states of India. *Indian J Med Res.* 1969;57(6):975-82. Epub 1969/06/01. PubMed PMID: 5823182.
6. Kalunda M, Mukwaya LG, Mukuye A, Lule M, Sekyalo E, Wright J, et al. Kasokero virus: a new human pathogen from bats (*Rousettus aegyptiacus*) in Uganda. *Am J Trop Med Hyg.* 1986;35(2):387-92. Epub 1986/03/01. PubMed PMID: 3082234.
7. L'Vov D K, Kostiuikov MA, Daniiarov OA, Tukhtaev TM, Sherikov BK. [Outbreak of arbovirus infection in the Tadzhik SSR due to the Issyk-Kul virus (Issyk-Kul fever)]. *Vopr Virusol.* 1984;29(1):89-92. Epub 1984/01/01. PubMed PMID: 6143452.

8. Rao CV, Dandawate CN, Rodrigues JJ, Rao GL, Mandke VB, Ghalsasi GR, et al. Laboratory infections with Ganjam virus. *Indian J Med Res.* 1981;74:319-24. Epub 1981/09/01. PubMed PMID: 6797936.
9. Treib J, Dobler G, Haass A, von Blohn W, Strittmatter M, Pindur G, et al. Thunderclap headache caused by Erve virus? *Neurology.* 1998;50(2):509-11. Epub 1998/03/04. PubMed PMID: 9484383.
10. Spengler JR, Bergeron E, Rollin PE. Seroepidemiological Studies of Crimean-Congo Hemorrhagic Fever Virus in Domestic and Wild Animals. *PLoS Negl Trop Dis.* 2016;10(1):e0004210. Epub 2016/01/08. doi: 10.1371/journal.pntd.0004210. PubMed PMID: 26741652; PubMed Central PMCID: PMC4704823.
11. Spengler JR, Estrada-Pena A, Garrison AR, Schmaljohn C, Spiropoulou CF, Bergeron E, et al. A chronological review of experimental infection studies of the role of wild animals and livestock in the maintenance and transmission of Crimean-Congo hemorrhagic fever virus. *Antiviral Res.* 2016;135:31-47. Epub 2016/10/28. doi: 10.1016/j.antiviral.2016.09.013. PubMed PMID: 27713073; PubMed Central PMCID: PMC45102700.
12. Davies FG. Nairobi sheep disease. *Parassitologia.* 1997;39(2):95-8. Epub 1997/06/01. PubMed PMID: 9530691.
13. Ishii A, Ueno K, Orba Y, Sasaki M, Moonga L, Hang'ombe BM, et al. A nairovirus isolated from African bats causes haemorrhagic gastroenteritis and severe hepatic disease in mice. *Nat Commun.* 2014;5:5651. Epub 2014/12/03. doi: 10.1038/ncomms6651. PubMed PMID: 25451856; PubMed Central PMCID: PMC4268697.
14. Montgomery E. On a Tick-borne Gastroenteritis of Sheep and Goats occurring in British East Africa. *Journal of Comparative Pathology and Therapeutics.* 1917;30(1):28-57.
15. Converse JD, Hoogstraal H, Moussa MI, Feare CJ, Kaiser MN. Soldado virus (Hughes group) from *Ornithodoros (Alectorobius) capensis* (Ixodoidea: Argasidae) infesting Sooty Tern colonies in the Seychelles, Indian Ocean. *Am J Trop Med Hyg.* 1975;24(6 Pt 1):1010-8. Epub 1975/11/01. PubMed PMID: 1200252.
16. Crabtree MB, Sang R, Miller BR. Kupe virus, a new virus in the family bunyaviridae, genus nairovirus, kenya. *Emerg Infect Dis.* 2009;15(2):147-54. Epub 2009/02/06. PubMed PMID: 19193256; PubMed Central PMCID: PMC2657624.
17. Sang R, Onyango C, Gachoya J, Mabinda E, Konongoi S, Ofula V, et al. Tickborne arbovirus surveillance in market livestock, Nairobi, Kenya. *Emerg Infect Dis.* 2006;12(7):1074-80. Epub 2006/07/14. doi: 10.3201/eid1207.060253. PubMed PMID: 16836823; PubMed Central PMCID: PMC163291068.
18. Durfee LA, Lyon N, Seo K, Huibregtse JM. The ISG15 conjugation system broadly targets newly synthesized proteins: implications for the antiviral function of ISG15. *Mol*

Cell. 2010;38:722-32. Epub 2010/06/15. doi: 10.1016/j.molcel.2010.05.002. PubMed PMID: 20542004.

19. Bakshi S, Holzer B, Bridgen A, McMullan G, Quinn DG, Baron MD. Dugbe virus ovarian tumour domain interferes with ubiquitin/ISG15-regulated innate immune cell signalling. *J Gen Virol.* 2013;94(Pt 2):298-307. Epub 2012/11/09. doi: 10.1099/vir.0.048322-0. PubMed PMID: 23136361; PubMed Central PMCID: PMC3709621.

20. Frias-Staheli N, Giannakopoulos NV, Kikkert M, Taylor SL, Bridgen A, Paragas J, et al. Ovarian tumor domain-containing viral proteases evade ubiquitin- and ISG15-dependent innate immune responses. *Cell Host and Microbe.* 2007;2:404-16.

21. Holzer B, Bakshi S, Bridgen A, Baron MD. Inhibition of interferon induction and action by the nairovirus Nairobi sheep disease virus/Ganjam virus. *PLoS One.* 2011;6(12):e28594. Epub 2011/12/14. doi: 10.1371/journal.pone.0028594. PubMed PMID: 22163042; PubMed Central PMCID: PMC3230622.

22. Scholte FEM, Zivcec M, Dzimianski JV, Deaton MK, Spengler JR, Welch SR, et al. Crimean-Congo Hemorrhagic Fever Virus Suppresses Innate Immune Responses via a Ubiquitin and ISG15 Specific Protease. *Cell Rep.* 2017;20(10):2396-407. Epub 2017/09/07. doi: 10.1016/j.celrep.2017.08.040. PubMed PMID: 28877473; PubMed Central PMCID: PMC5616139.

23. Niemeyer D, Mösbauer K, Klein EM, Sieberg A, Mettelman RC, Mielech AM, et al. The papain-like protease determines a virulence trait that varies among members of the SARS-coronavirus species. *PLoS pathogens.* 2018;14:e1007296. doi: 10.1371/journal.ppat.1007296. PubMed PMID: 30248143.

24. Arimoto K-iI, Löchte S, Stoner SA, Burkart C, Zhang Y, Miyauchi S, et al. STAT2 is an essential adaptor in USP18-mediated suppression of type I interferon signaling. *Nature Structural & Molecular Biology.* 2017;24:279-89. doi: 10.1038/nsmb.3378. PubMed PMID: 28165510.

25. Bogunovic D, Byun M, Durfee LA, Abhyankar A, Sanal O, Mansouri D, et al. Mycobacterial Disease and Impaired IFN- γ Immunity in Humans with Inherited ISG15 Deficiency. *Science.* 2012;2:1684-9.

26. D'Cunha J, Ramanujam S, Wagner RJ, Witt PL, Knight Jr. E, Borden EC. In vitro and in vivo secretion of human ISG15, an IFN-induced immunomodulatory cytokine. *J Immunol.* 1996;157:4100-8. Epub 1996/11/01. PubMed PMID: 8892645.

27. Du Y, Duan T, Feng Y, Liu Q, Lin M, Cui J, et al. LRRC25 inhibits type I IFN signaling by targeting ISG15-associated RIG-I for autophagic degradation. *The EMBO Journal.* 2017:e96781. doi: 10.15252/embj.201796781.

28. Knight Jr. E, Cordova B. IFN-induced 15-kDa protein is released from human lymphocytes and monocytes. *J Immunol.* 1991;146:2280-4. Epub 1991/04/01. PubMed PMID: 2005397.
29. Malakhov MP, Malakhova OA, Kim KI, Ritchie KJ, Zhang DE. UBP43 (USP18) specifically removes ISG15 from conjugated proteins. *J Biol Chem.* 2002;277:9976-81. Epub 2002/01/15. doi: 10.1074/jbc.M109078200. PubMed PMID: 11788588.
30. Malakhova OA, Yan M, Malakhov MP, Yuan Y, Ritchie KJ, Kim KI, et al. Protein ISGylation modulates the JAK-STAT signaling pathway. *Genes Dev.* 2003;17:455-60. Epub 2003/02/26. doi: 10.1101/gad.1056303. PubMed PMID: 12600939.
31. Recht M, Borden EC, Knight Jr. E. A human 15-kDa IFN-induced protein induces the secretion of IFN-gamma. *J Immunol.* 1991;147:2617-23. Epub 1991/10/25. PubMed PMID: 1717569.
32. Speer SD, Li Z, Buta S, Payelle-Brogard B, Qian L, Vigant F, et al. ISG15 deficiency and increased viral resistance in humans but not mice. *Nat Commun.* 2016;7:11496. Epub 2016/05/20. doi: 10.1038/ncomms11496. PubMed PMID: 27193971.
33. Swaim CD, Scott AF, Canadeo LA, Huibregtse JM. Extracellular ISG15 Signals Cytokine Secretion through the LFA-1 Integrin Receptor. *Mol Cell.* 2017;68(3):581-90 e5. Epub 2017/11/04. doi: 10.1016/j.molcel.2017.10.003. PubMed PMID: 29100055; PubMed Central PMCID: PMC5690536.
34. Zhang X, Bogunovic D, Payelle-Brogard B, Francois-Newton V, Speer SD, Yuan C, et al. Human intracellular ISG15 prevents interferon-alpha/beta over-amplification and auto-inflammation. *Nature.* 2015;517(7532):89-93. Epub 2014/10/14. doi: 10.1038/nature13801. PubMed PMID: 25307056; PubMed Central PMCID: PMC4303590.
35. Daczkowski CM, Dzimianski JV, Clasman JR, Goodwin O, Mesecar AD, Pegan SD. Structural Insights into the Interaction of Coronavirus Papain-Like Proteases and Interferon-Stimulated Gene Product 15 from Different Species. *J Mol Biol.* 2017;429(11):1661-83. Epub 2017/04/26. doi: 10.1016/j.jmb.2017.04.011. PubMed PMID: 28438633; PubMed Central PMCID: PMC5634334.
36. Jiang Y, Wang X. Structural insights into the species preference of the influenza B virus NS1 protein in ISG15 binding. *Protein & cell.* 2018. doi: 10.1007/s13238-018-0598-4. PubMed PMID: 30519829.
37. Langley C, Goodwin O, Dzimianski JV, Daczkowski CM, Pegan SD. Structure of interferon-stimulated gene product 15 (ISG15) from the bat species *Myotis davidii* and the impact of interdomain ISG15 interactions on viral protein engagement. *Acta Crystallographica Section D Structural Biology.* 2019;75. doi: 10.1107/S2059798318015322.

38. Dzimianski JV, Scholte FEM, Bergeron É, Pegan SD. ISG15: it's Complicated. *Journal of Molecular Biology*. 2019. doi: <https://doi.org/10.1016/j.jmb.2019.03.013>.
39. Zhao C, Sridharan H, Chen R, Baker DP, Wang S, Krug RM. Influenza B virus non-structural protein 1 counteracts ISG15 antiviral activity by sequestering ISGylated viral proteins. *Nat Commun*. 2016;7:12754. Epub 2016/09/03. doi: 10.1038/ncomms12754. PubMed PMID: 27587337.
40. Guan R, Ma LC, Leonard PG, Amer BR, Sridharan H, Zhao C, et al. Structural basis for the sequence-specific recognition of human ISG15 by the NS1 protein of influenza B virus. *Proc Natl Acad Sci U S A*. 2011;108:13468-73. Epub 2011/08/03. doi: 10.1073/pnas.1107032108. PubMed PMID: 21808041.
41. Sridharan H, Zhao C, Krug RM. Species specificity of the NS1 protein of influenza B virus: NS1 binds only human and non-human primate ubiquitin-like ISG15 proteins. *J Biol Chem*. 2010;285(11):7852-6. Epub 2010/01/23. doi: 10.1074/jbc.C109.095703. PubMed PMID: 20093371; PubMed Central PMCID: PMC2832935.
42. Versteeg GA, Hale BG, van Boheemen S, Wolff T, Lenschow DJ, Garcia-Sastre A. Species-specific antagonism of host ISGylation by the influenza B virus NS1 protein. *J Virol*. 2010;84:5423-30. Epub 2010/03/12. doi: 10.1128/JVI.02395-09. PubMed PMID: 20219937.
43. Deaton MK, Dzimianski JV, Daczkowski CM, Whitney GK, Mank NJ, Parham MM, et al. Biochemical and Structural Insights into the Preference of Nairoviral DeISGylases for Interferon-Stimulated Gene Product 15 Originating from Certain Species. *J Virol*. 2016;90(18):8314-27. Epub 2016/07/15. doi: 10.1128/JVI.00975-16. PubMed PMID: 27412597; PubMed Central PMCID: PMC5008091.
44. Dzimianski JV, Beldon BS, Daczkowski CM, Goodwin OY, Scholte FEM, Bergeron E, et al. Probing the impact of nairovirus genomic diversity on viral ovarian tumor domain protease (vOTU) structure and deubiquitinase activity. *PLoS Pathog*. 2019;15(1):e1007515. Epub 2019/01/11. doi: 10.1371/journal.ppat.1007515. PubMed PMID: 30629698; PubMed Central PMCID: PMC6343935.
45. Daczkowski CM, Goodwin OY, Dzimianski JV, Farhat JJ, Pegan SD. Structurally Guided Removal of DeISGylase Biochemical Activity from Papain-Like Protease Originating from Middle East Respiratory Syndrome Coronavirus. *J Virol*. 2017;91. Epub 2017/09/22. doi: 10.1128/JVI.01067-17. PubMed PMID: 28931677.
46. Deaton MK, Spear A, Faaberg KS, Pegan SD. The vOTU domain of highly-pathogenic porcine reproductive and respiratory syndrome virus displays a differential substrate preference. *Virology*. 2014;454-455:247-53. Epub 2014/04/15. doi: 10.1016/j.virol.2014.02.026. PubMed PMID: 24725951.
47. Capodagli GC, Deaton MK, Baker EA, Lumpkin RJ, Pegan SD. Diversity of ubiquitin and ISG15 specificity among nairoviruses' viral ovarian tumor domain proteases.

J Virol. 2013;87(7):3815-27. Epub 2013/01/25. doi: 10.1128/JVI.03252-12. PubMed PMID: 23345508; PubMed Central PMCID: PMC3624237.

48. Akutsu M, Ye Y, Virdee S, Chin JW, Komander D. Molecular basis for ubiquitin and ISG15 cross-reactivity in viral ovarian tumor domains. *Proc Natl Acad Sci U S A*. 2011;108(6):2228-33. Epub 2011/01/27. doi: 10.1073/pnas.1015287108. PubMed PMID: 21266548; PubMed Central PMCID: PMC3038727.

49. Capodagli GC, McKercher MA, Baker EA, Masters EM, Brunzelle JS, Pegan SD. Structural analysis of a viral ovarian tumor domain protease from the Crimean-Congo hemorrhagic fever virus in complex with covalently bonded ubiquitin. *J Virol*. 2011;85(7):3621-30. Epub 2011/01/14. doi: 10.1128/JVI.02496-10. PubMed PMID: 21228232; PubMed Central PMCID: PMC3067871.

50. James TW, Frias-Staheli N, Bacik J-P, Livingston Macleod JM, Khajehpour M, García-Sastre A, et al. Structural basis for the removal of ubiquitin and interferon-stimulated gene 15 by a viral ovarian tumor domain-containing protease. *Proceedings of the National Academy of Sciences of the United States of America*. 2011;108:2222-7.

51. Spengler JR, Estrada-Pena A. Host preferences support the prominent role of Hyalomma ticks in the ecology of Crimean-Congo hemorrhagic fever. *PLoS Negl Trop Dis*. 2018;12(2):e0006248. Epub 2018/02/09. doi: 10.1371/journal.pntd.0006248. PubMed PMID: 29420542; PubMed Central PMCID: PMC5821391.

52. Choy A, Severo MS, Sun R, Girke T, Gillespie JJ, Pedra JH. Decoding the ubiquitin-mediated pathway of arthropod disease vectors. *PLoS One*. 2013;8(10):e78077. Epub 2013/11/10. doi: 10.1371/journal.pone.0078077. PubMed PMID: 24205097; PubMed Central PMCID: PMC3804464.

53. Bente DA, Alimonti JB, Shieh WJ, Camus G, Stroher U, Zaki S, et al. Pathogenesis and immune response of Crimean-Congo hemorrhagic fever virus in a STAT-1 knockout mouse model. *J Virol*. 2010;84(21):11089-100. Epub 2010/08/27. doi: 10.1128/JVI.01383-10. PubMed PMID: 20739514; PubMed Central PMCID: PMC302953203.

54. Zivcec M, Safronetz D, Scott D, Robertson S, Ebihara H, Feldmann H. Lethal Crimean-Congo hemorrhagic fever virus infection in interferon alpha/beta receptor knockout mice is associated with high viral loads, proinflammatory responses, and coagulopathy. *J Infect Dis*. 2013;207(12):1909-21. Epub 2013/02/19. doi: 10.1093/infdis/jit061. PubMed PMID: 23417661; PubMed Central PMCID: PMC3654741.

55. Haddock E, Feldmann F, Hawman DW, Zivcec M, Hanley PW, Saturday G, et al. A cynomolgus macaque model for Crimean-Congo haemorrhagic fever. *Nat Microbiol*. 2018;3(5):556-62. Epub 2018/04/11. doi: 10.1038/s41564-018-0141-7. PubMed PMID: 29632370.

56. Gill SC, von Hippel PH. Calculation of protein extinction coefficients from amino acid sequence data. *Anal Biochem.* 1989;182(2):319-26. Epub 1989/11/01. PubMed PMID: 2610349.
57. Wilkinson KD, Gan-Erdene T, Kolli N. Derivatization of the C-terminus of ubiquitin and ubiquitin-like proteins using intein chemistry: methods and uses. *Methods Enzymol.* 2005;399:37-51. Epub 2005/12/13. doi: 10.1016/S0076-6879(05)99003-4. PubMed PMID: 16338347.
58. Deaton MK, Dzimianski JV, Daczkowski CM, Whitney GK, Mank NJ, Parham MM, et al. Biochemical and Structural Insights into the Preference of Nairoviral DeISGylases for Interferon-Stimulated Gene Product 15 Originating from Certain Species. *Journal of Virology.* 2016;90(18):8314-27. doi: 10.1128/jvi.00975-16.
59. Otwinowski Z, Minor W. Processing of X-ray Diffraction Data Collected in Oscillation Mode. C.W. Carter J, Sweet RM, editors. New York: Academic Press; 1997. 307-26 p.
60. Winn MD, Ballard CC, Cowtan KD, Dodson EJ, Emsley P, Evans PR, et al. Overview of the CCP4 suite and current developments. *Acta Crystallogr D Biol Crystallogr.* 2011;67(Pt 4):235-42. Epub 2011/04/05. doi: 10.1107/S0907444910045749. PubMed PMID: 21460441; PubMed Central PMCID: PMCPMC3069738.
61. McCoy AJ, Grosse-Kunstleve RW, Adams PD, Winn MD, Storoni LC, Read RJ. Phaser crystallographic software. *J Appl Crystallogr.* 2007;40(Pt 4):658-74. Epub 2007/08/01. doi: 10.1107/S0021889807021206. PubMed PMID: 19461840; PubMed Central PMCID: PMCPMC2483472.
62. Webb B, Sali A. Comparative Protein Structure Modeling Using MODELLER. *Curr Protoc Protein Sci.* 2016;86:2 9 1-2 9 37. Epub 2016/11/02. doi: 10.1002/cpps.20. PubMed PMID: 27801516.
63. Akutsu M, Ye Y, Virdee S, Chin JW, Komander D. Molecular basis for ubiquitin and ISG15 cross-reactivity in viral ovarian tumor domains. *Proc Natl Acad Sci U S A.* 2011. Epub 2011/01/27. doi:1015287108 [pii]
10.1073/pnas.1015287108. PubMed PMID: 21266548.
64. Terwilliger TC, Grosse-Kunstleve RW, Afonine PV, Moriarty NW, Zwart PH, Hung L-W, et al. Iterative model building, structure refinement and density modification with the PHENIX AutoBuild wizard. *Acta Crystallographica Section D.* 2008;64(1):61-9. doi: doi:10.1107/S090744490705024X.
65. Emsley P, Cowtan K. Coot: model-building tools for molecular graphics. *Acta Crystallographica Section D.* 2004;60(12):2126-32. doi: 10.1107/S0907444904019158.
66. Adams PD, Afonine PV, Bunkoczi G, Chen VB, Davis IW, Echols N, et al. PHENIX: a comprehensive Python-based system for macromolecular structure solution.

Acta Crystallogr D Biol Crystallogr. 2010;66(Pt 2):213-21. Epub 2010/02/04. doi: 10.1107/S0907444909052925. PubMed PMID: 20124702; PubMed Central PMCID: PMC2815670.

67. Emsley P, Cowtan K. Coot: model-building tools for molecular graphics. Acta Crystallogr D Biol Crystallogr. 2004;60(Pt 12 Pt 1):2126-32. Epub 2004/12/02. doi: 10.1107/S0907444904019158. PubMed PMID: 15572765.

68. Goujon M, McWilliam H, Li W, Valentin F, Squizzato S, Paern J, et al. A new bioinformatics analysis tools framework at EMBL-EBI. Nucleic Acids Res. 2010;38(Web Server issue):W695-9. Epub 2010/05/05. doi: 10.1093/nar/gkq313. PubMed PMID: 20439314; PubMed Central PMCID: PMC2896090.

69. Sievers F, Wilm A, Dineen D, Gibson TJ, Karplus K, Li W, et al. Fast, scalable generation of high-quality protein multiple sequence alignments using Clustal Omega. Mol Syst Biol. 2011;7:539. Epub 2011/10/13. doi: 10.1038/msb.2011.75. PubMed PMID: 21988835; PubMed Central PMCID: PMC3261699.

70. Robert X, Gouet P. Deciphering key features in protein structures with the new ENDscript server. Nucleic Acids Res. 2014;42(Web Server issue):W320-4. Epub 2014/04/23. doi: 10.1093/nar/gku316. PubMed PMID: 24753421; PubMed Central PMCID: PMC4086106.

71. Kabsch W, Sander C. Dictionary of protein secondary structure: pattern recognition of hydrogen-bonded and geometrical features. Biopolymers. 1983;22(12):2577-637. Epub 1983/12/01. doi: 10.1002/bip.360221211. PubMed PMID: 6667333.

CHAPTER 5

DISCUSSION

The implications of OTU-substrate activity and preference

The emergence and re-emergence of viruses possessing DUBs has led to concerted efforts to study their function and potential as therapeutic targets. The clear demonstration of an impact on the innate immune response and examples of the association of DUB activity with virulence have largely validated this approach [48, 59-61]. This certainly seems to be consistent with CCHFV, which compared to many other nairoviruses possesses enhanced DUB and deISGylase activity and also shows the greatest pathogenicity in humans. This observation could suggest a model where DUB activity is a contributor in nairoviruses to causing severe pathogenicity. However, viewing viral DUBs strictly as a virulence factor may create an unhelpfully strict perspective. For one, the evolutionary driver for viruses is not to be pathogenic per se, but to replicate in greater total numbers. In some cases pathogenic effects may aid in this, for example by increasing virus dissemination as might be the case for some respiratory viruses, but at the other extreme severe disease may actually hinder spread through lethality or malaise that restricts host-host interactions. For another, in nairoviruses the presence or absence of deubiquitinating activity does not necessarily correlate with the ability to trigger illness. While the deubiquitinating and deISGylating activity of NSDV, for example, does not appear to be much different from CCHFV biochemically, the pathogenic effects do not match for the same hosts. A better perspective of the OTU may be to view it as a mechanism for host

adaptation, and that in the presence of other factors and host interactions can result in pathogenicity.

General trends in OTU activity and host associations

Viewing the OTU from this more general view (that it reflects adaptation to viral hosts) yields interesting observations for nairoviruses. It is particularly noteworthy that activity for Ub and ISG15 largely coincides with the viruses that are mostly closely centered phylogenetically around CCHFV. To a large degree, these viruses are known to either infect, replicate in, or be present in ticks known to associate with vertebrate hosts. This strongly suggests that the OTU specifically adapted within this subgroup of viruses to accommodate circulation through vertebrate, particularly mammalian, hosts. This does not exclude the possibility that other nairoviruses do not utilize other mechanisms for adaptation and cannot replicate in vertebrates. LPHV, for example, was isolated from bats and can cause disease in mice upon experimental infection [9], yet it apparently lacks notable activity for both Ub and most, if not all, species' ISG15. On the whole, however, there appears to be a selective advantage for DUB and deISGylase that has driven the development of this activity in some nairovirus lineages that have long-term associations with mammalian hosts.

Implications for cellular pathways targeted by OTU activity

An additional point of significance for those OTUs possessing substantial DUB activity is the fact that it is not universal to all forms of Ub, but that there are preferences for specific poly-Ub linkages. The particular activities that OTUs possess towards these different forms implies that they target specific pathways. On one level, the common trend of OTUs interacting with the same four linkages, K6, K11, K48, and K63, suggests that

there are consistent processes that nairoviruses target. The fact that the relative preference can vary, however, suggests that there is individual malleability available to a virus for adaptation. The targeted linkages are largely consistent with a model of the OTU suppressing immune signaling and effects. Activity for K63 in particular makes sense due to its involvement in activating components of the RIG-I pathway, and suppression of RIG-I signaling is a known effect of the OTU. Targeting K48 also stands out due to its wide usage in regulating cellular processes through specific protein degradation. It can be easily envisioned how this activity of the OTU could be advantageous either by disrupting the regulation of immune signaling or by preserving viral proteins from K48-mediated degradation. With K6 and K11 more details will be needed to better grasp the functional outcome of OTU activity for these forms. However, the association of K11 with regulating TNF signaling [76] may provide a connection to OTUs impacting immune pathways other than RIG-I. For K6, on the other hand, the only significant cytoplasmic role identified so far is in the regulation of mitophagy [68, 69], which opens larger questions on how the OTU might be involved in manipulating host responses.

A convergence on mitochondria?

Mitochondria play important, but often unmentioned roles in cellular antiviral responses. This includes in the activation of the innate immune response through MAVS, which associates with activated, poly-ubiquitinated RIG-I as a part of signal transduction process. In addition, mitochondria play a critical part in the intrinsic pathway of apoptosis, a mechanism that can either combat viruses or be exploited by viruses [89]. Interestingly, the induction of mitophagy to eliminate faulty mitochondria is primarily driven by K6 poly-Ub, but can also involve K11, K48, and K63 [90]. This corresponds remarkably with the

general trend of nairovirus OTU activity. In addition, ISGylation has also been proposed to regulate mitochondrial function, including mitophagy, during infection [91, 92]. The activity antagonizing these poly-Ub linkages and ISG15 strongly suggest the potential of the OTU to be disruptive for mitophagy. If this is the case, it would result in faulty mitochondria persisting in the cellular environment. Whether this occurs and the benefit it would have for nairoviruses is an open question. Another thing to consider, however, is the potential role of the NSs in causing apoptosis in later stages of viral infection. The study describing this function of NSs reported that it was relatively unstable in the cellular environment, suggesting that it may be targeted for degradation [41]. Though the mechanism is currently unknown, it is within the realm of possibility that K48 poly-Ub could be involved. If this is the case, the OTU could serve a protective function for the NSs that allows to perform its function. Examination of potential connections that OTU activity might have to mitochondrial disruption would merit further investigation and may provide further insight into the impact of nairoviruses on larger scale cellular processes.

The OTU: more than a deubiquitinase/deISGylase?

Given all the potential benefits that DUB/deISGylase activity can have for a virus, it is somewhat surprising that many nairovirus OTUs apparently lack activity towards either substrate. For ISG15, in principle the lack of activity could just reflect high specificity for a particular species that isn't represented in the panel. However, the overall trend of which viruses do or do not appear to interact with ISG15 suggests there to be a genuine absence of ISG15 for some, if not many, of the nairoviruses. This raises questions as to whether there could be other functions that the OTU may be performing. One possibility is that there are other Ub-like modifiers that the OTU interacts with rather than

Ub or ISG15. This includes proteins such as SUMO, Nedd8, and FAT10, that can have regulatory roles during innate and adaptive immune signaling [93, 94]. While CCHFV lacks substantial activity for Nedd8 [95], interactions with these and other Ub-like proteins have not been fully investigated. It is possible that other OTUs may be able to interact with these proteins even if CCHFV does not. In addition, some proteins contain Ub-like domains that could serve as candidates for the OTU could interact with. The 2'-5'-Oligoadenylate Synthetase Like (OASL) protein, for example, contains two Ub-like domains at its C-terminus and is able to activate RIG-I signaling independently of K63 poly-ubiquitination [96, 97]. Perhaps the OTU is able to engage with Ub-like domains in these or other proteins in a way that is disruptive to immune function.

In addition to interactions with cellular proteins, it is possible that the OTU could be fulfilling a currently unknown, internal function that promotes viral replication. Although a minigenome system showed the OTU is not necessary for polymerase function [44], this does not exclude the possibility that it could performing a function in the context of the whole virus, for example by contributing to localization or a structural scaffold for viral protein association.

Remaining questions for OTU function

Although this work and others have provided extensive biochemical characterization of nairovirus OTUs, the full relationship of *in vitro* data to *in vivo* effects is still an unknown. Mutants to probe cellular effects typically aim for a knockout in function, making it unclear whether there is a biological threshold of activity that is sufficient, or if there is a gradient effect dependent on the relative activity. This is complicated by factors such as localization effects since *in vivo* proximity of substrates can

increase the effective activity of an enzyme. For example, some DUBs involved with the proteasome only have appreciable catalytic activity when in association with the other accessory proteins [98]. Further work will be needed to determine whether relatively poor affinity *in vitro* translates to poor activity *in vivo* for nairovirus OTUs, and what levels of *in vitro* activity may translate to *in vivo* effects.

Related to this, although multiple structures exist of the OTU domain, the overall structural features of the L protein are unknown. Thus, it is not currently apparent what the spatial characteristics of the OTU are relative to the protein as a whole and whether it could have a role in contributing to a particular structure. With the recent advancements in cryo-electron microscopy, opportunities may now exist to pursue this type of data. Attempts to obtain a structure of the full-length L protein would be warranted and could provide useful insights into this aspect of nairoviruses.

Utilizing structure-function: opportunities to develop novel applications

This work provides an unprecedented breadth and depth of knowledge into a family of viral DUB interactions with Ub and ISG15. The six novel OTU structures reported in CHAPTERS 3 and 4 expands the representation to nine unique nairoviruses, the most diverse representation of a DUB from any one family of viruses. Five of them have been solved in complex with either Ub, ISG15, or both in the case of CCHFV. In addition, three different ISG15 species are represented in these structures, presenting the most diverse structural information on the impact of ISG15 diversity within the DUB-substrate interface. This work also reports the biochemical interactions of fourteen OTUs with Ub and 12 different species' ISG15, which is the most comprehensive look of any viral DUB family

into substrate interactions. Taken together, this wealth of knowledge provides a strong basis for designing practical tools and applications.

Opportunities for bioinformatics and predictive studies

The rapidly growing availability of genomic data has outpaced the experimental characterization of the biological sources. With nairoviruses in particular, it could be argued that the most we know about many of them is the sequence itself, and little about how sequence diversity impacts function. This work provides a basis to connect OTU sequence with function in a predictive manner. In particular, the identification of the correlative relationship between the composition of the OTU selectivity pocket and Ub activity will allow early assessment of whether a nairovirus OTU is likely to interact extensively with Ub. Furthermore, the demonstration that particular ISG15 species preferences can also be impacted by specific residues presents the possibility that other motifs can be mapped that predict ISG15 activity. Such *in silico* approaches would provide a valuable starting point in assessing the probability that a virus will target Ub and ISG15 pathways.

As a complement to computational approaches, the knowledge that OTU preferences for ISG15 relates to host range provides a rationale to develop high-throughput assays for viral DUB-ISG15 interactions. This would help account for the surprises that biology has in store when attempting to computationally parameterize interactions in nature. In addition to confirming initial bioinformatic assessments, it can also provide information that strengthens the robustness of the computational methodology. Utilizing predictive methods such as these possesses the potential to increase the efficiency of virus surveillance and isolation. For example, it may suggest potential hosts in which the virus

could reside, prioritizing surveillance in these rather than relying on random sampling. In addition, these predictive studies could also flag viruses for the potential to jump from one host to another and discern the presence of overall trends in virus evolution.

Potential to target specific OTU-substrate interactions and cellular pathways

Probing the specific functions of the OTU and its impact during nairovirus infection depends on examining it in the context of altered or deficient activity. Accomplishing this practically can prove challenging, as it can be difficult to predict whether a mutation will accomplish the desired effect, cause more effects than intended, or compromise the overall integrity of the enzyme. Previous attempts with the CCHFV OTU have been partially successful, with the ability to selectively eliminate Ub activity and assess the impact on virus infection [48, 99]. Doing the same with ISG15, however, has been more challenging as Ub activity seems to also be largely impacted. The data in this study provides a wider range of information upon which to base such targeted mutants that could help solve this problem. In addition, it adds the possibility that interactions with specific species' ISG15 could be targeted, which would provide insights into whether it is a direct or passive player in host adaptation.

Another avenue opened up by this data is the potential to evaluate the importance of different poly-Ub linkages in a nairovirus infection. To date, virus studies utilizing viral DUB mutants, including nairoviruses, arteriviruses, and coronaviruses, have targeted Ub or ISG15 activity as a whole and focused the “selectivity” on separating it from ISG15 activity or role in polyprotein processing (arteriviruses and coronaviruses). The tools have been lacking to experimentally determine whether activity for one linkage over another is significant. The identification of the secondary binding site in the FARV OTU opens the

door to examine how this site in different OTUs impacts poly-Ub preference. Because the proximal Ub in this interaction presents a different surface for binding with the OTU, in principle specific mutations could be designed that favor some poly-Ub linkage types over others. To this point, designing such mutants has been limited by the lack of structural information providing the details of these interactions. Recently, however, di-Ub suicide probes, analogous to Ub-PA and ISG15-PA, have been successfully developed and employed to obtain structures of mammalian OTU enzymes with different di-Ub types [100, 101]. Increasing availability of these substrates will present opportunities to pursue different nairovirus OTU-di-Ub complexes. This would yield crucial insights into factors that could allow specific alteration of poly-Ub preference. With such tools, the potential exists to probe whether activities for linkages such as K6 and K11 are critical for nairoviruses, or if such activity is beneficial in the absence of K48 and K63 activity. Concurrently, it would uncover mechanistic insights into the particular mode by which OTUs influence particular pathways such as RIG-I, i.e. if it is strictly dependent on engaging one particular poly-Ub linkage type.

Evaluating the OTU: thinking beyond CCHFV

Considering the public health impact of CCHFV, it is not surprising that most of the tools to evaluate nairoviruses are designed with this virus. Although work has also been done to study infection with NSDV and HAZV, currently the only reverse genetics system existing for nairoviruses has been developed for CCHFV [23, 48]. While this focus is understandable and critically important, in the long run this narrow toolkit may hinder the ability to fully understand the role that the OTU plays. In part, this is due to the necessity of BSL4 level containment required to work with CCHFV, presenting practical

obstacles to routine study. Beyond this, however, the fact that OTU activity varies so extensively among nairoviruses implies the possibility that it can have different functions in different nairoviruses. This could be at the level of how it interacts with its hosts, including the particular factors and pathways it targets, or internally such as facilitating a particular structural architecture of the L protein or association with the NP. The development of reverse genetics systems with other nairoviruses would be beneficial to the field in assessing these possibilities. In the meantime, performing domain swaps with different nairovirus OTUs in the CCHFV reverse genetics system could yield insights into some of these questions. It could show, for example, whether there is cross-compatibility of the OTUs and if differences in function are qualitative or merely quantitative.

Conclusion

OTUs present an important component in nairovirus-host interfaces. The activity of the OTU is largely understood to be involved in immune suppression, making understanding its function important to evaluating potential pathogenicity and whether it can be targeted therapeutically. This work uncovered the structural and biochemical complexity of OTU interactions with Ub and ISG15, revealing a broad functional diversity that mirrors nairovirus and host diversity. The trends observed provide key insights into the connection between OTU structure, activity, and the hosts in which nairoviruses circulate. In addition, it presents a strong foundation for the development of new tools and approaches to assess the mechanisms of OTU function and the countermeasures employed by the host against viral infection.

REFERENCES ¹

1. Davies FG. Nairobi sheep disease. *Parassitologia*. 1997;39(2):95-8. Epub 1997/06/01. PubMed PMID: 9530691.
2. Montgomery E. On a Tick-borne Gastroenteritis of Sheep and Goats occurring in British East Africa. *Journal of Comparative Pathology and Therapeutics*. 1917;30(1):28-57.
3. Kuhn JH, Wiley MR, Rodriguez SE, Bao Y, Prieto K, Travassos da Rosa AP, et al. Genomic Characterization of the Genus Nairovirus (Family Bunyaviridae). *Viruses*. 2016;8(6). Epub 2016/06/15. doi: 10.3390/v8060164. PubMed PMID: 27294949; PubMed Central PMCID: PMC4926184.
4. Maes P, Adkins S, Alkhovsky SV, Avsic-Zupanc T, Ballinger MJ, Bente DA, et al. Taxonomy of the order Bunyvirales: second update 2018. *Arch Virol*. 2019;164(3):927-41. Epub 2019/01/22. doi: 10.1007/s00705-018-04127-3. PubMed PMID: 30663021.
5. Maes P, Alkhovsky SV, Bao Y, Beer M, Birkhead M, Briese T, et al. Taxonomy of the family Arenaviridae and the order Bunyvirales: update 2018. *Arch Virol*. 2018;163(8):2295-310. doi: 10.1007/s00705-018-3843-5. PubMed PMID: 29680923.
6. Walker PJ, Widen SG, Firth C, Blasdel KR, Wood TG, Travassos da Rosa AP, et al. Genomic Characterization of Yogue, Kasokero, Issyk-Kul, Keterah, Gossas, and Thiafora Viruses: Nairoviruses Naturally Infecting Bats, Shrews, and Ticks. *Am J Trop Med Hyg*. 2015;93(5):1041-51. Epub 2015/09/02. doi: 10.4269/ajtmh.15-0344. PubMed PMID: 26324724; PubMed Central PMCID: PMC4703270.
7. Walker PJ, Widen SG, Wood TG, Guzman H, Tesh RB, Vasilakis N. A Global Genomic Characterization of Nairoviruses Identifies Nine Discrete Genogroups with Distinctive Structural Characteristics and Host-Vector Associations. *Am J Trop Med Hyg*. 2016;94(5):1107-22. Epub 2016/02/24. doi: 10.4269/ajtmh.15-0917. PubMed PMID: 26903607; PubMed Central PMCID: PMC4856612.
8. Chastel C, Main AJ, Richard P, Le Lay G, Legrand-Quillien MC, Beaucournu JC. Erve virus, a probable member of Bunyviridae family isolated from shrews (*Crocidura russula*) in France. *Acta Virol*. 1989;33(3):270-80. Epub 1989/05/01. PubMed PMID: 2570514.
9. Ishii A, Ueno K, Orba Y, Sasaki M, Moonga L, Hang'ombe BM, et al. A nairovirus isolated from African bats causes haemorrhagic gastroenteritis and severe hepatic disease

¹ For citations in chapters 1 and 5

in mice. *Nat Commun.* 2014;5:5651. Epub 2014/12/03. doi: 10.1038/ncomms6651. PubMed PMID: 25451856; PubMed Central PMCID: PMC4268697.

10. Kalunda M, Mukwaya LG, Mukuye A, Lule M, Sekyalo E, Wright J, et al. Kasokero virus: a new human pathogen from bats (*Rousettus aegyptiacus*) in Uganda. *Am J Trop Med Hyg.* 1986;35(2):387-92. Epub 1986/03/01. PubMed PMID: 3082234.

11. Lvov DK, Karas FR, Timofeev EM, Tsyarkin YM, Vargina SG, Veselovskaya OV, et al. "Issyk-Kul" virus, a new arbovirus isolated from bats and *Argas (Carios) vespertilionis* (Latr., 1802) in the Kirghiz S.S.R. Brief report. *Arch Gesamte Virusforsch.* 1973;42(2):207-9. Epub 1973/01/01. PubMed PMID: 4747048.

12. Bente DA, Forrester NL, Watts DM, McAuley AJ, Whitehouse CA, Bray M. Crimean-Congo hemorrhagic fever: history, epidemiology, pathogenesis, clinical syndrome and genetic diversity. *Antiviral Res.* 2013;100(1):159-89. Epub 2013/08/03. doi: 10.1016/j.antiviral.2013.07.006. PubMed PMID: 23906741.

13. Burt FJ, Spencer DC, Leman PA, Patterson B, Swanepoel R. Investigation of tick-borne viruses as pathogens of humans in South Africa and evidence of Dugbe virus infection in a patient with prolonged thrombocytopenia. *Epidemiol Infect.* 1996;116(3):353-61. Epub 1996/06/01. PubMed PMID: 8666081; PubMed Central PMCID: PMC2271429.

14. Dandawate CN, Work TH, Webb JK, Shah KV. Isolation of Ganjam virus from a human case of febrile illness: a report of a laboratory infection and serological survey of human sera from three different states of India. *Indian J Med Res.* 1969;57(6):975-82. Epub 1969/06/01. PubMed PMID: 5823182.

15. L'Vov D K, Kostjukov MA, Daniyarov OA, Tukhtaev TM, Sherikov BK. [Outbreak of arbovirus infection in the Tadzhik SSR due to the Issyk-Kul virus (Issyk-Kul fever)]. *Vopr Virusol.* 1984;29(1):89-92. Epub 1984/01/01. PubMed PMID: 6143452.

16. Treib J, Dobler G, Haass A, von Blohn W, Strittmatter M, Pindur G, et al. Thunderclap headache caused by Erve virus? *Neurology.* 1998;50(2):509-11. Epub 1998/03/04. PubMed PMID: 9484383.

17. Bente DA, Alimonti JB, Shieh WJ, Camus G, Stroher U, Zaki S, et al. Pathogenesis and immune response of Crimean-Congo hemorrhagic fever virus in a STAT-1 knockout mouse model. *J Virol.* 2010;84(21):11089-100. Epub 2010/08/27. doi: 10.1128/JVI.01383-10. PubMed PMID: 20739514; PubMed Central PMCID: PMC2953203.

18. Haddock E, Feldmann F, Hawman DW, Zivcec M, Hanley PW, Saturday G, et al. A cynomolgus macaque model for Crimean-Congo haemorrhagic fever. *Nat Microbiol.* 2018;3(5):556-62. Epub 2018/04/11. doi: 10.1038/s41564-018-0141-7. PubMed PMID: 29632370.

19. Zivcec M, Safronetz D, Scott D, Robertson S, Ebihara H, Feldmann H. Lethal Crimean-Congo hemorrhagic fever virus infection in interferon alpha/beta receptor

knockout mice is associated with high viral loads, proinflammatory responses, and coagulopathy. *J Infect Dis.* 2013;207(12):1909-21. Epub 2013/02/19. doi: 10.1093/infdis/jit061. PubMed PMID: 23417661; PubMed Central PMCID: PMC3654741.

20. Sanchez AJ, Vincent MJ, Nichol ST. Characterization of the glycoproteins of Crimean-Congo hemorrhagic fever virus. *J Virol.* 2002;76(14):7263-75. Epub 2002/06/20. PubMed PMID: 12072526; PubMed Central PMCID: PMC36317.

21. Sanchez AJ, Vincent MJ, Erickson BR, Nichol ST. Crimean-congo hemorrhagic fever virus glycoprotein precursor is cleaved by Furin-like and SKI-1 proteases to generate a novel 38-kilodalton glycoprotein. *J Virol.* 2006;80(1):514-25. Epub 2005/12/15. doi: 10.1128/JVI.80.1.514-525.2006. PubMed PMID: 16352575; PubMed Central PMCID: PMC1317557.

22. Bergeron E, Vincent MJ, Nichol ST. Crimean-Congo hemorrhagic fever virus glycoprotein processing by the endoprotease SKI-1/S1P is critical for virus infectivity. *J Virol.* 2007;81(23):13271-6. Epub 2007/09/28. doi: 10.1128/JVI.01647-07. PubMed PMID: 17898072; PubMed Central PMCID: PMC2169102.

23. Bergeron É, Zivcec M, Chakrabarti AK, Nichol ST, Albariño CG, Spiropoulou CF. Recovery of Recombinant Crimean Congo Hemorrhagic Fever Virus Reveals a Function for Non-structural Glycoproteins Cleavage by Furin. *PLOS Pathogens.* 2015;11:e1004879. doi: 10.1371/journal.ppat.1004879.

24. Vincent MJ, Sanchez AJ, Erickson BR, Basak A, Chretien M, Seidah NG, et al. Crimean-Congo hemorrhagic fever virus glycoprotein proteolytic processing by subtilase SKI-1. *J Virol.* 2003;77(16):8640-9. Epub 2003/07/30. PubMed PMID: 12885882; PubMed Central PMCID: PMC167219.

25. Honig JE, Osborne JC, Nichol ST. Crimean-Congo hemorrhagic fever virus genome L RNA segment and encoded protein. *Virology.* 2004;321(1):29-35. Epub 2004/03/23. doi: 10.1016/j.virol.2003.09.042. PubMed PMID: 15033562.

26. Levingston Macleod JM, Marmor H, Garcia-Sastre A, Frias-Staheli N. Mapping of the interaction domains of the Crimean-Congo hemorrhagic fever virus nucleocapsid protein. *J Gen Virol.* 2015;96(Pt 3):524-37. Epub 2014/11/13. doi: 10.1099/vir.0.071332-0. PubMed PMID: 25389186; PubMed Central PMCID: PMC4336859.

27. Zivcec M, Scholte FE, Spiropoulou CF, Spengler JR, Bergeron E. Molecular Insights into Crimean-Congo Hemorrhagic Fever Virus. *Viruses.* 2016;8(4):106. Epub 2016/04/26. doi: 10.3390/v8040106. PubMed PMID: 27110812; PubMed Central PMCID: PMC4848600.

28. Lasecka L, Baron MD. The molecular biology of nairoviruses, an emerging group of tick-borne arboviruses. *Arch Virol.* 2014;159(6):1249-65. Epub 2013/12/12. doi: 10.1007/s00705-013-1940-z. PubMed PMID: 24327094.

29. Garrison AR, Radoshitzky SR, Kota KP, Pegoraro G, Ruthel G, Kuhn JH, et al. Crimean-Congo hemorrhagic fever virus utilizes a clathrin- and early endosome-dependent entry pathway. *Virology*. 2013;444(1-2):45-54. Epub 2013/06/25. doi: 10.1016/j.virol.2013.05.030. PubMed PMID: 23791227.
30. Bertolotti-Ciarlet A, Smith J, Strecker K, Paragas J, Altamura LA, McFalls JM, et al. Cellular localization and antigenic characterization of Crimean-Congo hemorrhagic fever virus glycoproteins. *J Virol*. 2005;79(10):6152-61. Epub 2005/04/29. doi: 10.1128/JVI.79.10.6152-6161.2005. PubMed PMID: 15858000; PubMed Central PMCID: PMC1091677.
31. Jin H, Elliott RM. Non-viral sequences at the 5' ends of Dugbe nairovirus S mRNAs. *J Gen Virol*. 1993;74 (Pt 10):2293-7. Epub 1993/10/01. doi: 10.1099/0022-1317-74-10-2293. PubMed PMID: 8409954.
32. Altamura LA, Bertolotti-Ciarlet A, Teigler J, Paragas J, Schmaljohn CS, Doms RW. Identification of a novel C-terminal cleavage of Crimean-Congo hemorrhagic fever virus PreGN that leads to generation of an NSM protein. *J Virol*. 2007;81(12):6632-42. Epub 2007/04/06. doi: 10.1128/JVI.02730-06. PubMed PMID: 17409136; PubMed Central PMCID: PMC1900101.
33. Lasecka L, Bin-Tarif A, Bridgen A, Juleff N, Waters RA, Baron MD. Antibodies to the core proteins of Nairobi sheep disease virus/Ganjam virus reveal details of the distribution of the proteins in infected cells and tissues. *PLoS One*. 2015;10(4):e0124966. Epub 2015/04/24. doi: 10.1371/journal.pone.0124966. PubMed PMID: 25905707; PubMed Central PMCID: PMC14407892.
34. Connolly-Andersen AM, Magnusson KE, Mirazimi A. Basolateral entry and release of Crimean-Congo hemorrhagic fever virus in polarized MDCK-1 cells. *J Virol*. 2007;81(5):2158-64. Epub 2006/12/15. doi: 10.1128/JVI.02070-06. PubMed PMID: 17166898; PubMed Central PMCID: PMC1865934.
35. Gack MU, Shin YC, Joo CH, Urano T, Liang C, Sun L, et al. TRIM25 RING-finger E3 ubiquitin ligase is essential for RIG-I-mediated antiviral activity. *Nature*. 2007;446(7138):916-20. Epub 2007/03/30. doi: 10.1038/nature05732. PubMed PMID: 17392790.
36. Okamoto M, Kouwaki T, Fukushima Y, Oshiumi H. Regulation of RIG-I Activation by K63-Linked Polyubiquitination. *Front Immunol*. 2017;8:1942. Epub 2018/01/23. doi: 10.3389/fimmu.2017.01942. PubMed PMID: 29354136; PubMed Central PMCID: PMC5760545.
37. Peisley A, Wu B, Xu H, Chen ZJ, Hur S. Structural basis for ubiquitin-mediated antiviral signal activation by RIG-I. *Nature*. 2014;509(7498):110-4. Epub 2014/03/05. doi: 10.1038/nature13140. PubMed PMID: 24590070; PubMed Central PMCID: PMC136653.

38. Loo YM, Gale M, Jr. Immune signaling by RIG-I-like receptors. *Immunity*. 2011;34(5):680-92. Epub 2011/05/28. doi: 10.1016/j.immuni.2011.05.003. PubMed PMID: 21616437; PubMed Central PMCID: PMC3177755.
39. Garcin D, Lezzi M, Dobbs M, Elliott RM, Schmaljohn C, Kang CY, et al. The 5' ends of Hantaan virus (Bunyaviridae) RNAs suggest a prime-and-realign mechanism for the initiation of RNA synthesis. *J Virol*. 1995;69(9):5754-62. Epub 1995/09/01. PubMed PMID: 7637020; PubMed Central PMCID: PMC189436.
40. Holm T, Kopicki JD, Busch C, Olschewski S, Rosenthal M, Uetrecht C, et al. Biochemical and structural studies reveal differences and commonalities among cap-snatching endonucleases from segmented negative-strand RNA viruses. *J Biol Chem*. 2018;293(51):19686-98. Epub 2018/10/24. doi: 10.1074/jbc.RA118.004373. PubMed PMID: 30348898; PubMed Central PMCID: PMC6314124.
41. Barnwal B, Karlberg H, Mirazimi A, Tan YJ. The Non-structural Protein of Crimean-Congo Hemorrhagic Fever Virus Disrupts the Mitochondrial Membrane Potential and Induces Apoptosis. *J Biol Chem*. 2016;291(2):582-92. Epub 2015/11/18. doi: 10.1074/jbc.M115.667436. PubMed PMID: 26574543; PubMed Central PMCID: PMC4705379.
42. Karlberg H, Tan YJ, Mirazimi A. Crimean-Congo haemorrhagic fever replication interplays with regulation mechanisms of apoptosis. *J Gen Virol*. 2015;96(Pt 3):538-46. Epub 2014/12/08. doi: 10.1099/jgv.0.000011. PubMed PMID: 25481756.
43. Karlberg H, Tan YJ, Mirazimi A. Induction of caspase activation and cleavage of the viral nucleocapsid protein in different cell types during Crimean-Congo hemorrhagic fever virus infection. *J Biol Chem*. 2011;286(5):3227-34. Epub 2010/12/03. doi: 10.1074/jbc.M110.149369. PubMed PMID: 21123175; PubMed Central PMCID: PMC3030327.
44. Bergeron E, Albarino CG, Khristova ML, Nichol ST. Crimean-Congo hemorrhagic fever virus-encoded ovarian tumor protease activity is dispensable for virus RNA polymerase function. *J Virol*. 2010;84(1):216-26. Epub 2009/10/30. doi: 10.1128/JVI.01859-09. PubMed PMID: 19864393; PubMed Central PMCID: PMC2798392.
45. Frias-Staheli N, Giannakopoulos NV, Kikkert M, Taylor SL, Bridgen A, Paragas J, et al. Ovarian tumor domain-containing viral proteases evade ubiquitin- and ISG15-dependent innate immune responses. *Cell Host and Microbe*. 2007;2:404-16.
46. Bakshi S, Holzer B, Bridgen A, McMullan G, Quinn DG, Baron MD. Dugbe virus ovarian tumour domain interferes with ubiquitin/ISG15-regulated innate immune cell signalling. *J Gen Virol*. 2013;94(Pt 2):298-307. Epub 2012/11/09. doi: 10.1099/vir.0.048322-0. PubMed PMID: 23136361; PubMed Central PMCID: PMC3709621.

47. Holzer B, Bakshi S, Bridgen A, Baron MD. Inhibition of interferon induction and action by the nairovirus Nairobi sheep disease virus/Ganjam virus. *PLoS One*. 2011;6(12):e28594. Epub 2011/12/14. doi: 10.1371/journal.pone.0028594. PubMed PMID: 22163042; PubMed Central PMCID: PMC3230622.
48. Scholte FEM, Zivcec M, Dzimianski JV, Deaton MK, Spengler JR, Welch SR, et al. Crimean-Congo Hemorrhagic Fever Virus Suppresses Innate Immune Responses via a Ubiquitin and ISG15 Specific Protease. *Cell Rep*. 2017;20(10):2396-407. Epub 2017/09/07. doi: 10.1016/j.celrep.2017.08.040. PubMed PMID: 28877473; PubMed Central PMCID: PMC5616139.
49. Ratia K, Saikatendu KS, Santarsiero BD, Barretto N, Baker SC, Stevens RC, et al. Severe acute respiratory syndrome coronavirus papain-like protease: structure of a viral deubiquitinating enzyme. *Proc Natl Acad Sci U S A*. 2006;103(15):5717-22. Epub 2006/04/04. doi: 10.1073/pnas.0510851103. PubMed PMID: 16581910; PubMed Central PMCID: PMC1458639.
50. Barretto N, Jukneliene D, Ratia K, Chen Z, Mesecar AD, Baker SC. The papain-like protease of severe acute respiratory syndrome coronavirus has deubiquitinating activity. *J Virol*. 2005;79(24):15189-98. Epub 2005/11/25. doi: 10.1128/JVI.79.24.15189-15198.2005. PubMed PMID: 16306590; PubMed Central PMCID: PMC1316023.
51. Lindner HA, Fotouhi-Ardakani N, Lytvyn V, Lachance P, Sulea T, Menard R. The papain-like protease from the severe acute respiratory syndrome coronavirus is a deubiquitinating enzyme. *J Virol*. 2005;79(24):15199-208. Epub 2005/11/25. doi: 10.1128/JVI.79.24.15199-15208.2005. PubMed PMID: 16306591; PubMed Central PMCID: PMC1316033.
52. Sulea T, Lindner HA, Purisima EO, Menard R. Deubiquitination, a new function of the severe acute respiratory syndrome coronavirus papain-like protease? *J Virol*. 2005;79(7):4550-1. Epub 2005/03/16. doi: 10.1128/JVI.79.7.4550-4551.2005. PubMed PMID: 15767458; PubMed Central PMCID: PMC1061586.
53. Lindner HA, Lytvyn V, Qi H, Lachance P, Ziomek E, Menard R. Selectivity in ISG15 and ubiquitin recognition by the SARS coronavirus papain-like protease. *Arch Biochem Biophys*. 2007;466:8-14. Epub 2007/08/19. doi: 10.1016/j.abb.2007.07.006. PubMed PMID: 17692280.
54. Baez-Santos YM, Mielech AM, Deng X, Baker S, Mesecar AD. Catalytic function and substrate specificity of the papain-like protease domain of nsp3 from the Middle East respiratory syndrome coronavirus. *J Virol*. 2014;88(21):12511-27. Epub 2014/08/22. doi: 10.1128/JVI.01294-14. PubMed PMID: 25142582; PubMed Central PMCID: PMC4248884.
55. Chen Y, Savinov SN, Mielech AM, Cao T, Baker SC, Mesecar AD. X-ray Structural and Functional Studies of the Three Tandemly Linked Domains of Non-structural Protein 3 (nsp3) from Murine Hepatitis Virus Reveal Conserved Functions. *J*

Biol Chem. 2015;290(42):25293-306. Epub 2015/08/25. doi: 10.1074/jbc.M115.662130. PubMed PMID: 26296883; PubMed Central PMCID: PMC4646180.

56. Mielech AM, Kilianski A, Baez-Santos YM, Mesecar AD, Baker SC. MERS-CoV papain-like protease has deISGylating and deubiquitinating activities. *Virology*. 2014;450-451:64-70. Epub 2014/02/08. doi: 10.1016/j.virol.2013.11.040. PubMed PMID: 24503068.

57. Bester SM, Daczkowski CM, Faaberg KS, Pegan SD. Insights into the Porcine Reproductive and Respiratory Syndrome Virus Viral Ovarian Tumor Domain Protease Specificity for Ubiquitin and Interferon Stimulated Gene Product 15. *ACS Infect Dis*. 2018;4:1316-26. Epub 2018/06/02. doi: 10.1021/acsinfecdis.8b00068. PubMed PMID: 29856201.

58. Deaton MK, Spear A, Faaberg KS, Pegan SD. The vOTU domain of highly-pathogenic porcine reproductive and respiratory syndrome virus displays a differential substrate preference. *Virology*. 2014;454-455:247-53. Epub 2014/04/15. doi: 10.1016/j.virol.2014.02.026. PubMed PMID: 24725951.

59. van Kasteren PB, Bailey-Elkin BA, James TW, Ninaber DK, Beugeling C, Khajehpour M, et al. Deubiquitinase function of arterivirus papain-like protease 2 suppresses the innate immune response in infected host cells. *Proceedings of the National Academy of Sciences of the United States of America*. 2013;110:E838-47. doi: 10.1073/pnas.1218464110. PubMed PMID: 23401522.

60. van Kasteren PB, Beugeling C, Ninaber DK, Frias-Staheli N, van Boheemen S, Garcia-Sastre A, et al. Arterivirus and Nairovirus Ovarian Tumor Domain-Containing Deubiquitinases Target Activated RIG-I To Control Innate Immune Signaling. *Journal of Virology*. 2011;86:773-85.

61. Niemeyer D, Mosbauer K, Klein EM, Sieberg A, Mettelman RC, Mielech AM, et al. The papain-like protease determines a virulence trait that varies among members of the SARS-coronavirus species. *PLoS Pathog*. 2018;14(9):e1007296. doi: 10.1371/journal.ppat.1007296. PubMed PMID: 30248143; PubMed Central PMCID: PMC6171950.

62. van Kasteren PB, Knaap RCM, van den Elzen P, Snijder EJ, Balasuriya UBR, van den Born E, et al. In vivo assessment of equine arteritis virus vaccine improvement by disabling the deubiquitinase activity of papain-like protease 2. *Veterinary microbiology*. 2015;178:132-7. doi: 10.1016/j.vetmic.2015.04.018. PubMed PMID: 25975520.

63. Baez-Santos YM, St John SE, Mesecar AD. The SARS-coronavirus papain-like protease: structure, function and inhibition by designed antiviral compounds. *Antiviral Res*. 2015;115:21-38. Epub 2015/01/03. doi: 10.1016/j.antiviral.2014.12.015. PubMed PMID: 25554382; PubMed Central PMCID: PMC4646180.

64. Bailey-Elkin BA, Knaap RCM, Kikkert M, Mark BL. Structure and Function of Viral Deubiquitinating Enzymes. *J Mol Biol.* 2017;429(22):3441-70. Epub 2017/06/20. doi: 10.1016/j.jmb.2017.06.010. PubMed PMID: 28625850.
65. Zhang W, Bailey-Elkin BA, Knaap RCM, Khare B, Dalebout TJ, Johnson GG, et al. Potent and selective inhibition of pathogenic viruses by engineered ubiquitin variants. *PLoS Pathog.* 2017;13(5):e1006372. Epub 2017/05/26. doi: 10.1371/journal.ppat.1006372. PubMed PMID: 28542609; PubMed Central PMCID: PMC5451084.
66. Capodagli GC, Deaton MK, Baker EA, Lumpkin RJ, Pegan SD. Diversity of ubiquitin and ISG15 specificity among nairoviruses' viral ovarian tumor domain proteases. *J Virol.* 2013;87(7):3815-27. Epub 2013/01/25. doi: 10.1128/JVI.03252-12. PubMed PMID: 23345508; PubMed Central PMCID: PMC3624237.
67. Zuin A, Isasa M, Crosas B. Ubiquitin signaling: extreme conservation as a source of diversity. *Cells.* 2014;3(3):690-701. Epub 2014/07/12. doi: 10.3390/cells3030690. PubMed PMID: 25014160; PubMed Central PMCID: PMC4197634.
68. Yau R, Rape M. The increasing complexity of the ubiquitin code. *Nat Cell Biol.* 2016;18(6):579-86. Epub 2016/05/28. doi: 10.1038/ncb3358. PubMed PMID: 27230526.
69. Swatek KN, Komander D. Ubiquitin modifications. *Cell Res.* 2016;26(4):399-422. Epub 2016/03/26. doi: 10.1038/cr.2016.39. PubMed PMID: 27012465; PubMed Central PMCID: PMC4822133.
70. Hu H, Sun SC. Ubiquitin signaling in immune responses. *Cell Res.* 2016;26(4):457-83. Epub 2016/03/26. doi: 10.1038/cr.2016.40. PubMed PMID: 27012466; PubMed Central PMCID: PMC4822134.
71. Spit M, Rieser E, Walczak H. Linear ubiquitination at a glance. *J Cell Sci.* 2019;132(2). Epub 2019/01/20. doi: 10.1242/jcs.208512. PubMed PMID: 30659056.
72. Morris JR, Solomon E. BRCA1 : BARD1 induces the formation of conjugated ubiquitin structures, dependent on K6 of ubiquitin, in cells during DNA replication and repair. *Hum Mol Genet.* 2004;13(8):807-17. Epub 2004/02/21. doi: 10.1093/hmg/ddh095. PubMed PMID: 14976165.
73. Durcan TM, Fon EA. USP8 and PARK2/parkin-mediated mitophagy. *Autophagy.* 2015;11(2):428-9. Epub 2015/02/24. doi: 10.1080/15548627.2015.1009794. PubMed PMID: 25700639; PubMed Central PMCID: PMC4502724.
74. Durcan TM, Tang MY, Perusse JR, Dashti EA, Aguilera MA, McLelland GL, et al. USP8 regulates mitophagy by removing K6-linked ubiquitin conjugates from parkin. *EMBO J.* 2014;33(21):2473-91. Epub 2014/09/14. doi: 10.15252/embj.201489729. PubMed PMID: 25216678; PubMed Central PMCID: PMC4283406.

75. Wickliffe KE, Williamson A, Meyer HJ, Kelly A, Rape M. K11-linked ubiquitin chains as novel regulators of cell division. *Trends Cell Biol.* 2011;21(11):656-63. Epub 2011/10/08. doi: 10.1016/j.tcb.2011.08.008. PubMed PMID: 21978762; PubMed Central PMCID: PMC3205209.
76. Dynek JN, Goncharov T, Dueber EC, Fedorova AV, Izrael-Tomasevic A, Phu L, et al. c-IAP1 and UbcH5 promote K11-linked polyubiquitination of RIP1 in TNF signalling. *EMBO J.* 2010;29(24):4198-209. Epub 2010/11/30. doi: 10.1038/emboj.2010.300. PubMed PMID: 21113135; PubMed Central PMCID: PMC3018797.
77. Palicharla VR, Maddika S. HACE1 mediated K27 ubiquitin linkage leads to YB-1 protein secretion. *Cell Signal.* 2015;27(12):2355-62. Epub 2015/09/08. doi: 10.1016/j.cellsig.2015.09.001. PubMed PMID: 26343856.
78. Liu Z, Chen P, Gao H, Gu Y, Yang J, Peng H, et al. Ubiquitylation of autophagy receptor Optineurin by HACE1 activates selective autophagy for tumor suppression. *Cancer Cell.* 2014;26(1):106-20. Epub 2014/07/16. doi: 10.1016/j.ccr.2014.05.015. PubMed PMID: 25026213; PubMed Central PMCID: PMC34166492.
79. Gatti M, Pinato S, Maiolica A, Rocchio F, Prato MG, Aebersold R, et al. RNF168 promotes noncanonical K27 ubiquitination to signal DNA damage. *Cell Rep.* 2015;10(2):226-38. Epub 2015/01/13. doi: 10.1016/j.celrep.2014.12.021. PubMed PMID: 25578731.
80. Kim W, Bennett EJ, Huttlin EL, Guo A, Li J, Possemato A, et al. Systematic and quantitative assessment of the ubiquitin-modified proteome. *Mol Cell.* 2011;44(2):325-40. Epub 2011/09/13. doi: 10.1016/j.molcel.2011.08.025. PubMed PMID: 21906983; PubMed Central PMCID: PMC3200427.
81. Besche HC, Sha Z, Kukushkin NV, Peth A, Hock EM, Kim W, et al. Autoubiquitination of the 26S proteasome on Rpn13 regulates breakdown of ubiquitin conjugates. *EMBO J.* 2014;33(10):1159-76. Epub 2014/05/09. doi: 10.1002/emboj.201386906. PubMed PMID: 24811749; PubMed Central PMCID: PMC34193922.
82. Fei C, Li Z, Li C, Chen Y, Chen Z, He X, et al. Smurf1-mediated Lys29-linked nonproteolytic polyubiquitination of axin negatively regulates Wnt/beta-catenin signaling. *Mol Cell Biol.* 2013;33(20):4095-105. Epub 2013/08/21. doi: 10.1128/MCB.00418-13. PubMed PMID: 23959799; PubMed Central PMCID: PMC3811687.
83. Licchesi JD, Mieszczanek J, Mevissen TE, Rutherford TJ, Akutsu M, Virdee S, et al. An ankyrin-repeat ubiquitin-binding domain determines TRABID's specificity for atypical ubiquitin chains. *Nat Struct Mol Biol.* 2011;19(1):62-71. Epub 2011/12/14. doi: 10.1038/nsmb.2169. PubMed PMID: 22157957; PubMed Central PMCID: PMC35260945.

84. Huang H, Jeon MS, Liao L, Yang C, Elly C, Yates JR, 3rd, et al. K33-linked polyubiquitination of T cell receptor-zeta regulates proteolysis-independent T cell signaling. *Immunity*. 2010;33(1):60-70. Epub 2010/07/20. doi: 10.1016/j.immuni.2010.07.002. PubMed PMID: 20637659; PubMed Central PMCID: PMCPMC2927827.
85. Yuan WC, Lee YR, Lin SY, Chang LY, Tan YP, Hung CC, et al. K33-Linked Polyubiquitination of Coronin 7 by Cul3-KLHL20 Ubiquitin E3 Ligase Regulates Protein Trafficking. *Mol Cell*. 2014;54(4):586-600. Epub 2014/04/29. doi: 10.1016/j.molcel.2014.03.035. PubMed PMID: 24768539.
86. Fu B, Wang L, Ding H, Schwamborn JC, Li S, Dorf ME. TRIM32 Senses and Restricts Influenza A Virus by Ubiquitination of PB1 Polymerase. *PLoS Pathog*. 2015;11(6):e1004960. Epub 2015/06/10. doi: 10.1371/journal.ppat.1004960. PubMed PMID: 26057645; PubMed Central PMCID: PMCPMC4461266.
87. Seissler T, Marquet R, Paillart JC. Hijacking of the Ubiquitin/Proteasome Pathway by the HIV Auxiliary Proteins. *Viruses*. 2017;9(11). Epub 2017/11/01. doi: 10.3390/v9110322. PubMed PMID: 29088112; PubMed Central PMCID: PMCPMC5707529.
88. Zeng W, Xu M, Liu S, Sun L, Chen ZJ. Key role of Ubc5 and lysine-63 polyubiquitination in viral activation of IRF3. *Mol Cell*. 2009;36(2):315-25. Epub 2009/10/27. doi: 10.1016/j.molcel.2009.09.037. PubMed PMID: 19854139; PubMed Central PMCID: PMCPMC2779157.
89. Galluzzi L, Brenner C, Morselli E, Touat Z, Kroemer G. Viral control of mitochondrial apoptosis. *PLoS Pathog*. 2008;4(5):e1000018. Epub 2008/06/03. doi: 10.1371/journal.ppat.1000018. PubMed PMID: 18516228; PubMed Central PMCID: PMCPMC2376094.
90. Harper JW, Ordureau A, Heo JM. Building and decoding ubiquitin chains for mitophagy. *Nat Rev Mol Cell Biol*. 2018;19(2):93-108. Epub 2018/01/24. doi: 10.1038/nrm.2017.129. PubMed PMID: 29358684.
91. Albert M, Becares M, Falqui M, Fernandez-Lozano C, Guerra S. ISG15, a Small Molecule with Huge Implications: Regulation of Mitochondrial Homeostasis. *Viruses*. 2018;10(11). Epub 2018/11/16. doi: 10.3390/v10110629. PubMed PMID: 30428561; PubMed Central PMCID: PMCPMC6265978.
92. Baldanta S, Fernandez-Escobar M, Acin-Perez R, Albert M, Camafeita E, Jorge I, et al. ISG15 governs mitochondrial function in macrophages following vaccinia virus infection. *PLoS Pathog*. 2017;13:e1006651. Epub 2017/10/28. doi: 10.1371/journal.ppat.1006651. PubMed PMID: 29077752.
93. Li K, Zhong B. Regulation of Cellular Antiviral Signaling by Modifications of Ubiquitin and Ubiquitin-like Molecules. *Immune Netw*. 2018;18(1):e4. Epub 2018/03/06.

doi: 10.4110/in.2018.18.e4. PubMed PMID: 29503737; PubMed Central PMCID: PMC583123.

94. Mah MM, Basler M, Groettrup M. The ubiquitin-like modifier FAT10 is required for normal IFN-gamma production by activated CD8(+) T cells. *Mol Immunol.* 2019;108:111-20. Epub 2019/03/01. doi: 10.1016/j.molimm.2019.02.010. PubMed PMID: 30818228.

95. Capodagli GC, McKercher MA, Baker EA, Masters EM, Brunzelle JS, Pegan SD. Structural analysis of a viral ovarian tumor domain protease from the Crimean-Congo hemorrhagic fever virus in complex with covalently bonded ubiquitin. *J Virol.* 2011;85(7):3621-30. Epub 2011/01/14. doi: 10.1128/JVI.02496-10. PubMed PMID: 21228232; PubMed Central PMCID: PMC3067871.

96. Zhu J, Ghosh A, Sarkar SN. OASL-a new player in controlling antiviral innate immunity. *Curr Opin Virol.* 2015;12:15-9. Epub 2015/02/14. doi: 10.1016/j.coviro.2015.01.010. PubMed PMID: 25676874; PubMed Central PMCID: PMC4470762.

97. Zhu J, Zhang Y, Ghosh A, Cuevas RA, Forero A, Dhar J, et al. Antiviral activity of human OASL protein is mediated by enhancing signaling of the RIG-I RNA sensor. *Immunity.* 2014;40(6):936-48. Epub 2014/06/17. doi: 10.1016/j.immuni.2014.05.007. PubMed PMID: 24931123; PubMed Central PMCID: PMC4101812.

98. Ventii KH, Wilkinson KD. Protein partners of deubiquitinating enzymes. *Biochem J.* 2008;414(2):161-75. Epub 2008/08/09. doi: 10.1042/BJ20080798. PubMed PMID: 18687060; PubMed Central PMCID: PMC2724835.

99. Akutsu M, Ye Y, Virdee S, Chin JW, Komander D. Molecular basis for ubiquitin and ISG15 cross-reactivity in viral ovarian tumor domains. *Proc Natl Acad Sci U S A.* 2011;108(6):2228-33. Epub 2011/01/27. doi: 10.1073/pnas.1015287108. PubMed PMID: 21266548; PubMed Central PMCID: PMC3038727.

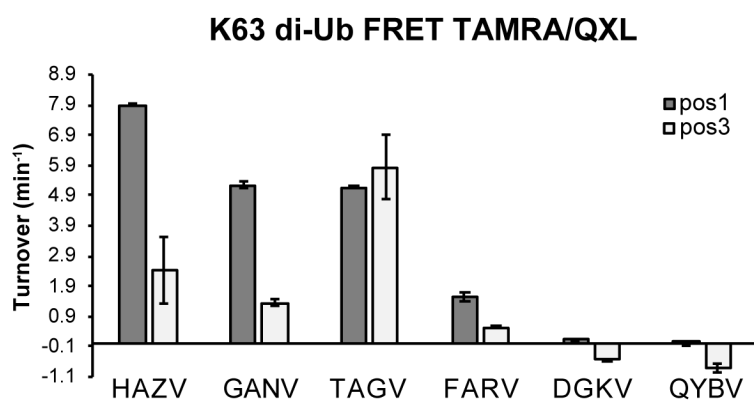
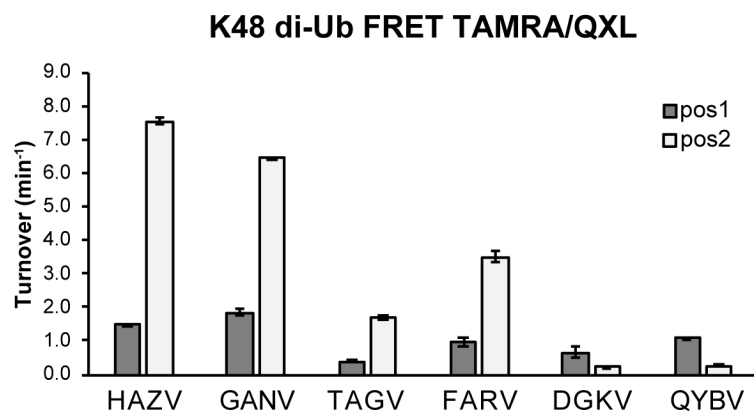
100. Mevissen TET, Kulathu Y, Mulder MPC, Geurink PP, Maslen SL, Gersch M, et al. Molecular basis of Lys11-polyubiquitin specificity in the deubiquitinase Cezanne. *Nature.* 2016;538(7625):402-5. Epub 2016/10/21. doi: 10.1038/nature19836. PubMed PMID: 27732584; PubMed Central PMCID: PMC5295632.

101. Weber A, Elliott PR, Pinto-Fernandez A, Bonham S, Kessler BM, Komander D, et al. A Linear Diubiquitin-Based Probe for Efficient and Selective Detection of the Deubiquitinating Enzyme OTULIN. *Cell Chem Biol.* 2017;24(10):1299-313 e7. Epub 2017/09/19. doi: 10.1016/j.chembiol.2017.08.006. PubMed PMID: 28919039; PubMed Central PMCID: PMC5658516.

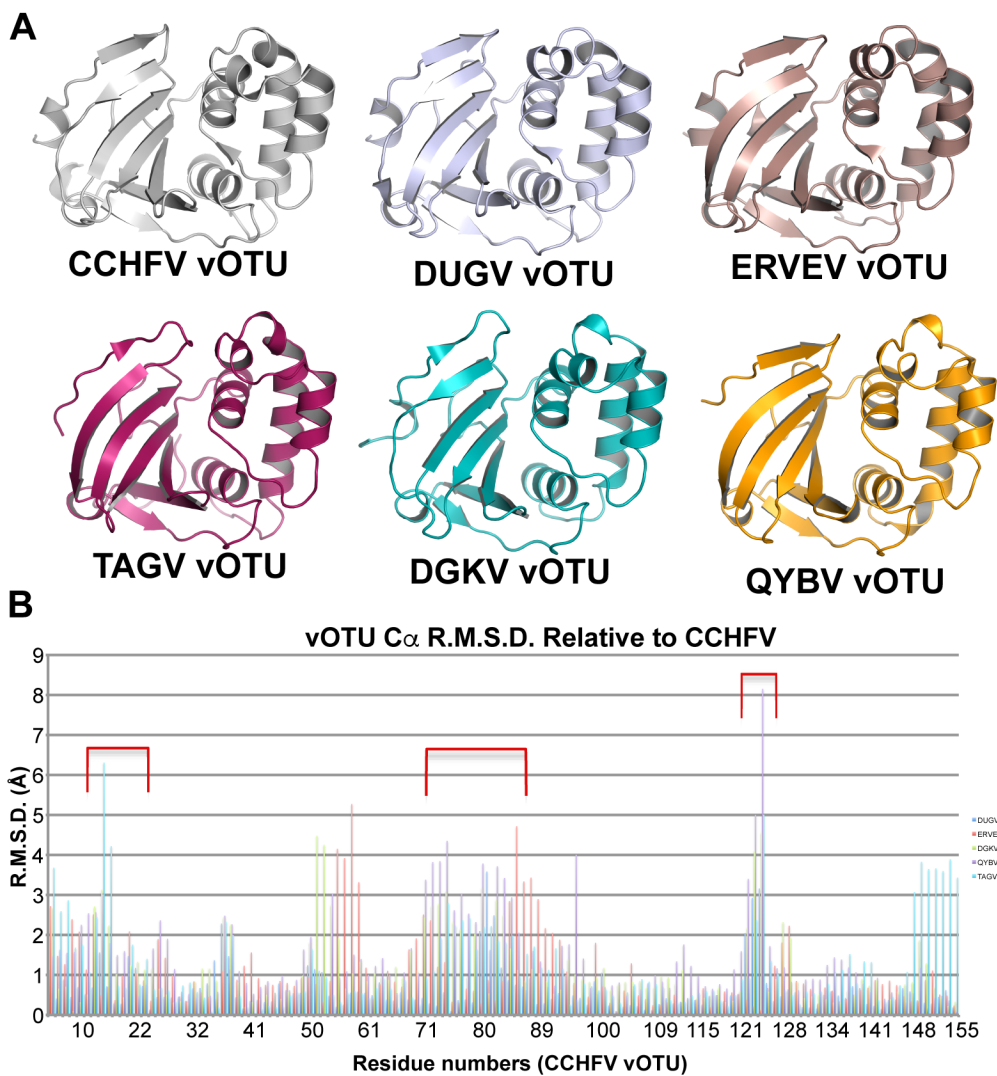
APPENDIX A
SUPPLEMENTAL INFORMATION FOR CHAPTER 3

3.S1 Table. Viruses and sequence accession numbers

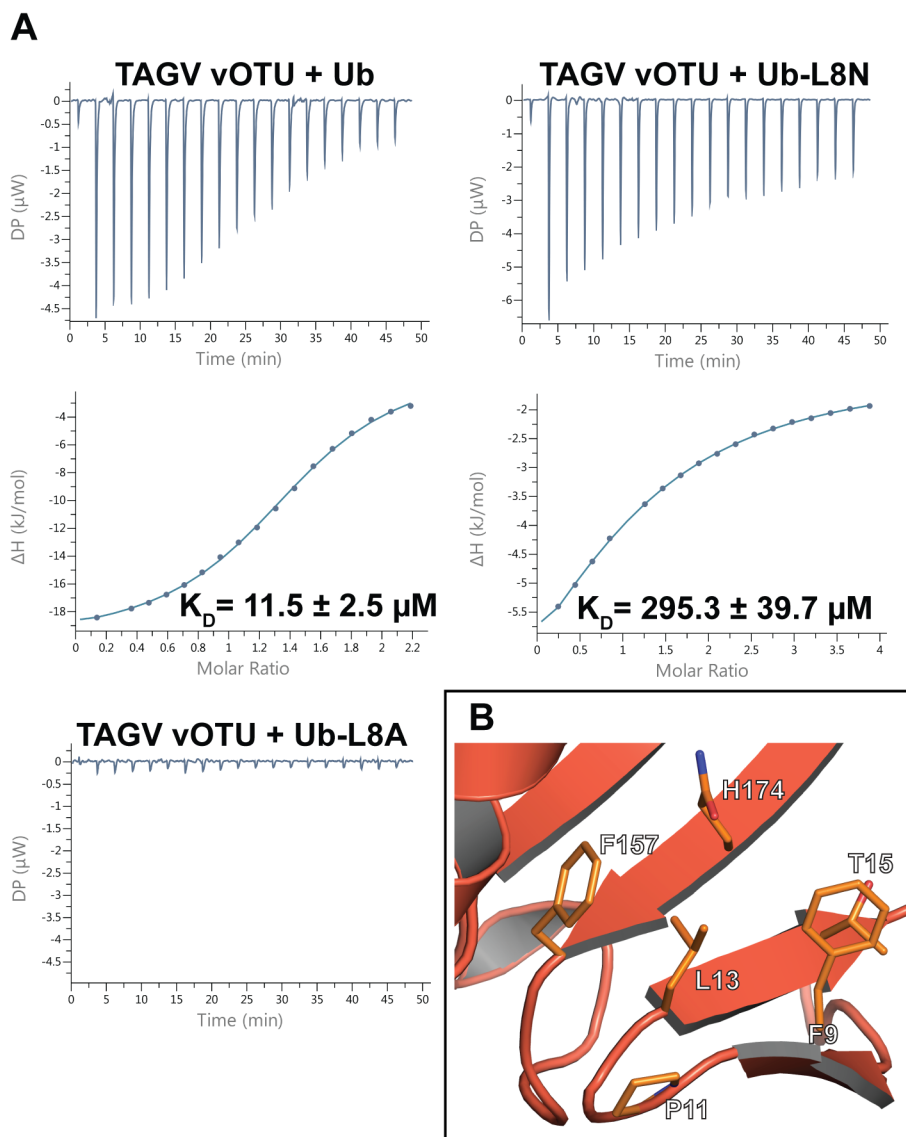
Name	Abbreviation	Species	Accession number	
Crimean-Congo hemorrhagic fever virus	CCHFV	<i>Crimean-Congo hemorrhagic fever orthonavivirus</i>	AAQ98866.2	
Ganjam virus	GANV	<i>Nairobi sheep disease orthonavivirus</i>	AMT75401.1	
Nairobi sheep disease virus	NSDV		ACH99799.1	
Dugbe virus	DUGV	<i>Dugbe orthonavivirus</i>	AAB18834.1	
Kupe virus	KUPEV		ABY82502.1	
Hazara virus	HAZV	<i>Hazara orthonavivirus</i>	AAZ38668.1	
Tofla virus	TFLV		YP_009227122.1	
Taggert virus	TAGV	<i>Sakhalin orthonavivirus</i>	AMT75428.1	
Tillamook virus	TILLV		AMT75431.1	
Paramushir virus	PRMV		AKC89337.1	
Avalon virus	AVAV		AMT75377.1	
Artashat virus	ARTSV	<i>Artashat orthonavivirus</i>	AKC89352.1	
Thiafora virus	TFAV	<i>Thiafora orthonavivirus</i>	ALD84355.1	
Erve virus	ERVEV		AFH89032.1	
Hughes virus	HUGV	<i>Hughes orthonavivirus</i>	AKC89316.1	
Farallon virus	FARV		AMT75398.1	
Raza virus	RAZAV		AMT75416.1	
Punta Salinas virus	PSV		AMT75410.1	
Zirqa virus	ZIRV		AMT75437.1	
Soldado virus	SOLV		AMT75425.1	
Great Saltee virus	GRSV		AMT75404.1	
Caspiy virus	CASV		AKC89346.1	
Abu Hammad virus	AHV		<i>Dera Ghazi Khan orthonavivirus</i>	AMT75434.1
Dera Ghazi Khan virus	DGKV			AMT75389.1
Sapphire II virus	SAPV	AMT75422.1		
Wēnzhōu tick virus	WzTV	<i>Tamdy orthonavivirus</i>	YP_009304993.1	
Burana virus	BURV		AKC89349.1	
Huángpí tick virus 1	HpTV-1		YP_009293587.1	
Tǎchéng tick virus 1	TcTV-1		YP_009304986.1	
Tamdy virus	TDYV		AKC89328.1	
Yogue virus	YOGV	<i>Kasokero orthonavivirus</i>	YP_009246486.1	
Leopards Hill virus	LPHV		BAP90971.1	
Qalyub virus	QYBV	<i>Qalyub orthonavivirus</i>	AKC89319.1	
Geran virus	GERV		AKC89340.1	
Chim virus	CHIMV	<i>Chim orthonavivirus</i>	AKC89343.1	
Gossas virus	GOSV	<i>Keterah orthonavivirus</i>	ALD83626.1	
Issyk-kul virus	ISKV		AII79373.1	
Uzun Agach virus	UZAV		AKC89313.1	
Keterah virus	KTRV		YP_009361838.1	



3.S1 Fig. Comparison of commercially available di-Ub FRET TAMRA/QXL substrates. Activities of the vOTUs towards the different donor-quencher pair positions of K48 and K63 di-Ub FRET substrates. Values shown are the mean \pm standard deviation of two independent experiments.



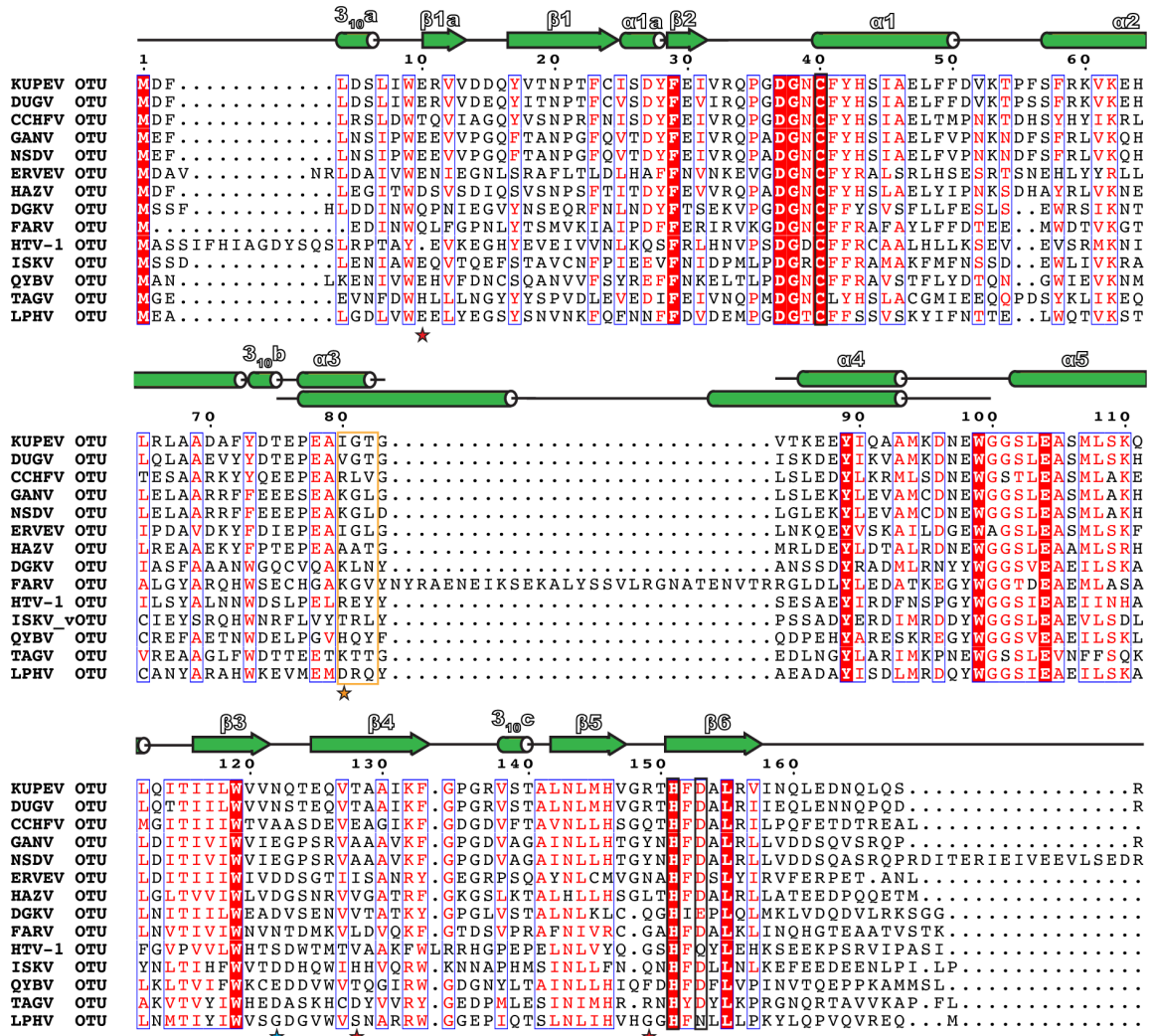
3.S2 Fig. Global structural comparison of vOTUs. (A) Overall structures of the TAGV, DGKV, and QYBV vOTUs with those of the previously solved CCHFV (PDB ID 3PRP), DUGV (PDB ID 4HXD), and ERVEV (PDB ID 5JZE) vOTUs. (B) Histogram of root mean square deviation of vOTU alpha carbons when measured against CCHFV vOTU. General regions highlighted in the text are indicated by red brackets.



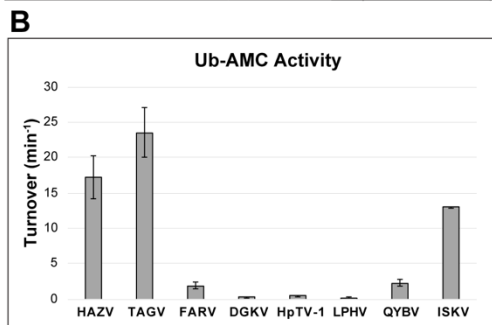
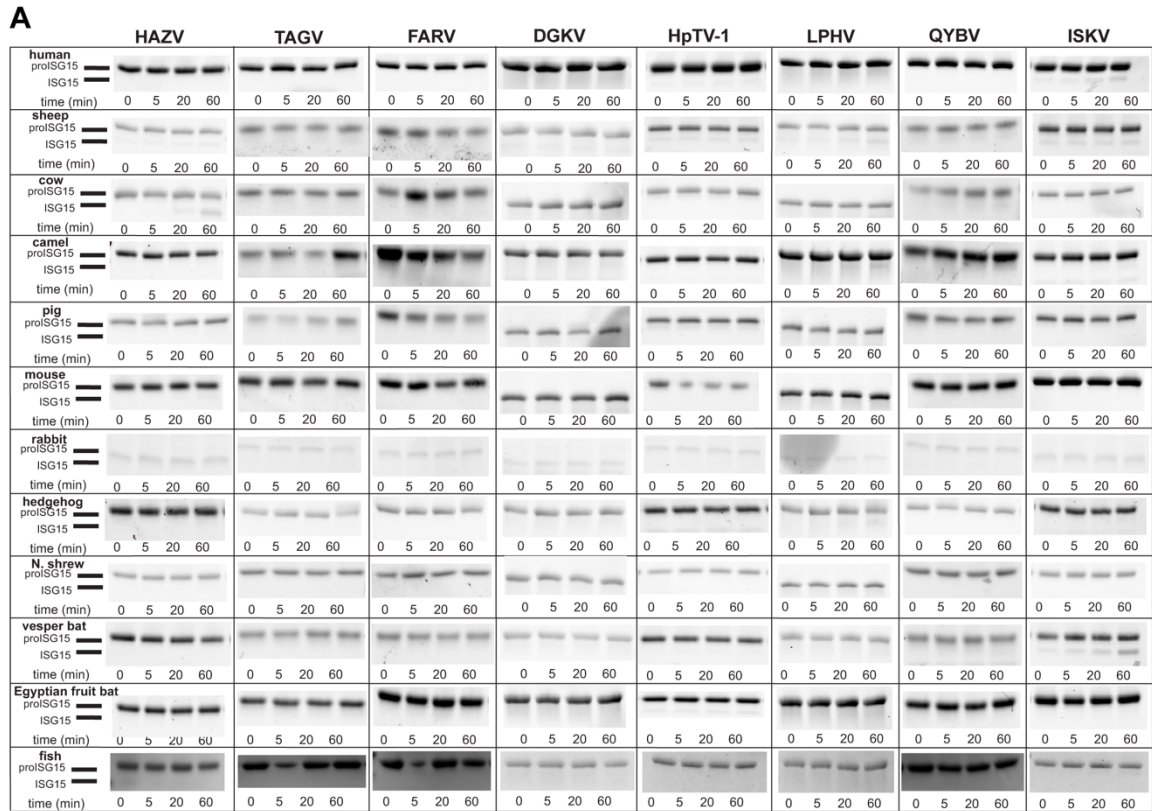
3.S3 Fig. ITC Isotherms of TAGV vOTU-Ub binding and biochemical environment of FARV vOTU Leu13. (A) Raw heat and integrated curves where binding occurs for representative runs of TAGV vOTU binding with Ub, Ub-L8A, and Ub-L8N. (B) Closeup of Leu13 and the surrounding hydrophobic region.

APPENDIX B

SUPPLEMENTAL INFORMATION FOR CHAPTER 4



4.S1 Fig. Expanded nairovirus OTU sequence alignment. Sequence alignment of the OTUs from the fourteen viruses included in this study. Annotated as in Fig 4.1A.



4.S2 Fig. Related to Fig 4.2. (A) OTU-proISG15 cleavage assays for HAZV, TAGV, FARV, DGKV, HpTV-1, LPHV, QYBV, and ISKV. Data obtained as described in Fig 4.2 and the Materials and Methods. (B) Reference Ub-AMC activity for OTUs. DGKV, HpTV-1, and LPHV are known to have poor/negligible DUB activity [44]. Values are the mean \pm standard deviation of three independent experiments.